AIRBORNE ELECTROMAGNETIC SEA ICE SOUNDING MEASUREMENTS DURING SIMMS'95

J.S. Holladay, R.Z. Moucha and S.J. Prinsenberg

Ocean Sciences Division
Maritimes Region
Fisheries and Oceans Canada

Bedford Institute of Oceanography
P.O. Box 1006
Dartmouth, Nova Scotia
Canada B2Y 4A2

1998

Canadian Contractor Report of Hydrography and Ocean Sciences 50

Fisheries and Oceans | Pêches et Océans

Canada

Canadian Contractor Report of Hydrography and Ocean Sciences 50

1998

Airborne Electromagnetic Sea Ice Sounding Measurements During SIMMS'95

by

J.S. Holladay,[*] R.Z. Moucha,[*] and S.J. Prinsenberg

Ocean Sciences Division
Maritimes Region
Fisheries and Oceans Canada

Bedford Institute of Oceanography
P.O. Box 1006
Dartmouth, Nova Scotia
Canada, B2Y 4A2

[*] Vanguard Geophysics Inc.
66 Mann Avenue
Toronto, Ontario M4S 2Y3
(formerly employed by Aerodat Inc.)

Public Works And Government Services 1998
Cat. No. Fs 98-17/50E ISSN 0711-6748

Correct Citation for this publication:

Holladay, J.S., R. Z. Moucha and S.J. Prinsenberg. 1998. Airborne Electromagnetic Sea Ice Sounding Measurements During SIMMS'95. Can. Contract. Rep. Hydrogr. Ocean Sci. 50: vii + 179.

TABLE OF CONTENTS

ABSTRACT

Holladay, J.S., R. Z. Moucha and S.J. Prinsenberg. 1998. Airborne Electromagnetic Sea Ice Sounding Measurements During SIMMS'95. Can. Contract. Rep. Hydrogr. Ocean Sci. 50: vii + 179.

An improved airborne electromagnetic ice sounding system was tested in conjunction with the Seasonal Ice Monitoring and Measurement Site (SIMMS'95) program near Resolute Bay, N.W.T., during the period 25 April to 10 May, 1995. Improvements made to the system included an improved EM transmitter and receiver, a more accurate laser altimeter and the addition of a precise orientation measurement system to the sensor bird.

In spite of helicopter and weather constraints, all of the primary objectives and most secondary objectives were achieved. Eight flights totalling 21.5 helicopter hours were executed with the system from the Polar Continental Shelf base during a 10 day window of helicopter availability. A further 5.5 helicopter hours were used for ground truth support. The first system flight acquired data north-west of Griffith Island to prepare an interim calibration of the system, and later flights used this calibration for estimation of real-time ice thickness and bulk ice conductivity over three marked sites at which ice and snow thickness data had been gathered. The most important of these sites was located at a margin between flat first-year (FY) ice and a multi-year (MY) ice floe near the Seasonal Ice Monitoring and Measurement Site (SIMMS'95) camp east of Lowther Island. A second site, located south of the camp, straddled a small pressure ridge, and a the third site consisted of two short east-west lines laid out on first-year ice at the "EM Site" just east of the camp.

This report presents data collected during the production phase of the project between May 1 and May 10, 1995 by the electromagnetic ice sounder. The snow-plus-ice thickness data set includes data from long flight traverses over the FY and MY ice, together with short intensive flight traverses in the immediate vicinity of ground truth lines on selected ice floes situated in both FY and MY ice. Improvements to the laser and to the pitch and roll sensor array were proven to be highly successful, effectively eliminating artefacts in measured ice thickness caused by bird swing. Analysis of the airborne measurements showed that the EM ice sounding technique can readily distinguish FY from MY pack ice through analysis of the measured thickness distribution, surface roughness, and bulk conductivity of the sea ice.

RÉSUMÉ

Holladay, J.S., R. Z. Moucha and S.J. Prinsenberg. 1998. Airborne Electromagnetic Sea Ice Sounding Measurements During SIMMS'95. Can. Contract. Rep. Hydrogr. Ocean Sci. 50: vii + 179.

Un nouveau système électromagnétique aéroporté d'observation de la glace a été testé dans le cadre du programme du site de surveillance et de mesure de la glace saisonnière (SIMMS'95), près de Resolute Bay, dans les Territoires du Nord-Ouest, entre le 25 avril et le 10 mai 1995. Le nouveau système comportait les modifications suivantes : un meilleur émetteur-récepteur électromagnétique, un altimètre laser plus précis et l'ajout d'un système de mesure de l'orientation plus précis à l'oiseau instrumenté.

Malgré les contraintes liées aux hélicoptères et aux conditions météorologiques, on a pu atteindre tous les objectifs principaux et la plupart des objectifs secondaires. Huit sorties, soit 21,5 heures-hélicoptère, ont été effectuées à partir de la base de l'Étude du plateau continental polaire, pendant le créneau de 10 jours de disponibilité de l'hélicoptère. On a en outre utilisé 5,5 heures-hélicoptère pour les travaux de réalité de terrain. À la première sortie, on a recueilli des données au nord-ouest de l'île Griffith pour préparer un étalonnage provisoire du système, qui a été utilisé au cours des sorties suivantes pour l'estimation en temps réel de l'épaisseur de la glace et de sa conductivité interne à trois sites marqués pour lesquels on avait amassé des données d'épaisseur de la glace et de la neige. Le plus important de ces sites était situé dans une zone frontière entre de la glace plate de première année et un floe de plusieurs année près du camp de SIMMS'95, à l'est de l'île Lowther. Le second site, au sud du camp, chevauchait une petite crête de pression, et le troisième se composait de deux courtes lignes est-ouest sur la glace de première année au site EM, juste à l'est du camp.

Le rapport présente les données recueillies par le sondeur électromagnétique pendant la phase opérationnelle du projet, entre le 1er et le 10 mai 1995. L'ensemble de données sur l'épaisseur glace-plus-neige inclut les données acquises au cours de deux longs survols transversaux de la glace de première année et de la glace de plusieurs années, et de plusieurs courtes sorties intensives dans les environs immédiats des lignes de réalité de terrain sur certains floes situés dans la glace de première année et la glace de plusieurs années. Les améliorations apportées au laser et au système de détection de tangage-roulis se sont révélées très efficaces, éliminant très bien les erreurs de mesure de l'épaisseur de la glace causées par le balancement de l'oiseau. L'analyse des mesures aéroportées a montré que la technique d'observation électromagnétique de la glace peut facilement faire la distinction entre la banquise de première année et la banquise de plusieurs années, en analysant la distribution de l'épaisseur, la rugosité de la surface et la conductivité interne de la glace de mer.

LIST OF FIGURES

LIST OF TABLES

1. INTRODUCTION

1.1 Background

The Canadian Coast Guard Electromagnetic Ice Sounder (EIS), also known as the Ice Probe, was developed for rapid measurement of sea ice properties by the now-defunct Aerodat Inc. during the late 1980's and early 1990's. An early prototype was demonstrated near Tuktoyaktuk, NWT in 1991 and in the Gulf of St. Lawrence and off the Labrador Coast between 1992 and 1994 (Prinsenberg *et al*, 1992, 1993, 1996, Peterson *et al*, 1995, 1998, Holladay, 1995, Holladay and Moucha, 1998). A series of similar devices were developed for the U.S. Army Corps of Engineers Cold Regions Research and Engineering Laboratory during the same period (Kovacs, 1990, Holladay *et al*, 1990). The sounding technology was improved during the 1994 to 1995 period, resulting in a new system known as the Production Prototype, which was delivered to Coast Guard (CCG) in early 1995. This system incorporated a more advanced EM transmitter-receiver subsystem, a more accurate laser altimeter, and an orientation sensor capable of monitoring the absolute attitude of the sensor bird in real time. The EIS system is now being supported and maintained by Vanguard Geophysics Inc. of Toronto.

The EIS was briefly tested in the southern Gulf of St. Lawrence during the late winter of 1995. Ice conditions were not conducive to extensive testing, however, so that the first rigorous test of the improved system occurred during the field project near Resolute, NWT., which forms the subject of this report.

The Resolute field program was carried out in conjunction with the Seasonal Ice Monitoring and Measurement Site (SIMMS'95) program near Resolute Bay, N.W.T., during the period 25 April to 10 May, 1995 (Misurak *et al*, 1995). **Figure 1.2.1** shows a location map for the area.

1.2 Objectives

This work was funded by the Canadian Coast Guard as a way to evaluate the EIS system under Arctic conditions. Some of the principal objectives of the EIS field program therefore reflected Coast Guard priorities:

1. To establish that EIS could reliably discriminate between first-year and multi-year sea ice.
2. To demonstrate the increased resolution in ice thickness profiles computed by two-dimensional (2D) processing techniques compared to the standard 1D estimates.

Other scientific objectives were:

1. To obtain data traverses suitable for use in ground-truthing SAR and satellite imagery.
2. To gather data which could be used to study the relationship between estimated ice conductivity, salinity, thickness and temperature.

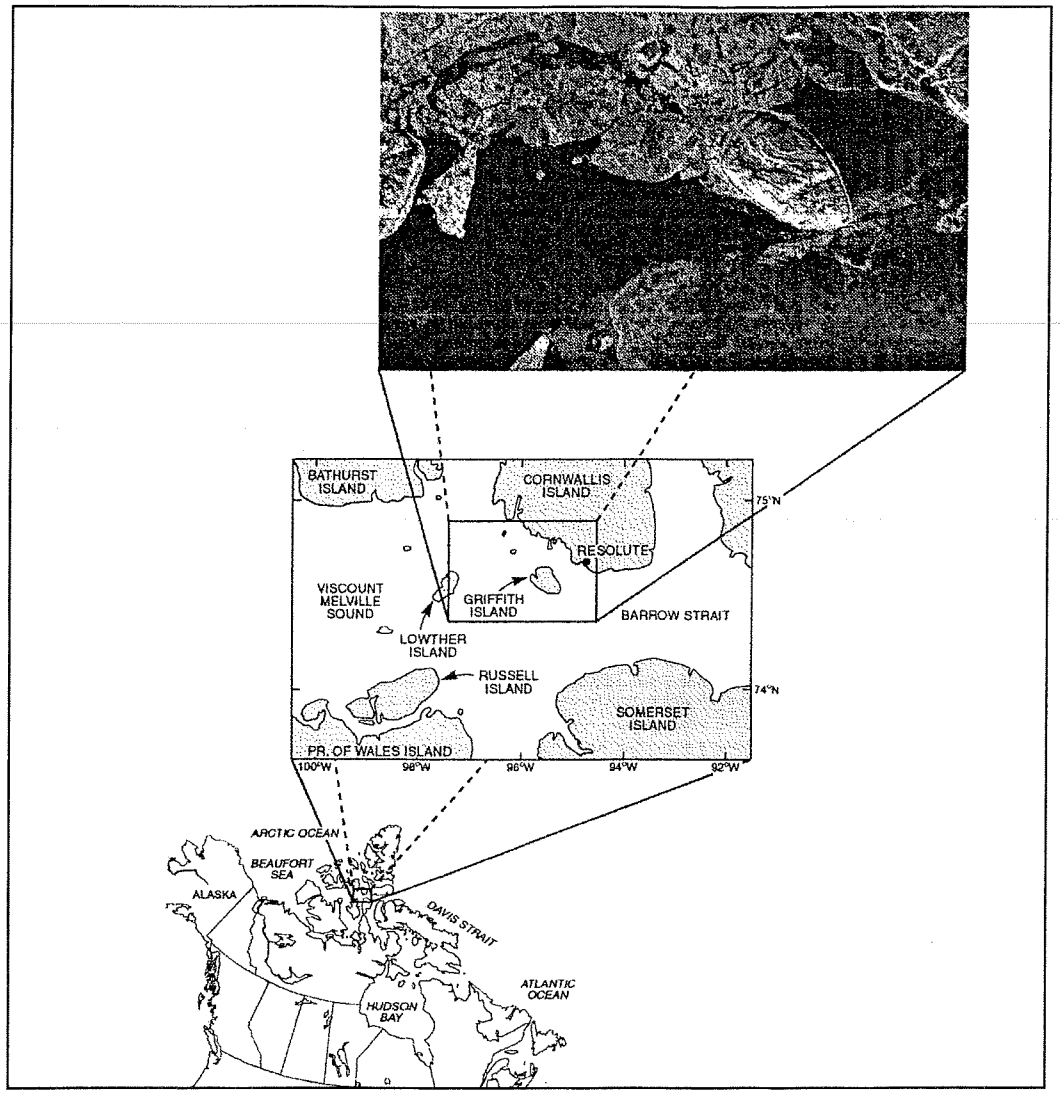

Figure 1.2.1: Location map for airborne survey work.[1]

1.3 Operational Issues

Prior to the initiation of the field program, a "moratorium zone" was declared by the local government which encompassed Resolute Bay out to Griffiths Island. Surface activities by non-aboriginals within the zone were forbidden. Very little low-level flying was performed in this area for the same reason, although it was not proscribed. The moratorium precluded the use of Resolute Bay itself as a site for ground truth calibration and test lines, which complicated activities during the airborne project start-up.

[1] From ICE PROBE Airborne Electromagnetic Sea Ice Sensor Measurements During SIMMS'95: Data Report, S. Holladay *et. al* (1995).

The first few days at the Polar Continental Shelf Project (PCSP) facility at Resolute were used for assembly and installation of the equipment and for initial testing. A preliminary calibration dataset was obtained on April 27. This was used to prepare a set of calibration factors for the system, which were tested on recorded data until flights were resumed on 1 May following a period of poor weather. This calibration was used during the rest of the field program, despite its preliminary nature, in order to minimise the complexity of the dataset. A new set of calibration factors were computed near the end of the field program, using data obtained on May 1 at the FY ridge site, and the results of post-processing performed at PCSP were compared to ground truth. The preliminary calibration was found to have been in error by approximately 0.07 m in snow plus ice thickness (for 2 m ice) at this time. The re-calibrated results showed excellent fidelity to ground truth (negligible systematic error over level ice) and a high degree of internal consistency. The results in this report are based on re-calibrated data.

From May 1 to May 6, EIS data was obtained in repeated passes over four surface measurement sites and along a series of long traverses in the Resolute area, with one traverse on May 6 extending up to the Polaris mine site on Little Cornwallis Island.

EIS flights departed from and returned to the PCSP helicopter facility at the Resolute airport. For extended operations near the SIMMS'95 camp, refuelling was performed at the fuel cache located at the camp's airstrip, known as the "Y" airstrip for the forked ridge which bracketed it.

Data were typically acquired during the day, with an immediate assessment being performed by monitoring the system's output on the chart recorder, and summarised in the evening for reporting and post-processing purposes. System maintenance and repairs were performed as required to make the best use of the available good flying weather.

Flight operations with the bird required a minimum 1000 foot ceiling and VFR conditions. Winds strong enough to cause whiteout conditions and deteriorating ceilings curtailed flights on some days, while ice fog was present on others.

The EIS system was still relatively "new" at the time of this project. It was therefore very useful to have an engineer on site for immediate diagnosis and correction of problems. In one case, the cold, dry conditions led to a transmitter failure through static discharge during a landing at the Y airstrip. This severe problem was repaired and measures to prevent recurrences were taken in the field.

A detailed account of the field work is provided in Section 2.2.

1.4 Processing

Post-processing software was used to present data in *profile map* format and in *standard plot* format. The *profile map* consists of data presented in profile form superimposed on a map of the area in a Lambert Conic Conformal projection (**Appendix D**). The *standard plot* contains ice thickness and high-pass filtered laser altimeter histograms along with profile plots of ice thickness, laser altimeter and high-pass filtered laser altimeter (**Appendix E,** May 1 only). Each *standard plot* corresponds to a 2 km segment of the flight traverse.

2. STUDY AREA AND FIELD WORK

2.1 Study Area

The study area lay in the general vicinity of Resolute Bay, NWT, with most survey work concentrated near the SIMMS'95 ice camp. This camp was located west of Griffith Island, just off the east coast of Lowther Island on a large zone of first-year ice, close to a multi-year ice floe grounded at its south end on Lowther Shoal (**Figure 2.1.1**). Selection of the survey sites A-D was partially based on the desire to investigate features seen in SAR images such as this one.

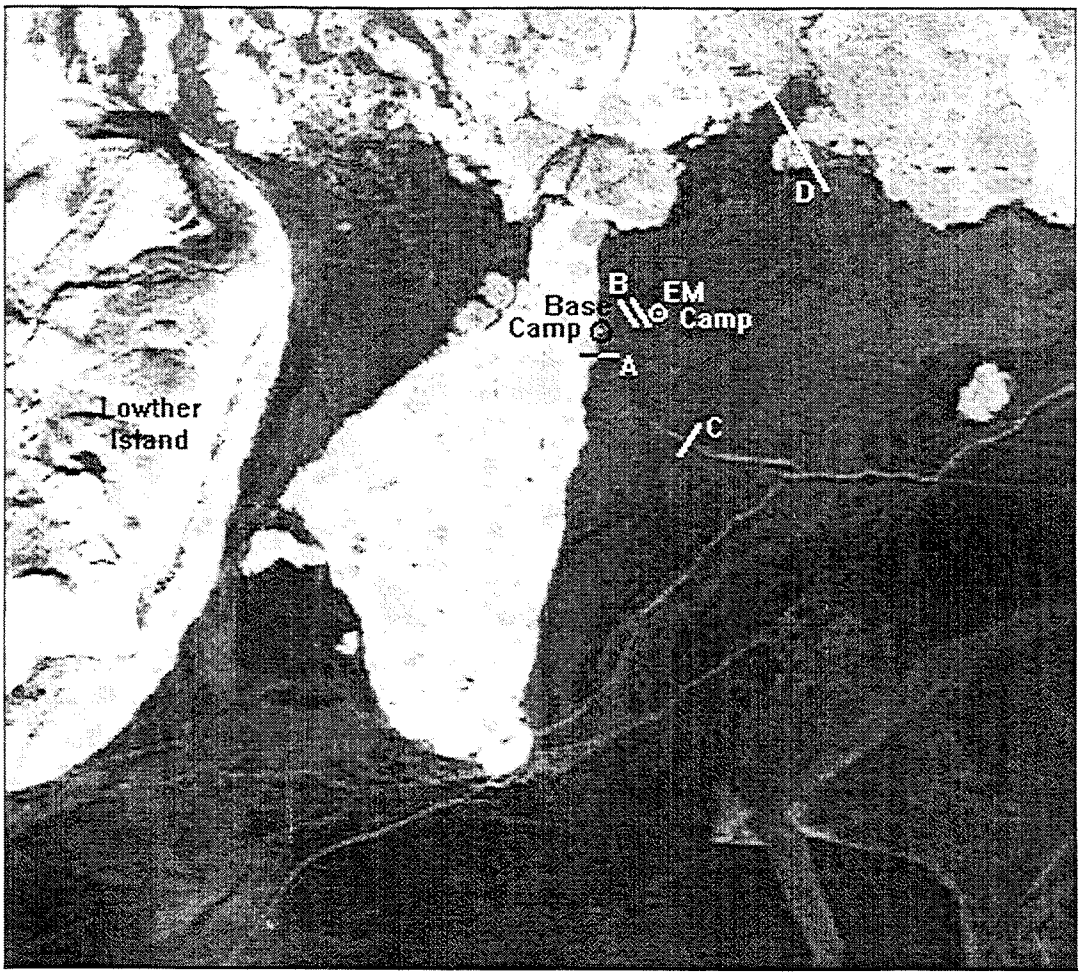

Figure 2.1.1: SIMMS'95 calibration sites.

2.2 Field Work

Surface verification data were gathered by Simon Prinsenberg and Roger Provost, with assistance from Mohammed Shokr and other SIMMS'95 participants. Four sites, designated A, B, C and D, were marked and drilled. Snow depth, ice thickness and ice salinity samples were obtained along

these ground truth lines (**Appendix C**). Snow depths were measured twice at Site A, both before and after the snowfall of April 29.

The Site A measurement line was selected to assess EIS' ability to distinguish between FY and MY ice based in EIS estimates of thickness and ice conductivity (which relates to ice salinity). Lines at Site B were along the edge of the "EM test site" used by other investigators. Site C was intended to test the new 2D ridge keel inversion capability of the system. The ridge at Line C turned out to be an anomalous ridge without a significant keel, so less quantitative tests were performed instead over features with more substantial keels. A number of traverses were undertaken in order to obtain for regional ice information, but also served to demonstrate the reconnaissance capability of the system.

Site A: FY/MY Line

The FY/MY Line was located to the south-west of the main SIMMS'95 camp, crossing the margin between thick MY ice at the west end of the line to level, snow-covered FY ice in the east (**Figure 2.2.1**). A total of 29 auger holes were drilled at this site, 25 of them at 20 m spacing along the line, two along the western extension of the line, and two just south of the line. Of these holes, twelve were in the FY ice, twelve in the MY ice and one at the interface.

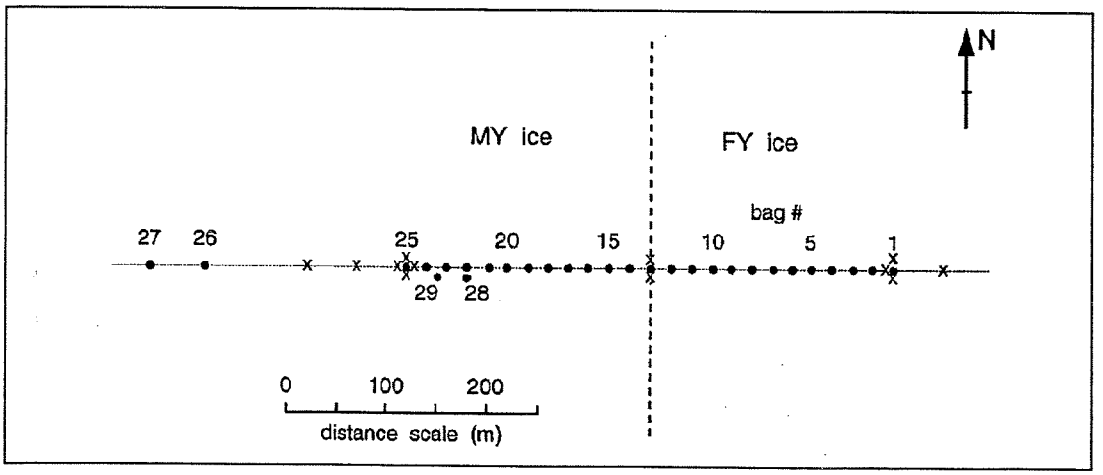

Figure 2.2.1: Marked line at Site A, FY/MY line.

Site B: EM Site Line

The EM Site marked lines consisted of two parallel tracks, roughly 75 m apart, located SW of the EM Site tent. The ice was all level FY with significant snow drifting. Along these two lines a total of 10 auger holes were drilled with a spacing of 25 m (**Figure 2.2.2**). The ice thickness ranged from 165 cm to 179 cm and snow depth from 10 cm to 30 cm.

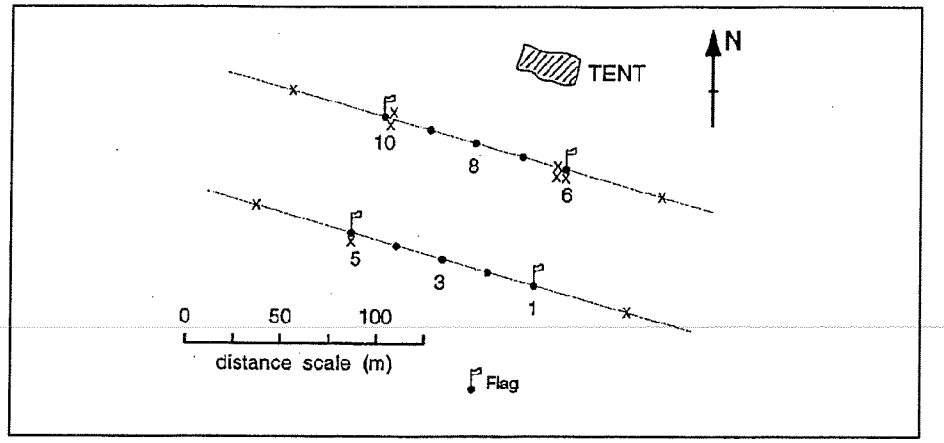

Figure 2.2.2: Marked and drilled lines at Site B, the SIMMS'95 "EM Site".

Site C: Ridge Line

The FY Ridge Line was located almost due south of Site B and consisted of 24 auger holes aligned approximately NS, crossing a small pressure ridge. Of the 24 holes, 21 were at 20 m intervals along the main line, one hole was 10 m north of the ridge, and the remaining two were located 5 m to either side of the line at the ridge crest (**Figure 2.2.3**). It appears that this was not a typical pressure ridge, but rather a linear "pop-up" feature, in which the ice on both sides of the ridge axis were forced up during the ridging event. As such, it had little or no keel beneath the ridge. The ridge line also provided good FY calibration data with snow-plus-ice thickness ranging from 190 and 210 cm.

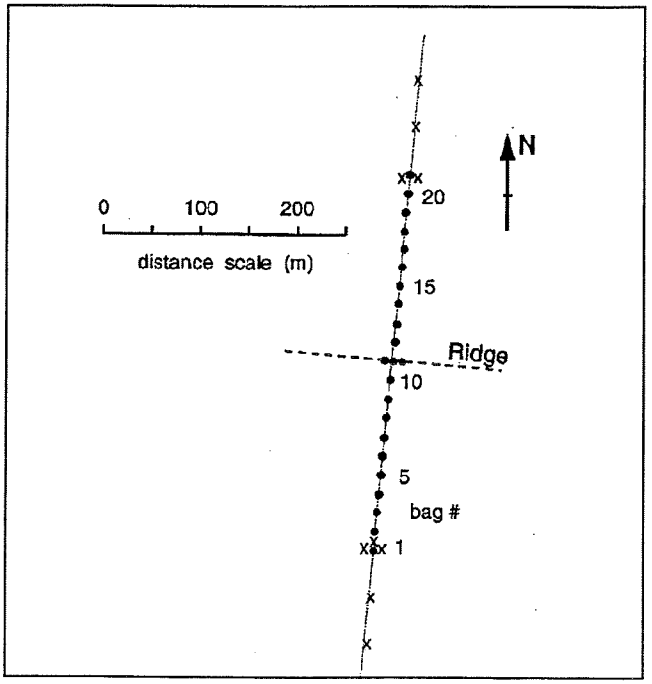

Figure 2.2.3: Calibration line site C, FY ridge.

Site D: SAR Validation Traverse

This line was constructed after EIS profiling in order to investigate certain features observed on the airborne results, and to assess features seen in the SAR imagery. Auger holes were sited to sample distinct portions of the FY and MY floe structure in the area. A total of 7 holes were drilled along this line (**Figure 2.2.4**).

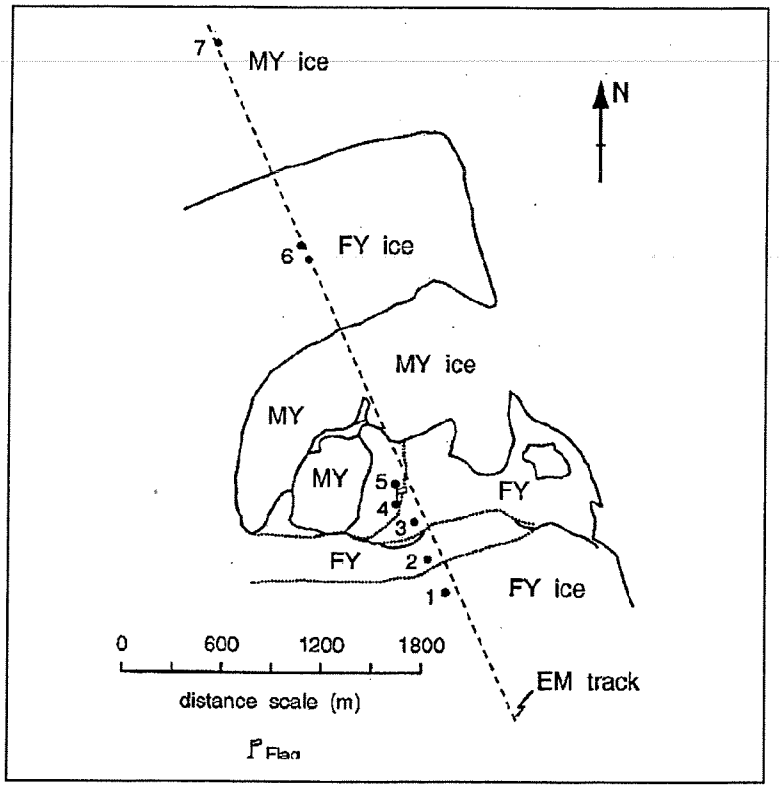

Figure 2.2.4: Measurement locations at Site D, SAR validation line.

2.3 Daily Summary of Field Activities

Tuesday, April 25, 1995
Weather: –5 °C, clear
EM Flight Files: none

1. Arrived Resolute approx. 1330.
2. All pre-shipped equipment had arrived on Saturday.
3. Met with PCSP Base Manager Dave Maloley in evening. Helicopter LMV was designated for EIS use. Met Canadian Helicopters pilot Bernard Maugim (BM) and helicopter engineer Terry Porter (TP), who were designated to work with EIS.

4. Assembled bird, checked console, checked bird operation, tested field computer and printer for post-processing.

Wednesday, 26 April, 1995
Weather -10°C ,clear, calm.
EM Flight Files: none

1. System installed and ground tested. Appears to be fully functional. The helicopter's chin bubble through which flight path video is monitored is in poor shape and will definitely mar picture quality.
2. Checked CV580 SAR imagery for survey line planning. Chuck Livingstone will provide a set of GPS co-ordinates to use in setting up our survey lines and grids. Simon has determined a location for the main ground truth line (Site A). Their mob to camp has been delayed to tomorrow morning.
3. A lag of 2 sec should be allowed for between manual fiducial (with resultant video output) and appearance of the corresponding ice thicknesses on the video display, due to time required for real-time processing.

Thursday, 27 April, 1995
Weather: -10 °C, clear.
EM Flight Files: 01 - 05

1. Start for EM flying delayed to noon due to pilot having to provide emergency assistance early in morning. Simon Prinsenberg (SP) and Roger Provost (RP) flew with the Twin Otter to SIMMS'95 field camp near Lowther Island to start collecting ice and snow surface measurements along calibration lines.
2. FLT001: Flew from Resolute to the N end of Griffith Island and performed some runs over a section of smooth ice for preliminary calibration purposes. Attempt to acquire a thickness measurement with surplus auger unsuccessful (auger dull). Observed snow plus ice thicknesses from EIS were in 1.8-1.9 m range, as opposed to 1.75 m ice thickness expected from SIMMS'95 briefing.
3. FLT002: flew to SIMMS'95 camp, located micro-met towers (obstacles for EIS flying) and flew two passes over MY floe. SP had already begun to mark a line: flew this in two directions.
4. FLT003: after refuelling at the "Y" runway, flew more passes over main FY/MY ground truth line (Site A, more marks now set out) and then to small MY floe to E of "Y" on border of large smooth area. Flew multiple passes over this margin. Initial tests of 2D inversion for ridge unsatisfactory.
5. FLT004 - 005: continued over the flat ice towards Resolute. About 3 hours helicopter time used.
6. JSH post-processed data (real-time inversion map plots) in evening. Also estimated new CAL1 complex calibration factors from smooth ice in FLT001 for fid range 699800 to 699900, based on briefed ice thickness of 1.75 m, for installation and testing Friday.
   New CAL1 factors: (0.9612 + 0.0121i), (0.9123 + 0.3079i), (1.2244 + 0.5464i)
   New/old factor ratios: (1.0091 + 0.0020i), (1.0135 + 0.0013i), (1.1548 - 0.1252i)

Friday, 28 April, 1995
Weather: -10 °C, cloudy
EM Flight Files: no EIS flying due to weather

1. SP has completed drilling of FY portion of Site A. JSH told Kevin Misurak (KM) that we'd observed 2 m ± 0.1 m along FY line with EIS. He indicated that the ice thickness is more like 1.8 m. Didn't ask at that time whether this number included snow depth. [It turned out that the snow-plus-ice thickness ranged from 1.8 to 2.1 m along this line, with drifted snow accounting for the .3 m of variability].
2. JSH re-inverted short extract over FLT001 calibration site to check revised calibration (called CAL1, the original from PEI was CAL0). Results are .05 m thinner and yield .02 S/m rather than .016 S/m for the FY ice, as intended.
3. Calibrated and inverted dataset from FLT003, Line 3, from 21:13:20 and 40 sec thereafter, from the Site A GT line. The FY ice shows a minimum thickness of about 1.80 ± 0.02 m and apparent snow drifting of up to 20 cm. This snow drift thickness is consistent with what was observed on flat ice closer to Resolute.
4. Sent a data plot for the main GT line to SP at camp with Mike Manore, who went out with the helicopter to fetch Mohammed Shokr (MS) and Rob Moucha (RM).

Saturday, 29 April, 1995
Weather: -2°C , cloudy, light snow, winds gale force with blowing snow by evening
EM Flight Files: no EIS flying due to weather

1. Brought detailed flight records up to date and performed data backups.
2. Printed maps at CHS chart scale (1:200,000) and CCRS SAR print scale (1:273,000) for comparison. The ice thickness and especially conductivity maps correlate very well to the imagery.

Sunday, 30 April, 1995
Weather: -8°C, winds < 10 kts, low ceiling breaking up
EM Flight Files: no EIS flying due to weather and pilot availability

MS suggested that the next flight to the vicinity of the camp be run over a slightly longer route that first goes W from Resolute, then N to camp. There were some interesting features on the SAR image that he wished to investigate.

Monday, 1 May, 1995
Weather: -12°C clear, north wind 15 kts and rising.
EM Flight Files: 008 - 011

1. Flew first mission (FLT008) starting about 0800, returning about 1300 without bird, because the wind had picked up and significant low cloud had developed at the "Y" landing strip. Refuelled twice at "Y", once just before return flight. During the first few lines of this flight, the system first yielded "good" ice conductivity estimates which discriminated well between FY and MY ice.

2. Second mission (FLT010 – 011) started about 1940, with a helicopter ferry to pick up bird at the "Y". Winds at the "Y" were <10 kts and visibility excellent.
3. FLT010: repeated passes over the FY Ridge Site, the Main MY ground truth line and the two EM site lines were made.
4. FLT011: started for final work near the camp and for the return ferry. Excellent stability of the ice thickness and conductivity parameters during this long ferry, accomplished in two data segments separated by a single background, demonstrated the performance of the system over extended periods: FY/MY discrimination was still performing well.
5. Most of the ground truth program for EIS validation has been completed
6. JSH processed data from these missions during the evening after the second flight. Noted weak crosstalk from the roll channel into the real-time ice thickness estimates, not present in inversions performed post-flight.

Tuesday, 2 May, 1995
Weather -10°C, cloudy, light NW winds, no flying
EM Flight Files: none

1. JSH analysed crosstalk observed Monday. Concluded that an error existed in real-time bird orientation corrections. Requested revised software from programmer in Toronto.
2. Plotted FLT007-FLT008 data for Mohammed Shokr (AES) at 1:273,000 (to match SAR image) and 1:50,000.
3. Obtained software updates for real-time 2D inversion.

Wednesday, 3 May, 1995
Weather: -15 °C, light NW winds, couldn't fly in morning. Improved in afternoon.
EM Flight Files: 16 - 18

1. JL loaded revised orientation correction routine of real-time inversion software. Weather had improved to fair-to-good, with some low cloud remaining to W.
2. During takeoff, tow cable was trapped under bird (from front). When helicopter ascended, bird was rolled over cable. No damage to bird.
3. System "hung" several times before becoming stable (problems due to tow cable damage.) Therefore had to abort acquisition several times (Files FLT012 to FLT017).
4. FLT018: after topping up fuel and inspecting system for obvious damage from takeoff incident, flew remainder of mission as one file (FLT018), starting south of Lowther Shoal, then running into MY ice NE of camp. From this point, flew due S, searching for an "ice island fragment" seen as a bright feature on the SAR image. After failing to locate any extremely thick ice in this area, moved on to profile the main FY/MY GT line, EM Site North and South GT lines, and FY Ridge GT line.
5. After completing multiple over-flights of FY Ridge GT line, flew to fuel cache at "Y" airstrip. After refuelling, attempts to start the system failed. It appeared that the bird was "zapped" by static build-up during touchdown
6. Could not re-establish link with bird after landing at Polar Shelf. Confirmed that tow cable was damaged during takeoff incident.
7. Transmitter determined to have been damaged, repairs initiated.

8. Twin Otter brought auger gear and SP back from field camp to Resolute.

Thursday, 4 May, 1995
Weather -18°C, clear, winds 15 kts from N.
EM Flight Files: none

1. SP, RP and MS used the EM helicopter LMV to drill GT holes at site D while EM transmitter and tow cable repairs were carried out.
2. EM and tow cable repairs completed in late evening
3. Tested system and confirmed ready for flight Friday morning.

Friday, 5 May, 1995
Weather -15°C, fog to W, winds light from N.
EM Flight Files: 19 - 24

1. FLT019: fog over ice prevented extension of survey lines outside Resolute Bay, so performed test profiles over bay in morning.
2. FLT020: tested 2D inversion over MY floe in bay. Weather truncated flight.
3. Returned to base and plotted 2D results.
4. Weather improved by afternoon, SP, RP and JSH flew out to sample Site D.
5. FLT021 – 024: Second EM flight in evening after dinner, including Site A and Site B. Terminated by weather.

Saturday, 6 May, 1995
Weather: -10°C, clear, winds light NW.
EM Flight Files: 25 – 27

1. JSH trained RP in EIS system operation.
2. FLT025: training flight north to Polaris Mine site at Little Cornwallis Island, following normal shipping route from Resolute Passage. Plotted results after flight with RP observing using real-time data.
3. FLT206: short profile over MY fragment in NW Resolute Bay.
4. FLT027: Solo training flight for RP (low ceiling, data not usable.)
5. SP, MS and RM flew out to perform further validation work north of the camp (including acquisition of ice cores and salinity measurements).
6. End of EIS flights. De-installed system to free up helicopter for next group of users.

Sunday, 7 May, 1995

1. JSH reprocessed FLT027 to assess usability.
2. RP was trained in data presentation, plotted FLT026, FLT027 from Monitor data files MAY06F26, MAY06F27.

Monday, 8 May, 1995

1. Further training for RP: plotted up some of the previous real-time data for extra practice.

2. Data assessment and plotting set-up for ground-truth comparisons.

Tuesday, 9 May, 1995

1. Measured and corrected for lag on comparison profiles, adjusted presentation format.
2. Video time picks were made for all passes over Site A, B and C lines (SH, SP, JL).
3. Assessed preliminary calibration results (used for real-time ice thickness estimates during flying.)
4. Agreement was good (within +/- .1 m in most cases) over "flat" FY ice, despite known variable snow cover ranging from 10 to 30 cm. Noted a systematic difference averaging 0.07m.
5. As expected, 1D performance over MY ice was not as good over flat ice, but tracked mean GT thickness very well. The ice conductivity estimates were typically over 0.1 S/m over the FY portion, but low (~.001 S/m) and much less variable over the MY ice.
6. Compared results obtained with this calibration and ground truth over the FY ridge line: these indicated a 7 cm systematic error.
7. The 0.07m systematic ice thickness error is almost certainly the result of the rather rough initial calibration.
8. A "Resolute Final" calibration for the system, based on flat ice near the FY ridge, was therefore undertaken. The resulting factors were all within 2% in amplitude of the initial calibration, as expected. An almost negligible phase rotation was observed as well. The new factors are:
   New factors: (0.9790 + 0.0177i) (0.9270 + 0.3193i) (1.2501 + 0.5689i)
   New/old factor ratios: (1.0186 + 0.0056i) (1.0182 + 0.0063i) (1.0244 + 0.0075i)
9. FLT018 was re-calibrated using the new factors, and lines extracted for comparison to GT values.
10. Packed most of the remaining equipment .

Wednesday, 10 May, 1995

1. Plotted re-calibrated ground truth comparison data. Good match observed with ground truth, systematic error has been removed by improved calibration. Noted a number of video mark picking and manual data entry errors.
2. Plotted all available data, and photocopied results for SP's use.

3. INSTRUMENTATION

3.1 Sensors In The Bird

The EM induction sensor package is towed in a bird about 30 m beneath the helicopter at altitudes of 10 to 25 m above the ice surface. Low frequency "primary" EM signals are transmitted by an antenna in the sensor bird and excite eddy currents in the sea water beneath the ice. These eddy currents in turn generate reflected or "secondary" EM fields which are measured by the receiver, also mounted in the bird. The distance of the bird to the water/ice interface can be determined by measuring the amplitude and phase of the secondary field relative to the transmitted field.

The frequencies in the EM sensor were 30 and 90 kHz. The antenna configuration was the horizontal coplanar mode, which has a larger footprint than the coaxial mode (3.75 times the bird altitude at the 90% level) but a much better signal/noise ratio for ice thickness measurement. The transmitter and receiver antennas were separated by 3.5 m. The overall length of the bird is approximately 4.2 m and its weight is about 100 kg. The bird is slung from the helicopter's cargo hook on a 30-meter tow cable, which carries power and digital control signals down to the bird and digital data up to the helicopter.

An IBEO PS100E laser profilometer mounted in the sensor bird was used to measure the distance from the bird to the snow/air interface. Its beam has a radius of less than .05 m when flying the sensor at an altitude of 15 to 20 m. A Trimble Navigation TANS Vector attitude monitoring system was also mounted in the bird. Provided that four or more GPS satellites are in view (this is normally the case), this GPS-based device uses carrier-phase interferometry techniques to continuously measure the orientation of the bird in pitch, roll and yaw to an accuracy of approximately 0.1°, and also provides a bird position estimate. Finally, a radar altimeter operating at about 2 GHz was mounted in the helicopter to assist the pilot in maintaining a steady survey attitude. Data from all of these ancillary sensors were logged on the helicopter computer along with the EM results.

3.2 Helicopter Instrumentation

The EIS system console was mounted on a rack in the back seat area of the Bell 206L helicopter. The operator could use the master computer/data logger and see the power distribution unit while viewing the annotated imagery from the video flight path monitoring camera on the CRT. A Panasonic AG-7400 S-VHS video recorder made an analog recording of this imagery for later use in assessing ice conditions below the helicopter. This camera was mounted in front of the forward passenger's seat, pointing downwards through the "chin bubble" of the helicopter, and observed the ice conditions and bird flight behaviour.

The master computer operated as the system controller. It collated, reduced and logged EM and other incoming data onto magnetic media. It also controlled an auxiliary processor which

inverted incoming data to ice thickness and other parameters, plotted the data on the GR33 graphic recorder, and generated a text overlay on the video flight path imagery including time, position and ice parameters. Positioning was carried out using the TANS Vector's position output, which was logged on the EM computer in WGS84 coordinates, displayed them on the CRT, and recorded them on the video flight path tape.

3.3 Other Instrumentation

Calibration and remotely sensed data were collected during the project to assess whether the EIS sensor could be used as a sampling technique to validate data collected by fixed-wing aircraft or satellite SAR.

Ice thickness, ice salinity and snow depth data collected during the experiment are listed in **Appendix C**. Ice holes where ice thickness measurements were taken were drilled by hand with a 2" diameter auger: the battery packs for the power drill did not last long in the cold temperatures (one 2 m FY ice hole per pack). Drilling holes in the MY ice was much more difficult: FY ice is relatively soft due to the presence of brine pockets, whereas MY ice has very low salinity and lacks such brine pockets. Ice chips were collected by 4" hand auger to determined the salinity of the ice by a hand-held refractometer once ice chips were melted at the base camp. 6-9 ppt average salinities were observed for FY ice using this procedure. Surface snow layer depths (8) were measured around each ice hole to obtain a more accurate average around the vicinity of the ice hole. Snow samples were also collected to determine snow salinity content. Although most samples were salt free, the snow layer above the FY ice (basal layer) contained salt ranging from 13 to 21 ppt. The basal layer thickness ranged from 0.5 to 4.0 cm. Other investigators investigated the effect of the salinity content of the basal layer on the reflective radar properties of sea ice (see Barber *et al.* 1995).

4. DATA COLLECTION AND ANALYSIS

4.1 Airborne Data Collection

Weather conditions during late April and early May of 1995 started out as moderate and sunny and deteriorated to light snow, fog, and cold temperatures (**Table 4.1.1**).

Table 4.1.1: Weather conditions summary

Date	Temperature (°C)	Sky/Precipitation	Wind
25/4/95	-8	clear	Calm
26/4/95	-10	clear	Calm
27/4/95	-10	clear	Light S
28/4/95	-10	cloudy	Light N
29/4/95	-5	cloudy/ afternoon snow storm	Light N
30/4/95	-5	cloudy	Light N
1/5/95	-12	clear	Strong NW
2/5/95	-10	cloudy	Light NW
3/5/95	-15	partly cloudy	Light NW
4/5/95	-18	clear	Strong NW
5/5/95	-15	cloudy	Light
6/5/95	-10	clear	Strong NW
7/5/95	-10		Light NW
8/5/95	-11		light N

Long-range data collection missions over FY and MY ice were undertaken from May 1 to 5, during which large quantities of airborne and surface ice thickness data were collected. Flights prior to this time were used for testing, setup and calibration purposes.

Table 4.1.2: EM data sets for the FY and MY ice traverses.

Date	FY ice (km)	MY ice (km)
1/5/94	82.129	86.157
3/5/94	152.178	39.604
5/5/94	174.886	129.435
Total	409.193	255.196

Of these flights[2] a total of 664 km of EM data was collected, 409 km over FY ice and 255 km over MY ice. (**Table 4.1.2** above.)

A summary of ice types according date and flight number can be found in **Table 4.1.3**. A detailed summary of EM data collected for each date, flight and survey line number may be found in **Appendix B**. A coastal map of the study area with survey line flight paths superimposed is shown by Figure 4.1.1. More detailed coastal maps of the areas surveyed for each flight with superimposed survey line flight paths are shown seen in **Figure 4.1.2 -- Figure 4.1.13**.

Table 4.1.3: Flight summary over FY and MY ice floes.

May 1, 1995			May 3, 1995			May 5, 1995			May 6, 1995		
FLT	Line #	Ice Type	FLT	Line #	Ice Type	FLT	Line #	Ice Type	FLT	Line #	Ice Type
8	10010	FY	16	10011	FY	19	10012	FY	25	10010	FY
	10020	FY		10012	FY		10020	FY		10020	MY
	10030	MY		10020	FY		10030	MY		10031	MY
	10040	FY	17	10010	FY		10040	MY		10032	MY
9	10012	FY		10020	FY	20	10011	MY		10040	MY
	10013	FY		10031	FY		10021	FY		10050	FY
	10020	FY		10032	FY	21	10010	FY		10061	FY
	10031	FY		10040	FY		10020	MY		10062	FY
	10032	FY		10051	FY		10031	FY		10080	FY
	10041	FY		10052	FY		10032	FY		10090	FY
	10042	FY		10060	FY		10033	FY		10100	FY
	10051	FY	18	10020	FY		10034	FY			
	10052	FY		10041	FY		10035	FY			
	1006	FY		10042	FY		10036	FY			

[2] Survey lines shorter than 400 m were omitted from the totals.

May 1, 1995			May 3, 1995			May 5, 1995			May 6, 1995		
FLT	Line #	Ice Type	FLT	Line #	Ice Type	FLT	Line #	Ice Type	FLT	Line #	Ice Type
	2										
	10063	FY		10043	FY		10037	FY			
	10081	FY		10050	MY		10041	FY			
	10092	FY		10061	FY		10042	MY			
	10100	FY		10062	FY		10043	MY			
	10121	FY		10071	FY		10044	MY			
	10122	FY		10072	FY		10045	MY			
	10123	FY		10073	MY		10051	MY			
	10131	FY		10074	MY		10071	FY			
	10132	MY		10081	FY		10081	MY			
	10141	FY		10082	FY		10091	FY			
	10142	MY		10092	MY		10092	FY			
	10150	MY		10093	FY		10110	FY			
	10160	MY		10094	FY		10121	FY			
	10173	FY		10101	FY		10122	FY			
	10180	FY		10111	MY		10131	FY			
10	10010	FY		10112	FY		10140	FY			
	10021	FY		10113	MY		10151	FY			
	10022	FY		10114	FY		10160	FY			
	10030	FY		10115	MY		10180	FY			
	10040	MY		10120	MY		10192	FY			

May 1, 1995			May 3, 1995			May 5, 1995			May 6, 1995		
FLT	Line #	Ice Type	FLT	Line #	Ice Type	FLT	Line #	Ice Type	FLT	Line #	Ice Type
	10060	MY		10130	MY		10201	FY			
	10070	MY		10141	FY	22	10011	MY			
	10092	FY		10151	FY		10020	FY			
	10111	FY		10161	FY	24	10010	FY			
	10112	FY		10163	FY		10020	FY			
	10113	FY		10171	FY		10050	FY			
	10121	FY		10172	FY		10070	FY			
11	10010	FY		10181	FY						
	10022	MY		10182	FY						
	10032	MY		10191	FY						
	10034	MY		10221	FY						
	10041	MY		10222	FY						
	10042	MY		10231	FY						
	10050	MY		10240	FY						
	10070	MY		10251	FY						
	10080	FY		10252	FY						

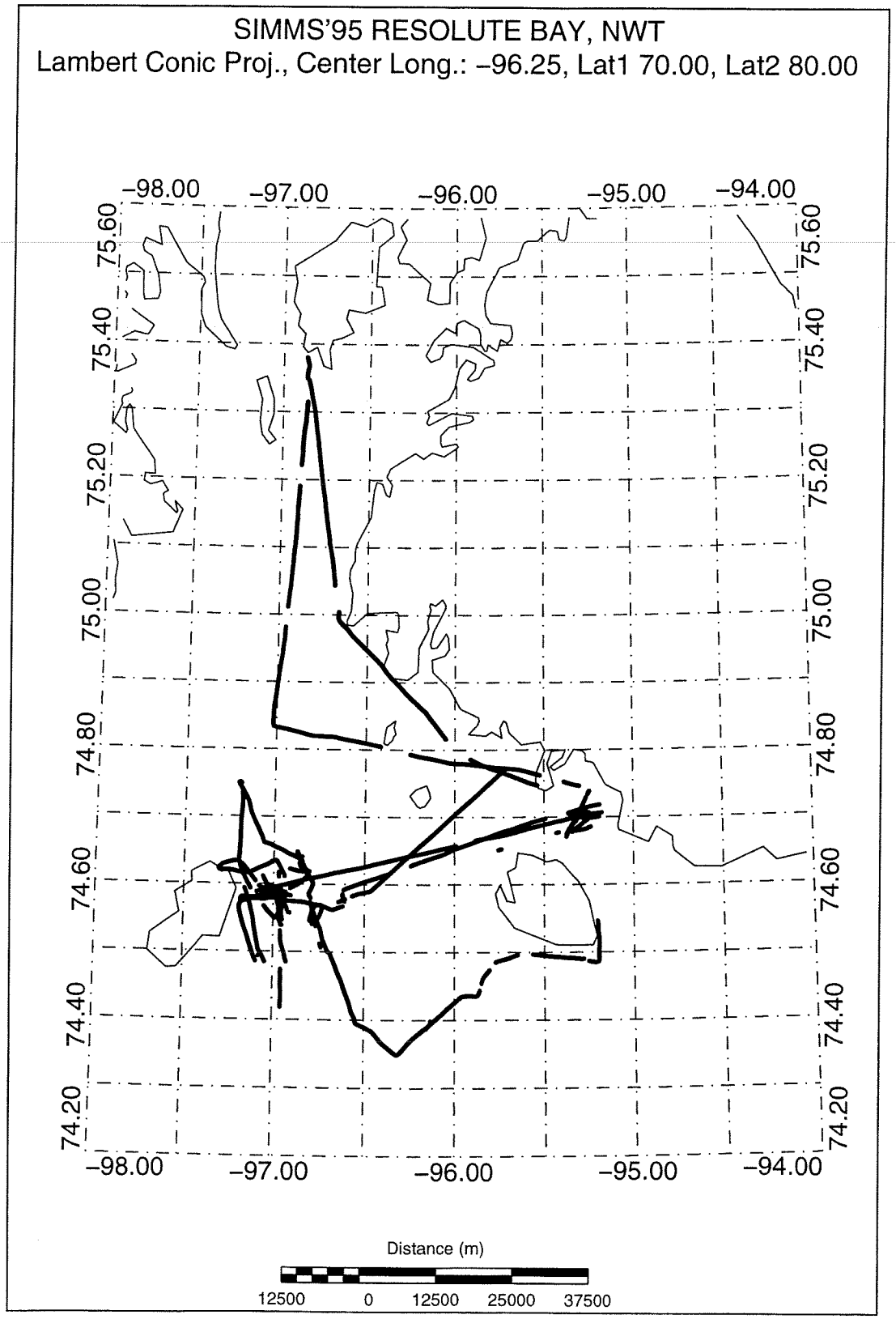

Figure 4.1.1: Resolute Bay area coastal map with superimposed survey line flight paths.

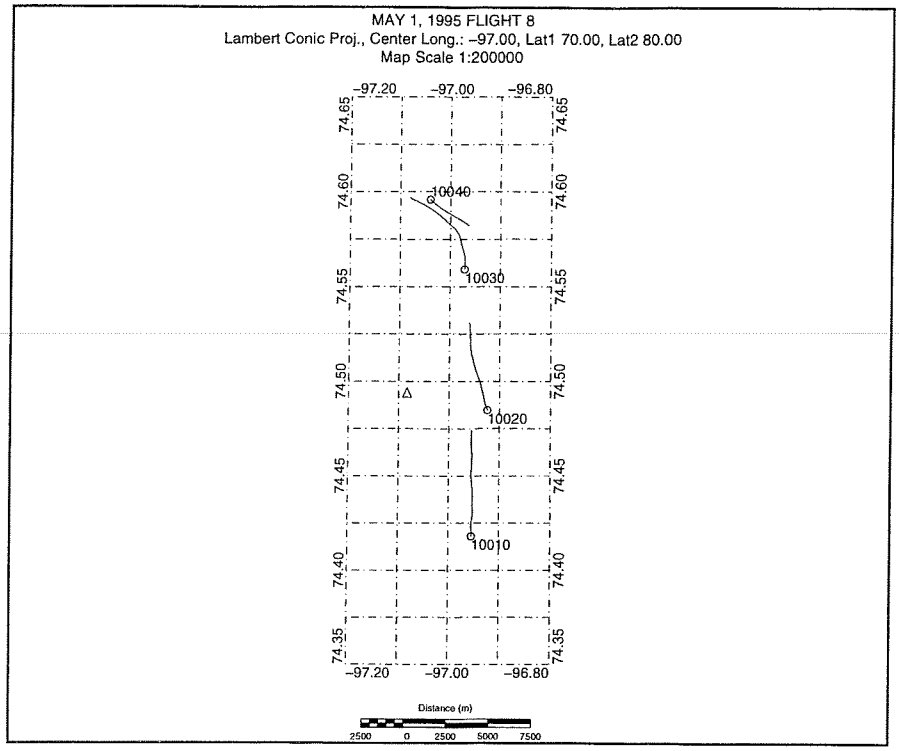

Figure 4.1.2: May 1, 1995 survey line flight path, FLT008.

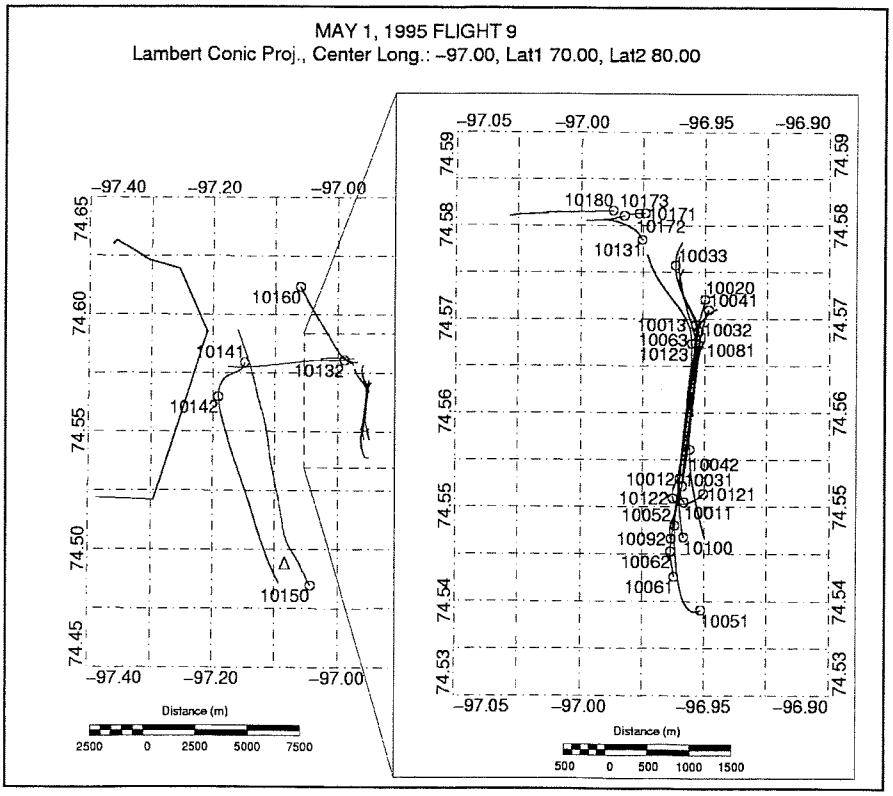

Figure 4.1.3: May 1, 1995 survey line flight path, FLT009.

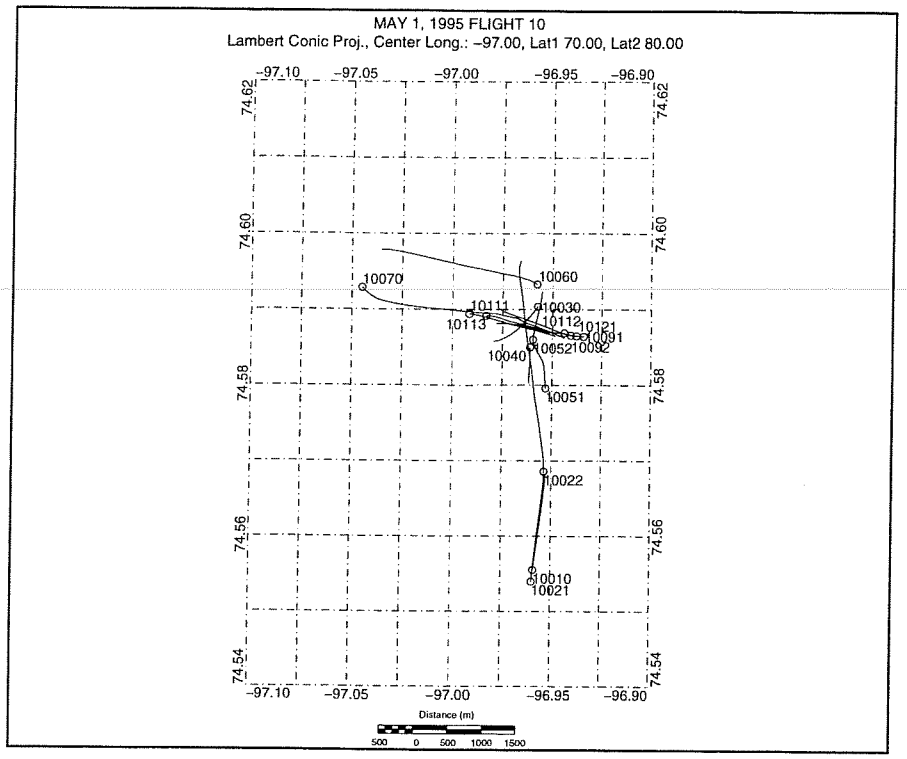

Figure 4.1.4: May 1, 1995 survey line flight path, FLT010.

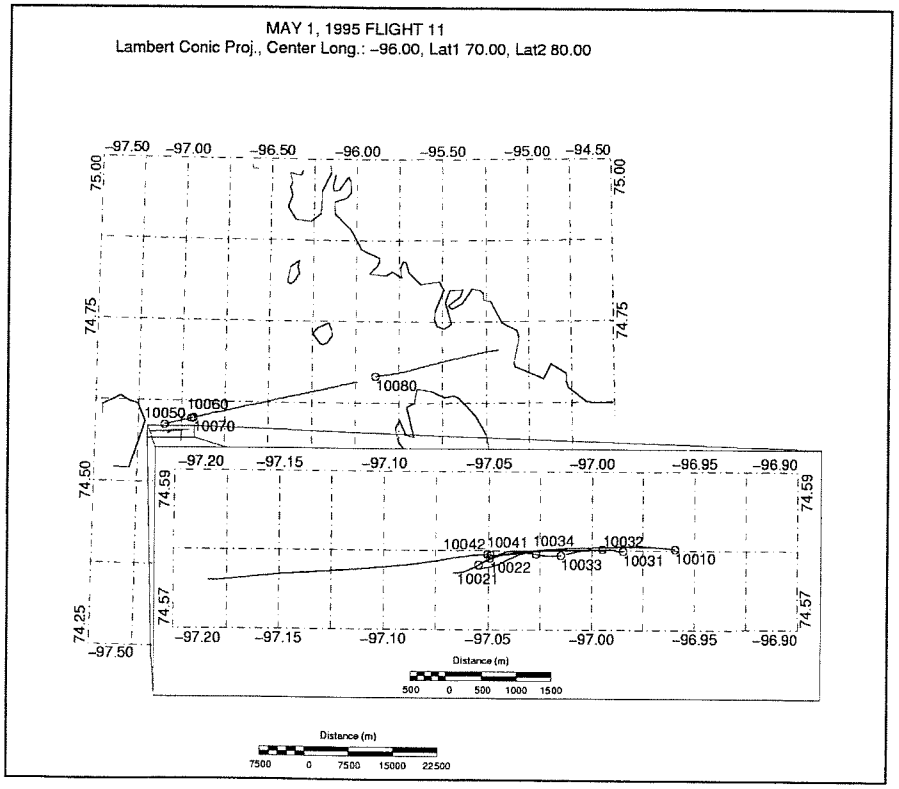

Figure 4.1.5: May 1, 1995 survey line flight path, FLT011.

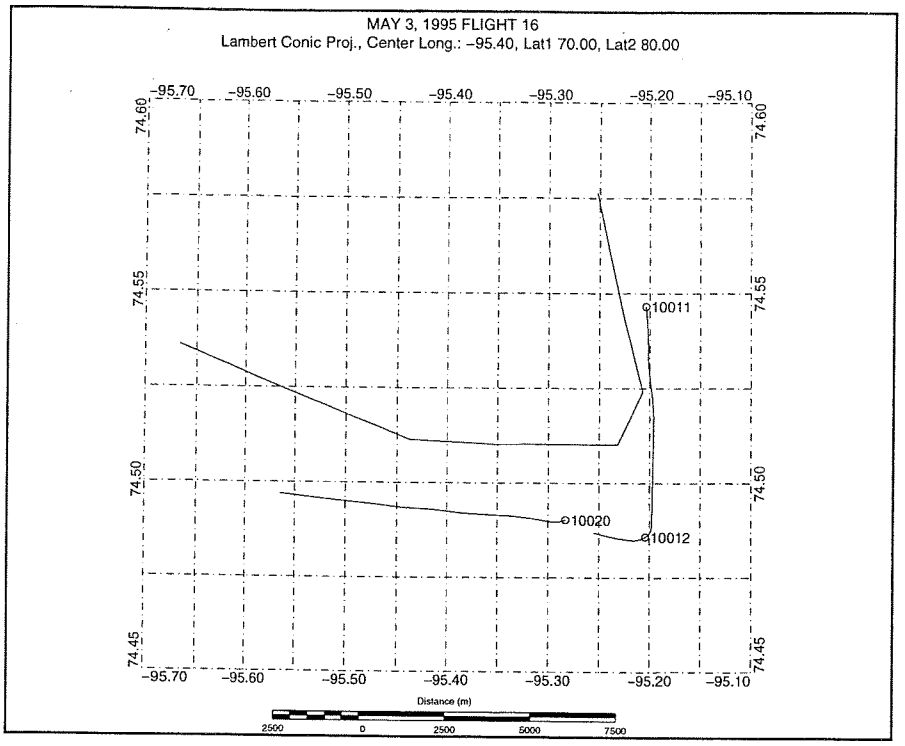

Figure 4.1.6: May 3, 1995 survey line flight path, FLT016.

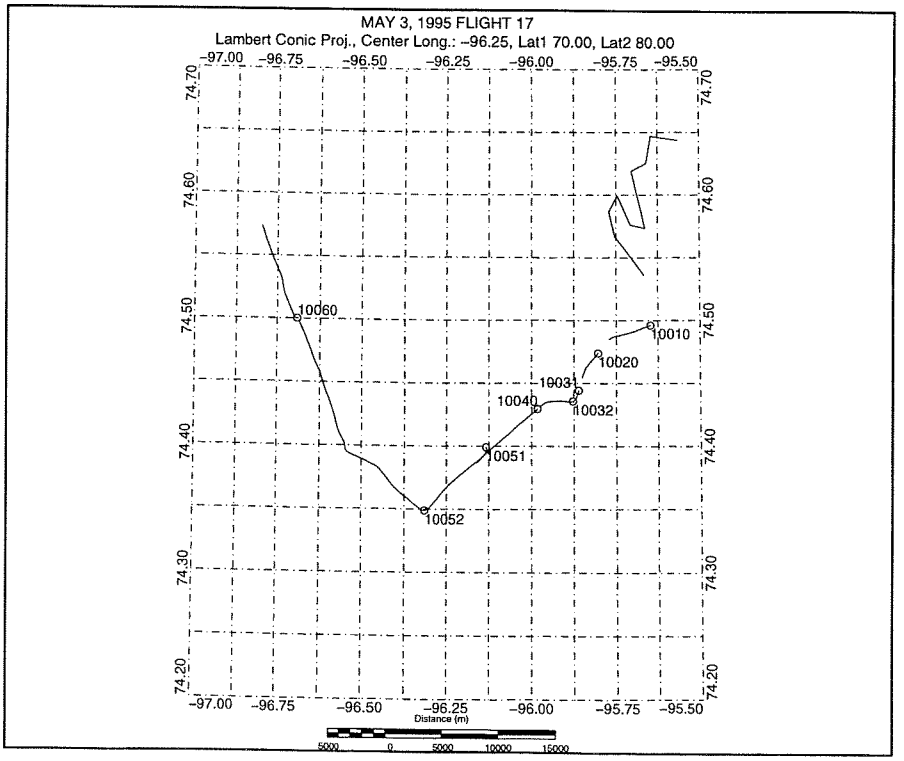

Figure 4.1.7: May 3, 1995 survey line flight path, FLT017.

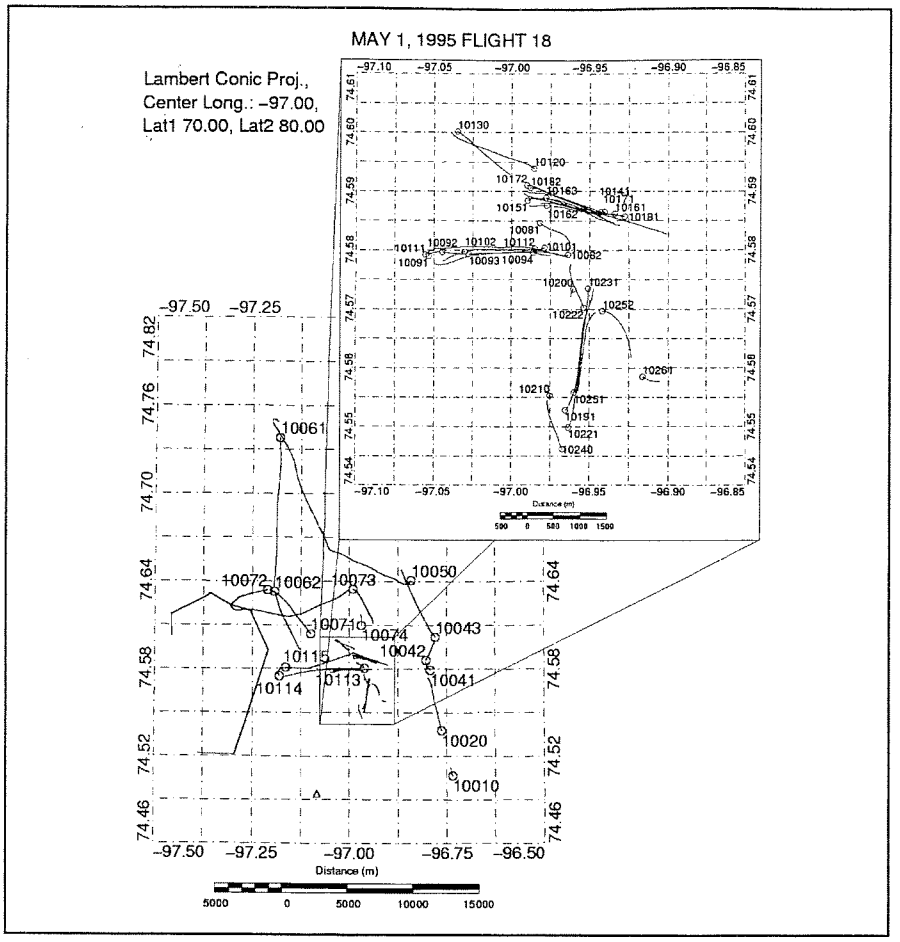

Figure 4.1.8: May 3, 1995 survey line flight path, FLT018.

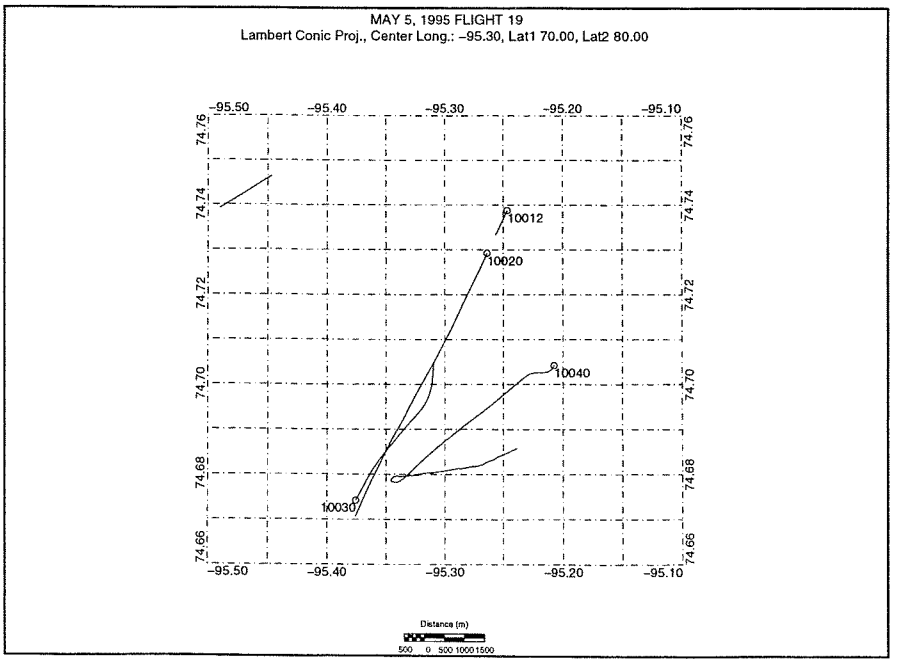

Figure 4.1.9: May 5, 1995 survey line flight path, FLT019.

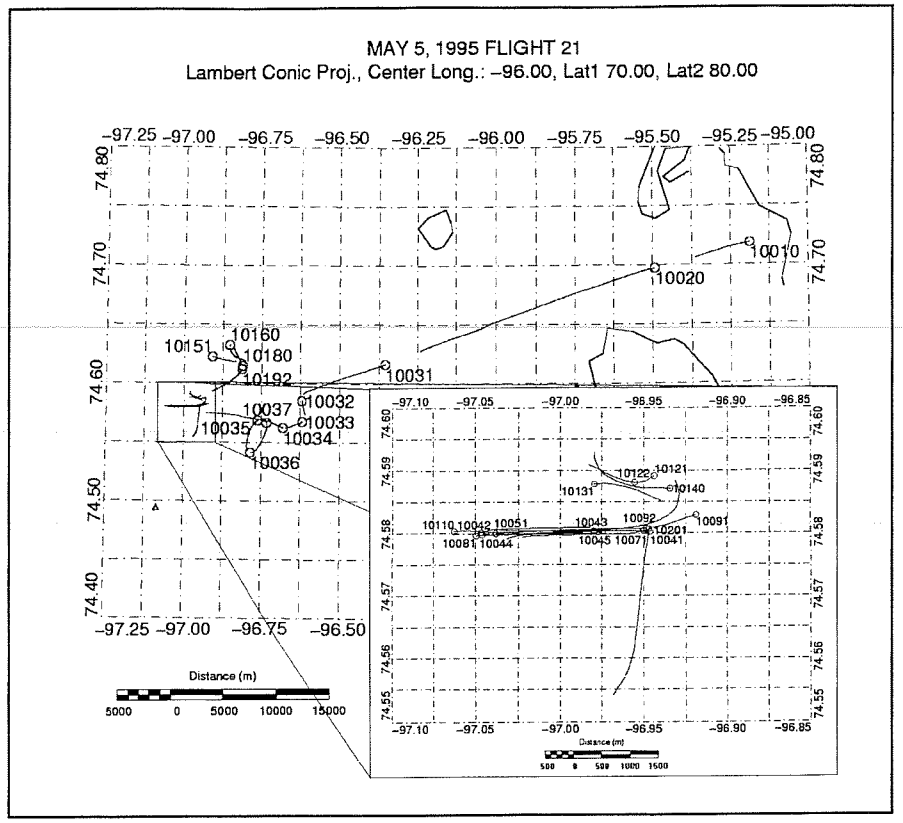

Figure 4.1.10: May 5, 1995 survey line flight path, FLT021.

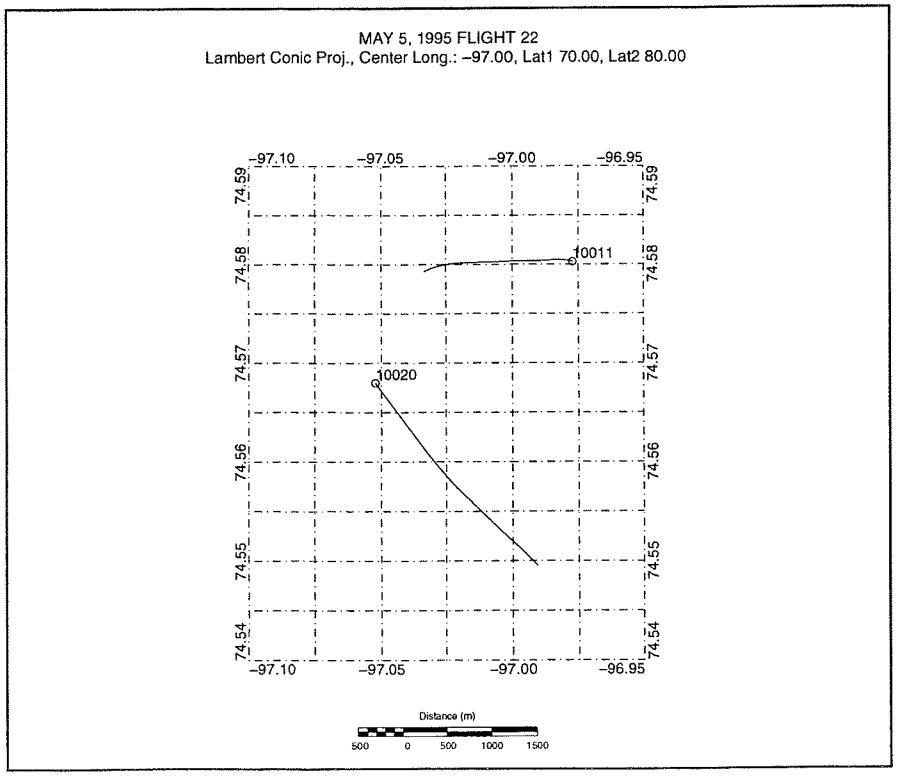

Figure 4.1.11: May 5, 1995 survey line flight path, FLT022.

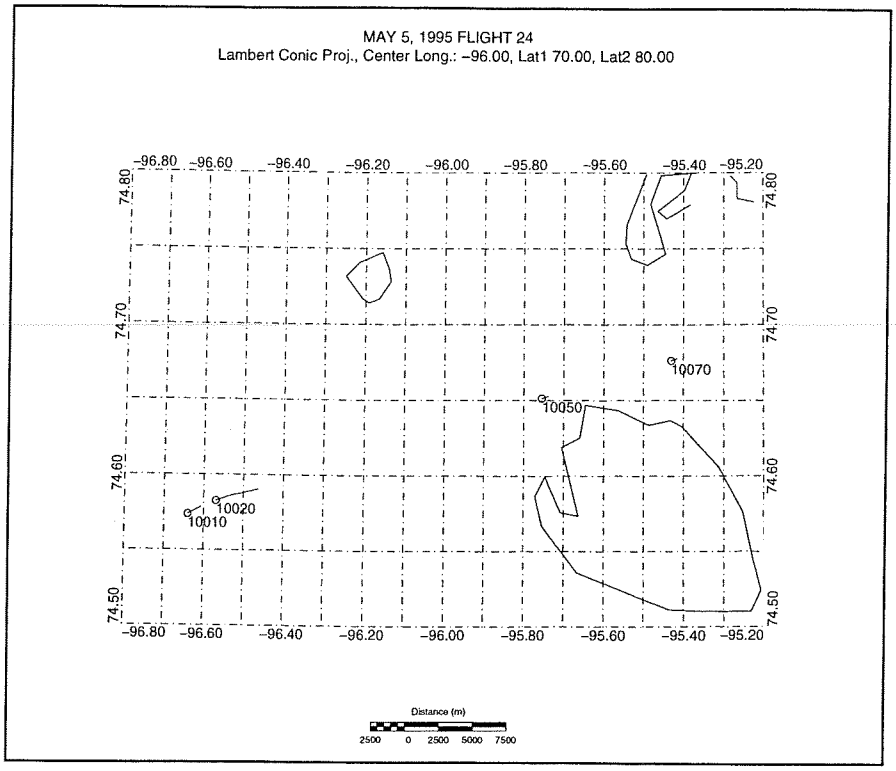

Figure 4.1.12: May 5, 1995 survey line flight path, FLT024.

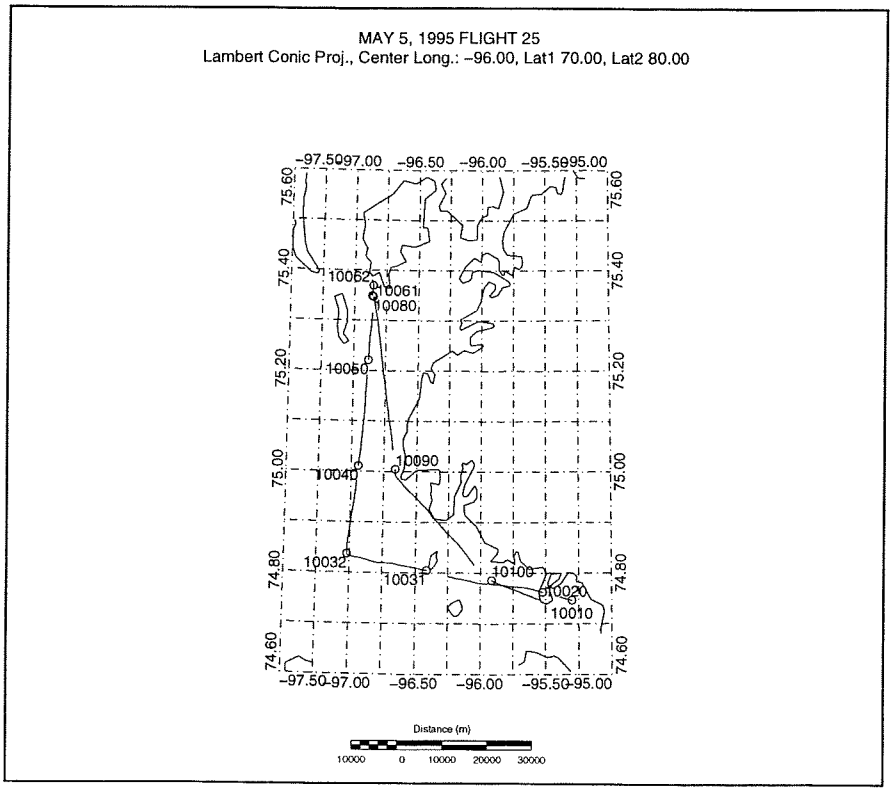

Figure 4.1.13: May 5, 1995 survey line flight path, FLT025.

4.2 Data Analysis

4.2.1 Real time processing

The snow plus ice thickness is effectively measured by estimating the bird-to-water distance, then subtracting the bird-snow distance measured with the laser altimeter, although in fact the calculations are combined as a joint inversion of the EM and laser altimeter measurements. This inversion operation is numerically intensive and is therefore performed on a secondary computer within the helicopter computer package.

The amplitude and phase of the measured EM signals depend not only on the bird's altitude above the ice surface, but also on the operating frequency, the ice conductivity and the sea water conductivity. The response can be numerically estimated for horizontally-layered ice and water layers of known thickness and conductivity (1D models). Approximations to more complex ice features such as ridges are more difficult and time-consuming to model and interpret. Using these models, the measured EM signals can be inverted to yield estimates of distances from the bird to the sea water surface on a point-by-point basis (1D model) or as a profile or grid data (2D and 3D models). The 1D inversion technique remains the standard approach for ice thickness calculations, and provides excellent accuracy over relatively smooth ice conditions.

4.2.2 Post-processing

Post-processing begins with the extraction of data from binary files to XYZ format (columnar ASCII), smoothing and resampling of GPS data, high-pass filtering of the laser altimeter, and manual editing of data. The extraction of data from binary files to XYZ files introduces repetition of GPS values since the GPS data are sampled at .5 to 1 Hz whereas the EM data are sampled at 10 Hz. Though the GPS data are quite stable, spikes in positioning do appear. Software was therefore developed to process the GPS data stream, specifically to despike, filter and resample it to match the sample rate for the ice thickness, conductivity and other data series derived from the EM data.

GPS filtering involves two procedures. The first procedure prepares the GPS data series (latitudes and longitudes) by removing anomalies (significant gaps and/or spikes in data) and adding synthesised or "contrived" data to minimise edge effects associated with filtering. The procedure also keeps track of where these anomalies occur to keep the user up to date. The second procedure utilises the information gathered by the first procedure to filter the GPS data series, using a weighted average filter. The filter is advanced in time through the prepared GPS data at the desired output sampling rate. The data points within the filter window are weighted, summed and output with a time stamp corresponding to the centre point of the filter window. The filtered GPS data stream is free of repeating values, spikes and large gaps. The associated data (ice thickness, laser altimeter, etc...) are then linearly interpolated to match the sampling rate of the filtered GPS data.

Ice and snow surface roughness can be estimated by removing the helicopter motion (altitude variations of the helicopter) from the laser altimeter (Dierking 1995). An automated three step filtering technique (referred to here as the *maximum technique)* was used to separate the different signals following the GPS filtering. The laser altimeter data are filtered via a Butterworth low pass filter (LPF) with a spatial cut off frequency of 0.01 m^{-1} and a Nyquist frequency equal to the spatial sampling rate divided by 2. The high-pass filtered laser altimeter data series (HPFL) is then obtained by subtracting the LPF laser altimeter result from the laser data.

Maxima in the HPFL are then located by numerical differentiation. The first derivative of the HPFL changes from positive to negative on each side of a peak (maximum). These changes in the slope are used to detected these peaks. The sequence of the maxima are then linearly interpolated to match the common sampling rate of the data series to give the estimated helicopter motion. The unfiltered laser altimeter is then subtracted from the estimated helicopter motion. The result is a generally positive laser profile of the surface roughness (surface topography). Small negative values in the surface roughness profile are due to the combination of the linear interpolation and the points of inflection. The laser profile of the surface roughness is referred to as the HPF laser altimeter throughout this report. A more complete description of the HPF laser data generation is given in Holladay and Moucha (1998).

One of the formats for presenting the data is the *standard plot* format (**Figure 4.2.1**). The *standard plot* includes ice thickness and HPF laser altimeter histograms along with profile plots of ice thickness, laser altimeter and HPF laser altimeter. The software that creates the *standard plots* excludes data corresponding to laser altimeter readings of 5 m or less and 35 m or greater from statistical calculations when the system is too low or high, respectively, to provide accurate measurements. In addition, data that is separated by ground speeds of 83.3 m/s or greater is also excluded. Survey lines are separated in 2 km segments. The start and end co-ordinates of each segment are displayed in the subtitle of the *standard plots*. **Figure 4.2.1** describes the *standard plots* format. Statistical tables are also created by the post-processing software (**Table 4.2.1**). These tables contain useful line and line segment information. The post-processing software also has the ability to overlay profiles onto a geo-referenced map (**Figure 4.2.2**).

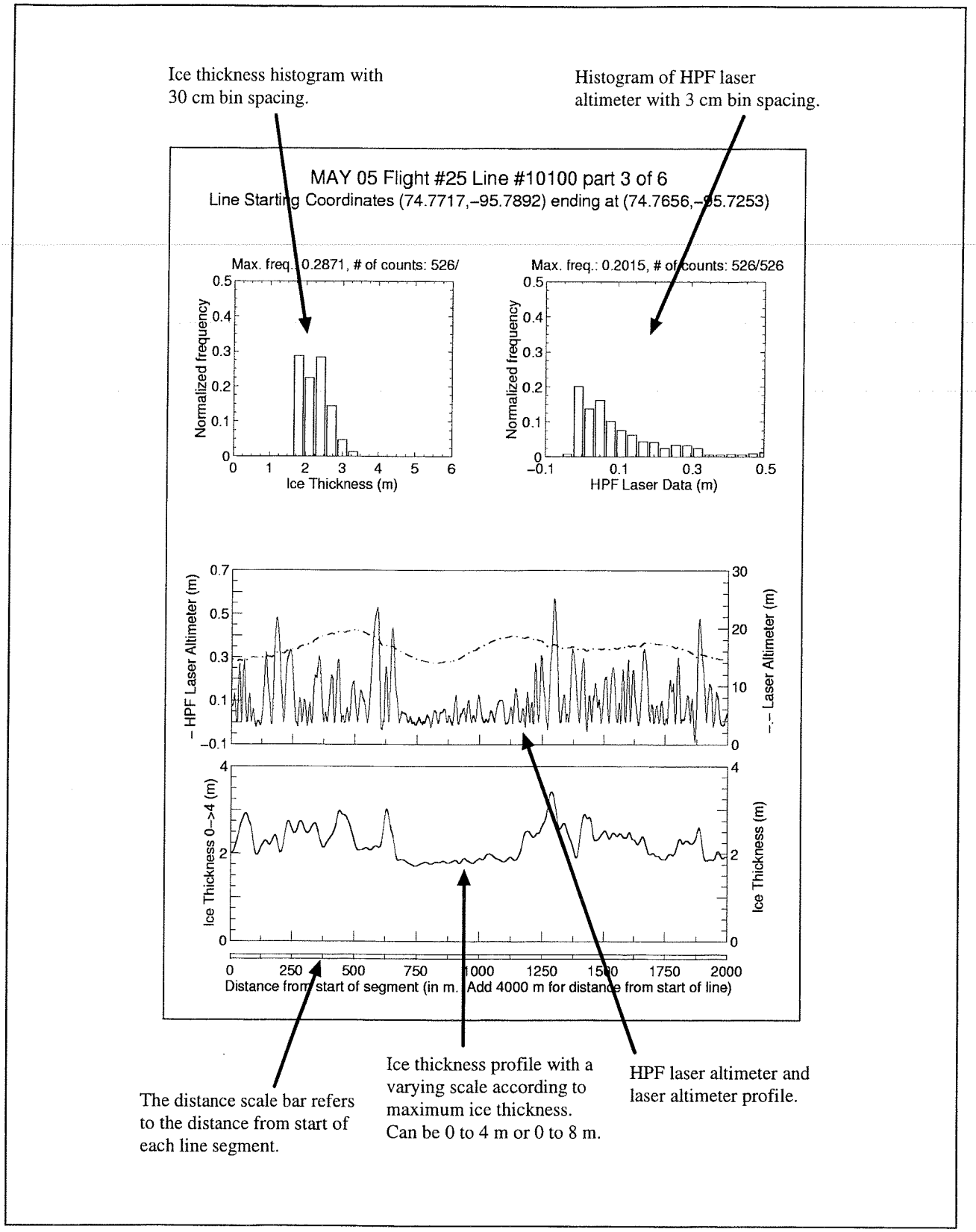

Figure 4.2.1: The *standard plot* format

Table 4.2.1: Sample profile statistics table created by the post-processing software.

Line Number	Start		End		Number of Samples ICE	Length of Line/Seg. (km)	Ice Thickness (m)		Average Spacing (s) ICE	Average Spacing (m) ICE
	Lat. (deg. N)	Long. (deg. W)	Lat. (deg. N)	Long. (deg. W)			Mean	Std.		
10010	53.7428	-56.1099	53.7280	-56.0544	222	4.012	3.53	1.385		
	53.7280	-56.0544	53.7130	-55.9993	219	3.993	3.31	1.793		
	53.7130	-55.9993	53.6972	-55.9446	225	4.011	5.00	1.937		
	53.6972	-55.9446	53.6937	-55.9324	56	0.896	6.66	1.252		
Total	53.7428	-56.1099	53.6937	-55.9324	719	12.911	4.16	1.971	0.4	17.96
10020	53.6547	-55.9566	53.6344	-55.9065	223	4.008	0.31	0.662		
	53.6344	-55.9065	53.6172	-55.8534	216	4.000	2.12	1.436		
	53.6172	-55.8534	53.6124	-55.8369	72	1.207	2.92	1.076		
Total	53.6547	-55.9566	53.6124	-55.8369	509	9.215	1.44	1.513	0.4	18.10
10030	53.6158	-55.7112	53.6060	-55.6747	160	2.646	1.69	0.658		
Total	53.6158	-55.7112	53.6060	-55.6747	160	2.646	1.69	0.658	0.4	16.54

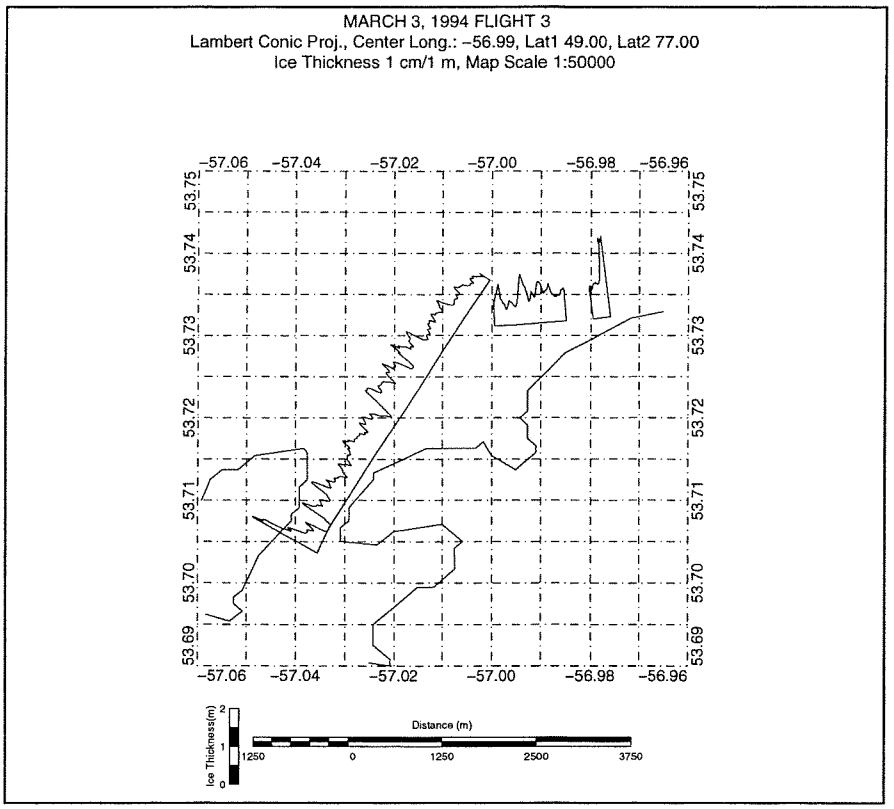

Figure 4.2.2: An ice thickness profile map (not to scale).

5. RESULTS

Errors in snow plus ice thickness observed during previous field studies which were caused by bird pitch and roll variation during bird swings can now be eliminated by real-time pitch and roll data provided by the GPS orientation sensor (Holladay *et al.* 1997). A pilot experienced with flying HEM systems can reduce the amount of bird swing considerably and improve data quality, but such improvements are now relatively small effects.

The first step in analysis of the results was the examination of profiles obtained over the surface measurement lines at Sites A – D. When this process had been completed, it was possible to categorise a given *standard plot* of data, based on ice thickness and surface roughness profiles and histograms, as being predominantly FY or MY ice. Ice conductivity estimates made by the system add a further parameter for assessment which also appears to be strongly linked to ice type, although these are not at present included on *standard plots*.

The post-processed data were categorised as FY or MY, based on surface observations at ground truth sites. Comparison to SAR images provided by M. Manore of the Canadian Center for Remote Sensing and ground truth data assisted in this process. The *standard plots* for FY ice were then compared to the *standard plots* for MY ice. Obvious differences between FY and MY ice profile characteristics appeared during this comparison. These differences are illustrated in the following sections with the use of selected histograms and profiles.

5.1 Surface Measurement Sites

As indicated in Section 2.2, four surface measurement sites were set up, two of which (Sites A and C) will be discussed here. Site A was a measurement line that crossed a margin between FY and MY ice. This margin can be clearly distinguished in the ice thickness profile, and even in the HPF laser altimeter profile (Figure 5.1.1). The snow-plus-ice thickness histogram of **Figure 5.1.1** clearly shows the two populations of ice thickness present along this line. The FY snow plus ice estimates fall into a narrow peak at 1.9 m, while the MY snow plus ice thickness estimates have a broader distribution ranging from 2 to 6+ m, with a modal peak at 3.6m. The snow plus ice profiles over the FY/MY margin were also compared to the surface data collected on April 27th and 30th (**Figure 5.1.2**). This plot includes results from multiple airborne passes over the calibration line. Note the consistency of the thickness and conductivity results from pass to pass and between flights. The short wavelength fluctuations in FY ice thickness are due to snow drifts which were profiled by the laser altimeter. **Figure 5.1.2** also includes a plot of the bulk ice conductivity estimated along the profile. The bulk ice conductivity is a function of the average salinity of sea ice and of its temperature. It is also enhanced by the presence of entrained seawater, such as occurs between blocks in a rafted zone, ridge keel or rubble field, and by the degree of consolidation and weathering of such deformed features. It was during this project that EIS first demonstrated its ability to profile bulk ice conductivity in real time over long traverses. At Site A, the contrast between FY and MY conductivity estimates is unambiguous.

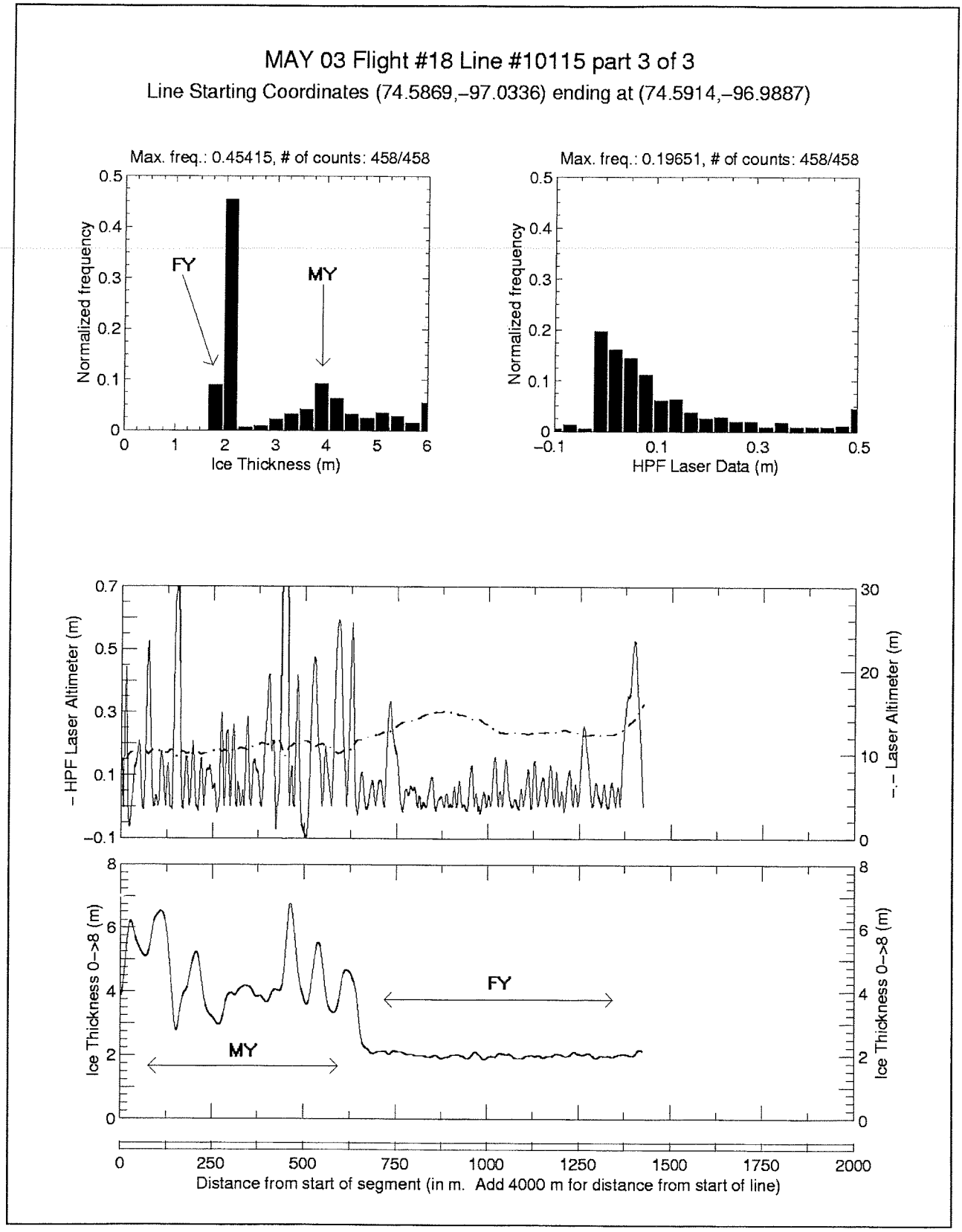

Figure 5.1.1: EIS profile from *standard plot* over Site A.

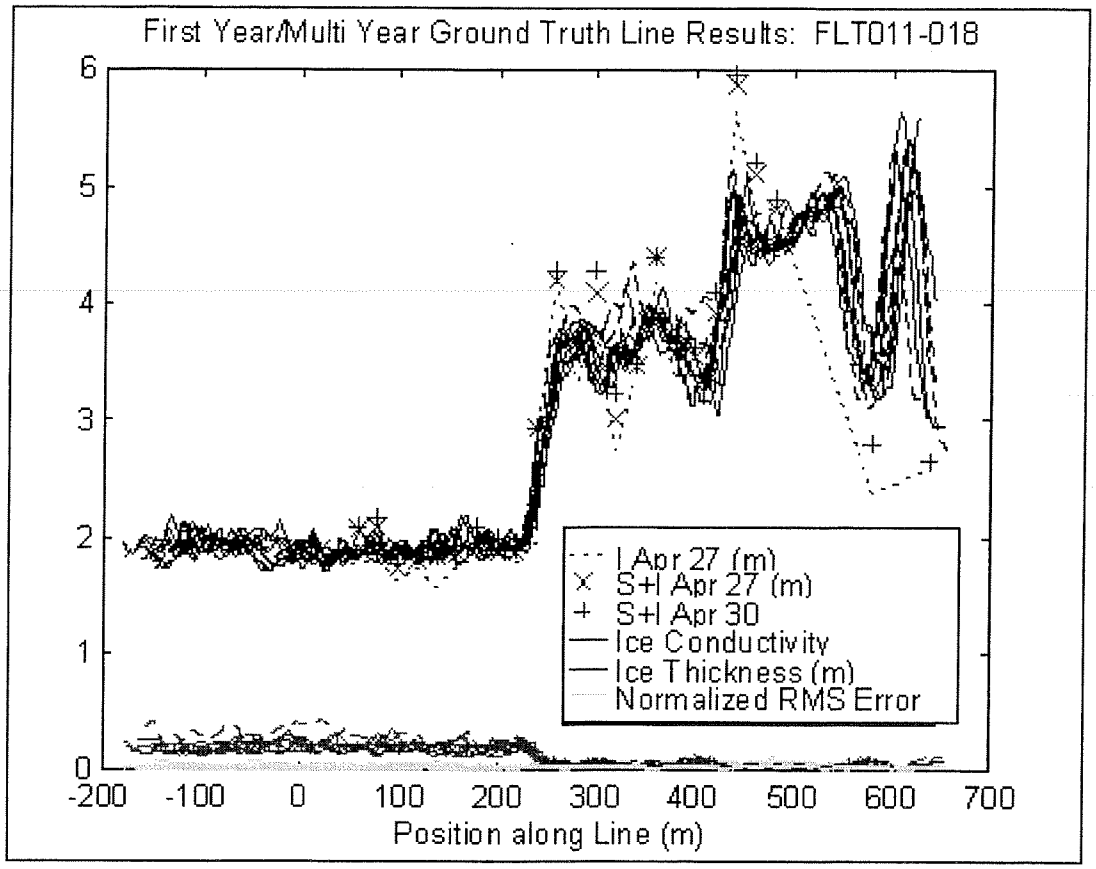

Figure 5.1.2: EIS results for multiple passes over site A and surface measurements along profile. I and S+I refer to Ice and Snow plus Ice thickness, respectively.

At Site C, the system's capability for measurement of narrow features in FY ice was tested. The small FY ridge is easily seen in the *standard plot* ice thickness profile (**Figure 5.1.3**). The mean snow plus ice thickness of 2.1 ± 0.2 m observed along the level portion of this line was consistent with ground truth observations indicating that the level ice thickness was 1.84 ± 0.12 m (2 σ) with snow cover of 0.17 ± 0.17 m in quasi-periodic drifts. The snow drifts, as profiled by the laser altimeter, are visible on the EIS profile.

No ridge keel was detected by EIS at this site, which was in agreement with the surface measurements obtained close to the ridge. It appears that this ridge formed by the up-tilting of the ice blocks without any ridging or rafting occurring, at least in the vicinity of this line. The EIS estimate for the peak ridge thickness was 3.5 ± 0.1 m, compared to 3.6 m ± 0.3 m as estimated from surface measurements of 2.3 ± 0.2 m thickness plus a freeboard change of 1.3 ± 0.1 m. The unusually high degree of accuracy seen in this ridge thickness estimate is attributed to the lack of a ridge keel in this case, which largely eliminates the averaging effect of the EM footprint and permitted direct use of the laser altimeter results for estimation of the ridge thickness.

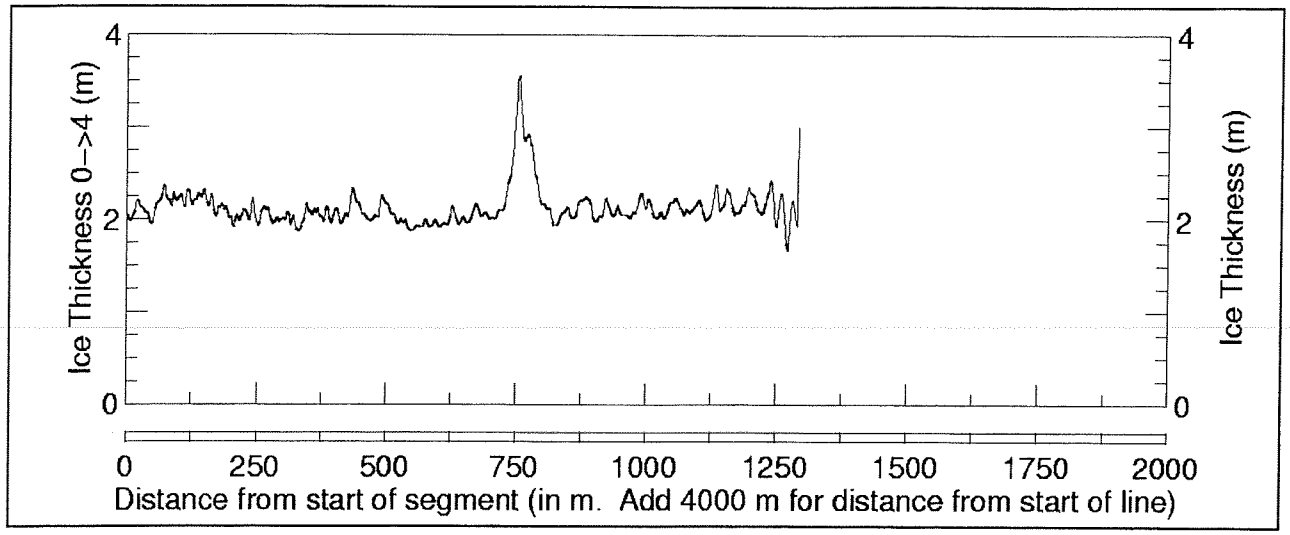

Figure 5.1.3: Standard plot ice thickness profile over the FY ridge line (Site C).

5.2 First Year Ice

Level or mildly deformed FY ice is easily classified using *standard plots*. The snow-plus-ice thickness histograms were found to have very narrow distributions, typically ranging from 1.75 m to 2.25 m with a maximum average count at 2.0 m. Usually the maximum count was extremely high in comparison to the other counts, indicating very homogeneous FY ice conditions. **Figure 5.2.1** shows the general characteristics of FY thickness histograms. The snow-plus-ice thickness profiles for FY ice were found to be smooth with minimal variance in the thickness. **Figure 5.2.2** shows the typical characteristics of thickness profiles for FY ice. Surface roughness can be most easily studied using the high-pass filtered (HPF) laser altimeter profile. As expected, the FY ice surface is smooth in comparison to a MY ice surface (**Figure 5.3.3**).

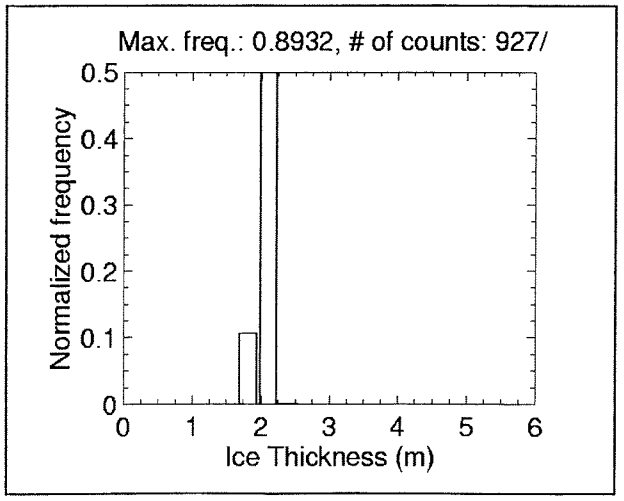

(a)

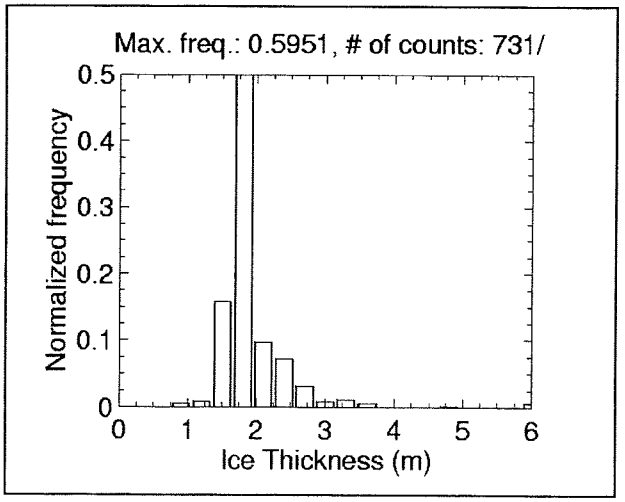

(b)

Figure 5.2.1: Typical ice thickness histogram characteristics for FY ice.

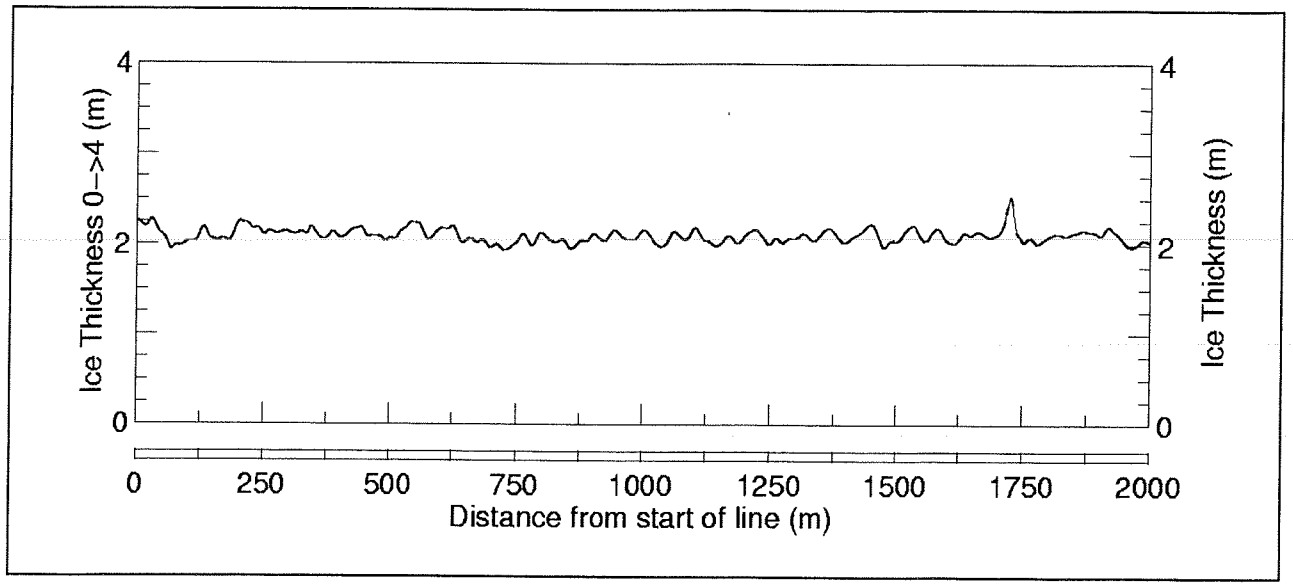

Figure 5.2.2: Typical snow plus ice thickness profile for FY ice.

5.3 Multi-year Ice

The *standard plots* for MY ice differed substantially from those obtained over FY ice. For example, the snow-plus-ice thickness histograms were found to have a wide bell-shaped or irregular distribution of thickness in contrast to the FY case, for which the distributions were narrow. The majority of the counts for the snow-plus-ice thickness histogram for MY ice were found to be above 2 m with an average maximum count at 3.5 m.

Figure 5.3.1 shows some of the characteristics pertaining to the thickness histograms of MY ice. The MY snow-plus-ice thickness profiles were found to have a high variance in thickness from 2 to 6+ m. A typical snow-plus-ice thickness profile for MY ice is shown in **Figure 5.3.2**. Surface roughness profiles of FY and MY ice are compared in **Figure 5.3.3.** The MY ice surface was found to be rough in comparison to FY ice topography as indicated by the HPF laser altimeter profile.

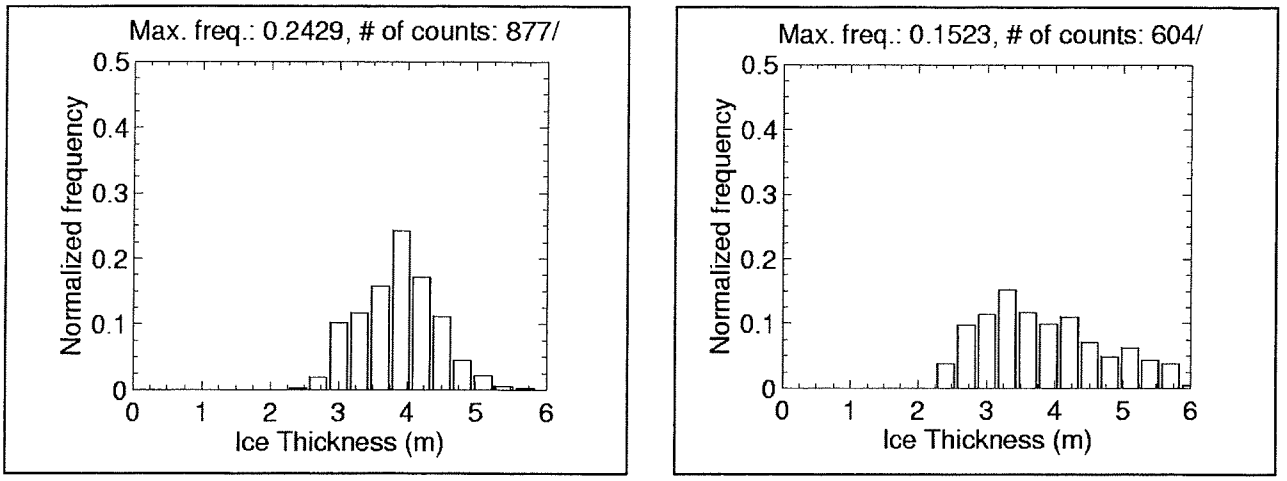

Figure 5.3.1: Typical snow plus ice thickness histogram characteristics for MY ice.

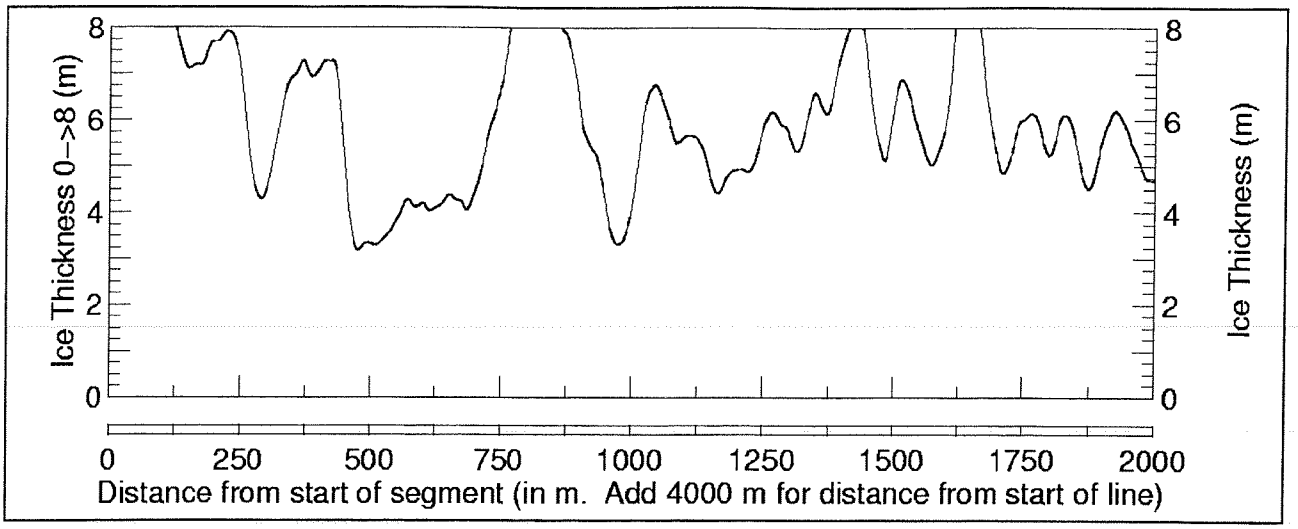

Figure 5.3.2: Typical ice thickness profile for MY ice.

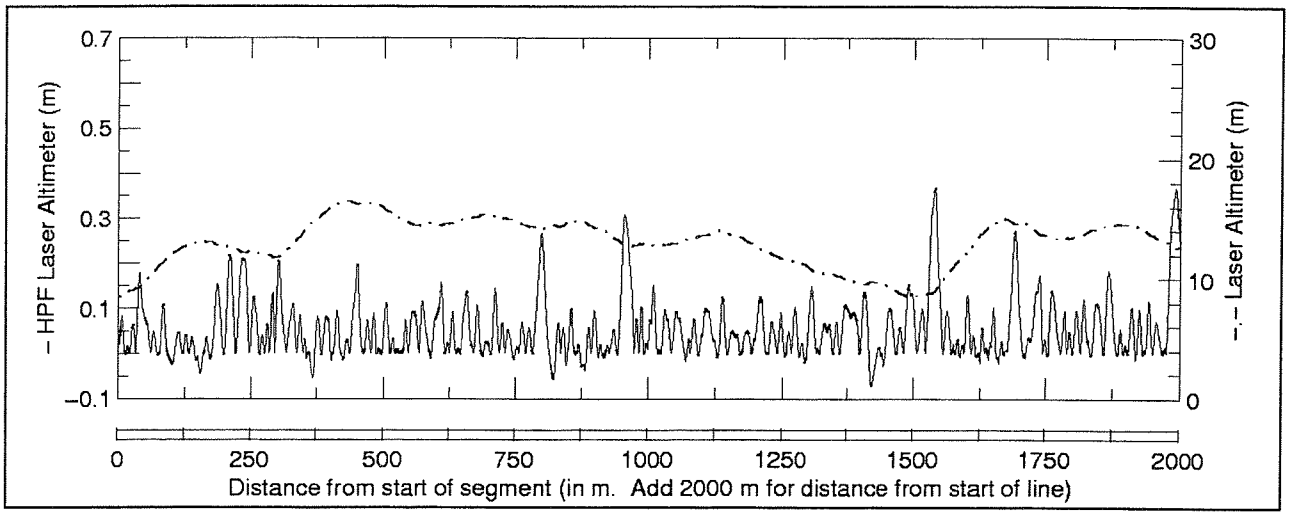

(a)

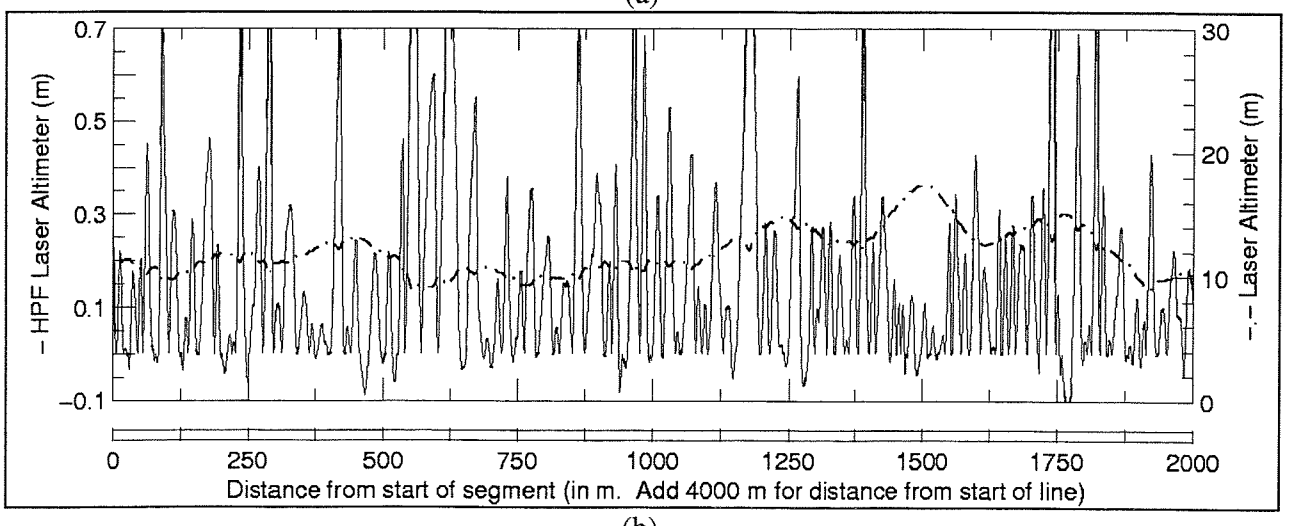

(b)

Figure 5.3.3: Typical HPF laser altimeter profiles for; (a) FY ice and (b) MY ice.

5.4 First Year Rubble

FY ice which has been extensively ridged and rubbled may exhibit thickness and surface roughness profiles which are difficult to distinguish from those due to MY ice. During FLT025, zones of FY ice crushed between large MY floes provided an example in which flat FY, a small block of MY and an area of rubbled FY ice were present (**Figure 5.4.1**).

Level FY ice may be seen at the far left side of the figure, with an EIS-estimated snow plus ice thickness of about 1.6 m. A block of MY ice (confirmed visually) with a thickness of almost 5 m separates the level FY ice from the moderately rubbled FY ice which extends off to the right side. The lower profile in the figure represents EIS-estimated ice conductivity in units of 0.1 S/m: the level FY ice has a conductivity of about 0.03 S/m, the MY block exhibits very low conductivity, on the order of 0.001 S/m, while the FY rubble shows a highly variable bulk conductivity which remains well above 0.1 S/m at almost all points along the profile.

In this example, the MY ice block is considerably thicker than the rubbled blocks. However, it is common to encounter large areas of FY rubble with thicknesses of 5 m or more in active Arctic ice regimes, such as that of the Beaufort Sea. Under these circumstances, a two-parameter ice classification scheme based on thickness and surface roughness could well break down where a three-parameter approach which includes ice conductivity estimates would prove robust.

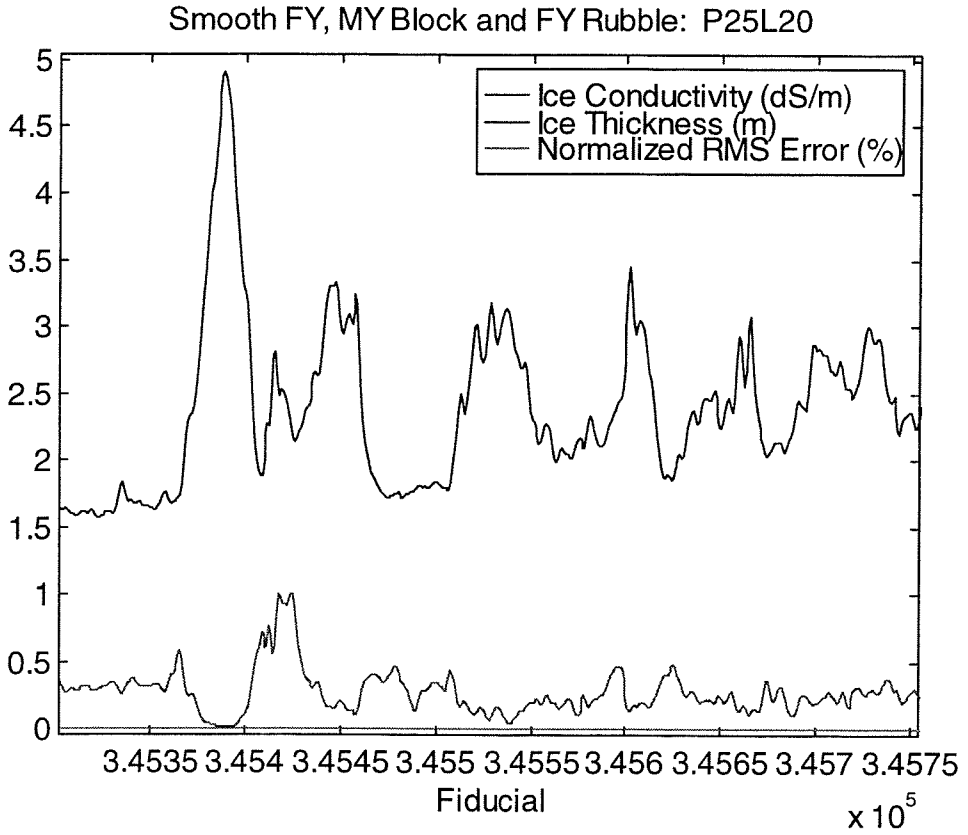

Figure 5.4.1 : Ice thickness and conductivity profiles over level FY, MY and FY rubble.

6. CONCLUSIONS

The 1995 Arctic test program, executed in conjunction with the SIMMS'95 project, provided the first extensive trials of the improved CCG airborne sea ice measurement system.

The bulk conductivity estimates for the sea ice, as estimated using the 30 kHz and 90 kHz frequencies of the system, clearly distinguish FY saline ice from MY low-salinity ice, at least under the prevailing cold Arctic conditions. FY rubbled ice is also easily distinguished from MY ice of similar thickness by its much higher conductivity.

Through the comparison of post-processed data for known first-year (FY) and multi-year (MY) sea ice profiles, it was possible to identify other data characteristics pertaining to these ice types. These characteristics were identified in three data products: the snow-plus-ice thickness histogram, the snow-plus-ice thickness profile plot, and the HPF laser altimeter profile plot.

The snow-plus-ice thickness histograms for FY ice were found to have a very narrow spike-shaped distribution. The histogram distribution ranged from 1.75 m to 2.25 m with a peak centred at 2.0 m. The MY snow-plus-ice thickness histograms were found to display a wide bell-shaped or irregular distribution, with thicknesses greater than 2 m and having an average maximum count at 3.5 m. The snow-plus-ice thickness profile plots for most FY ice were generally smooth with low variance in thickness whereas the MY profiles were generally rough with a high variance in thickness from 2 to 6+ m.

The HPF laser altimeter profile over the typically flat, undeformed ice present in the study area was smoother and contained a smaller number of sharp features than did the MY HPF laser altimeter profile. The differences between the FY and MY HPF laser altimeter profiles was significant enough to permit discrimination between undeformed FY and MY ice regimes with confidence, at least within the context of this dataset.

A classification technique based on ice thickness and surface roughness was therefore set up and applied to the dataset as a whole, using *standard plots* to identify characteristic differences in ice type. It was found to be consistent with other visual and surface measurements and with SAR imagery.

These results, taken in isolation, might suggest that it is possible to distinguish FY from MY ice solely on the basis of EIS-derived total snow plus ice thickness and surface roughness. This would be a false conclusion. Thick and extensive FY rubble fields were not profiled during this field program, and since weathered or snow-smoothed FY rubble fields would be expected to be to yield both surface roughness and thickness profiles similar to those for MY floes, it is likely that a classification scheme based on these two characteristics alone would fail to perform in circumstances where level FY, ridged and rubbled FY and MY ice regimes are all present.

EIS ice conductivity estimates provide the additional information required to distinguish FY rubble from MY ice. They can be obtained from the same EIS data used to estimate ice thickness. Further work will be required to study the relationship between EIS-measured bulk ice conductivity and the average salinity of sea ice. While this relationship is complicated by the presence of snow and by temperature effects, it should be possible to draw conclusions regarding ice strength which will prove useful for icebreaking or ice engineering applications.

ACKNOWLEDGEMENTS

It was a privilege to be included in the SIMMS'95 program, which provided logistical and tactical support for this field project. The assistance of Kevin Misurak and Dave Barber of SIMMS'95 is gratefully acknowledged. Roger Provost of the Canadian Ice Centre assisted Dr. Prinsenberg during the acquisition of the surface measurements. The skills and know-how of engineer James Lee during the field phase of this project was vital to its success. The facilities and helicopter support provided by the Polar Continental Shelf Project base at Resolute and its manager, Dave Maloley, is gratefully acknowledged, as are the contributions of pilot Bernard Maugim. Ian St. John and Louis Lalumiere provided excellent remote support during the field work. Funding for this project was provided by the Canadian Coast Guard and by the Panel on Energy Research and Development to Dr. Prinsenberg.

REFERENCES

Barber, D.G., S.P. Reddan, E.F. LeDrew, 1995. Statistical characterization of the geophysical and electrical properties of snow on landfast first year sea ice. *JGR 100(C2), 2673-2686.*

Dierking, W., 1995. Laser profiling of the ice surface topography during the Winter Weddell Gyre Study 1992. J. Geophys. Res., 100(C3), 4807-4820.

Holladay, J.S., 1995. Analysis of Electromagnetic/laser data over the Newfoundland Shelf in 1992. Can. Contract. Rep Hydrogr. Ocean Sci. 44: v + 318pp.

Holladay, J.S., R. Lo, and S.J. Prinsenberg, 1997, Bird orientation effects in quantitative airborne electromagnetic interpretation of pack ice thickness sounding, Oceans'97 Conference Proceedings, Halifax, NS.

Holladay, J.S. and R.Z. Moucha, 1998. Electromagnetic/laser ice thickness data from the Labrador Shelf, 1994, Can. Contract. Rep. Hydrogr. Ocean Sci. 49, v + 340pp.

Holladay, J.S., J.R. Rossiter and A. Kovacs, 1990. Airborne measurements of sea-ice thickness using Electromagnetic induction sounding. In: Pro. 9th Conf. of Offshore Mechanics and Arctic Eng.: 309-315.

Kovacs, A. and J.S. Holladay, 1989. Airborne Sea Ice Thickness Sounding. In: Proc. Int. Conf. on Port and Ocean Eng. under Arctic Conditions. Lulea Univ. of Techn.: 1042-1052.

Liu, G. and A. Becker, 1990. Two-dimensional mapping of sea-ice keels with airborne electromagnetics: Geophysics No.55: 239-248.

Misurak, K.M., C.P. Derksen, E.F. LeDrew and D.G. Baber, 1995. SIMMS 1995 data report, Earth Observations Laboratory Tecnical Report ISTS-EOL-SIMS-TR95-003, University of Waterloo.

Peterson, I.K., S.J. Prinsenberg and G.A. Fowler, 1995. Newfoundland Shelf sea ice program, 1993 and 1994. Can. Techn. Rep. of Hydrogr. and Ocean Sc., 167: vi + 129pp.

Peterson, I.K., S.J. Prinsenberg and J.S. Holladay and T. Carrieres, 1998. Ice thickness over Labrador shelf from EM-induction sounding: Comparison with ERS-1 SAR and airborne video data. J. Geophys. Res., Advances in Oceanography and Sea Ice Research using ERS-1 observations. In Press.

Prinsenberg, S.J., J.S. Holladay, J.R. Rossiter and L.A. Lalumiere, 1992. 1991 Beaufort Sea EM/Radar ice and snow sounding project. Can. Techn. Rep. of Hydrogr. and Ocean Sc., No 139: vi + 61pp.

Prinsenberg, S.J., J.S. Holladay and L.A. Lalumiere, 1993. 1992 Electromagnetic/Radar Ice and Snow Sounding Project over the Newfoundland Shelf in 1992. Can. Techn. Rep. of Hydrogr. and Ocean Sc., No 144: vii + 59pp.

Prinsenberg, S.J., I.K. Peterson and J.S. Holladay, 1996. Comparison of Airborne Electromagnetic Ice Thickness Data with NOAA/AVHRR and ERS-1/SAR Images. Atmosphere-Ocean 34(1): 185-205.

APPENDICES

A. Survey Line Listings

Date	Flight ID	Flight #	Line #	Remarks
				Flights 1 to 5 for test and calibration purposes.
27-Apr-95	APR27F01	1	100	Flat ice NW of Griffith Is., then MY pan
			200	Flat FY ice W of Griffith
			300	Flat FY ice W of Griffith
			400	Landing on flat FY ice
	APR27F02	2		No analog, so no log at this point
	APR27F03	3	100	BAD swings. FY flat ice, ridge after fid 5, then MY after 755930
			200	Pass 27-1 over Main GT Line near camp: E-W
			300	Pass 27-2 over Main GT Line near camp: W-E. MF20/22 start/end MY portion, MF23/24 start/end FY portion.
			400	Flat FY, MY pan, FY, ridge at 766750, FY flat
			500	Flat FY, ridge about 76530, flat, MY, flat FY
			600	Flat FY, ridges at MF32, just before MF33 (772550-772750), flat FY
	APR27F04	4	100	Flat FY, then MY
	APR27F05	5	100	MY with FY refrozen leads (old)
			200	MY with minor FY

Date	Flight ID	Flight #	Line #	Remarks
1-May-95	MAY01F06	6	100	Aborted, flight 6 to 17 had error in real-time attitude correction and displayed an intermittent calibration error (software corrected for flight 18 and later).
	MAY01F07	7	100	Times in this file are local time. Bad line--baseline inadequate
			200	Ending at WP 1.2
			300	Starting at WP1.2 Include smooth and rough FY ice, MY section, 6 ridges, terraced thicknesses near 321100, more MY, flat FY. Ends at WP1.3.
			400	Flat FY ice, approx. 2.1 m thick. Roll correction problems in large swings.
	MAY01F08	8	100	Flat FY ice. Again, roll correction problems in large swings (getting very windy).
			200	Line ends after run over ridge extending from S end of grounded MY ice on Lowther Shoal.
			300	Northbound toward camp. Crossed ridge, end of main GT line, Lowther camp, MY ice floe NW of camp.
			400	Short line, MY to FY near camp. S1 not trustworthy. Landed after this run. Note that bird touched down (hard) before landing.
	MAY01F09	9	100	Pass 1 S-N over marked FY Ridge Line #1. NB: bird was noisy after takeoff (possible effect of impact before landing?). Subsequent data therefore suspect. F1 not bad--could recover good thicknesses by reprocessing with F1 only.
			200	
			300	Very bad bird swing on line
			400	Heavy bird swing.
			500	Heavy bird swing.
			600	
			700	
			800	Main GT Line.
			900	FY, MY, FY

Date	Flight ID	Flight #	Line #	Remarks
			1000	Long S to N run over MY/FY pack
			1100	N to S run over MY/FY, then camp
			1200	E to W over Main GT Line, then go for fuel
	MAY01F10	10	100	S-N over FY Ridge line. Bad bird swing
			200	S-N over FY Ridge line. Bad bird swing. Extended to run up to vicinity of EM site.
			300	Run over EM site vicinity
			400	Run over large MY ridge in pan NW of camp
			500	Thicker FY adjacent to MY where Roger and Simon drilled test holes, NW of camp
			600	EM Site, N line, E-W
			700	EM Site, S line, W-E
			800	EM Site, S line, E-W
			900	Main GT line, E-W
	MAY01F11	11	100	Main GT line, E-W, bad swing
			200	Main GT line, W-E, bad swing
			300	Main GT line, E-W, bad swing
			400	Main GT line, W-E, small swing.
			500	Main GT line, continued across MY zone to FY zone
			600	Long run back to Resolute, leg 1
			700	Long run back to Resolute, leg 2
				NOTE: Post-processed ALL flights up to here. BL's OK, but need post-flight inversion to correct properly for roll.
3-May-95	MAY03F12-14			Bad takeoff--tow cable damaged. Aborts
	MAY03F15-17			Scratch
	MAY03F18	18	100	GOOD flight. FY ice S of S ridge, N of S ridge, N of N ridge (to WP 3.6)
			200	WP 3.6 to 3.7 to 3.8
			310	WP 3.8 to 3.9, 3.9 to 3.10 part 1
			320	WP 3.8 to 3.9, 3.9 to 3.10 part 2
			410	Due south from 3.10 , part 1
			420	Due south from 3.10 , part 2
			430	Due south from 3.10 , part 3
			500	Searching for v. thick ice (from SAR)
			600	Searching for v. thick ice (from SAR)
			700	Main GT Line, EW

Date	Flight ID	Flight #	Line #	Remarks
			800	Main GT Line, WE
			900	Main GT Line, EW
			1000	Main GT Line, WE
			1100	Main GT Line, EW, run out to FY ice on far side of floe
			1200	N on FY ice
			1300	E across MY/FY floe, ending N of Lowther camp
			1400	W across FY, MY ice, big ridge NW of camp
			1500	E across MY ice, big ridge NW of camp, FY
			1600	WE across EM site S line
			1700	EW across EM site S line
			1800	WE across EM site S line
			1900	WE across EM site N line
			2000	WE across EM site N line
			2200	EW across EM site N line
			2300	WE across EM site N line
			2400	NS along FY Ridge line
			2500	SN along FY Ridge line
			2600	NS along FY Ridge line
			2700	SN along FY Ridge line
5-May-95	MAY05F19	19	100	Test flight after Tx repairs. Resolute Bay, FY/MY/FY, southbound.
			200	Resolute Bay, FY/MY/FY, Northbound
			300	Southbound, note fissure.
			400	final pass of file
	MAY05F20	20	100	Southbound, new file
			200	NE, includes 2D acquisition pass
	MAY05F21	21	100	Ferry from Resolute: FY, ridge, thickened ice, MY, fair bg
			200	MY, FY, fair bg
			300	MY, then across main pressure ridge (back and forth
			400	EW Main GT Line, JSH operating fid button, 8-12 m
				WE Main GT Line, JSH operating fid button, 8-12 m
			500	EW Main GT Line, JL operating fid button, 10-15 m
			600	WE Main GT Line, JL operating fid button, 10-15

Date	Flight ID	Flight #	Line #	Remarks
			700	EW Main GT Line, JL operating fid button, 20-25 m (MFIDs not good)
			800	WE Main GT Line, JL operating fid button, 20-25 m
			900	EW Main GT Line, JL operating fid button, 25 m (MFIDs not good)
			1000	WE Main GT Line, JL operating fid button, 15 m
			1100	EW Main GT Line, JL, 25m (fair BG)
			1200	WE Main GT Line, JL , 25-30 m (too high for BG quality)
			1300	EW EM site N line
			1400	EW EM site N line
			1500	MY block in FY N of camp
			1600	MY and FY N of camp (too high)
			1700	MY and FY N of camp (where drilling took place in afternoon)
			1800	MY and FY N of camp (where drilling took place in afternoon)
			1900	FY heading W
			2000	FY Ridge Site, N S
			2100	FY Ridge Site, SN
			2200	FY Ridge Site, N S
			2300	FY Ridge Site, SN
			2400	FY Ridge Site, N S
			2500	Continuation from FY ridge site to south, past southern ridge
			2600	Run up to "Y" airstrip, land after BG
	MAY05F22	22	100	EW Main GT Line, poor BG, 13 m
			200	WE Main GT Line, 13 m, no fids
	MAY05F24	24	100	EW Main GT Line, 13 m, no fids, poor BG, remainder of file a write-off (weather)
6-May-95	MAY06F25	25	100	R. Provost operating, JSH instructing. Training run to Little Cornwallis Island along shipping route. Leg 1. BG OK
			200	Huge MY floe with minor FY near N end. BG OK
			300	More MY, minor FY rubble. BG poor
			400	FY, some MY. T1 OK, but S1 low due to poor BG. This effect was reduced during postproc.
			500	Bay at Little Cornwallis Island
			600	Southbound leg
			700	Southbound, mostly MY. Bad BG at end

Date	Flight ID	Flight #	Line #	Remarks
			800	Southbound, mostly MY. Good BG at end
			900	Mixed MY and FY rubble. End logging
	MAY06F26	26	100	FY, then MY. 2D ridge acquisition.
	MAY06F27	27		Ice Recco, solo by R. Provost. Windy air and flat light conditions led to large altitude variations, reduced data quality. No analog record.

B. Flight Line Ice Type Summary

It is important to note that the line numbers that do not end with 0 are the result of manual editing. These lines were split into numerous parts. For example, the line 10010 on May 1st, Flight 9 was split into three parts, therefore the line numbers 10011, 10012, and 10013. Also note, that lines shorter than 400 meters were omitted from the table (ex. 10011 of Flight 9 was shorter than 400 m.

Date	Flight #	First-Year Ice				Multi-Year Ice			
		Line #	Length (km)	Ave. Ice Thickness (m)	Subtotal Length (km)	Line #	Length (km)	Ave. Ice Thickness (m)	Subtotal Length (km)
1-May	8	10010	6.265	2.05					
		10020	5.276	2.14					
						10030	5.800	2.78	
		10040	2.771	2.44					
					14.312				5.800
	9	10012	1.837	2.15					
		10013	0.711	2.26					
		10020	1.351	2.46					
		10031	1.839	1.84					
		10032	0.842	2.04					
		10041	1.671	4.56					
		10042	1.075	3.52					
		10051	1.680	3.93					
		10052	2.284	2.04					
		10062	2.482	2.15					
		10063	1.059	2.25					
		10081	0.850	7.22					
		10092	2.403	2.67					
		10100	2.816	2.25					
		10121	0.427	3.75					
		10122	1.857	2.08					
		10123	1.199	2.86					
		10131	0.497	2.23					
						10132	5.546	3.40	
		10141	2.226	2.60					
						10142	9.292	4.12	
						10150	12.716	4.09	
						10160	4.689	3.11	
		10173	0.468	2.04					
		10180	1.225	2.81					

					30.799				32.243
	10	10010	1.437	1.98					
		10021	1.634	1.99					
		10022	3.122	2.04					
		10030	0.861	2.21					
						10040	0.530	2.67	
						10060	2.466	3.79	
						10070	3.045	3.30	
		10092	1.139	2.00					
		10111	1.323	1.90					
		10112	1.028	1.91					
		10113	1.217	1.91					
		10121	0.988	1.95					
					12.749				6.041
	11	10010	2.903	2.99					
						10022	1.802	3.17	
						10032	0.533	3.23	
						10034	1.233	3.62	
						10041	1.547	3.30	
						10042	3.955	3.68	
						10050	4.461	2.82	
						10070	28.542	3.49	
		10080	21.366	1.45					
					24.269				42.073
3-May	16	10011	6.843	1.84					
		10012	1.564	2.30					
		10020	8.416	2.39					
					16.823				
	17	10010	3.857	1.56					
		10020	2.645	1.27					
		10031	1.099	1.19					
		10032	3.050	1.39					
		10040	7.161	1.58					
		10051	7.988	1.84					
		10052	20.96	1.77					
		10060	8.862	1.93					
					55.622				
	18	10020	4.169	2.12					
		10041	0.732	2.16					
		10042	1.840	2.09					
		10043	5.785	2.80					
						10050	18.248	3.49	
		10061	11.307	2.49					

		10062	4.832	2.19					
		10071	4.596	2.25					
		10072	12.919	2.70					
						10073	3.130	3.79	
						10074	0.856	4.83	
		10081	0.703	2.20					
		10082	2.583	2.98					
						10092	0.397	3.86	
		10093	1.152	2.86					
		10094	0.410	2.01					
		10101	1.373	2.97					
						10111	2.104	3.10	
		10112	0.723	2.02					
						10113	6.410	3.39	
		10114	0.930	2.21					
						10115	5.425	3.50	
						10120	1.729	3.32	
						10130	1.305	3.34	
		10141	1.185	2.01					
		10151	1.999	2.20					
		10161	1.690	2.24					
		10163	1.406	2.06					
		10171	1.595	2.07					
		10172	1.998	2.03					
		10181	1.903	2.11					
		10182	2.736	2.05					
		10191	2.431	2.12					
		10221	2.164	2.09					
		10222	0.886	2.11					
		10231	1.949	2.16					
		10240	0.968	2.15					
		10251	1.645	2.10					
		10252	1.124	2.21					
					79.733				39.604
5-May	19	10012	0.665	2.55					
		10020	7.315	3.22					
						10030	3.999	4.87	
						10040	8.448	3.47	
					7.980				12.447
	20					10011	5.655	3.74	
		10021	1.863	2.17					
					1.863				5.655
	21	10010	5.397	2.48					

						10020	23.413	3.09	
		10031	8.179	2.78					
		10032	1.267	2.09					
		10033	1.728	1.89					
		10034	2.236	2.17					
		10035	2.925	2.18					
		10036	3.346	1.99					
		10037	5.997	2.11					
		10041	2.715	2.85					
						10042	1.920	3.01	
						10043	1.534	3.17	
						10044	1.722	3.20	
						10045	1.676	3.22	
						10051	1.541	3.41	
		10071	2.148	2.99					
						10081	1.875	3.27	
		10091	0.792	2.30					
		10092	2.260	2.72					
		10110	4.586	2.68					
		10121	0.373	2.06					
		10122	0.889	2.13					
		10131	1.234	2.12					
		10140	1.650	2.12					
		10151	2.228	2.37					
		10160	2.419	2.87					
		10180	2.560	3.17					
		10192	3.500	2.16					
		10201	3.305	2.10					
					61.734				33.681
	22					10011	1.740	2.98	
		10020	2.757	2.91					
					2.757				1.740
	24	10010	1.126	1.77					
		10020	3.260	2.55					
		10050	0.523	2.61					
		10070	0.461	2.34					
					5.370				
	25	10010	7.085	2.09					
						10020	21.613	3.21	
						10031	17.919	4.55	
						10032	16.281	4.86	
						10040	20.099	3.75	
		10050	10.520	2.37					

		10061	2.127	3.05					
		10062	1.298	2.59					
		10080	34.187	2.95					
		10090	28.110	2.69					
		10100	11.855	2.48					
					95.182				75.912
Total		125		2.13	409.193	39		3.51	255.196

C. Surface Measurements

The following surface measurement datasets were acquired by S. Prinsenberg, with assistance from Roger Provost.

Station A: FY-MY line, near base camp. 74° 34.86N
97° 00.00W

Sites (bags) separated by 20m, April 27.
Snow depths before storm of April 29.
Two lead-up bags at 50m and 100m east of site (bag) #1.

# of bags	site #	ice (cm)	free board (cm)	snow depth (cm)	mean snow (cm)	snow+ice (cm) 28 April	30*
4	01	172	10	22/23/06/08 14/15/17/14	15	187	190
1	02	177	13	04/04/04/05 14/18/18/09	10	187	192
1	03	179	14	03/04/04/06 06/06/03/03	4	183	190
1	04	176	14	22/24/26/32 42/46/36/28	32	208	210
1	05	181	13	20/21/18/23 21/21/20/23	21	209	217
1	06	162	11	10/11/14/08 06/06/06/08	11	173	177
1	07	174	13	06/05/06/05 06/05/05/07	6	180	183
1	08	155	8	45/28/20/25 28/23/28/30	28	183	184
1	09	176	12	06/06/08/10 08/08/11/15	9	185	194
1	10	181	14	15/24/20/17 12/15/24/16	18	199	209
1	11	185	15	01/01/02/03 01/01/03/05	2	187	200
1	12	178	15	06/07/18/12 08/07/11/08	10	188	190
0**	--	161	-3	31/34/31/32 35/38/38/35	34	195	---
2	13	295	110	00/00/00/00 00/00/00/00	0	295	295

* April 30 snow depths are the average of 3 depths near the bag.
** Location: 5m east of ridge in the FY ice.

Station A: FY-MY line, near base camp. Site #25 74 34.82°N 97 01.01°W

April 28, sites (bags) at 20m spacing.
2 lead up bags at 50m and 100m west of site (bag) #25.

# of bags	site #	ice (cm)	free board (cm)	snow depths (cm) April 28	snow depths (cm) April 30	mean snow depths/ snow+ice(cm) April 28	mean snow depths/ snow+ice(cm) April 30*
2	13	295	110	00/00/00/00 00/00/00/00	00/00/00/00 00/00/00/00	00/295	00/295
0**	--	228	-2	42/38/32/44 38/42/45/44	--/--/--/-- --/--/--/--	41/269	--/---
1	14	420	16	00/00/00/00 00/00/00/00	10/21/13/03 09/00/00/02	00/420	06/426
1	15	332	30	42/45/42/50 30/35/40/42	26/33/39/44 44/35/44/27	40/372	38/370
1	16	383	5	28/32/26/28 22/30/30/22	44/50/48/43 49/46/42/46	26/409	46/429
1	17	274	6	24/30/26/32 33/18/24/21	48/53/50/50 50/46/46/47	26/300	49/323
1	18	343	45	00/04/00/04 00/04/00/04	10/09/06/07 01/03/03/05	02/345	06/349
1	19	419	5	19/20/21/18 22/24/26/24	07/29/27/29 39/04/09/29	22/441	22/441
1	20	334	30	24/28/28/24 20/24/28/26	34/32/32/34 30/34/32/33	25/359	33/367
1	21	355	52	00/00/00/00 00/00/00/00	11/04/02/05 16/11/04/12	00/355	08/363
1	22	372	5	29/19/20/24 20/17/16/20	39/43/38/40 40/30/35/35	21/393	38/410
1	23	565	45	20/22/21/20 24/20/22/20	28/26/30/32 34/26/27/31	21/586	29/594
1 (rafted)	24	475 346	8	32/34/39/41 34/39/34/39	45/32/47/50 48/49/48/42	37/512	46/521
5	25	481	68	00/00/00/00 00/00/00/00	05/00/27/18 05/05/06/05	00/481	09/490

* April 30 snow depths are the average of 3 depths near the bag.
** Location: 5m west of ridge in the MY ice.

Stn A: Notes on topographic features along the calibration line in the MY section.

Site #14 on a gentle down slope of a hummock towards site #15.
Top of hummock towards site#13 is 20cm above hole.

Snow bump at 2m from 15 to 16, height 20cm above level at #15.

#16 low melt pond. Ice bump to #15 and to north (45cm).

From 17 to 18 level snow area, one ice bump of 15cm.
#18 on a gentle down slope of a hummock towards 19.
Hole 10cm below top hummock towards 17.

#19, ice bump at 3m and 10m towards #18 about 60cm above level at #19 (3m wide).
Hummock parallel to line 80-120cm high at 6-8m from line.

30cm hummock above snow level at #20 at 1m to north of line.
20cm hummock 2-3m south of #20.
From 20 to 21 same height as at #20.

At #21 level lower by 15cm relative to #20. #21 hummock base.
#22: Small (2mx2m) high hummock (60cm) 1m north and 1m to #23.

Very level from #22 to #23 (level of #23).
Hummocks to south generally 40cm high.
Large (1m) hummock running perpendicular to line and to north,
(4mx1m on top) at 5-10m from #23.

#24, rafting with about 30cm of water between ice sheets.
Large hummock (100cm) south (5m) of line at 2m to #25.
#25, ridge N to S, 4m wide, 25cm high at 1 to 5m from #25.

Station A: FY-MY line.

Extra MY ice depths from FY-MY line.
Melt ponds: April 29 (#26 and #27) and May 1 (#28 and #29)

location	site #	ice (cm)	free board (cm)	snow depths (cm)	mean snow depths/ snow+ice (cm)
100m west of #25	26	237	01	35/40/45/50 50/48/42/32	44/281
160m west of #25	27	260	09	00/00/00/05 05/05/10/10	05/265
10m south of #22	28	214	08	20	20/234
12m south of #23/24	29	308	-3	40	40/348

#28 and 29 were large 10m wide melt ponds south of the line.

Station A: FY-MY line, snow depths at ridge.

Snow depths at FY-MY ridge (Friday April 28).
Snow depths relative to surface ice levels at 5m from ridge taken at 1m intervals from centre of ridge.

m	FY ice	MY ice
1	--	--
2	80	90
3	55	65
4	43	45
5	34	41
6	28	44
7	23	50
8	14	60
9	13	80
10	13	90

Station A: FY-MY line.

Snow depths at 5m spacing along ridge line.
(Evening of April 30, after the snow storm).

Site #	Snow (cm)	mean snow (cm)	Site #	Snow (cm)	mean snow (cm)
	15				
1	24	17	7	15	9
	15			10	
	45			20	
	37			32	
2	5	15	8	30	29
	2			25	
	16			7	
	7			15	
3	11	11	9	20	18
	16			20	
	29			17	
	39			15	
4	38	34	10	30	28
	22			35	
	27			26	
	27			23	
5	36	36	11	22	15
	36			2	
	16			16	
	15			6	
6	19	15	12	14	12
	10			16	
	2			20	
	2			31	
7	15	9			

Station A: Ice Salinities at FY-MY line sites

1. MY floe at site #23.

(Thursday, April 27)

#	Depth (cm)	Salinity (ppt)
3	0-5	0
2	10-15	0
1	20-25	0
5	30-35	0
4	45-50	0

2. MY floe melt pond, 10m S of site #22.

(Tuesday, May 2)

#	Depth (cm)	Salinity (ppt)
10	05-10	0
5	20-25	1

3. FY ice at site #8

(Thursday, April 27)

#	Depth (cm)	Salinity (ppt)
10	snow	0
11	basal	15
6	0-5	10
7	10-15	6
9	20-25	9
8	35-40	8
7	50-55	10

10cm of snow, 3cm basal layer

4. FY ice at site # 1

(Friday, April 28)

#	Depth (cm)	Salinity (ppt)
3	snow	0
4	basal	9
8	0-5	11
7	10-15	8
10	20-25	8
6	30-35	7
9	40-45	7
5	50-55	7

20cm of snow, 3cm of basal layer

Station B: EM Camp, east of Base Camp

1.2km East of base camp, sites 1, 3, 5, 6, 8 and 10 done on May 1.
Two E-W 100m parallel lines 50m apart.
#1 E corner and #5 W corner of southern line.
#6 E corner and #10 W corner of northern line.
Sites (bags) 2, 4, 7, 9 and snow line done May 2.
Note: bags location are approximately 25m apart not 20m.

# of bags	site #	ice (cm)	free board (cm)	snow depth (cm)	mean snow depths/ snow+ice thickness (cm)
1	1	167	8	28/28/30/28 27/30/29/28	29/196
1	2	173	9	26/24/22/23 25/17/19/22	22/195
1	3	179	11	24/24/29/26 24/29/29/26	26/205
1	4	175	7	33/32/32/25 26/27/29/29	29/204
2	5	175	12	08/09/08/10 10/09/10/12	09/184
4	6	165	8	16/17/18/18 19/18/19/17	18/183
1	7	172	7	24/27/23/25 19/28/32/32	27/199
1	8	174	11	08/09/12/19 19/14/08/08	12/186
1	9	171	13	15/16/14/11 08/11/14/17	13/184
3	10	177	10	05/05/10/15 15/22/27/18	16/193
flag	11	179	10	21/21/18/16 15/16/18/15	18/197

Site (bag) #11 was the turning back flag to main base camp,
50m south of bag #2 on southern line.

Station B: EM Camp, snow depths of May 2.

Snow depths at approximately 5m intervals.
Sites are locations of ice thickness observations.

site #	snow (cm)	site #	snow (cm)
1	25	6	27
	21		30
	9		24
	10		29
	17		29
2	18	7	33
	26		24
	40		23
	24		18
	24		19
3	23	8	11
	19		16
	16		21
	23		8
	16		11
4	25	9	17
	19		17
	45		20
	25		31
	13		10
5	29	10	19

Station B: EM Camp, snow and salinities of May 2.

Location: site #7.
26cm of snow and 3cm basal layer.

#	Depth (cm)	Salinity (ppt)
4	basal	15
16	0-5	16
1	10-15	9
20	20-25	9
--	30-35	9
9	55-60	7

Station C: Ridge line (first location). 74 34.00°N
96 58.55°W

Saturday April 29, morning of storm
Ridge here 12m wide, 2m flat top surface.
55cm of snow, 17cm of free and 140cm of ice (no keel).
Moved farther east along ridge after the storm.

Station C: Ridge line (final location). 74 33.82°N
96 57.26°W

South of ridge, Monday May 1
3 bags on top of ridge in a straight line (site #11).
Square (4 bags) at south end site #1.
Two lead up bags at 50m and 100m from end of line.

# of bags	site #	ice (cm)	free board (cm)	snow depth (cm)	mean snow (cm)	snow +ice (cm)
4	1	190	11	28/28/29/22 24/27/27/17	26	216
1	2	183	10	25/25/26/21 33/32/25/25	26	209
1	3	179	9	22/22/27/32 25/33/43/25	28	207
1	4	184	10	15/15/14/14 15/15/14/10	14	198
1	5	188	10	15/22/16/18 34/34/22/28	23	211
1	6	187	15	07/07/11/11 09/06/05/05	07	194
1	7	175	10	10/10/26/25 18/14/08/14	15	190
1	8	190	15	03/03/04/04 06/05/04/06	04	194
1	9	176	15	12/10/11/06 06/17/24/20	13	189
1	10	174	12	07/10/22/23 20/21/16/17	17	191
-	--*	167	-13	20/23/26/25 21/21/22/23	23	190

* Location 10.75 or 5m south of ridge centre, site #11.

Station C: Ridge line (site #11: top of ridge). 74 33.82°N
Wednesday, May 3. 96 57.26°W

Ridge top marked by 3 bags.
Blocks of ridge 12-15cm thick.

depth (cm)	freeboard (cm)	location
230	145	ridge centre at line
195	148	3m east of line
210	141	3m west of line

Station C: Ridge line, Wednesday May 3.

Snow drift depths at distances from centre of ridge.
(note: more snow north of the ridge)

North of ridge		South of ridge	
distance (m)	depths (cm)	distance (m)	depths (cm)
2	180	2	80
3	80	3	30
4	72	5	23
5	71		
6	60		
10	50		
20	20		

Station C: Ridge line Ice Salinities.

1. Ridge line at site #11.5. 10cm of snow
10m north of ridge, Wednesday May 3. 2.5cm basal layer

#	Depth (cm)	Salinity (ppt)
14	snow	0
19	basal	21
11	2-5	13
13	10-15	9
12	20-25	9
17	30-35	9
18	45-50	8
15	60-65	9

---

2. Ridge line at site #10. 15cm of snow
20m south of ridge, Wednesday May 3. 2.5cm basal layer

#	Depth (cm)	Salinity (ppt)
37	snow	0
36	basal	18
35	2-5	9
32	10-15	11
31	20-25	15
33	35-40	11
34	55-60	14

Station C: Ridge line. 74 33.82°N
North of ridge, Monday May 1. 96 57.26°W

3 bags on ridge straight line.
Triangle (3 bags) at north end bag, site #21.
2 lead up bags at 50m and 100m from site #21.

# of bags	site #	ice (cm)	free board (cm)	snow depth (cm)	mean snow (cm)	snow +ice (cm)
-	11.5	168	-14	52/48/40/42 48/52/54/52	48	216
1	12	186	10	16/12/16/17 20/27/24/23	19	205
1	13	187	15	25/24/23/16 12/14/14/24	19	206
1	14	185	12	15/11/10/17 05/10/15/13	12	197
1	15	186	14	04/05/06/05 13/17/24/09	10	196
1	16	177	7	41/30/30/37 43/28/27/24	33	210
1	17	188	13	10/11/11/12 25/10/05/05	11	199
1	18	190	14	20/20/19/21 22/25/28/20	22	212
1	19	177	10	18/21/19/21 16/25/22/18	20	197
1	20	188	13	05/03/05/03 05/03/05/03	04	192
3	21	189	11	16/19/20/18 15/09/12/18	16	205

(site #11.5 is 10m north of ridge)

Station C: Ridge line, May 1.
Snow depths at approximately 5m intervals.

Site #	Snow (cm)	Site #	Snow (cm)	Site #	Snow (cm)
1	28	4	15	7	14
	11		23		21
	11		22		4
	17		16		4
2	30	5	25	8	5
	15		19		4
	15		16		10
	22		16		8
3	30	6	7	9	15
	25		6		4
	22		5		4
	29		32		4
4	15	7	14	10	18

Site #	Snow (cm)	Site #	Snow (cm)	Site #	Snow (cm)
12	16	15	9	18	25
	12		4		25
	14		10		20
	4		24		25
13	20	16	35	19	35
	6		28		13
	9		19		5
	20		13		8
14	12	17	12	20	7
	22		3		14
	22		10		17
	8		12		20
15	9	18	25	21	16

Base Camp: Salinity Stations.

Site 1: 1. 1km north of camp. 74° 35.24N
West of minor ridge 97° 00.75W
Block width 7cm

hole 1: 194cm ice, 13cm freeboard, 6cm snow and .5cm basal layer
hole 2: 176cm ice, 10cm freeboard, 10cm snow and .5cm basal layer

#	Depth (cm)	Salinity (ppt)
2	snow	0
6	basal	7
5	0-5	7
1	10-15	10
7	20-25	10
8	30-35	9
4	40-45	9

Site 2: 100m east of camp. 74° 35.09N
west of minor ridge 97° 00.56W

hole 1: 194cm ice, 14cm freeboard, 7cm snow and .5cm basal layer
hole 2: 189cm ice, 13cm freeboard, 3cm snow and .5cm basal layer

#	Depth (cm)	Salinity (ppt)
8	snow	0
5	basal	13
2	0-5	8
10	10-15	9
3	20-25	6
6	35-40	5
7	55-60	5

Large Ridge: East of air strip, May 4. 74° 23.5N
Surveyed by helicopter. 96° 42.0W

Site 1: South of secondary ridge (60m south of main ridge).

205cm of ice. snow depths: 13/06/13
.5cm basal layer. 08/11/09
18cm freeboard.

#	Depth (cm)	Salinity (ppt)
8	snow	0
10	basal	3
2	0-5	13
5	20-25	11
13	50-55	8

Site 2: South (4m) of main ridge.

258cm of ice. snow depths: 38/39/40
-3cm freeboard 40/38/38
220cm sail height above ice level.

Station D: Area north of base camp surveyed by helicopter.
(Thursday and Friday, May 4 and 5)

Site #1: Station D area: South of MY ice and south of ridge.
395m south of ridge and 120m south of site #2.
Surveyed by helicopter, Friday May 5.

190cm of ice.
3.5cm basal layer.
11cm freeboard.

snow depths: 05/06/10/08
05/04/05/05

#	Depth (cm)	Salinity (ppt)
34	basal	19
8	0-5	10

Site #2: Station D area.

South (275m) of ridge.
120m north of site #1.

74° 37.08N
96° 49.26W

179cm of ice.
4.0cm basal layer.
13cm freeboard.

snow depths: 09/10/08/06
08/09/08/09

#	Depth (cm)	Salinity (ppt)
19	basal	12
11	0-5	11
7	15-20	8
31	35-40	6
35	45-50	8

Site #3: Station D area: small ridge.
300 north of station #2.

192cm of ice.
2.0cm basal layer.
10cm freeboard.

snow depths: 20/17/22/16
14/13/16/18

#	Depth (cm)	Salinity (ppt)
15	snow	0
33	basal	21
17	0-5	11
18	15-20	9
12	35-40	7

Site #4: Station D area: FY ice south of MY ice rubble.

FY ice by SIMM"S flag.
5km northeast of base camp.
South of small SW-NE ridge.

74° 34.28N
96° 49.75W

208cm of ice,
11cm of freeboard,
3cm basal layer.

snow depths: 22/24/25/26
25/20/22/24

bag #	depth (cm)	salinity (ppt)
31	basal	14
18	0-5	7
7	10-15	5
36	20-25	6
15	30-35	7

Site #5: Station D are: North of ridge and flag.

400-500m north of ridge. 74° 37.38N
50m SE of a piece of MY ice. 96° 50.08W

209cm of ice. snow depths: 06/06/07/08
2.0cm basal layer. 07/07/08/08
Basal layer above 2cm refrozen snow.
13cm freeboard.

#	ice or snow	Depth (cm)	Salinity (ppt)
37	basal	2-4	13
36	snow*	0-2	6
14	ice	0-5	9

* 2cm refrozen snow layer between basal layer and ice surface.

Site #6: Station D area: FY ice north of MY ice rubble.

Two locations for ice thicknesses.
FY ice refrozen at edge of MY ice. 74° 38.1N
7km northeast of base camp. 96° 50.3W

a. 188cm of ice, snow depth 22cm
8.5cm of freeboard basal depth 2.5cm

b. 187cm of ice, snow depth 22cm
9cm of freeboard basal layer 2.5cm

bag #	ice or snow	depth (cm)	salinity (ppt)
8	basal	0-2	17
1	ice	0-5	11

Site #7: Station D area: MY flat floe.

Start of MY ice. 74° 38.68N
8km northeast of base camp. 96° 51.69W
Bare hummocks (1m) above snow surface.

333cm of ice, snow depths: 36/36/39/35
10cm of freeboard 42/39/36/44

North of Station D:

FY ice, refrozen lead between MY ice. 74° 42.59N
14km north of base camp. 97° 04.95W

a. 166cm of ice, snow depths: 21/20/25/25
2.5cm basal layer and 24/20/19/22
7cm of freeboard.

b. 160cm of ice, snow depths: 16/15/14/15
2.5cm basal layer and 14/16/15/16
8cm of freeboard.

bag #	depth (cm)	salinity (ppt)
2	basal	14
9	0-5	11
1	10-15	10
16	20-25	8
20	35-40	7

North of Station D:

Large homogeneous MY floe. 74° 49.0N
North of Base Camp, Thursday May 4. 96° 45.0W

5.02cm of ice and 85cm of freeboard.
Hummock 25m NE was 195cm above ice level at ice hole.
Station D area: Snow depths at 5m intervals.

FY ice north of EM site.

Starting at ridge as distances from ridge.
South to sites #2 and #1.

Distance (m)	depth (cm)	Distance (m)	depth (cm)	Distance (m)	depth (cm)
0	42	150	30	300	17
5	44	155	17	305	12
10	31	160	12	310	12
15	25	165	16	315	24
20	15	170	21	320	19
25	20	175	20	325	20
30	17	180	20	330	10
35	29	185	20	335	7
40	20	190	22	340	7
45	30	195	25	345	8
50	29	200	33	350	14
55	34	205	31	355	20
60	10	210	17	360	31
65	5	215	5	365	27
70	12	220	11	370	32
75	15	225	5	375	38
80	25	230	19	380	44
85	13	235	22	385	37
90	13	240	12	390	7
95	15	245	5	395**	4
100	12	250	11	400	10
105	13	255	8	405	17
110	5	260	13	410	24
115	10	265	16	415	12
120	5	270	5	420	21
125	5	275*	6	425	22
130	5	280	7	430	22
135	12	285	12	435	12
140	7	290	17	440	12
145	22	295	22		
150	30	300	17		

* location of stn. #2 south of ridge.
** location of stn. #1 south of ridge.

South Stations: Stations surveyed by helicopter.

Site #1: West of 40% MY floe (May 6). 74° 23.39N
22km SE of base camp. 96° 24.88W

9cm of snow had no distinct basal interface,
total snow layer was salty.

bag #	ice or snow	depth (cm)	salinity ppt
11	snow	7-9	3
34	snow	5-7	6
19	basal	3-5	13
12	basal	0-2	15
35	ice	0-2	13

Site #2: East of 40% MY floe (May 6). 74° 27.00N
27km ESE of base camp. 95° 53.39W

115cm of ice, snow depths: 06/08/03/05
6cm of freeboard. 03/08/08/06
7cm of snow with a 4cm basal layer.

bag #	ice or snow	depth (cm)	salinity (ppt)
13	snow	5-7	1
2	snow	2-4	6
10	basal	0-2	18
5	ice	0-2	10

D. Ice Thickness Profile Maps

This appendix presents snow plus ice thickness profile maps generated from the airborne EIS dataset. Although the legends on these maps identify a nominal scale for each map, they have been resized to fit into this document and so are no longer to scale. Distances may be estimated using the scale bar or the latitude/longitude grid.

MAY 1, 1995 FLIGHT 8
Lambert Conic Proj., Center Long.: −97.00, Lat1 70.00, Lat2 80.00
Ice Thickness 1 cm/2 m, Map Scale 1:300000

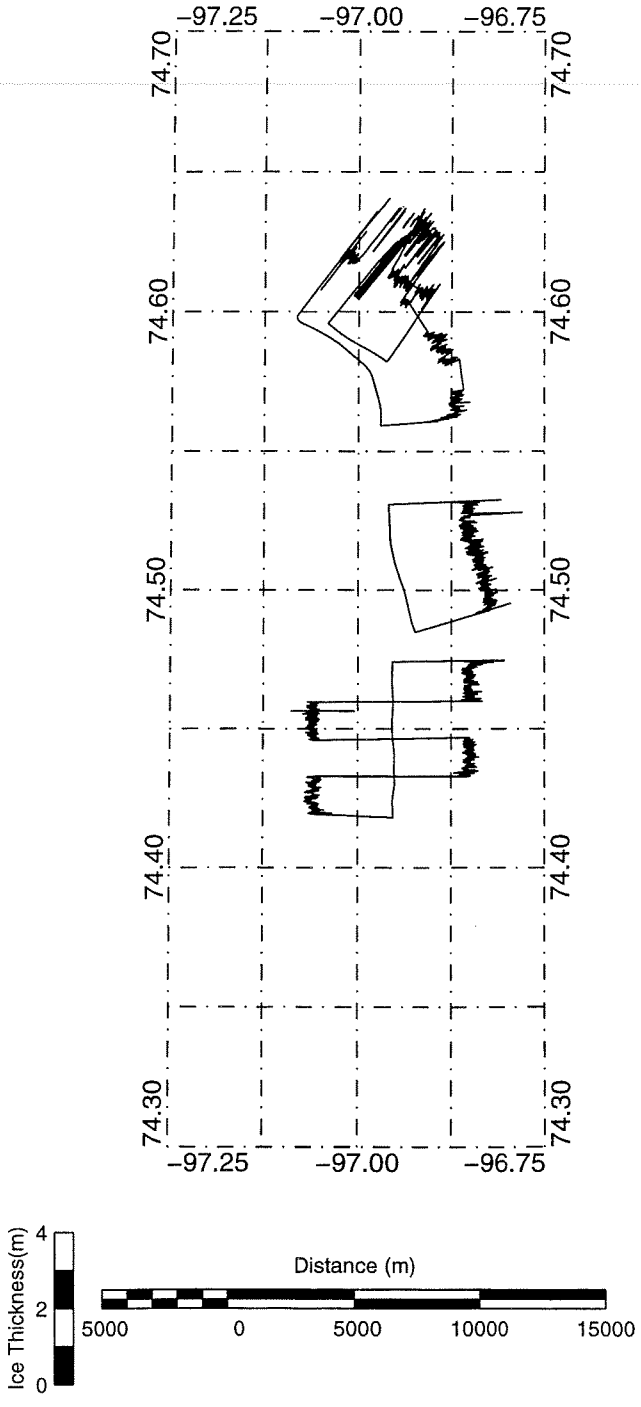

MAY 1, 1995 FLIGHT 9: Lines 10011 – 10052
Lambert Conic Proj., Center Long.: –97.00, Lat1 70.00, Lat2 80.00
Ice Thickness 1 cm/2 m, Map Scale 1:100000

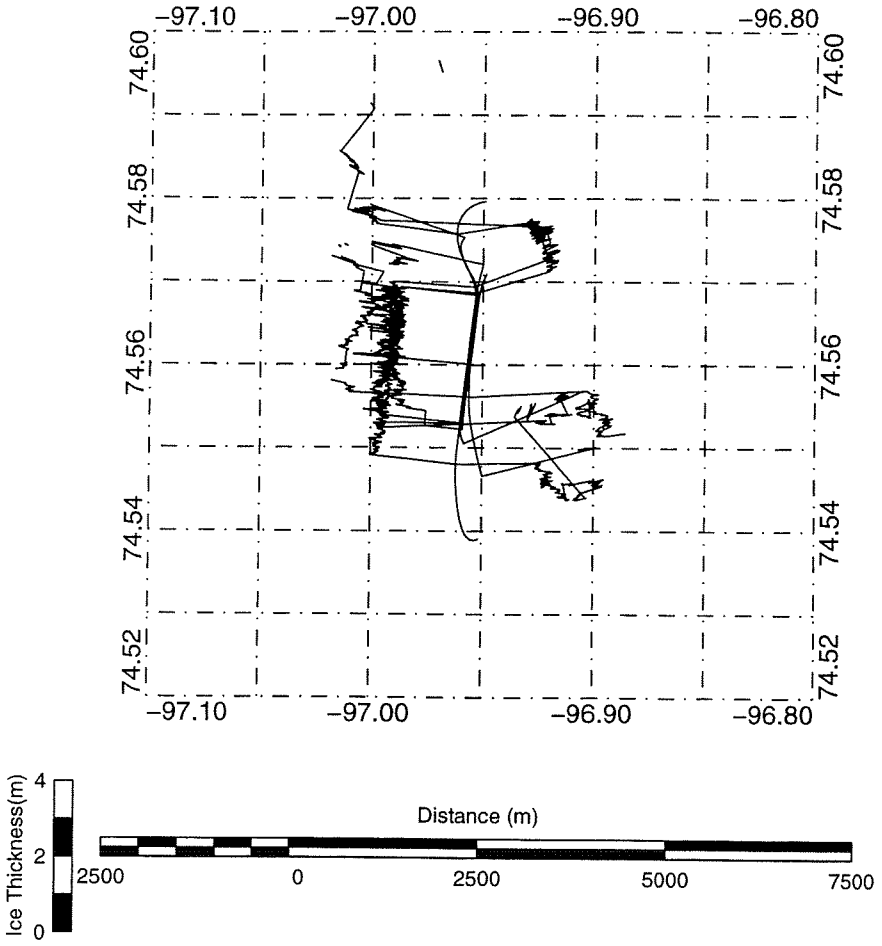

MAY 1, 1995 FLIGHT 9: Lines 10061 – 10123
Lambert Conic Proj., Center Long.: –97.00, Lat1 70.00, Lat2 80.00
Ice Thickness 1 cm/2 m, Map Scale 1:100000

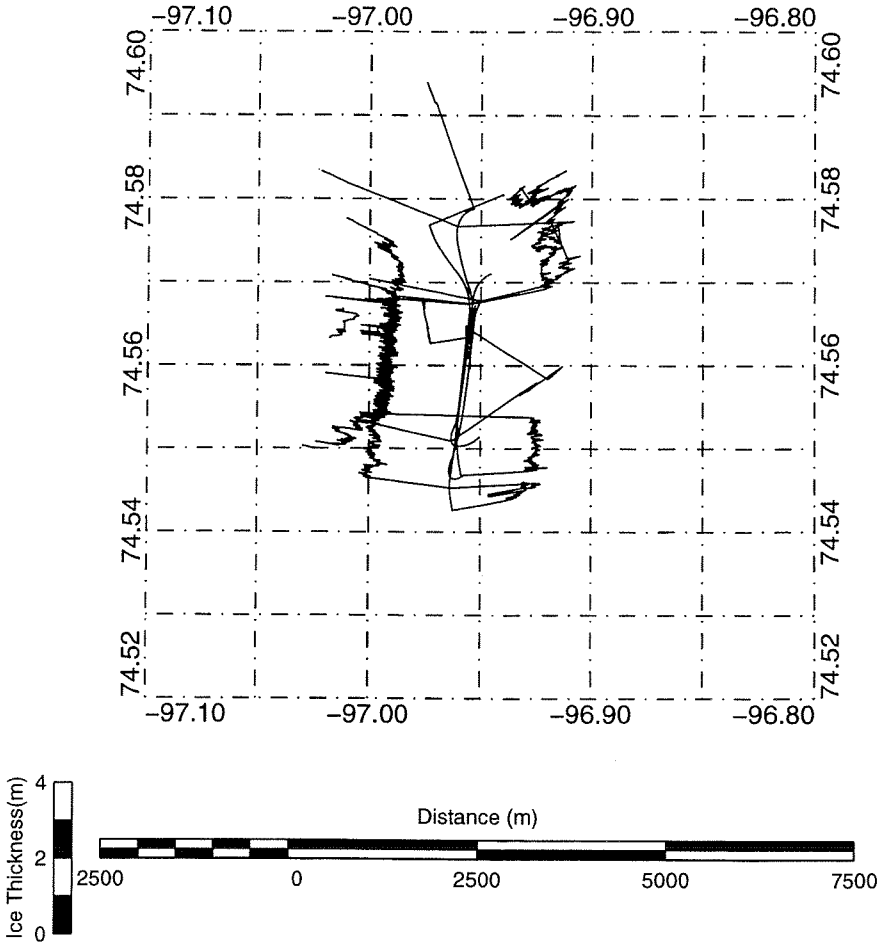

MAY 1, 1995 FLIGHT 9: Lines 10131 – 10190
Lambert Conic Proj., Center Long.: –97.00, Lat1 70.00, Lat2 80.00
Ice Thickness 1 cm/2 m, Map Scale 1:250000

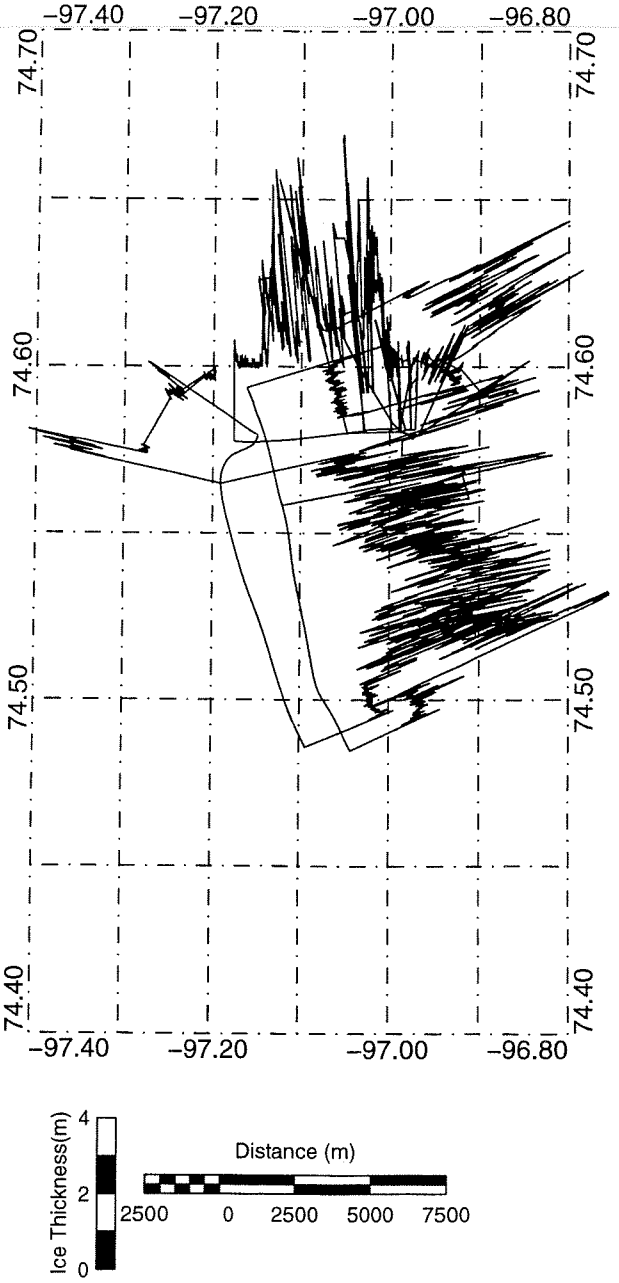

MAY 1, 1995 FLIGHT 10: Lines 10010 – 10052
Lambert Conic Proj., Center Long.: –97.00, Lat1 70.00, Lat2 80.00
Ice Thickness 1 cm/4 m, Map Scale 1:100000

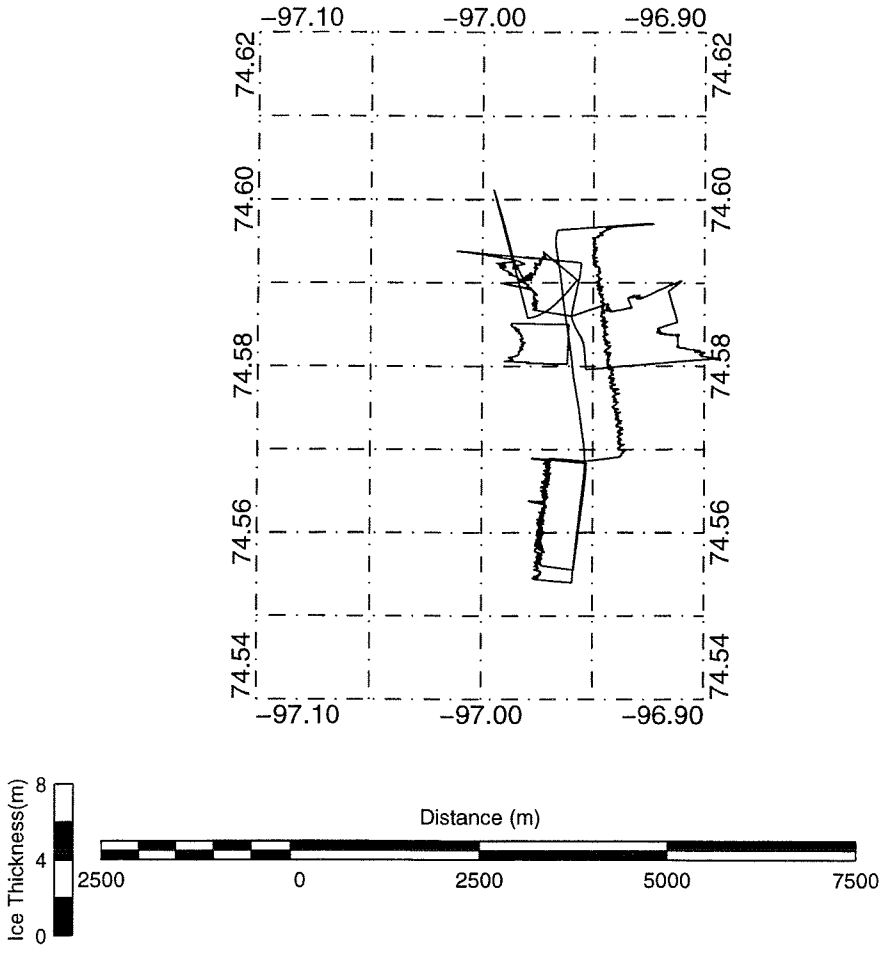

MAY 1, 1995 FLIGHT 10: Lines 10060 – 10130
Lambert Conic Proj., Center Long.: –97.00, Lat1 70.00, Lat2 80.00
Ice Thickness 1 cm/4 m, Map Scale 1:100000

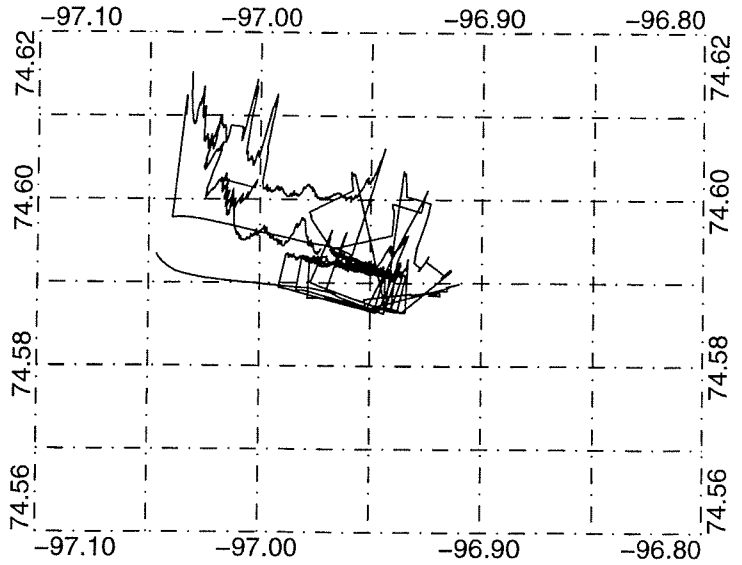

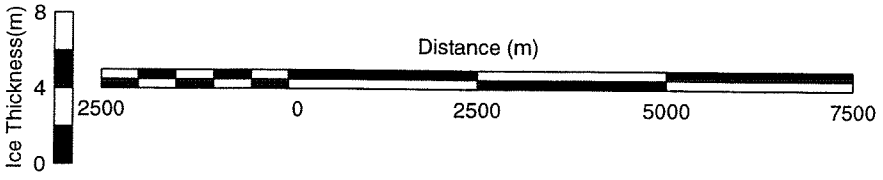

MAY 1, 1995 FLIGHT 11
Lambert Conic Proj., Center Long.: -96.00, Lat1 70.00, Lat2 80.00
Ice Thickness 1 cm/4 m, Map Scale 1:600000

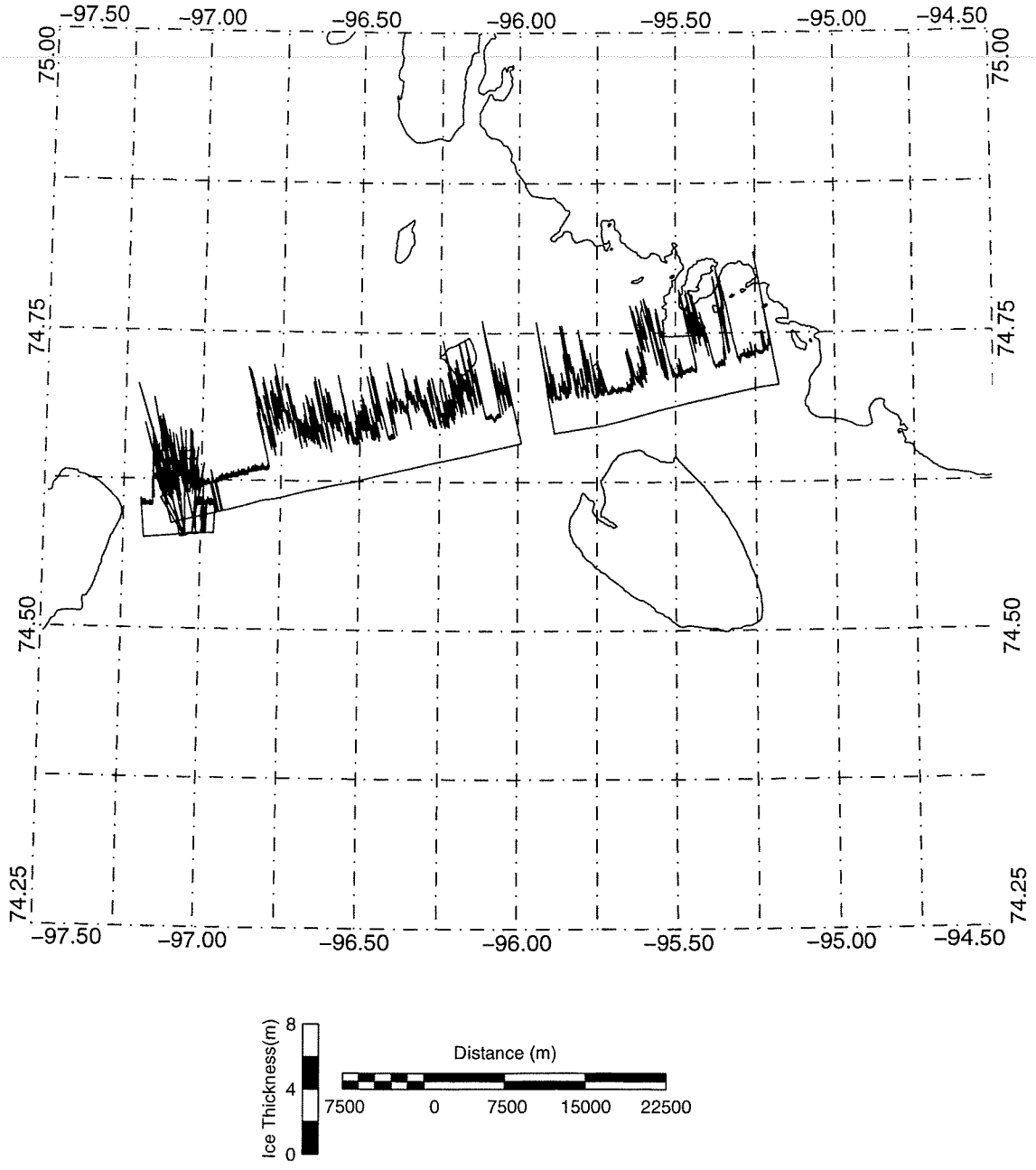

MAY 3, 1995 FLIGHT 16
Lambert Conic Proj., Center Long.: −95.50, Lat1 70.00, Lat2 80.00
Ice Thickness 1 cm/4 m, Map Scale 1:100000

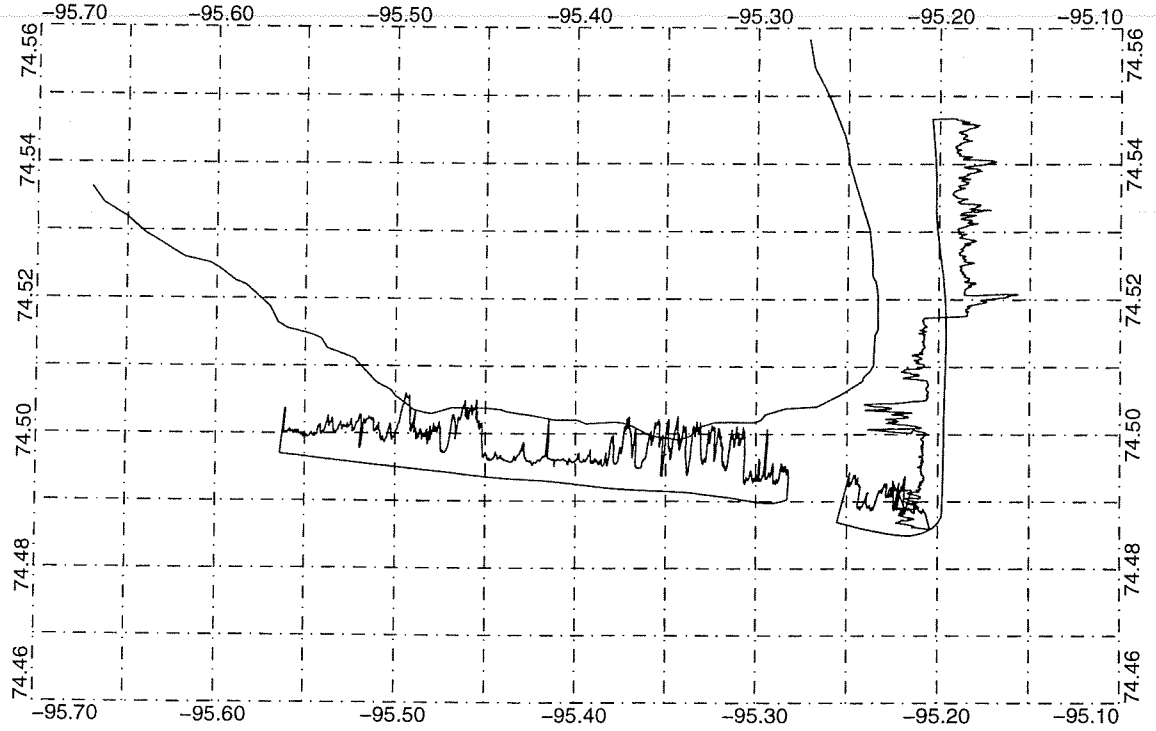

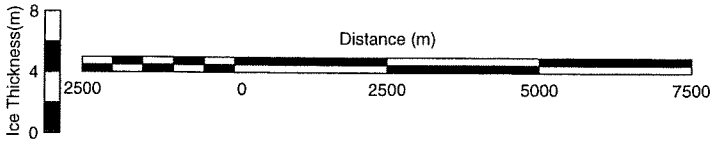

MAY 3, 1995 FLIGHT 17
Lambert Conic Proj., Center Long.: -96.20, Lat1 70.00, Lat2 80.00
Ice Thickness 1 cm/2 m, Map Scale 1:300000

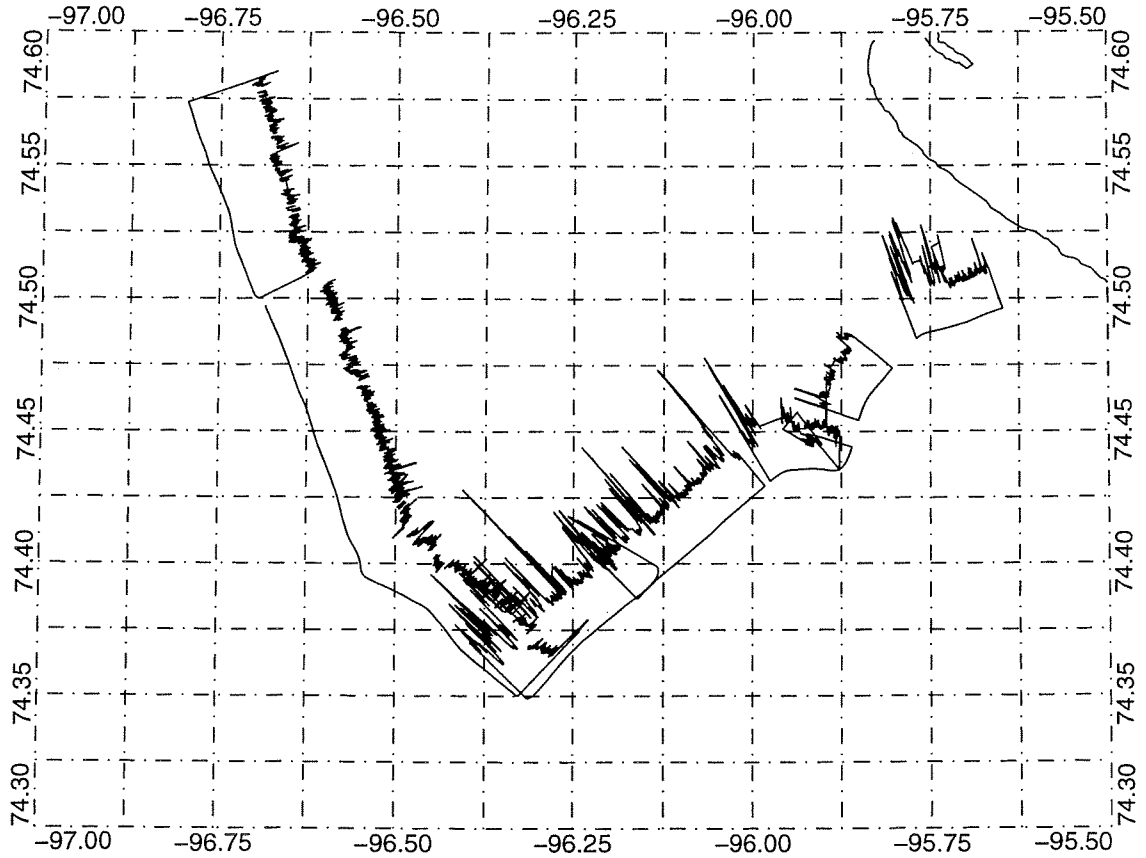

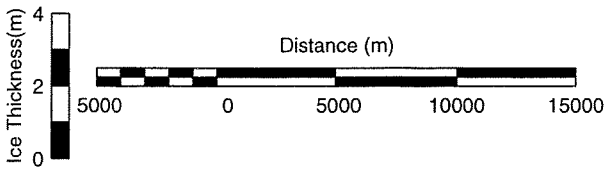

MAY 3, 1995 FLIGHT 18: Lines 10020 – 10061
Lambert Conic Proj., Center Long.: –97.00, Lat1 70.00, Lat2 80.00
Ice Thickness 1 cm/2 m, Map Scale 1:300000

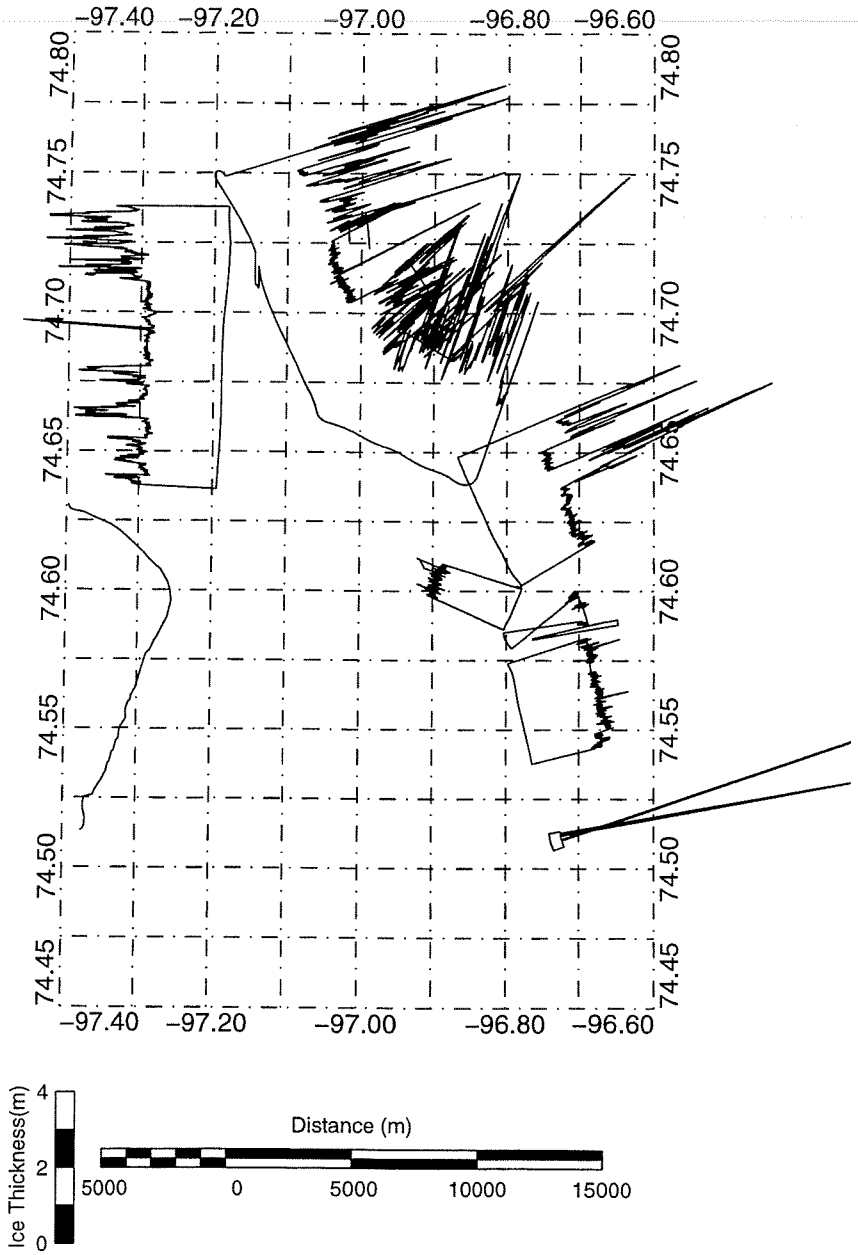

MAY 3, 1995 FLIGHT 18: Lines 10062 – 10094
Lambert Conic Proj., Center Long.: –97.00, Lat1 70.00, Lat2 80.00
Ice Thickness 1 cm/2 m, Map Scale 1:200000

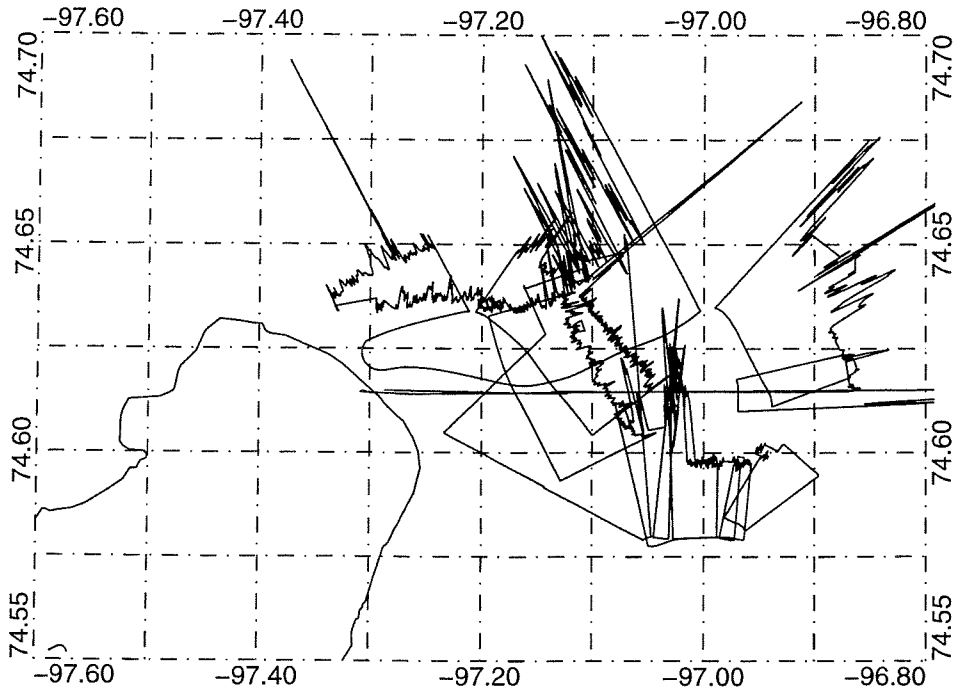

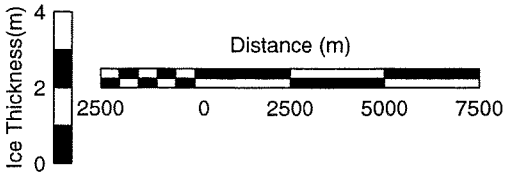

MAY 3, 1995 FLIGHT 18: Lines 10101 – 10151
Lambert Conic Proj., Center Long.: –97.00, Lat1 70.00, Lat2 80.00
Ice Thickness 1 cm/2 m, Map Scale 1:200000

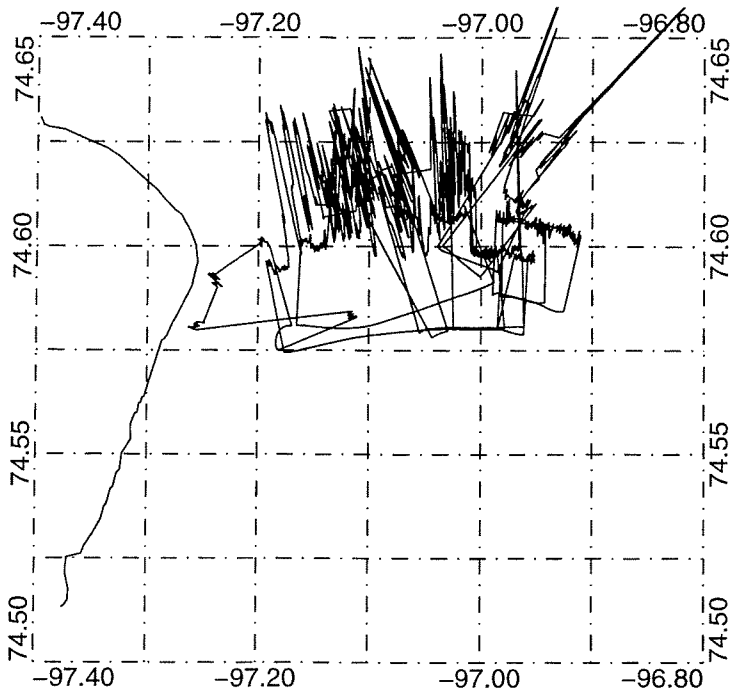

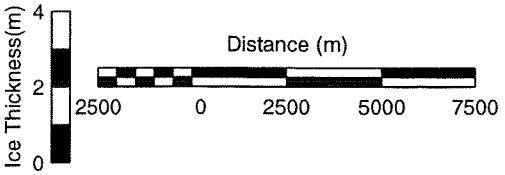

MAY 3, 1995 FLIGHT 18: Lines 10161 – 10262
Lambert Conic Proj., Center Long.: –97.00, Lat1 70.00, Lat2 80.00
Ice Thickness 1 cm/2 m, Map Scale 1:200000

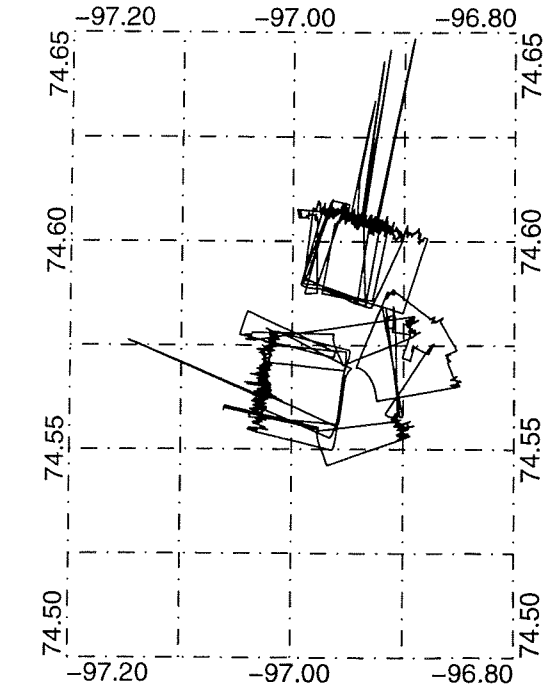

MAY 5, 1995 FLIGHT 19
Lambert Conic Proj., Center Long.: −95.30, Lat1 70.00, Lat2 80.00
Ice Thickness 1 cm/2 m, Map Scale 1:200000

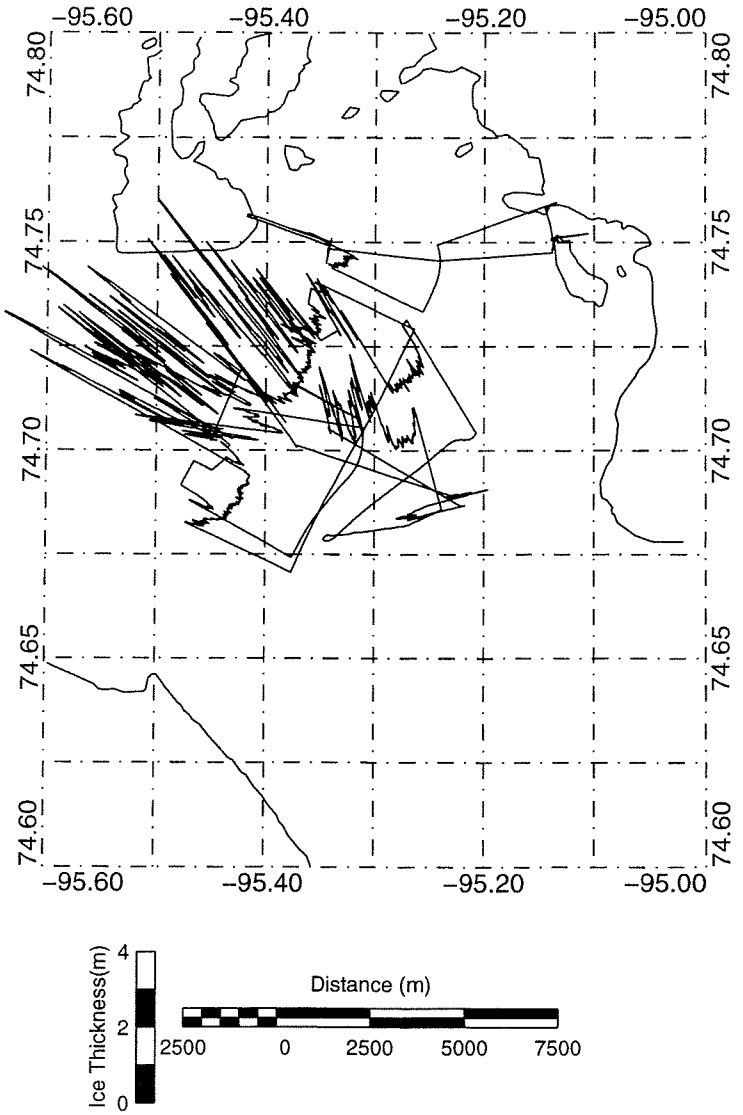

MAY 5, 1995 FLIGHT 20
Lambert Conic Proj., Center Long.: –95.30, Lat1 70.00, Lat2 80.00
Ice Thickness 1 cm/2 m, Map Scale 1:100000

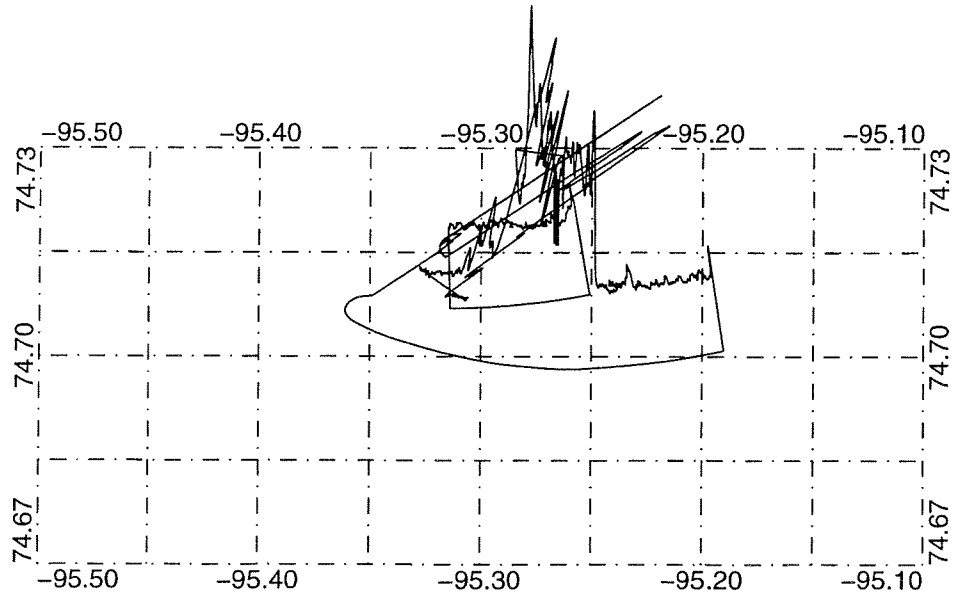

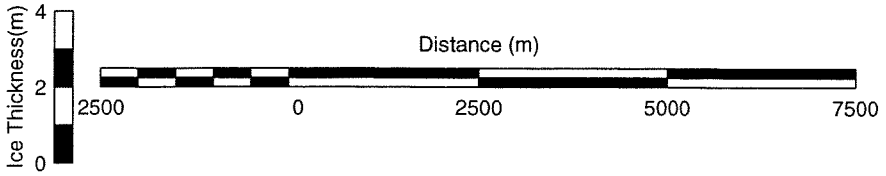

MAY 5, 1995 FLIGHT 21: Lines 10010 – 10031
Lambert Conic Proj., Center Long.: –96.00, Lat1 70.00, Lat2 80.00
Ice Thickness 1 cm/2 m, Map Scale 1:400000

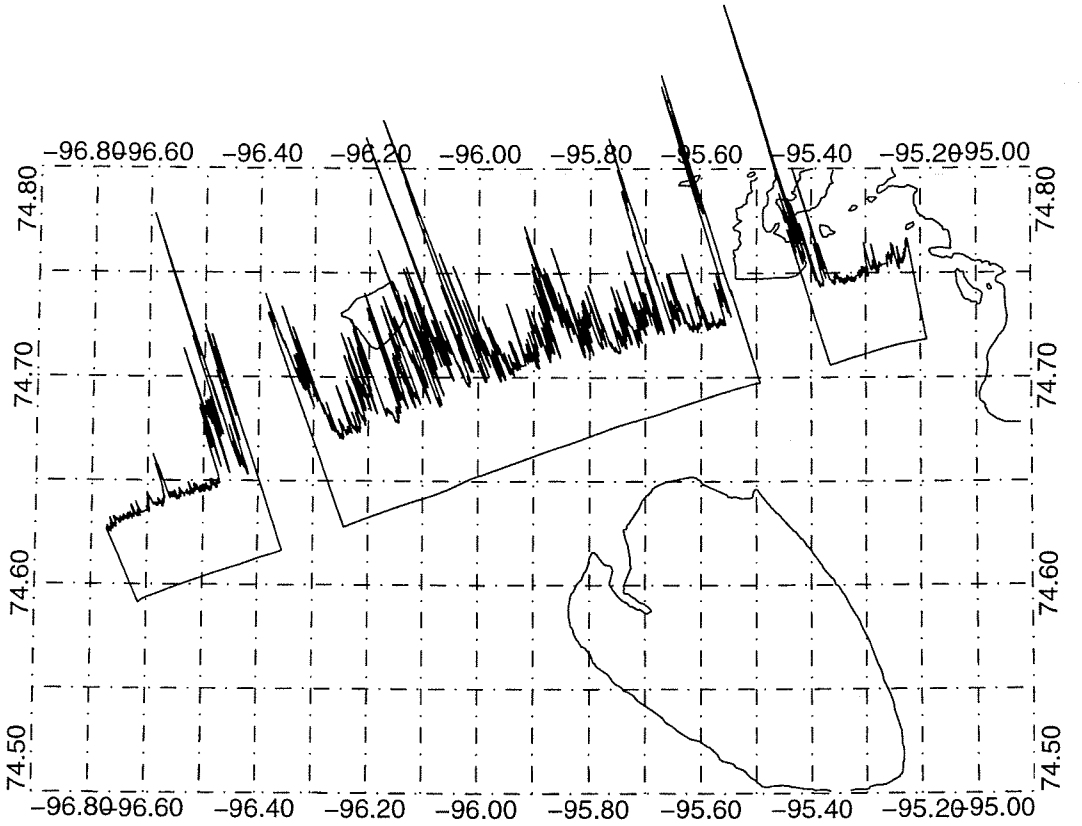

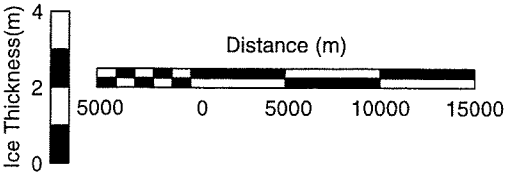

MAY 5, 1995 FLIGHT 21: Lines 10032 – 10081
Lambert Conic Proj., Center Long.: -96.80, Lat1 70.00, Lat2 80.00
Ice Thickness 1 cm/2 m, Map Scale 1:300000

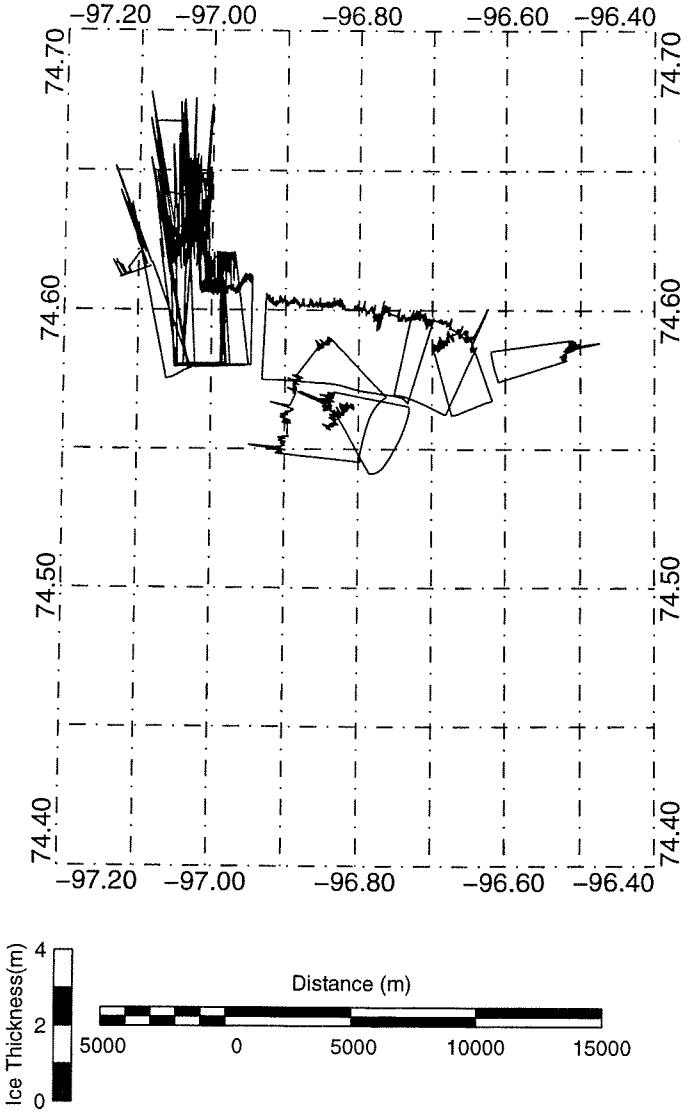

MAY 5, 1995 FLIGHT 21: Lines 10091 – 10201
Lambert Conic Proj., Center Long.: –96.80, Lat1 70.00, Lat2 80.00
Ice Thickness 1 cm/2 m, Map Scale 1:200000

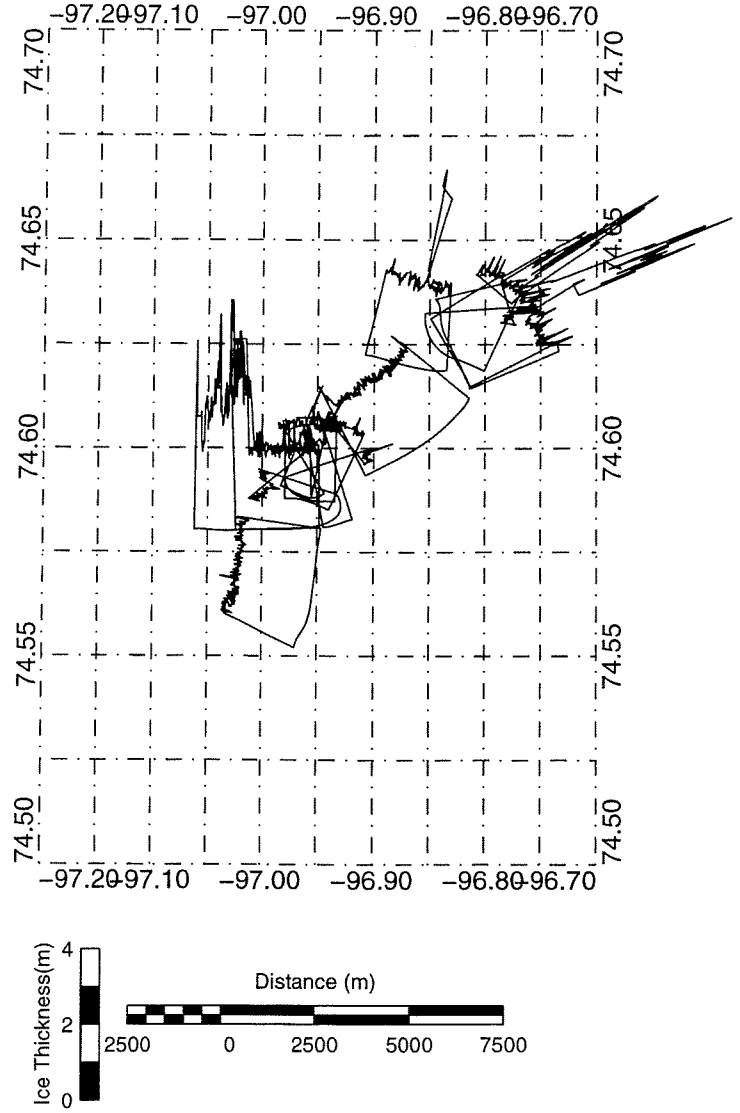

MAY 5, 1995 FLIGHT 22
Lambert Conic Proj., Center Long.: –97.00, Lat1 70.00, Lat2 80.00
Ice Thickness 1 cm/2 m, Map Scale 1:150000

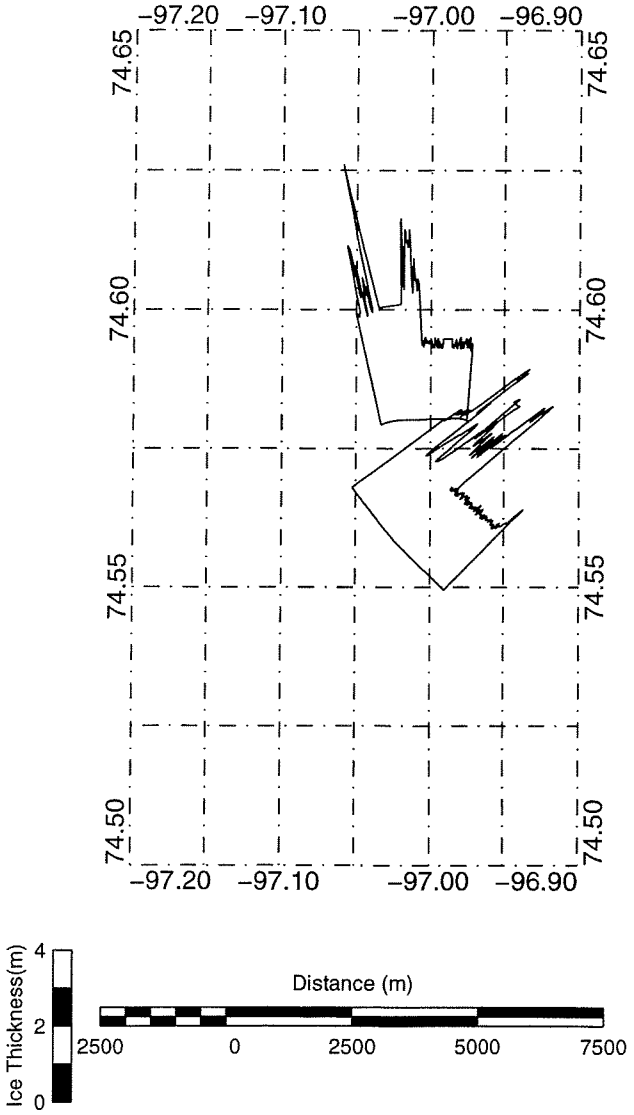

MAY 5, 1995 FLIGHT 24
Lambert Conic Proj., Center Long.: -96.00, Lat1 70.00, Lat2 80.00
Ice Thickness 1 cm/2 m, Map Scale 1:300000

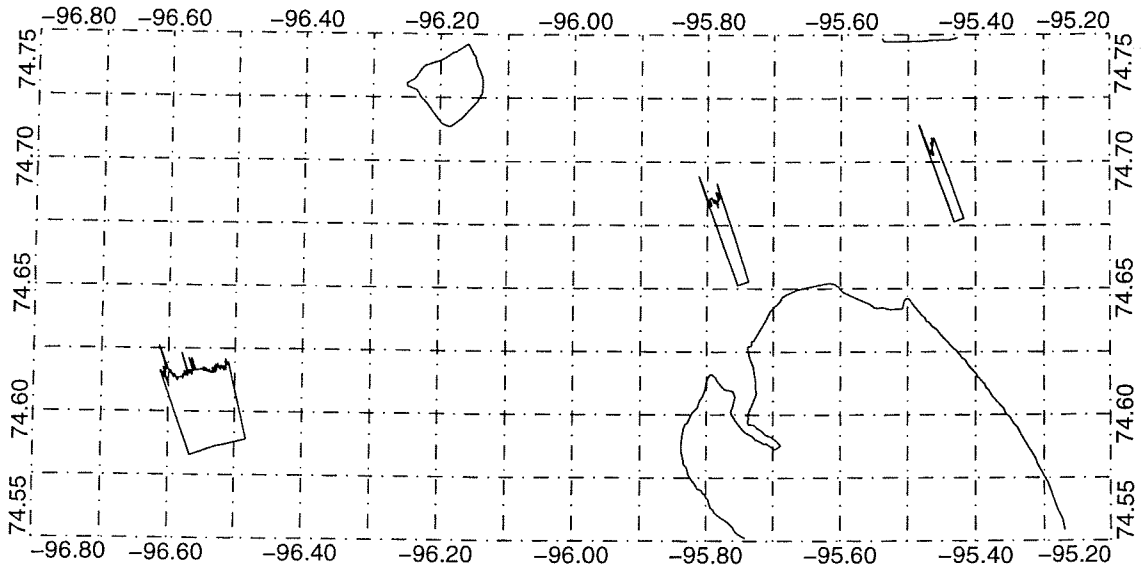

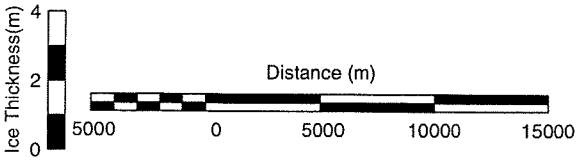

MAY 5, 1995 FLIGHT 25
Lambert Conic Proj., Center Long.: –96.00, Lat1 70.00, Lat2 80.00
Ice Thickness 1 cm/2 m, Map Scale 1:1000000

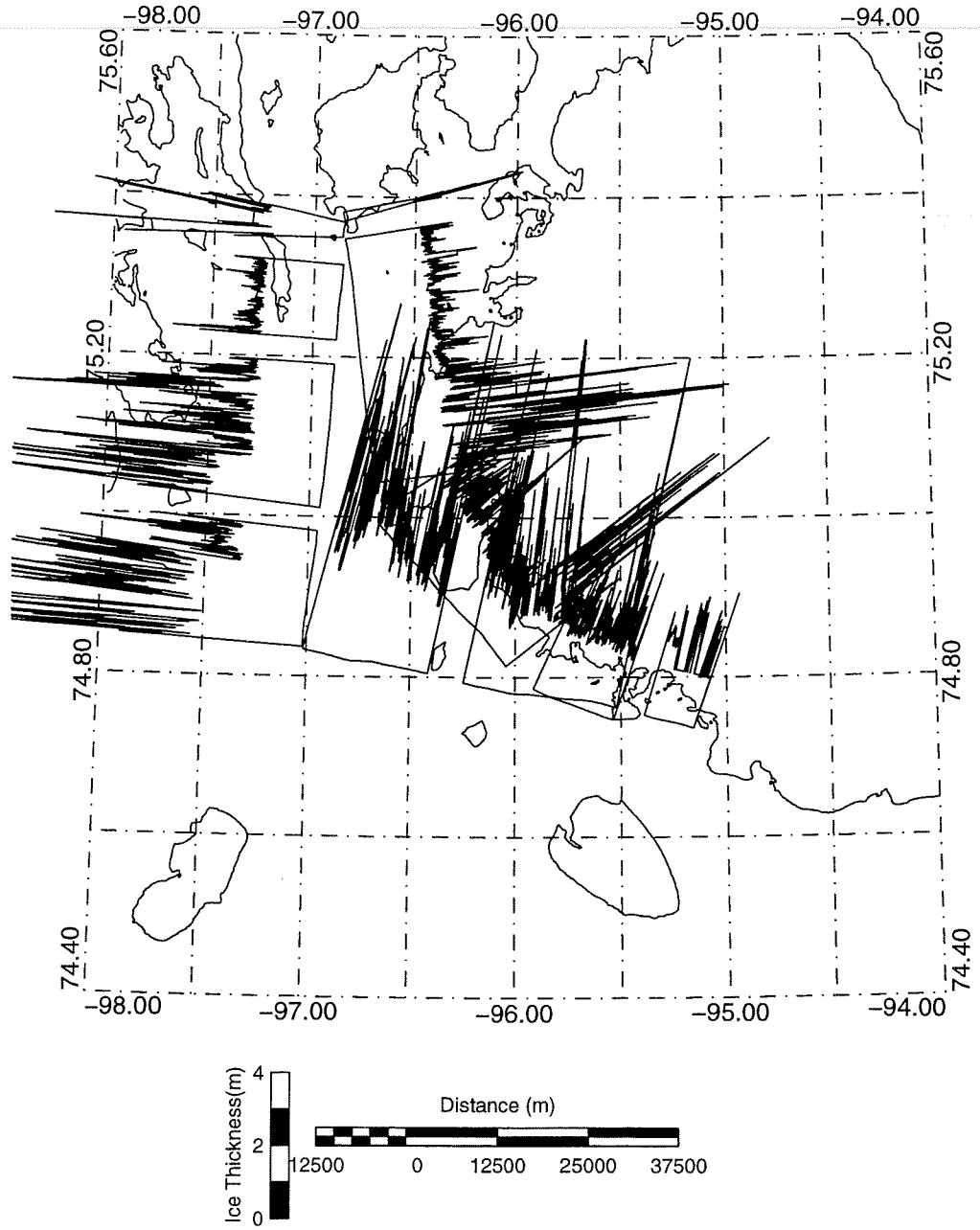

E. Standard Plots (May 1 only)

MAY 01 Flight #08 Line #10010 part 1 of 4

Line Starting Coordinates (74.4180,−96.9545) ending at (74.4360,−96.9531)

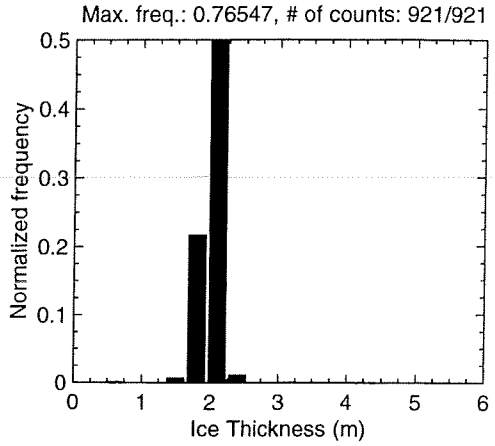

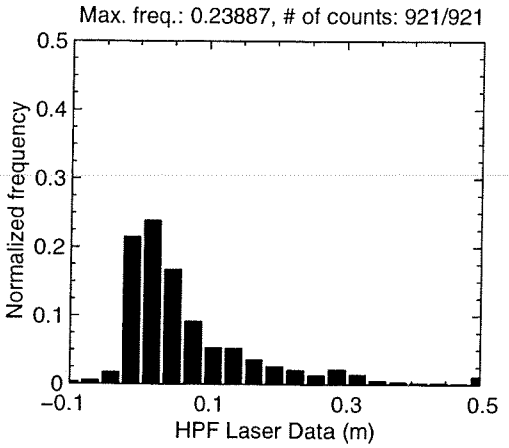

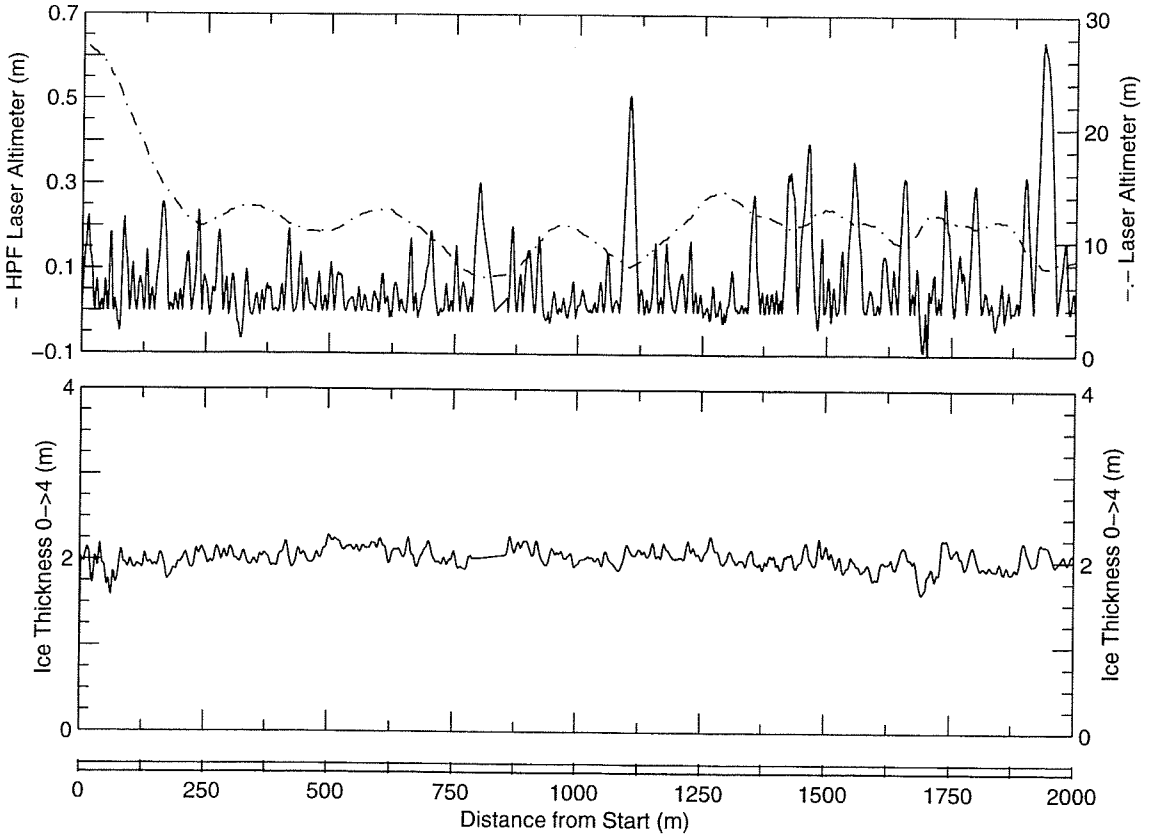

MAY 01 Flight #08 Line #10010 part 2 of 4

Line Starting Coordinates (74.4360,–96.9531) ending at (74.4539,–96.9552)

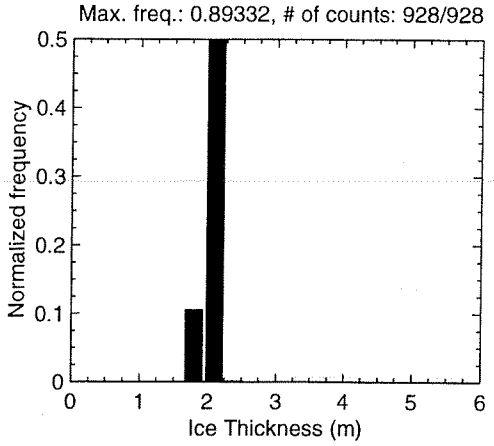

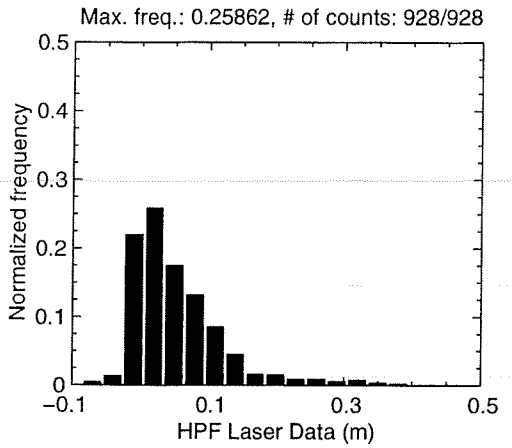

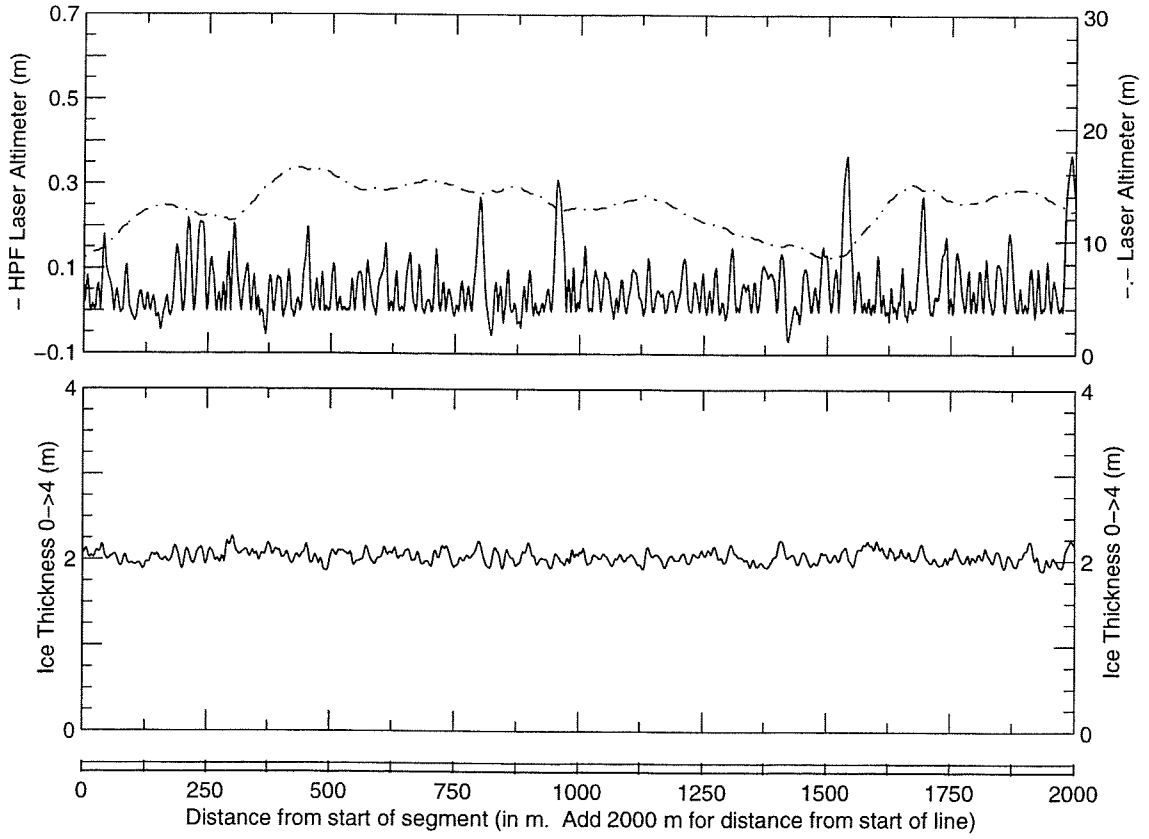

MAY 01 Flight #08 Line #10010 part 3 of 4

Line Starting Coordinates (74.4539,–96.9552) ending at (74.4718,–96.9554)

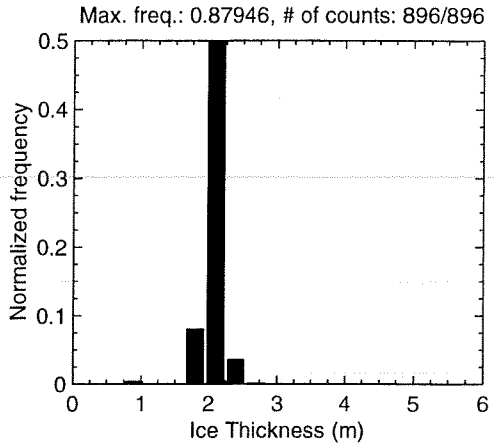

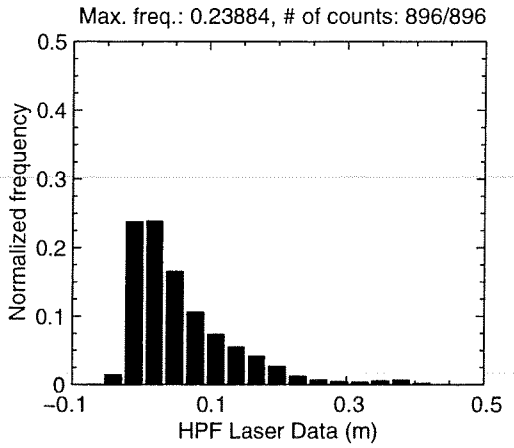

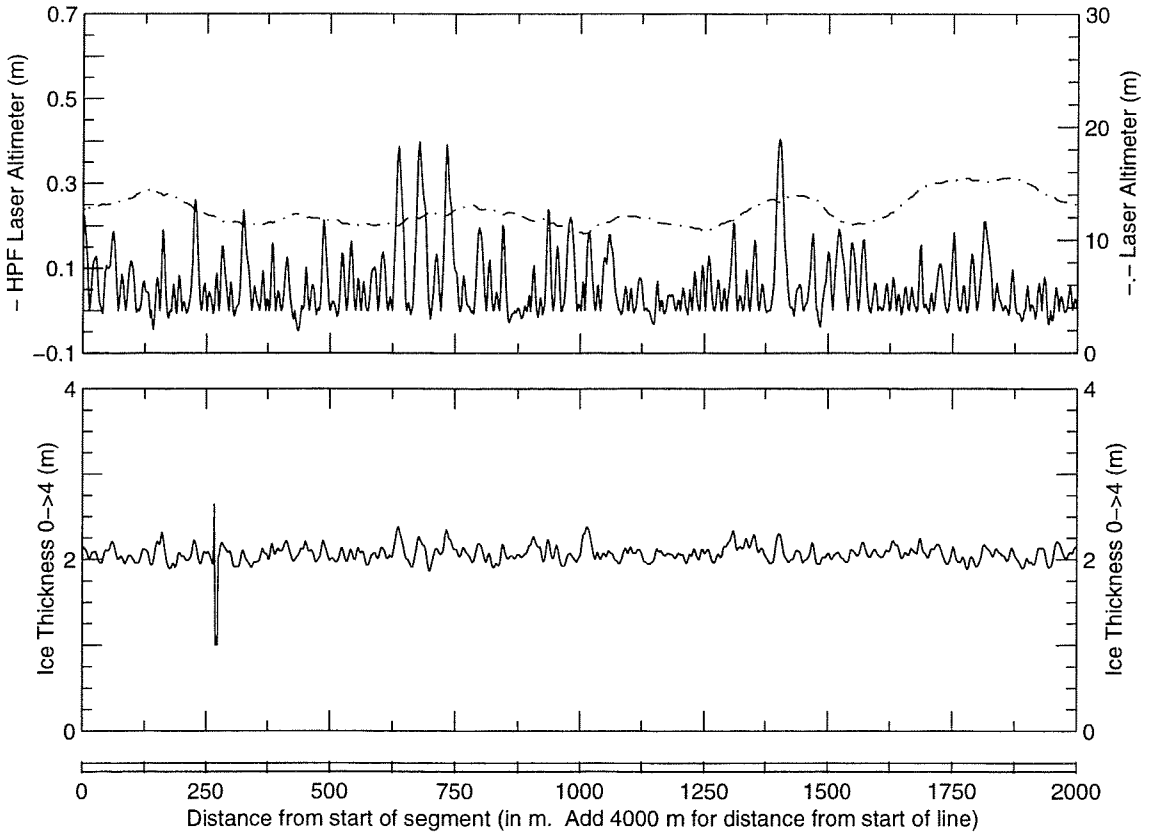

MAY 01 Flight #08 Line #10010 part 4 of 4

Line Starting Coordinates (74.4718,–96.9554) ending at (74.4742,–96.9550)

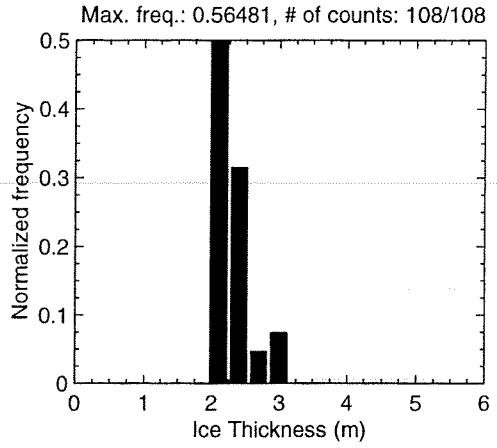

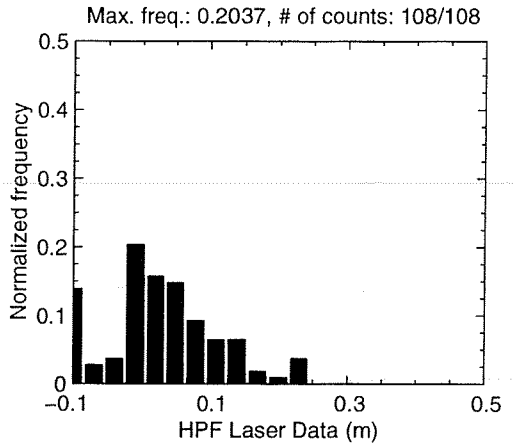

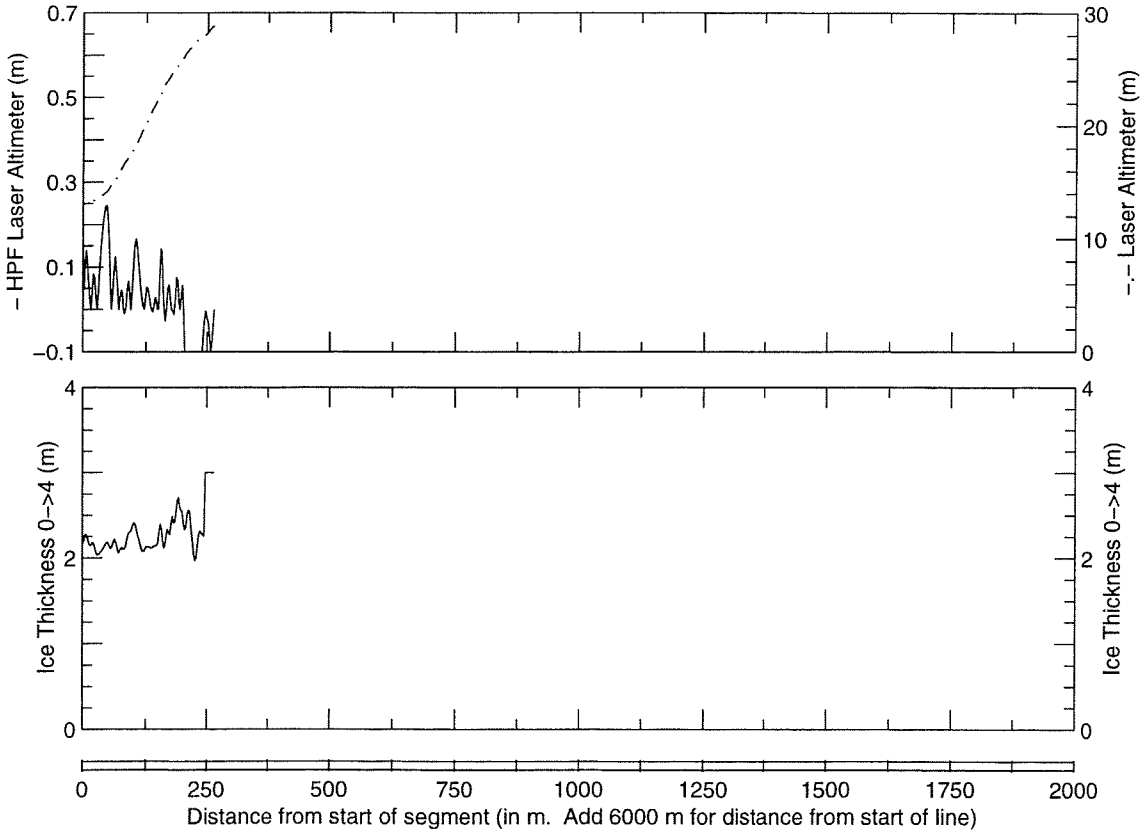

MAY 01 Flight #08 Line #10020 part 1 of 3

Line Starting Coordinates (74.4848,–96.9240) ending at (74.5020,–96.9426)

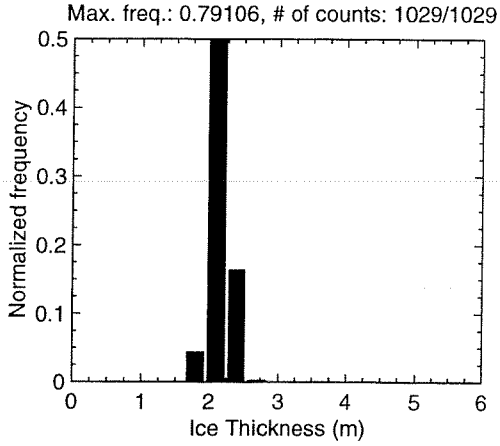

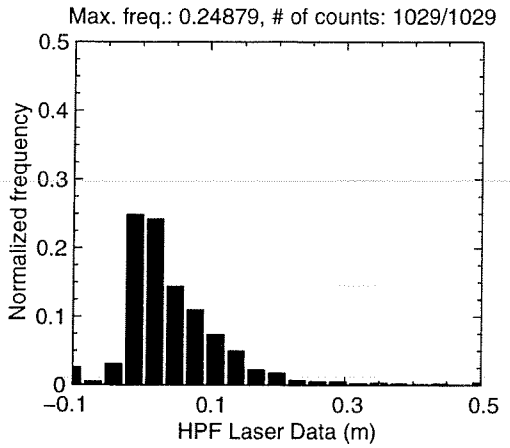

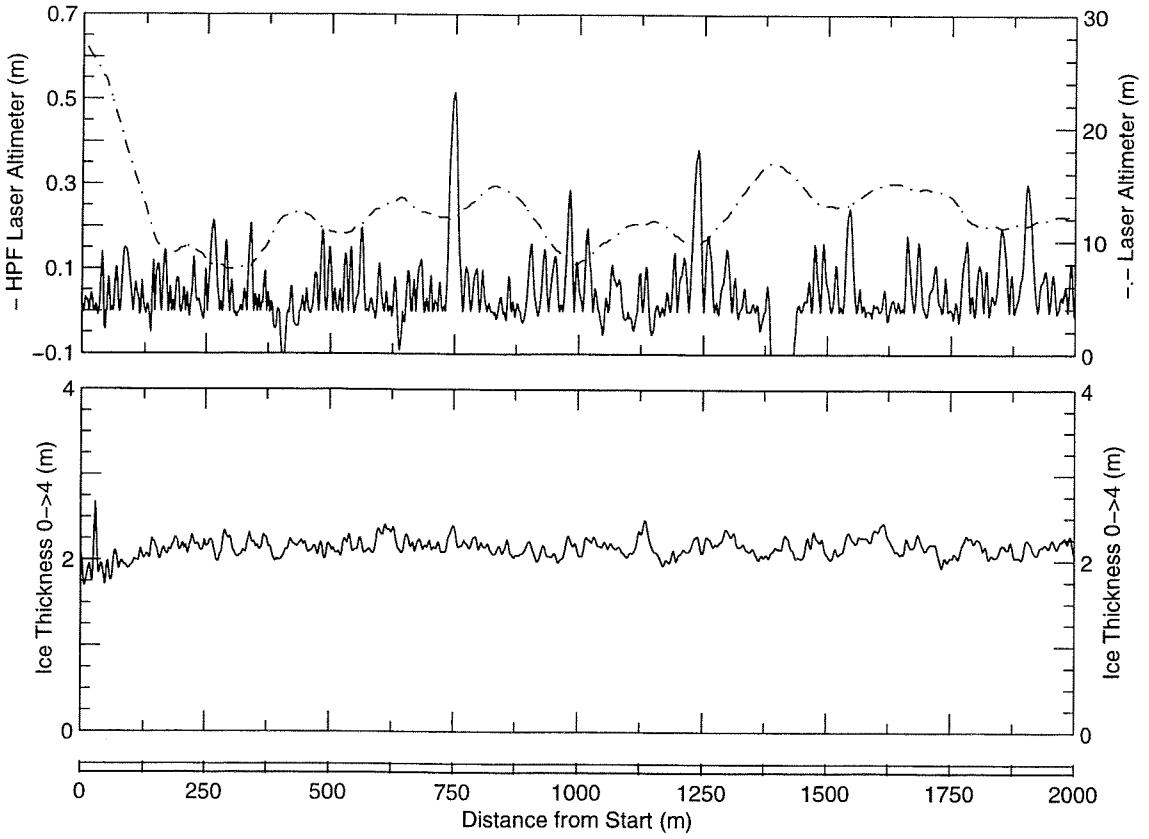

MAY 01 Flight #08 Line #10020 part 2 of 3

Line Starting Coordinates (74.5020,–96.9426) ending at (74.5194,–96.9586)

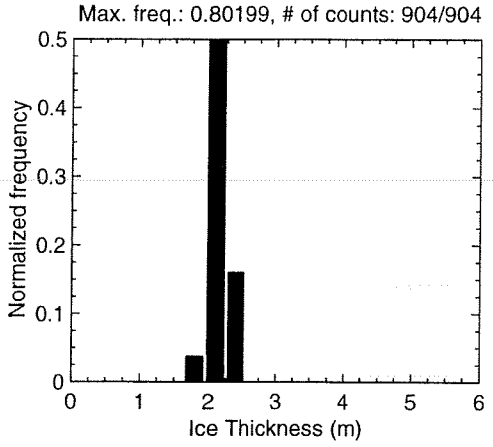

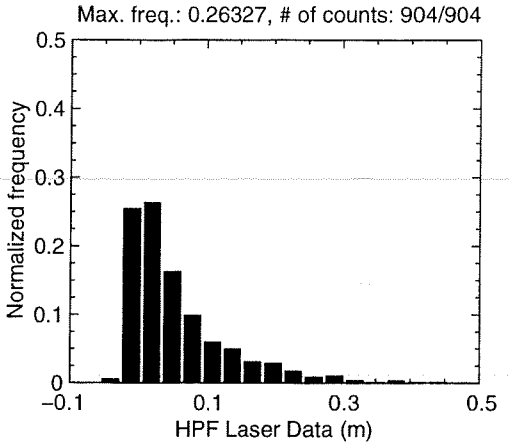

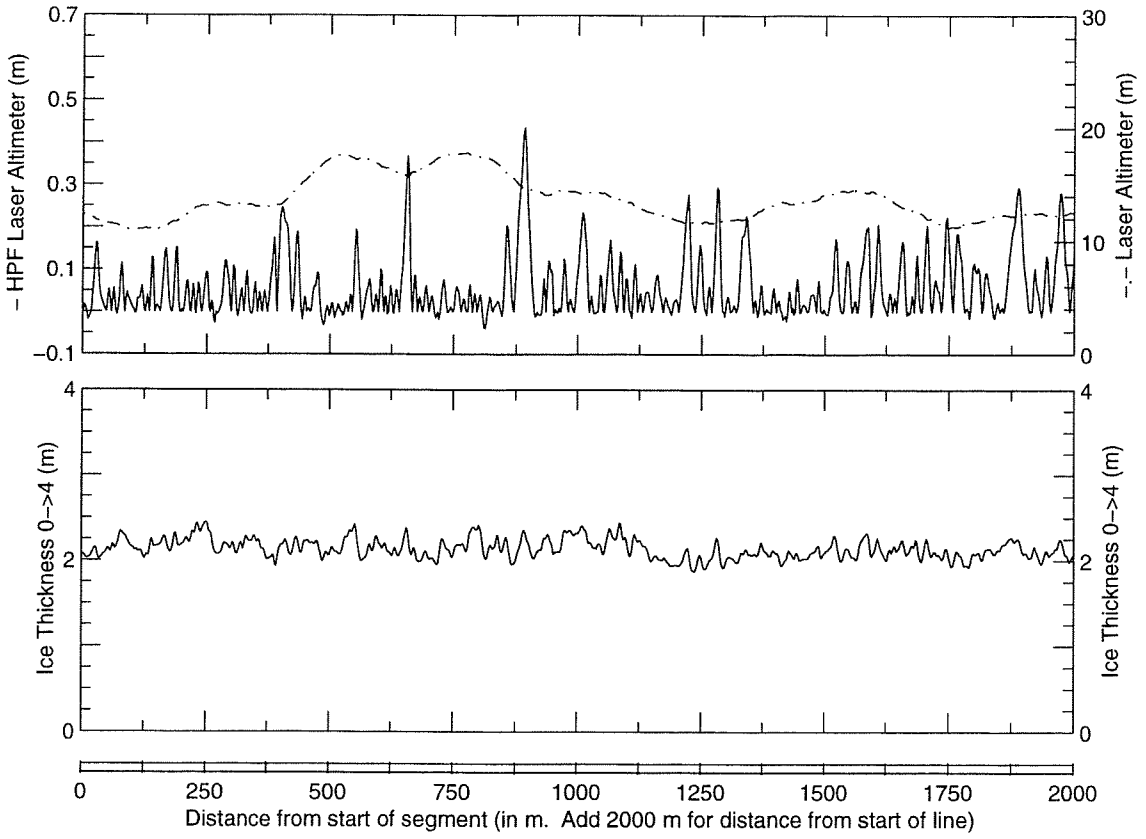

MAY 01 Flight #08 Line #10020 part 3 of 3

Line Starting Coordinates (74.5194,–96.9586) ending at (74.5309,–96.9603)

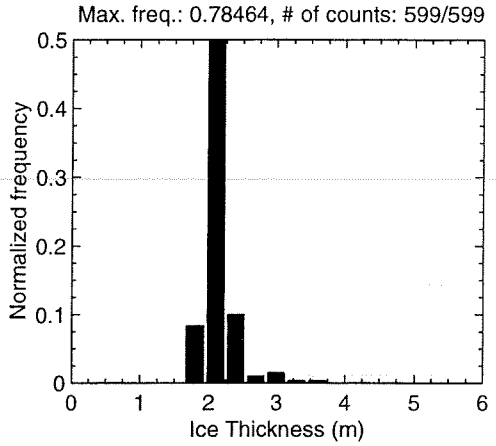

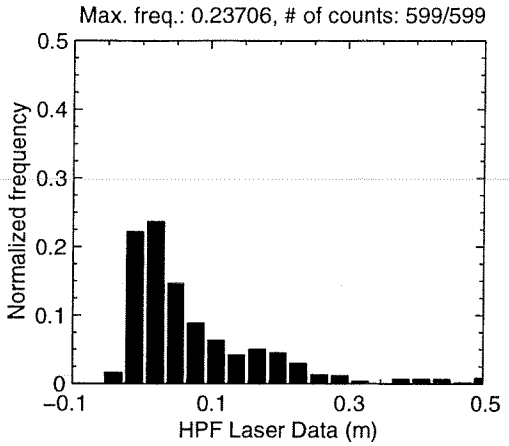

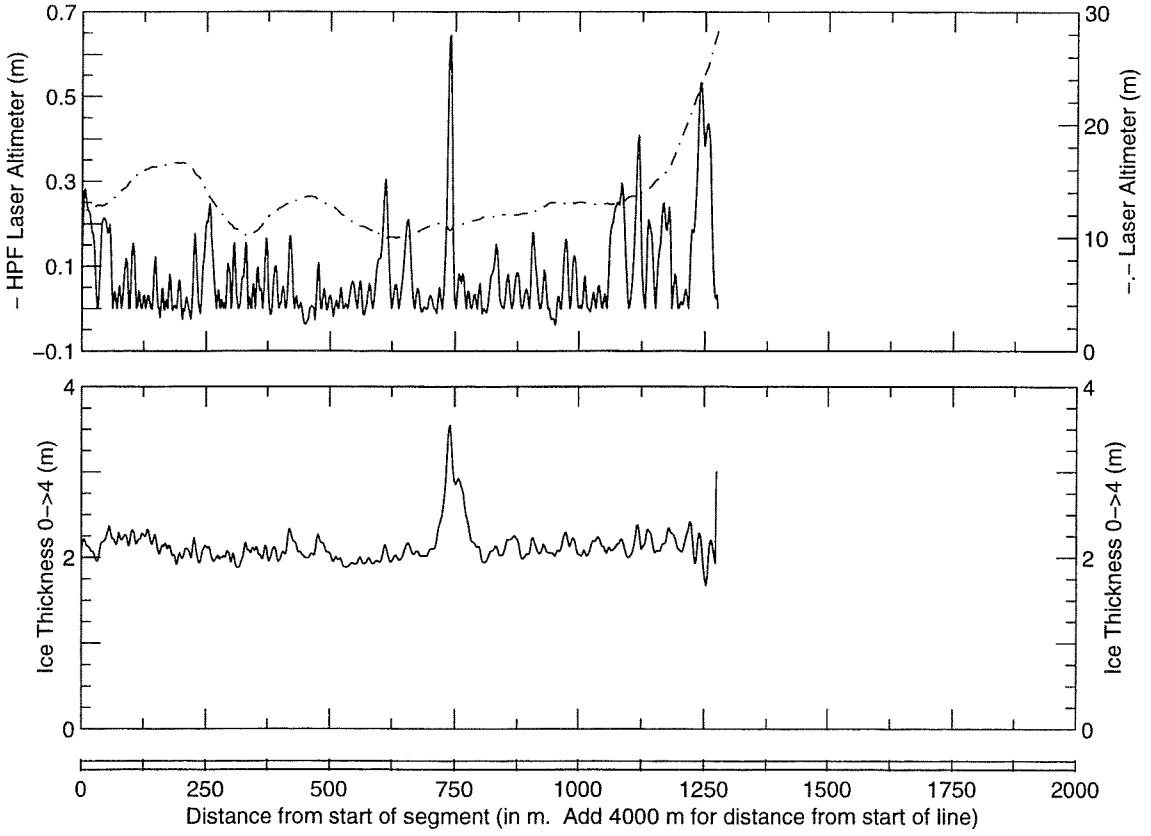

MAY 01 Flight #08 Line #10030 part 1 of 4

Line Starting Coordinates (74.5591,–96.9712) ending at (74.5767,–96.9821)

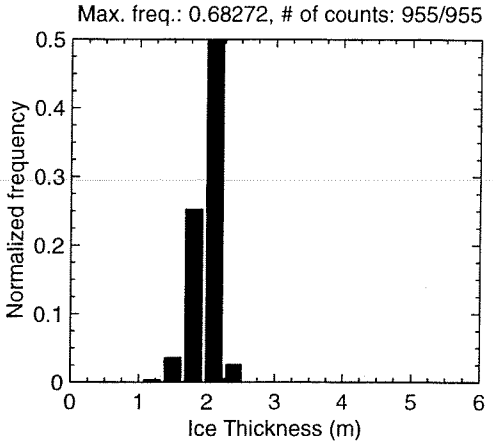

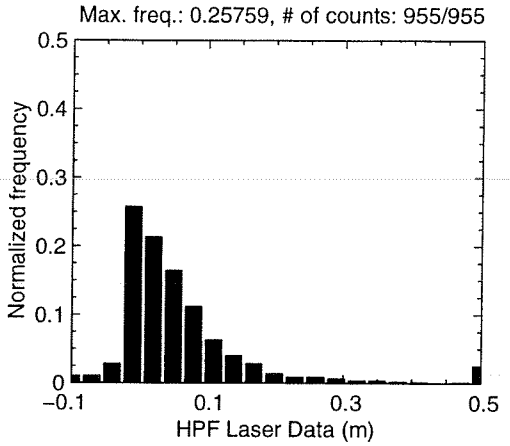

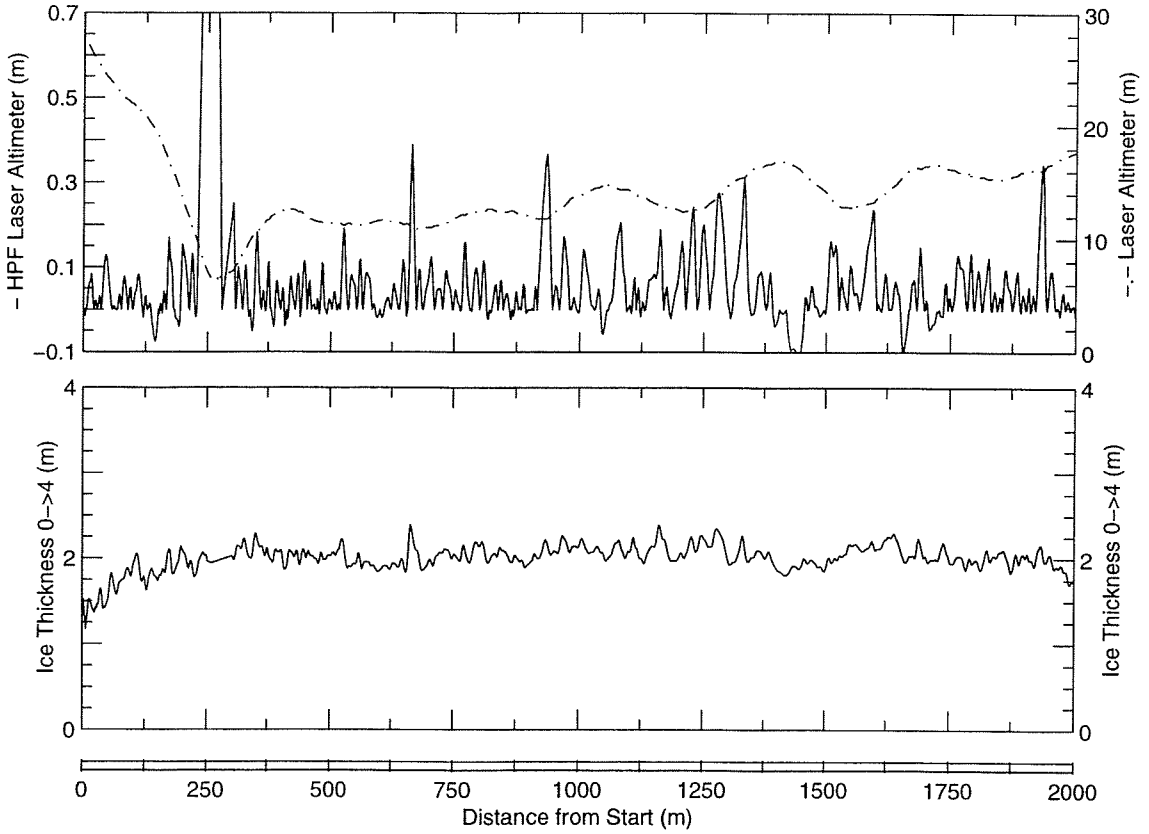

MAY 01 Flight #08 Line #10030 part 2 of 4

Line Starting Coordinates (74.5767,–96.9821) ending at (74.5892,–97.0296)

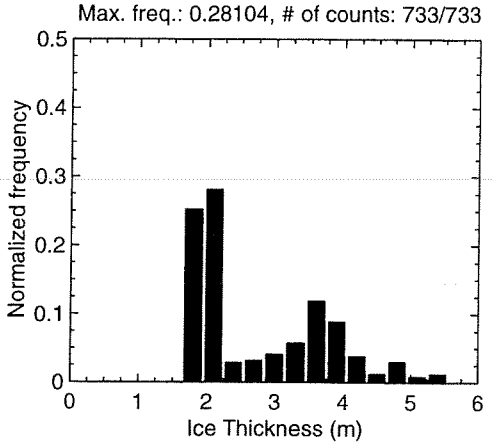

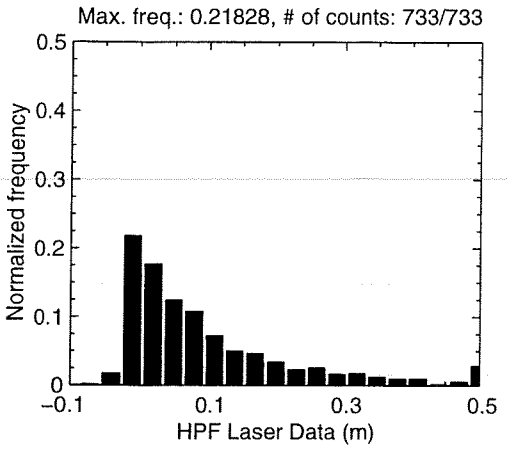

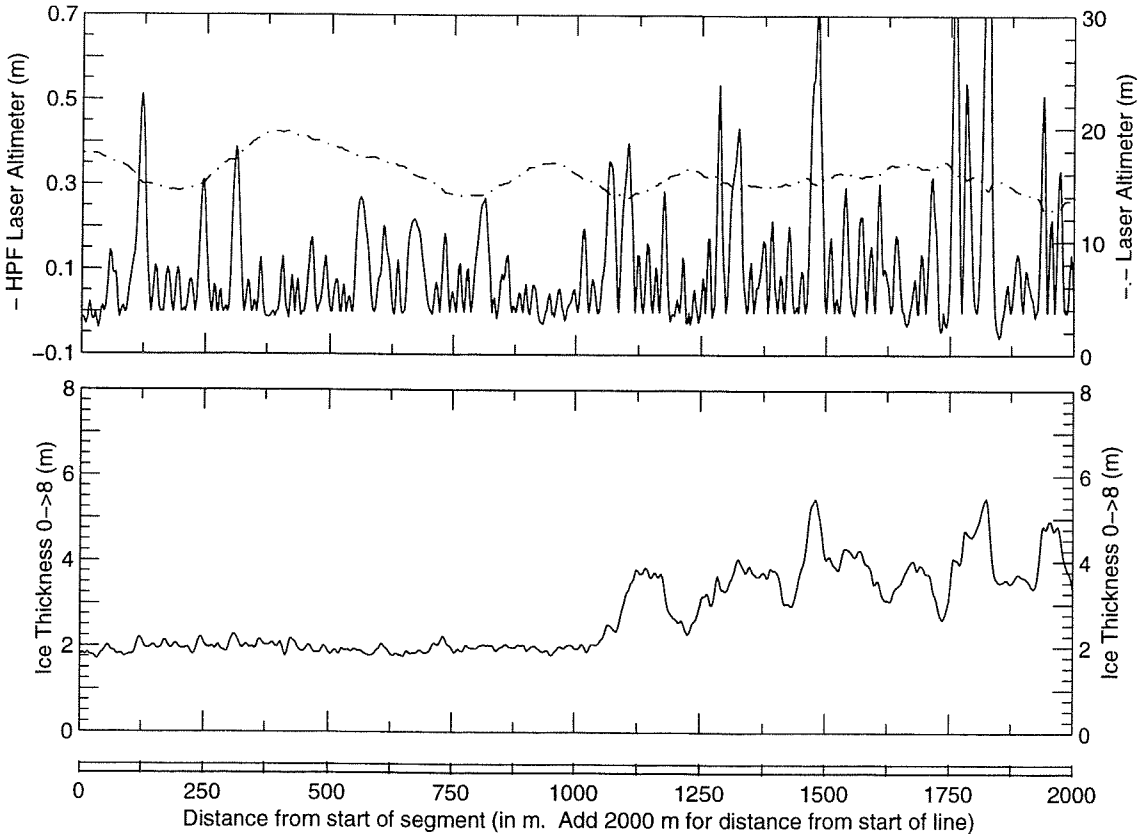

MAY 01 Flight #08 Line #10030 part 3 of 4

Line Starting Coordinates (74.5892,–97.0296) ending at (74.5990,–97.0810)

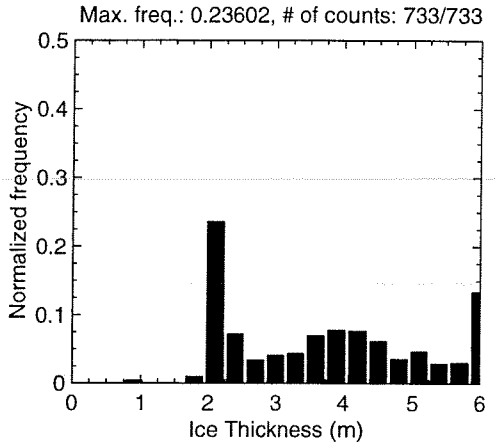

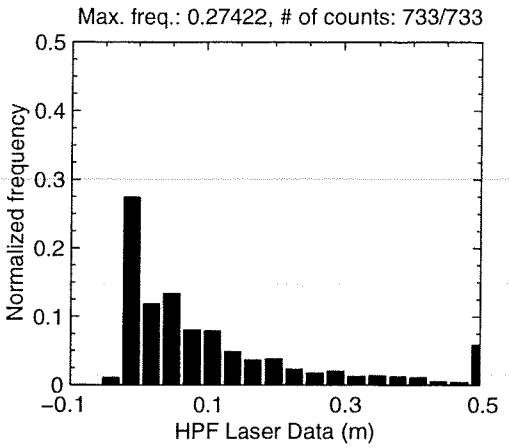

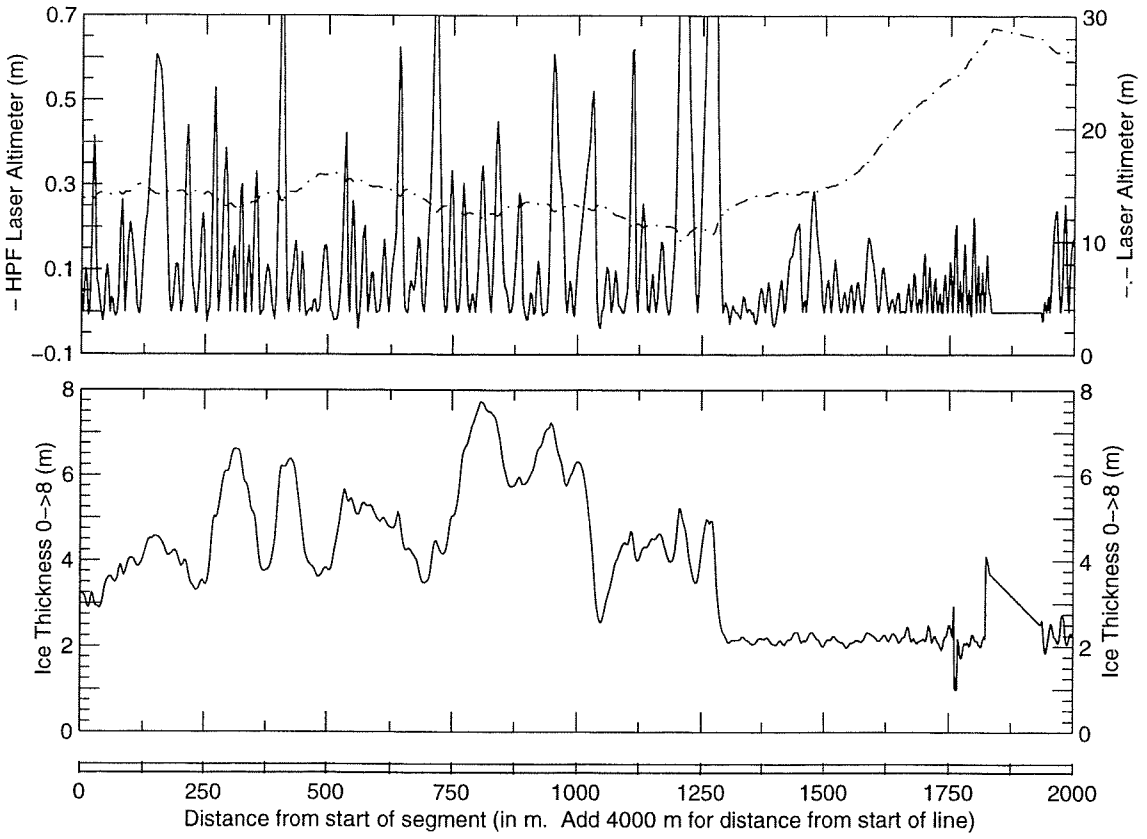

MAY 01 Flight #08 Line #10030 part 4 of 4

Line Starting Coordinates (74.5990,–97.0810) ending at (74.5991,–97.0805)

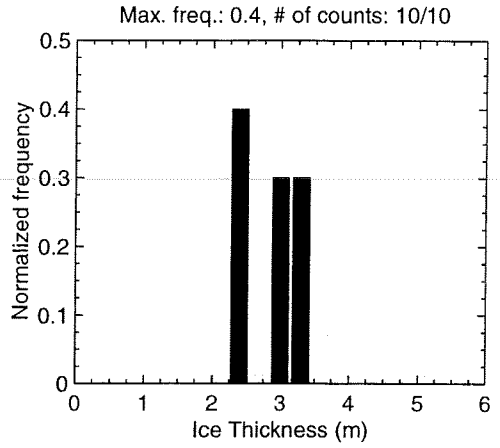

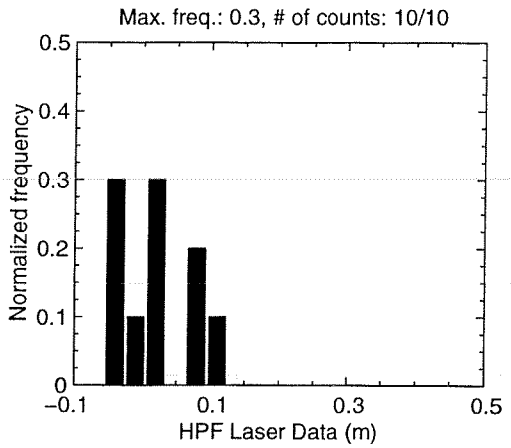

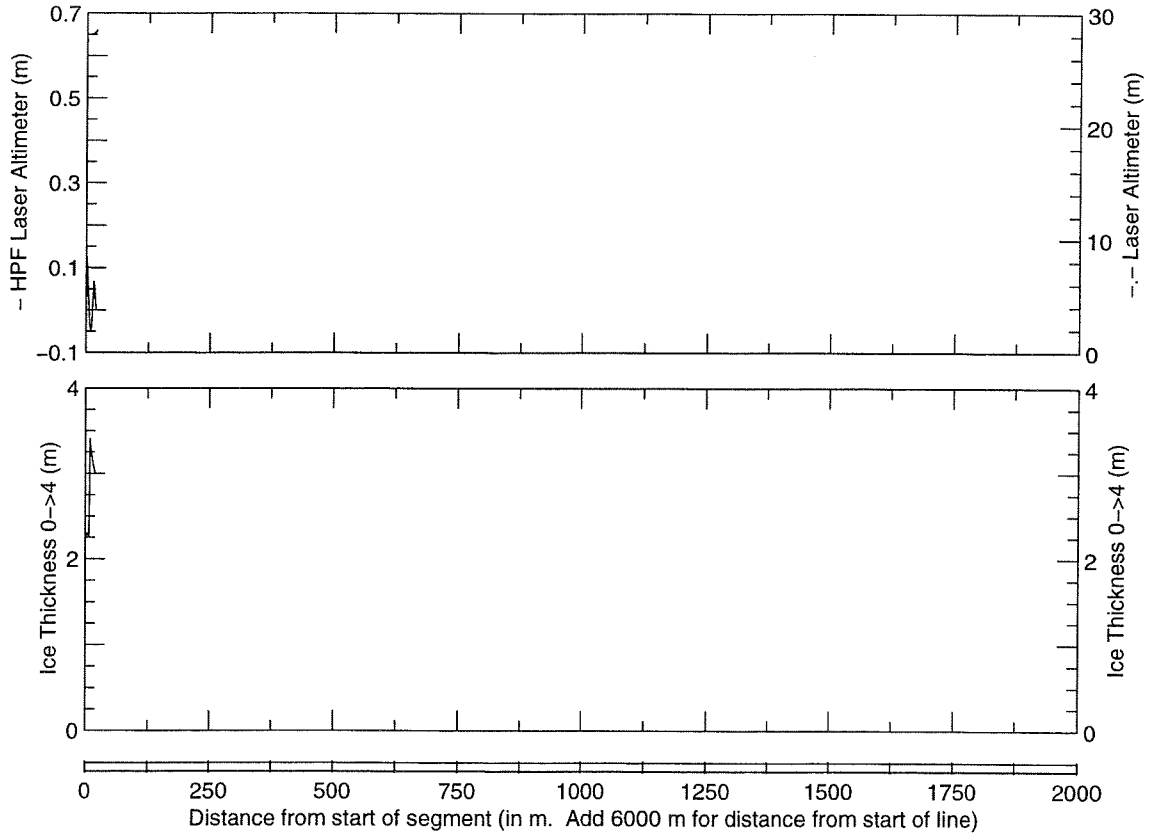

MAY 01 Flight #09 Line #10012 part 1 of 1

Line Starting Coordinates (74.5530,–96.9599) ending at (74.5694,–96.9537)

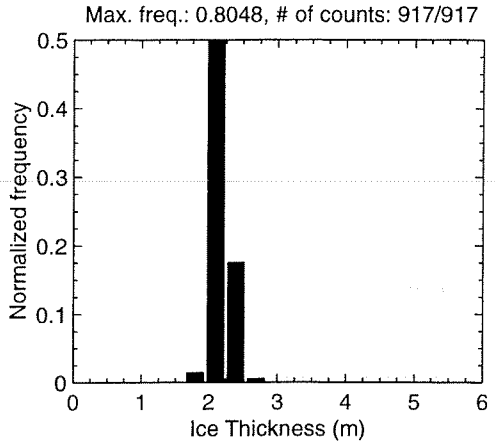

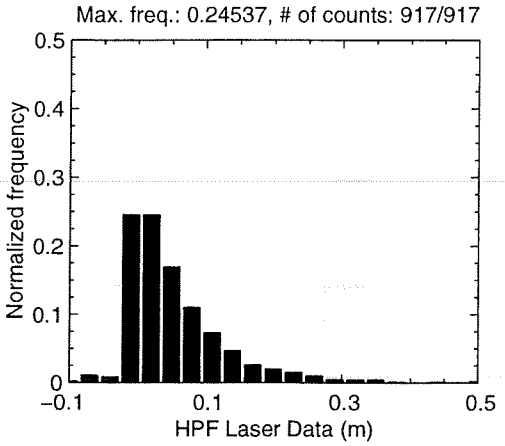

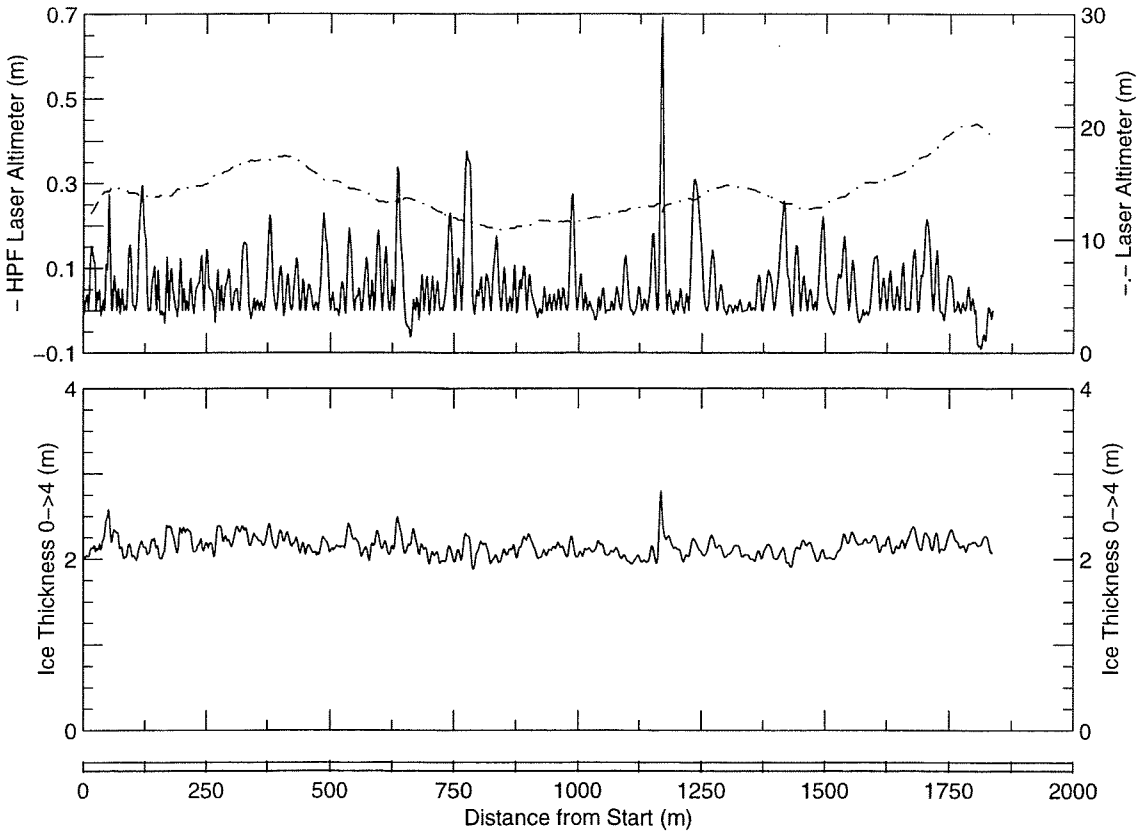

MAY 01 Flight #09 Line #10013 part 1 of 1

Line Starting Coordinates (74.5694,–96.9537) ending at (74.5753,–96.9585)

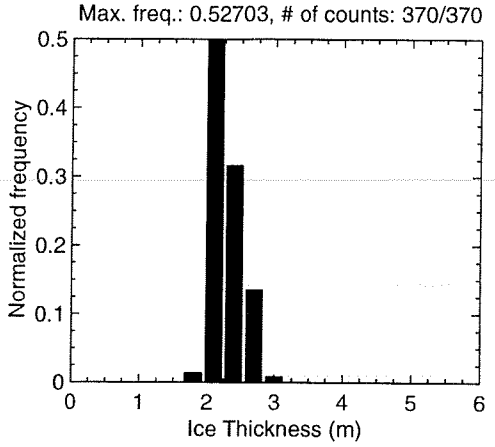

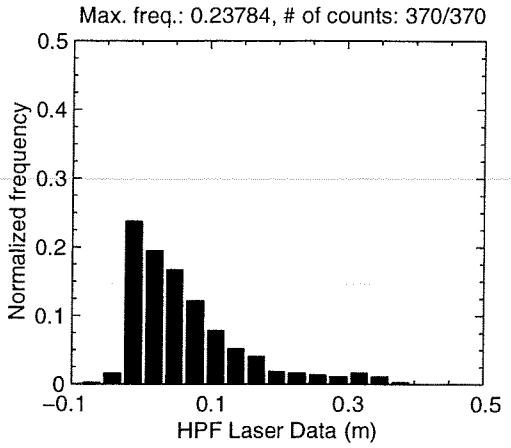

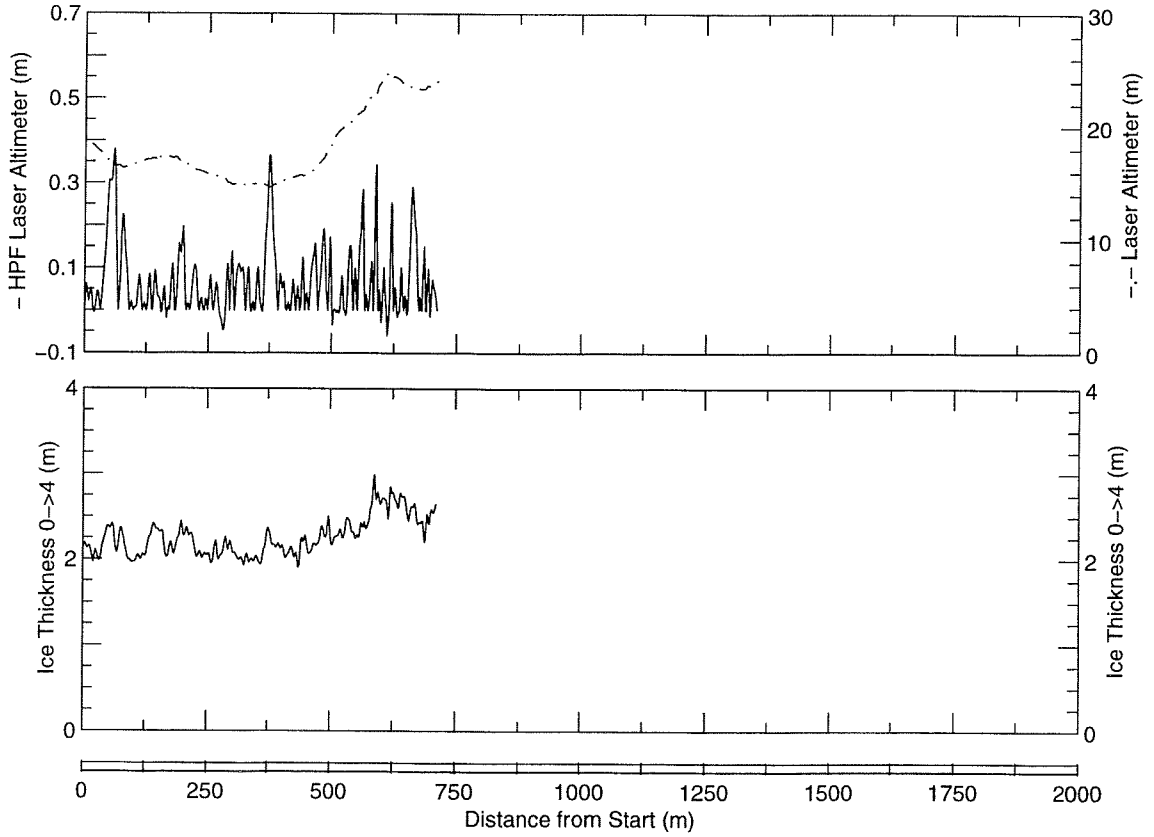

MAY 01 Flight #09 Line #10020 part 1 of 1

Line Starting Coordinates (74.5721,–96.9501) ending at (74.5601,–96.9560)

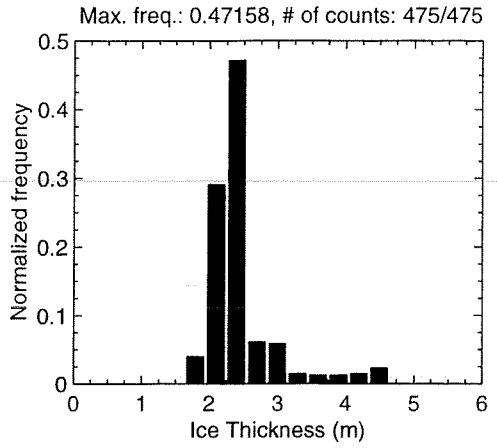

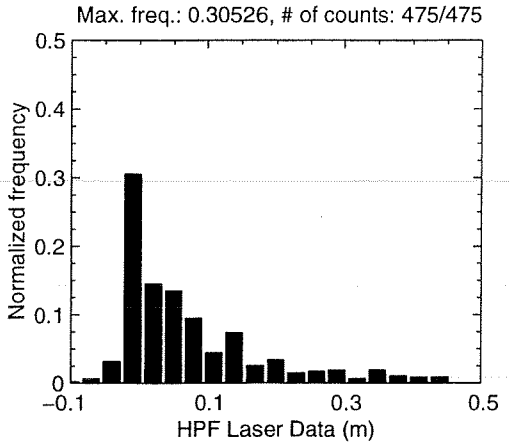

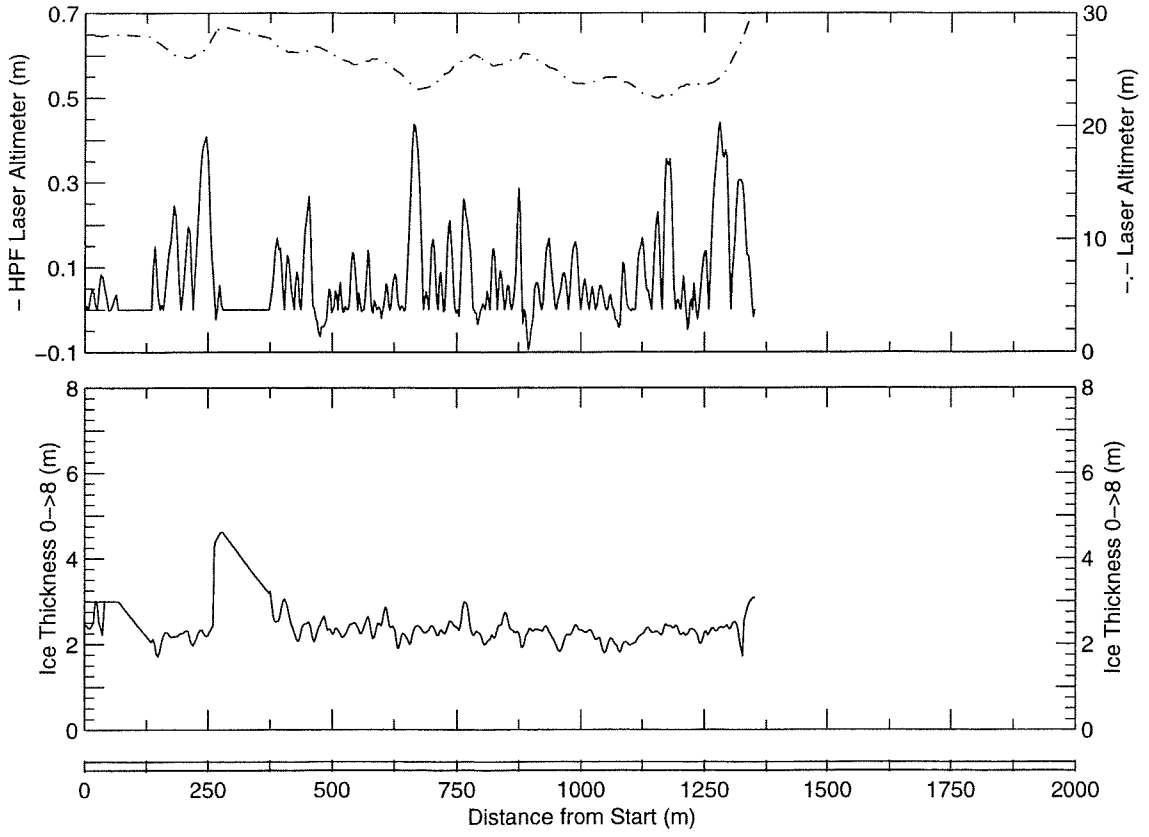

MAY 01 Flight #09 Line #10031 part 1 of 1

Line Starting Coordinates (74.5522,−96.9589) ending at (74.5686,−96.9525)

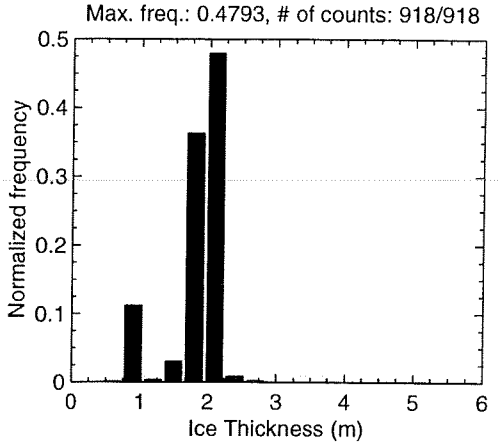

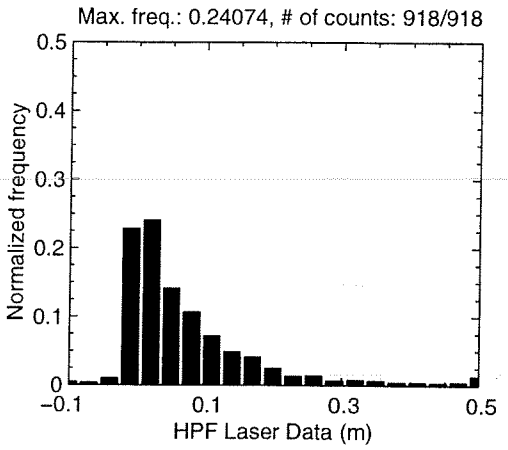

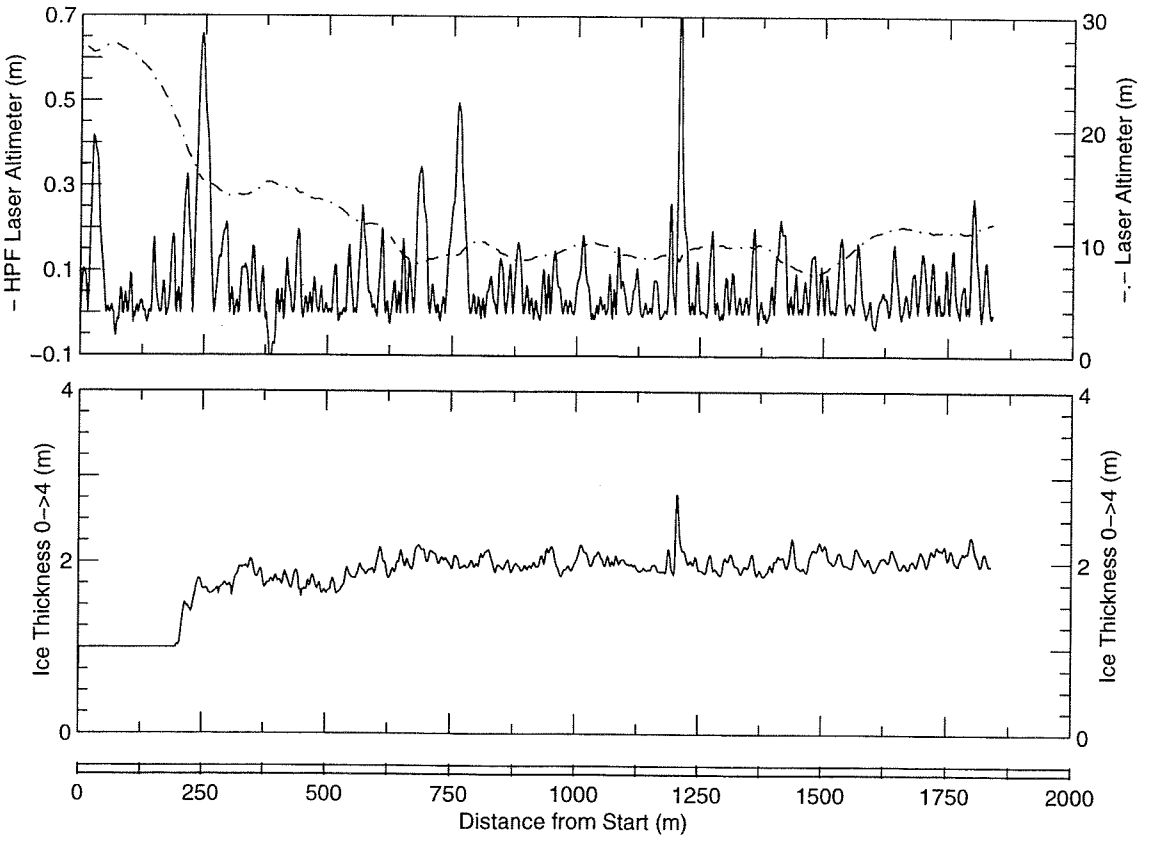

MAY 01 Flight #09 Line #10032 part 1 of 1

Line Starting Coordinates (74.5687,–96.9525) ending at (74.5757,–96.9619)

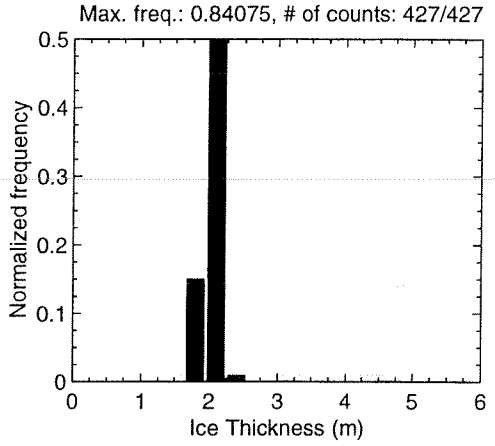

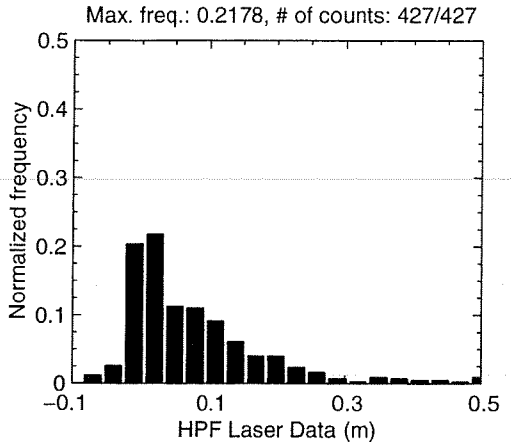

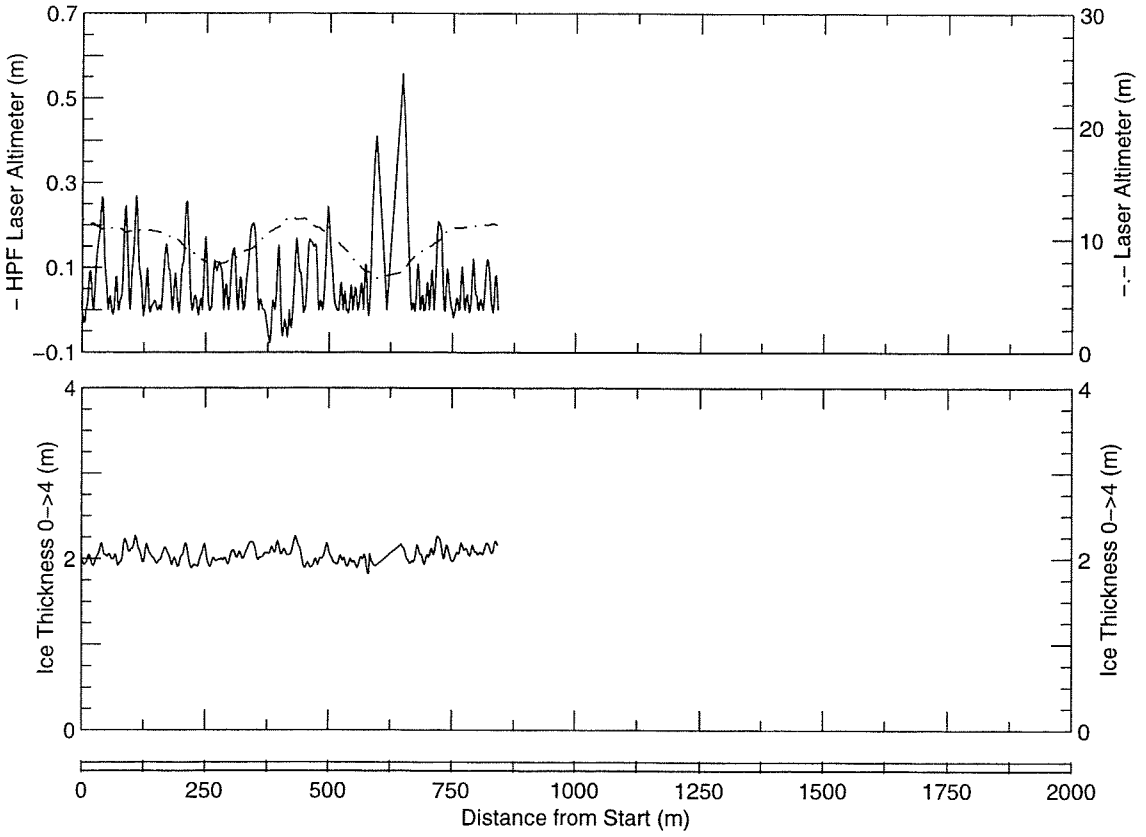

MAY 01 Flight #09 Line #10033 part 1 of 1

Line Starting Coordinates (74.5757,−96.9619) ending at (74.5796,−96.9493)

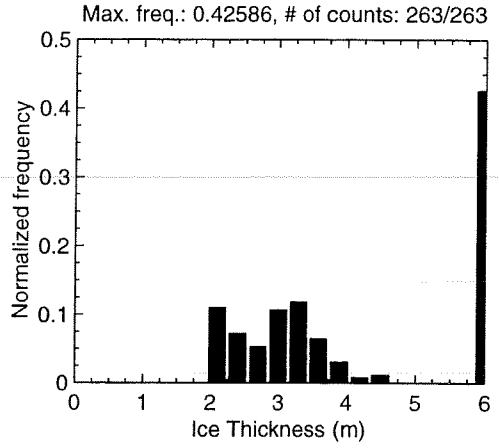

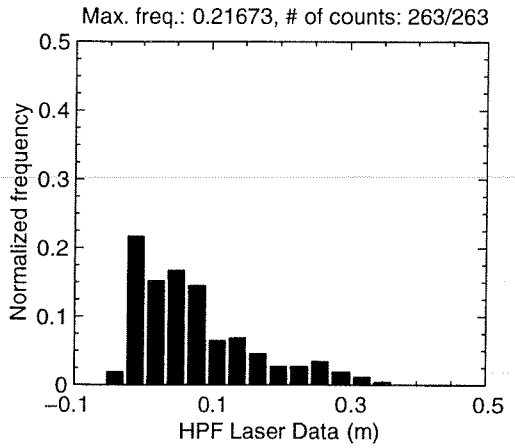

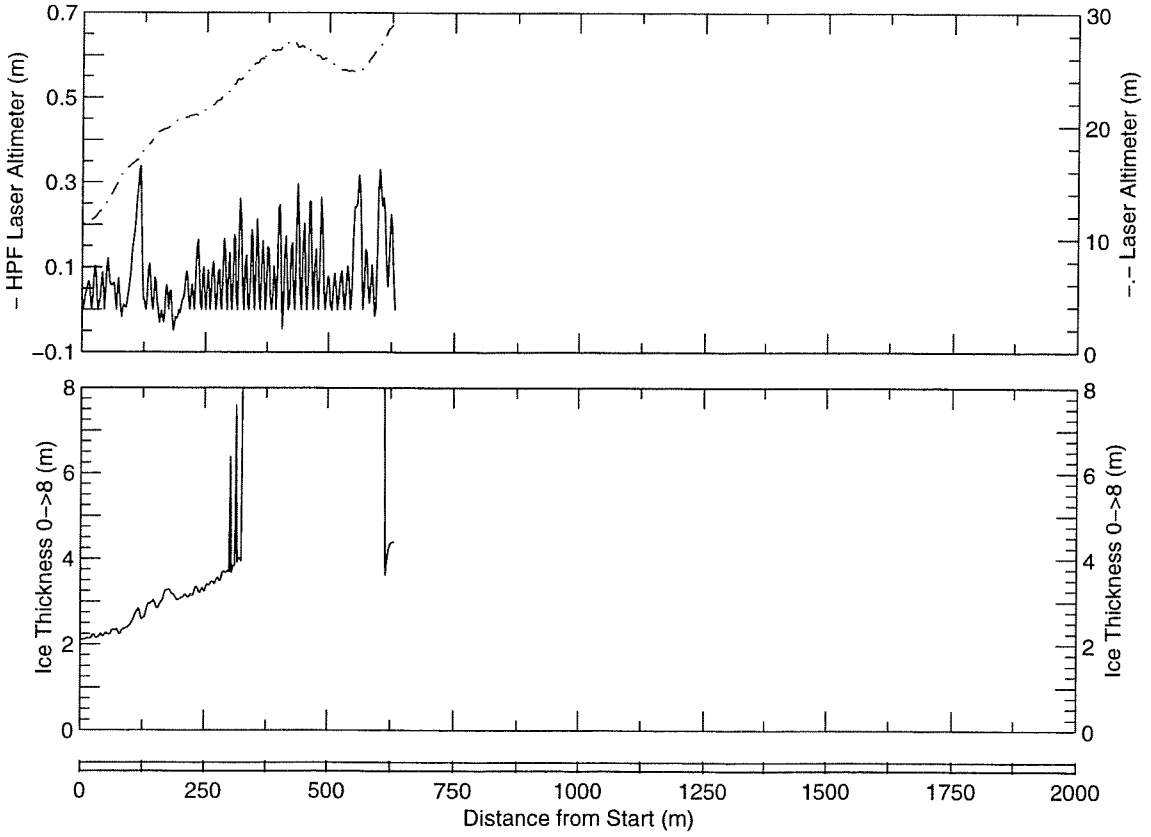

MAY 01 Flight #09 Line #10041 part 1 of 1

Line Starting Coordinates (74.5710,–96.9485) ending at (74.5561,–96.9560)

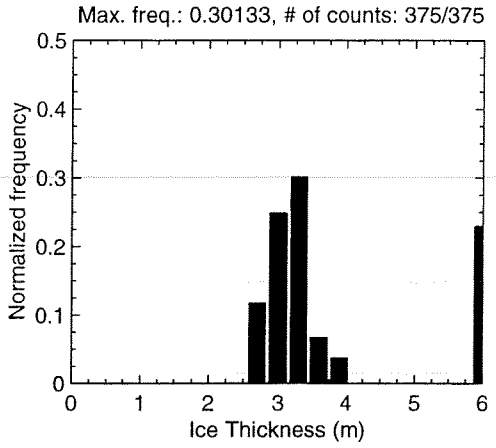

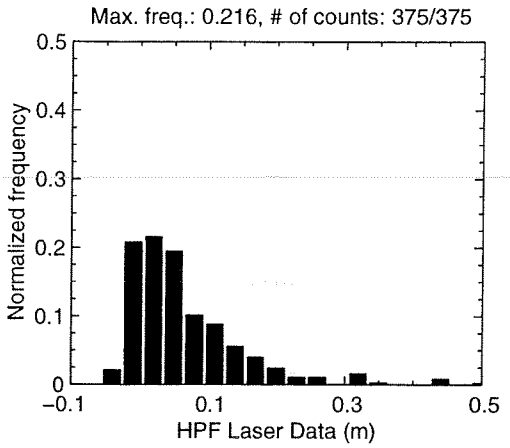

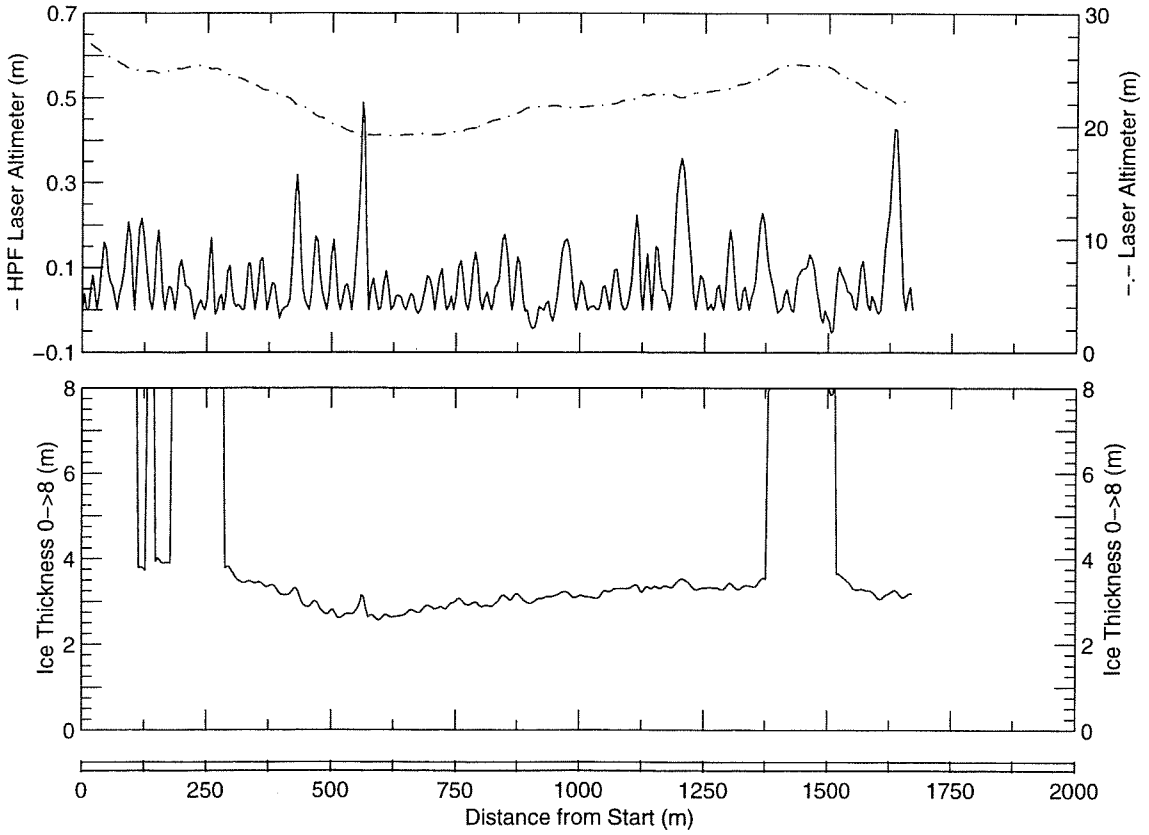

MAY 01 Flight #09 Line #10042 part 1 of 1

Line Starting Coordinates (74.5561,–96.9560) ending at (74.5466,–96.9499)

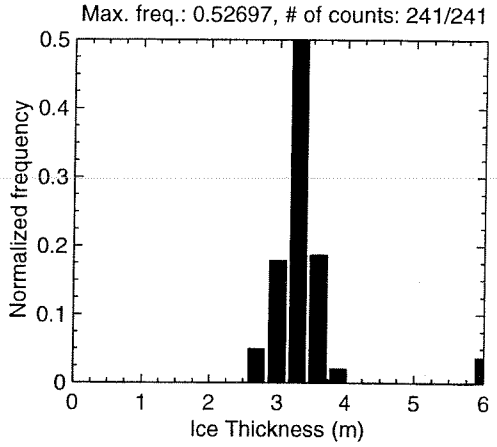

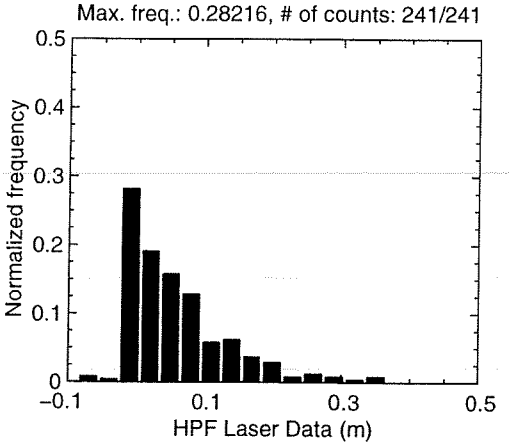

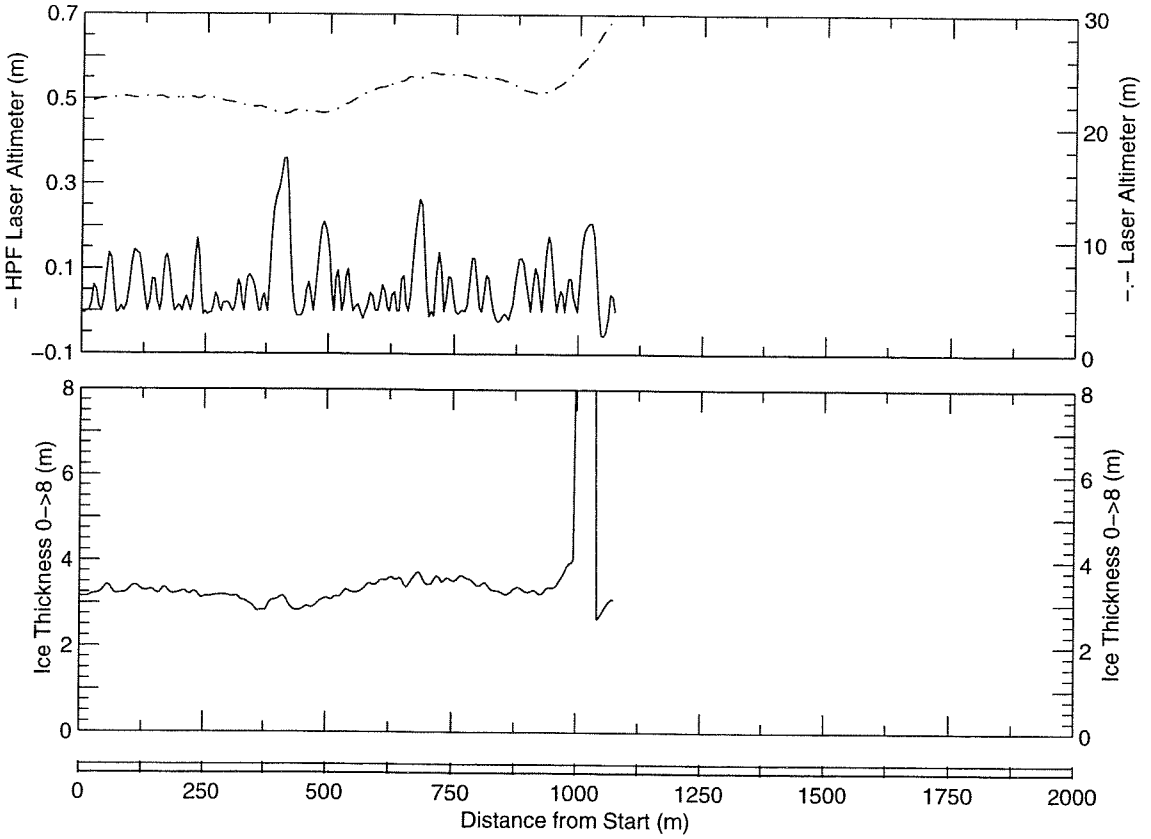

MAY 01 Flight #09 Line #10051 part 1 of 1

Line Starting Coordinates (74.5391,–96.9513) ending at (74.5480,–96.9618)

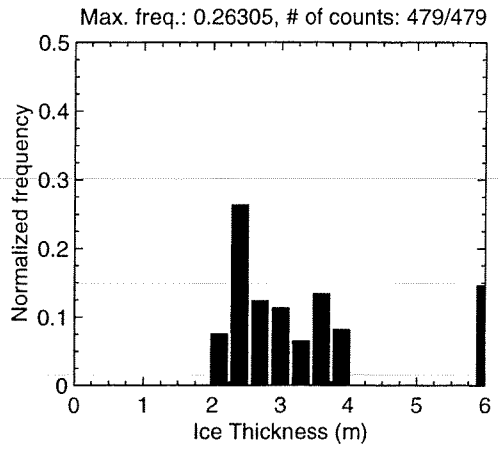

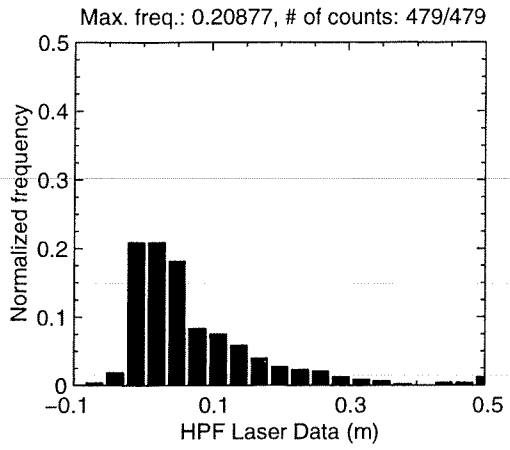

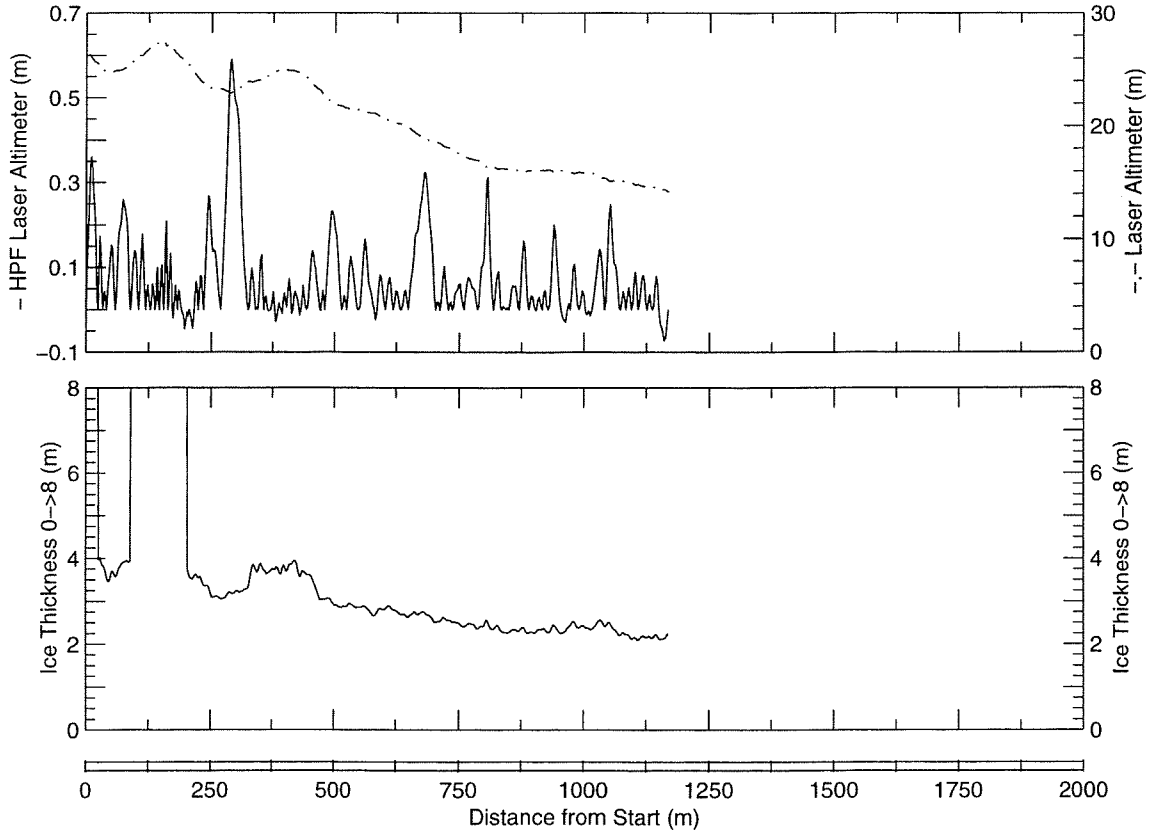

MAY 01 Flight #09 Line #10052 part 1 of 2

Line Starting Coordinates (74.5480,-96.9618) ending at (74.5659,-96.9539)

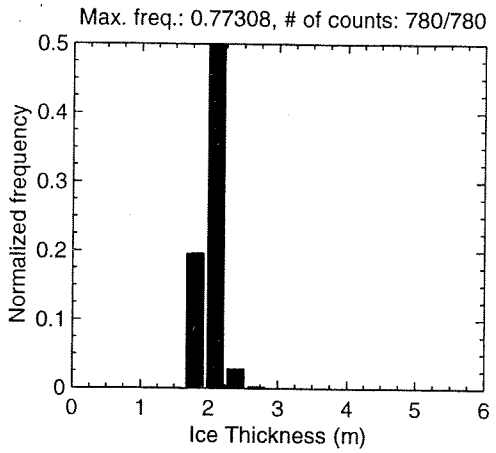

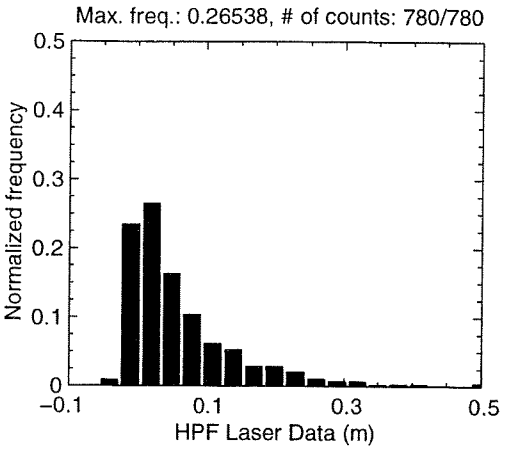

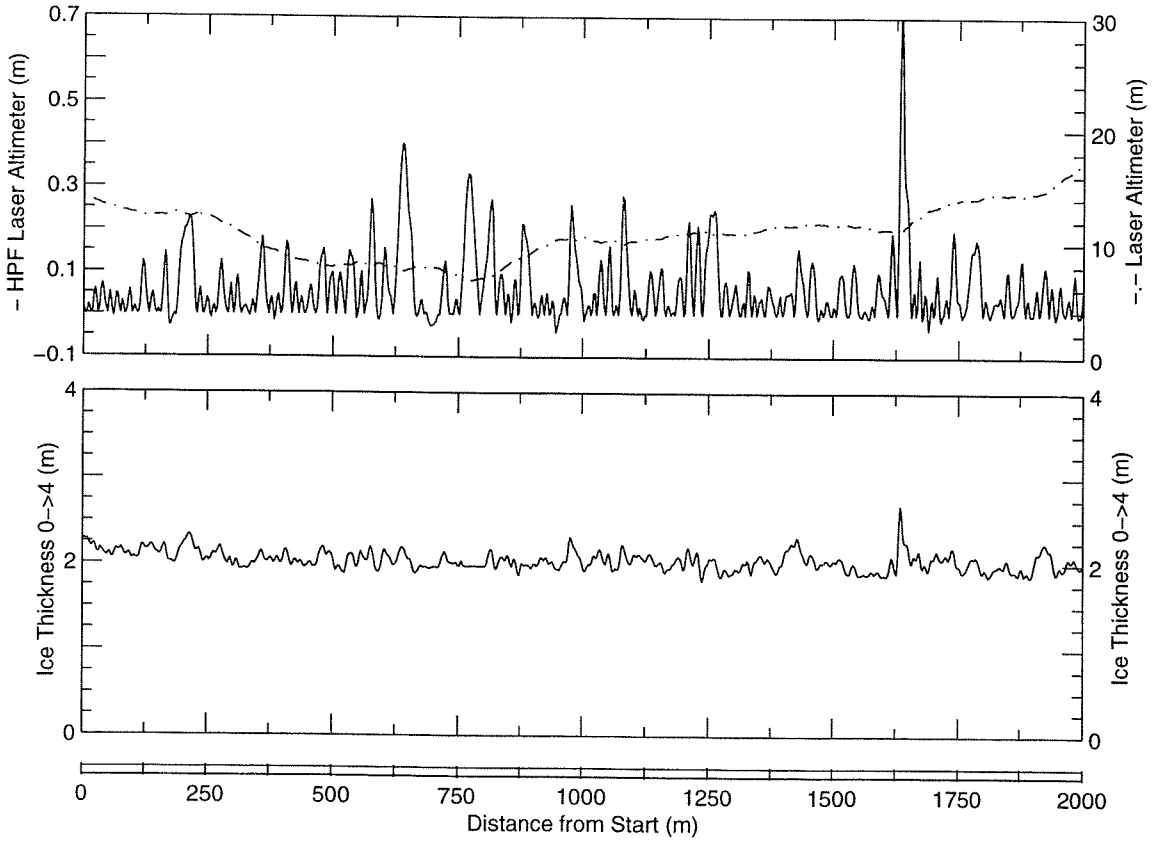

MAY 01 Flight #09 Line #10052 part 2 of 2

Line Starting Coordinates (74.5659,–96.9539) ending at (74.5684,–96.9530)

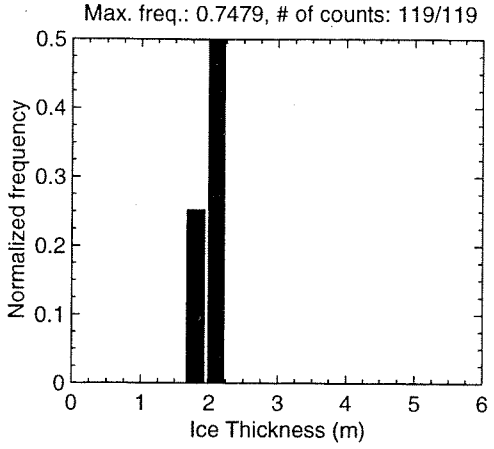

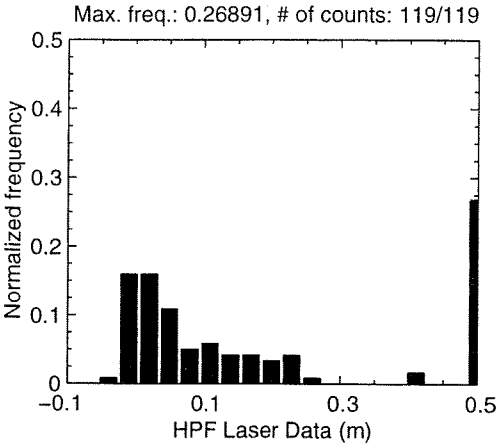

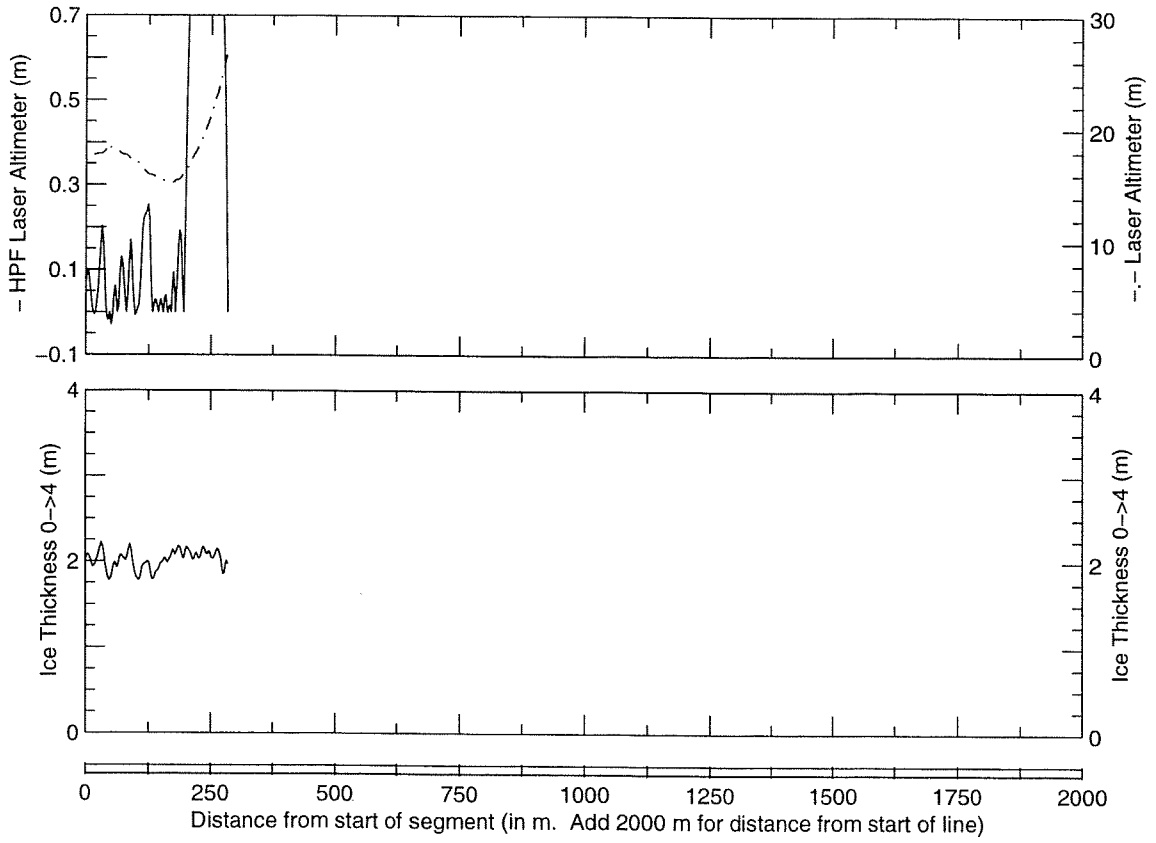

MAY 01 Flight #09 Line #10061 part 1 of 1

Line Starting Coordinates (74.5426,–96.9621) ending at (74.5453,–96.9636)

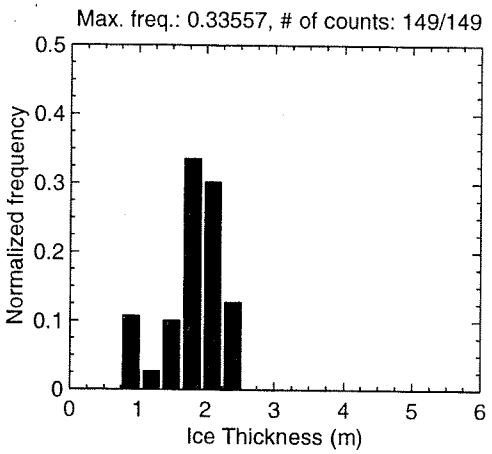

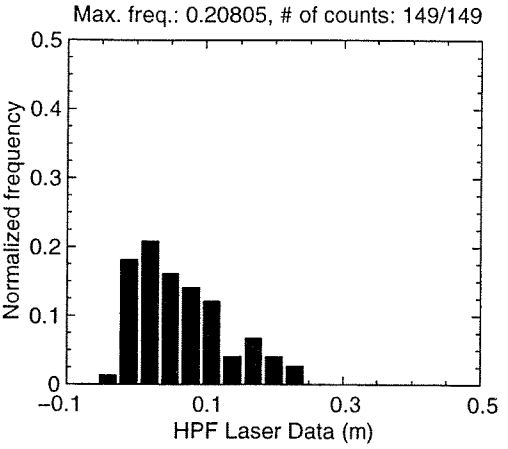

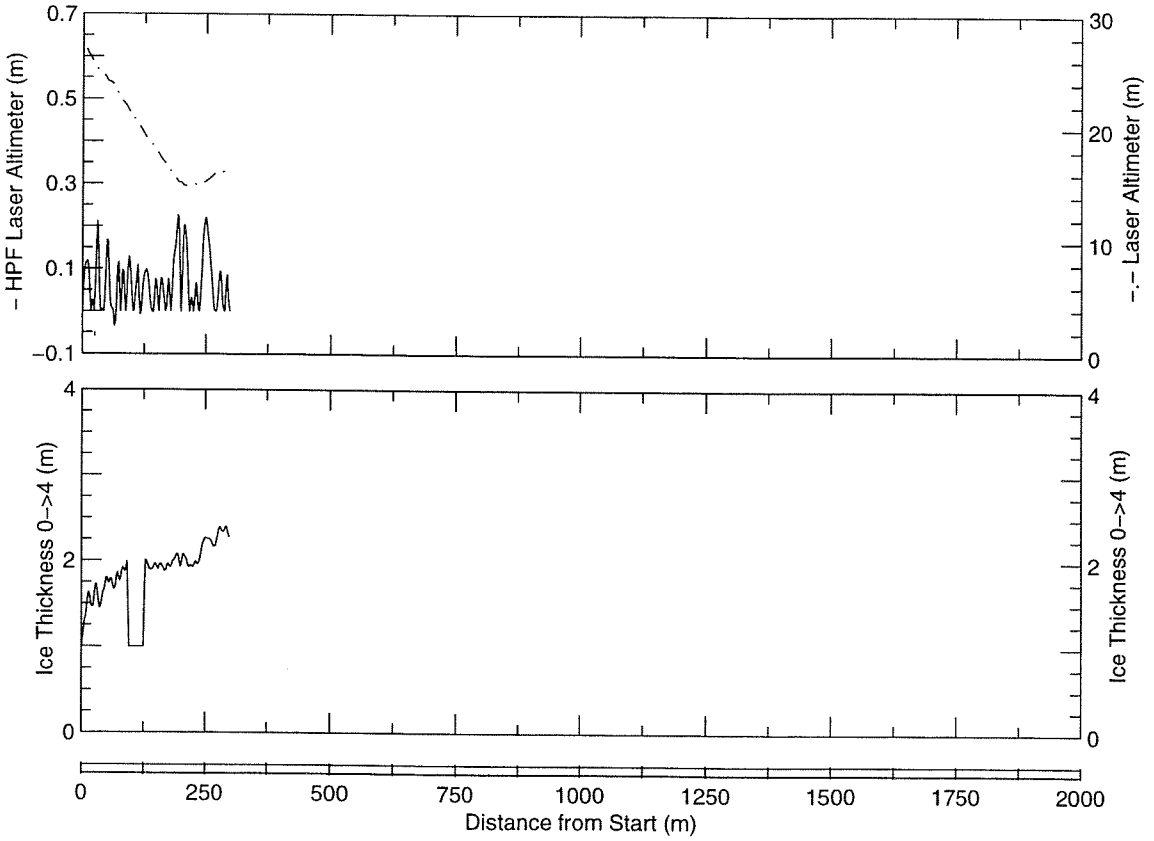

MAY 01 Flight #09 Line #10062 part 1 of 2

Line Starting Coordinates (74.5453,–96.9636) ending at (74.5631,–96.9553)

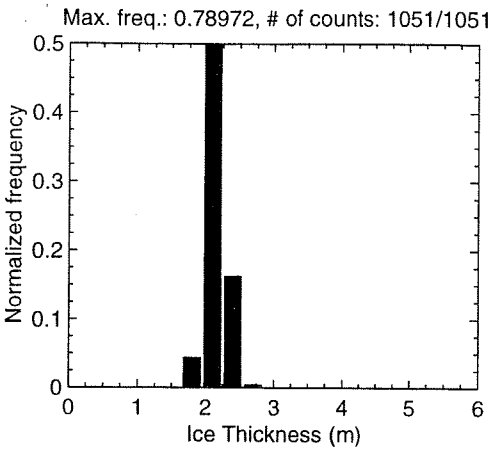

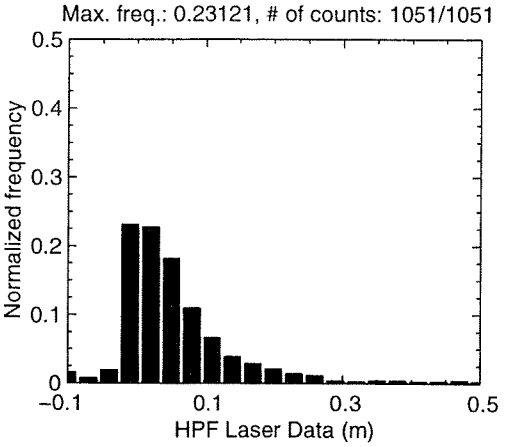

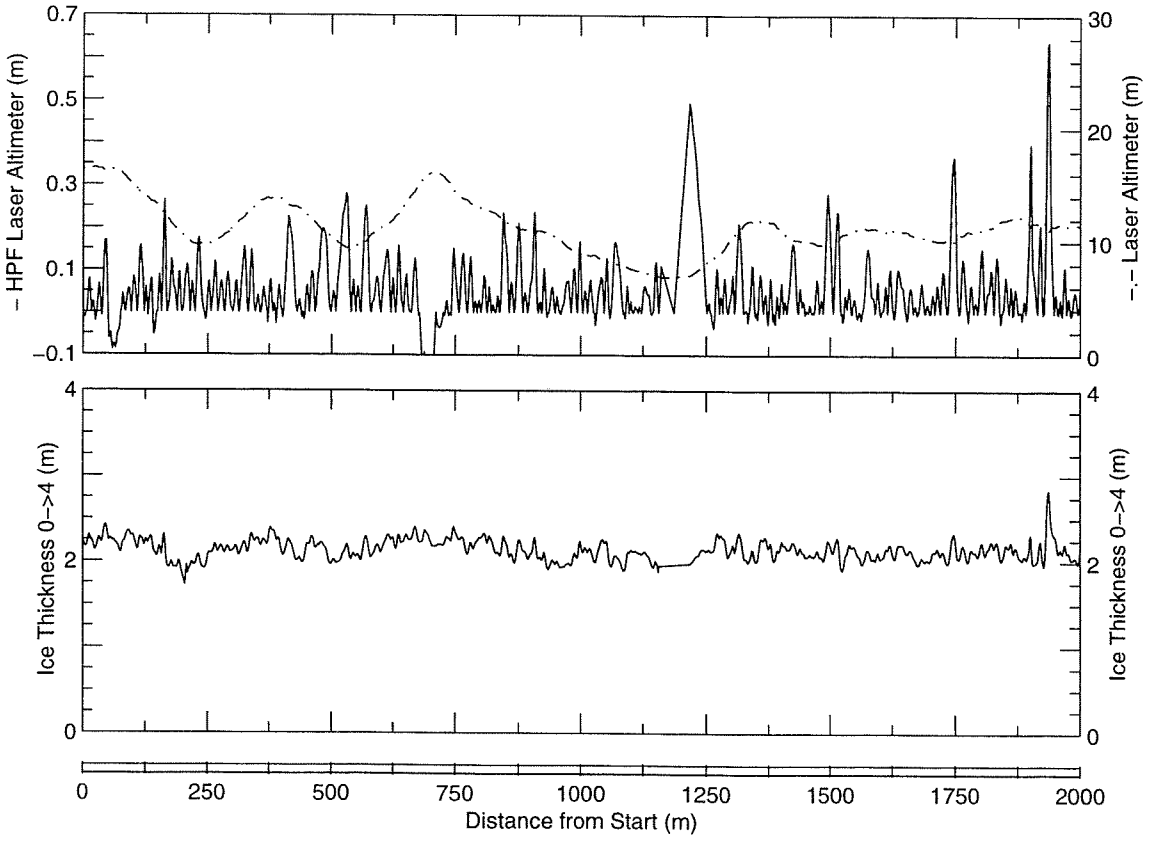

MAY 01 Flight #09 Line #10062 part 2 of 2

Line Starting Coordinates (74.5631,–96.9553) ending at (74.5674,–96.9538)

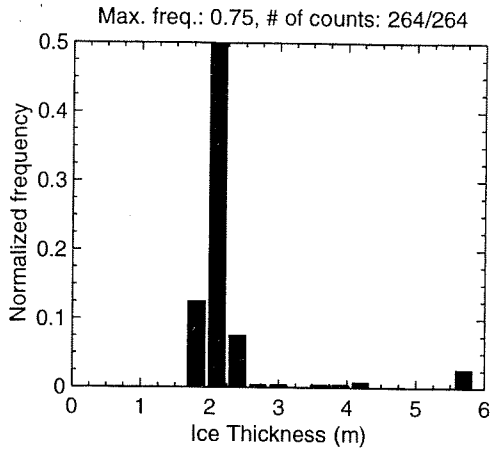

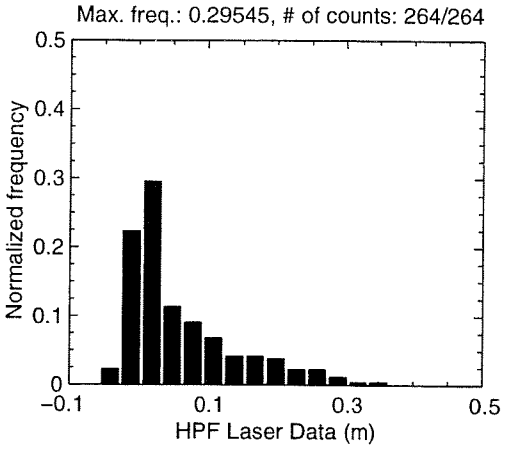

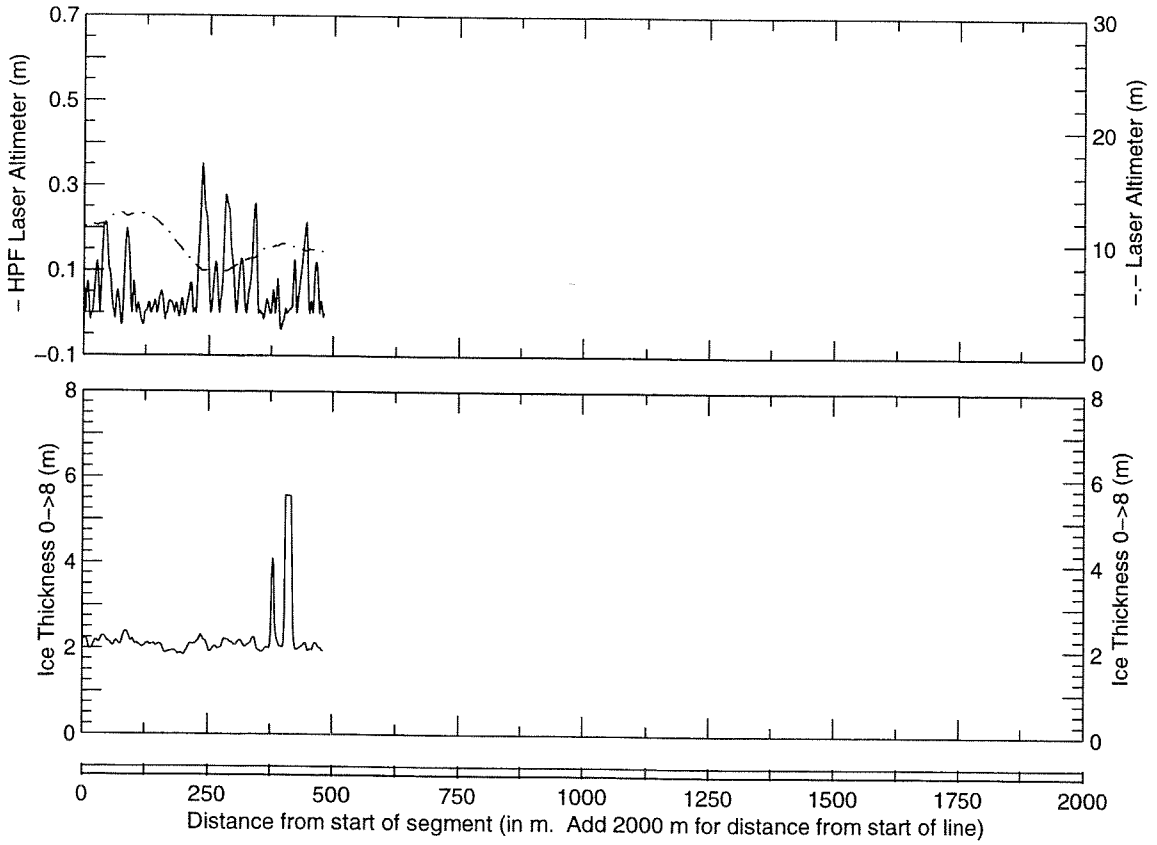

MAY 01 Flight #09 Line #10063 part 1 of 1

Line Starting Coordinates (74.5674,-96.9538) ending at (74.5767,-96.9603)

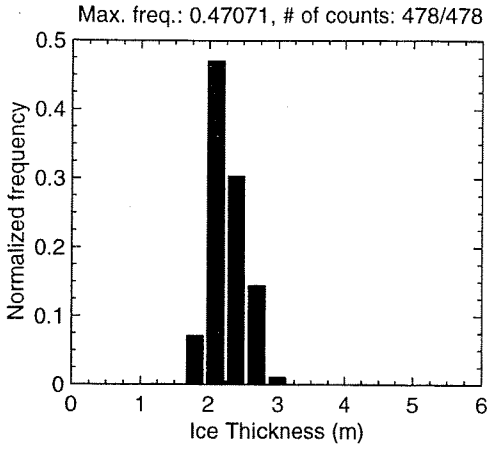

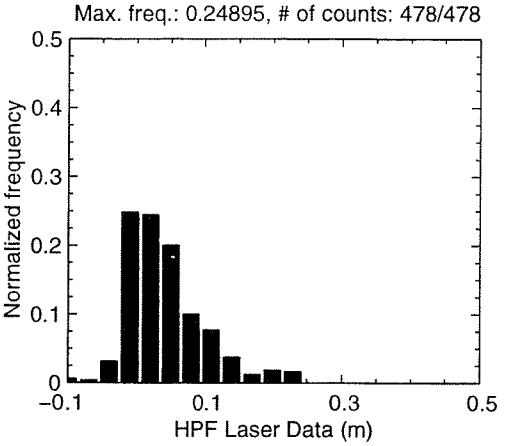

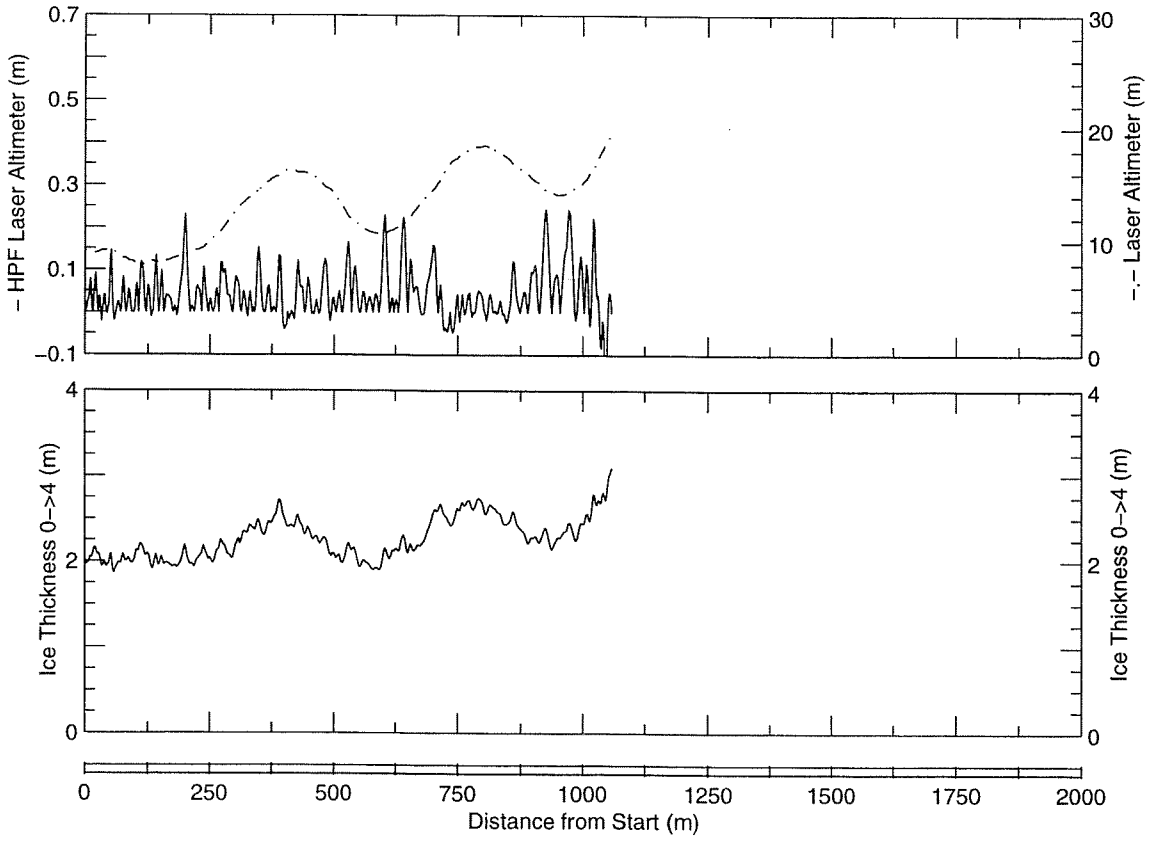

MAY 01 Flight #09 Line #10064 part 1 of 1

Line Starting Coordinates (74.5767,–96.9603) ending at (74.5788,–96.9531)

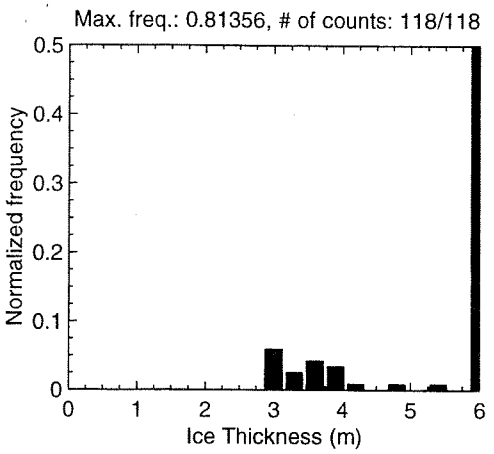

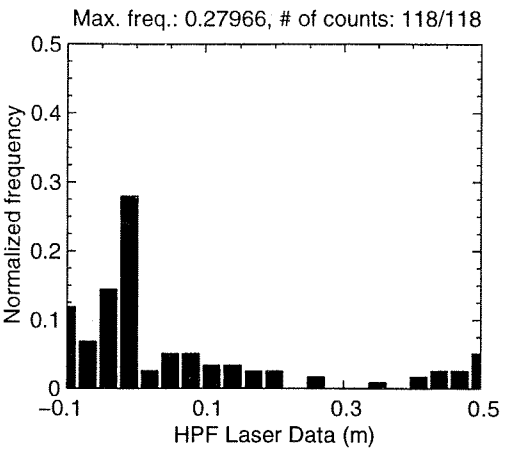

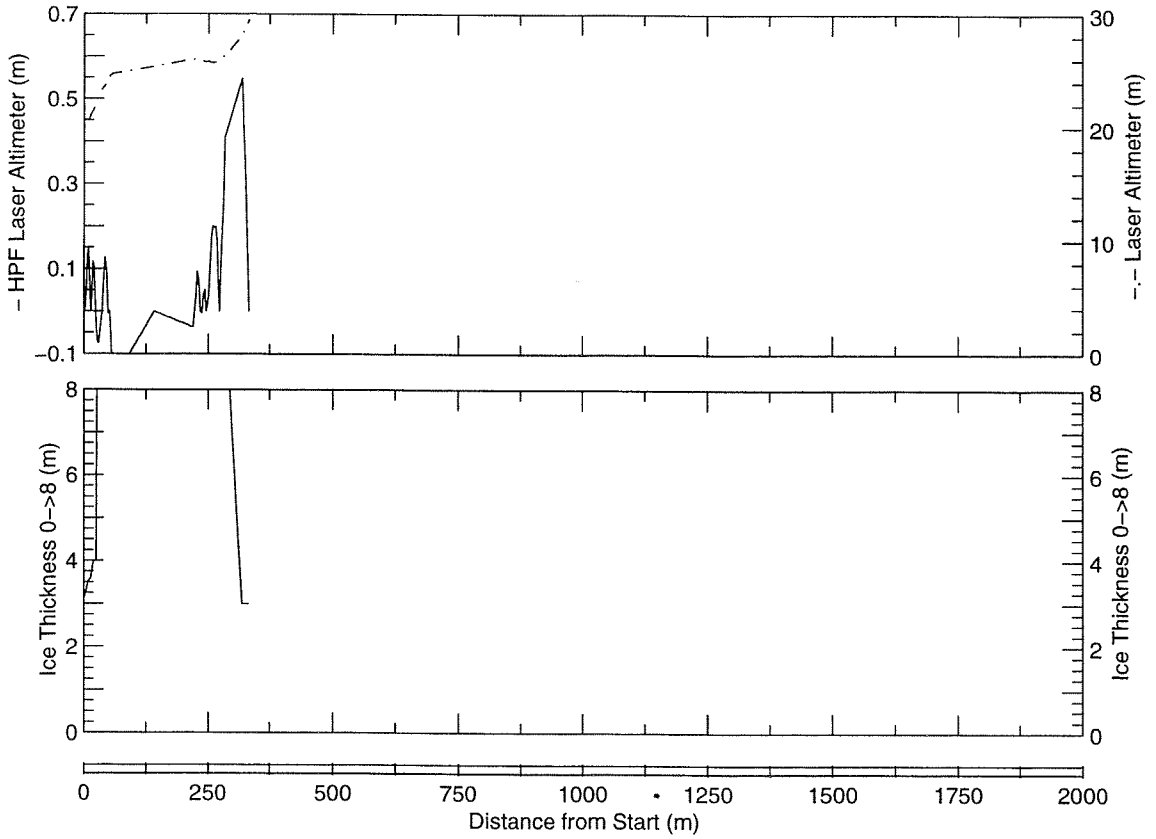

MAY 01 Flight #09 Line #10081 part 1 of 1

Line Starting Coordinates (74.5672,–96.9524) ending at (74.5596,–96.9546)

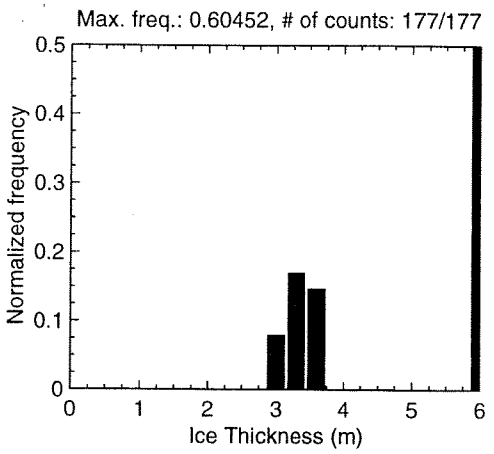

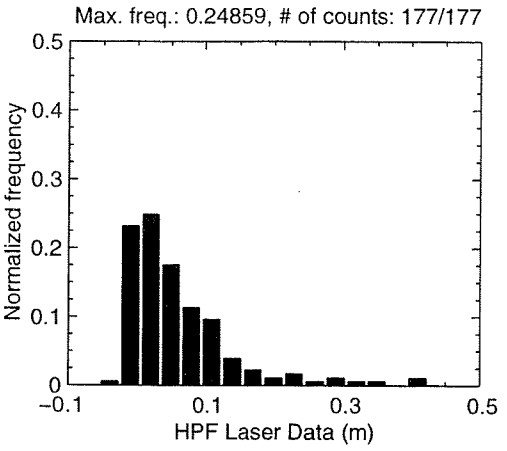

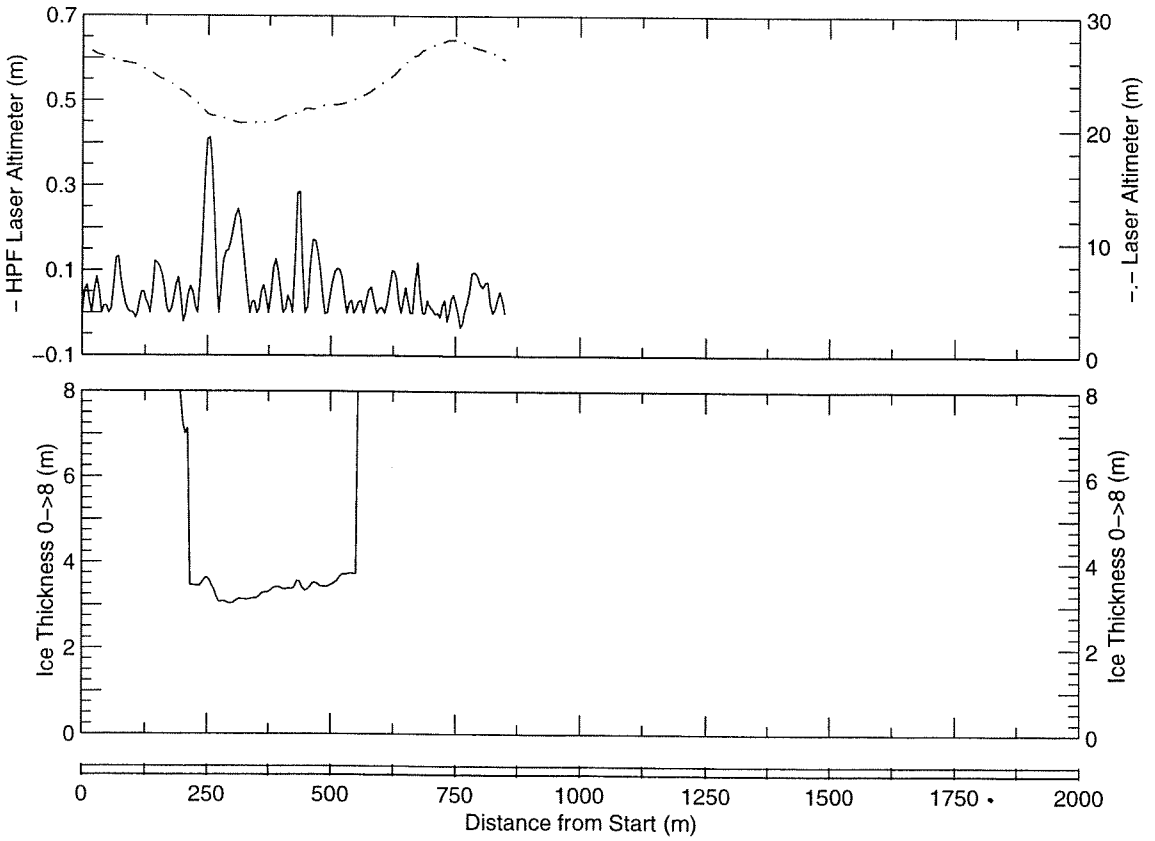

MAY 01 Flight #09 Line #10091 part 1 of 1

Line Starting Coordinates (74.5467,–96.9576) ending at (74.5466,–96.9633)

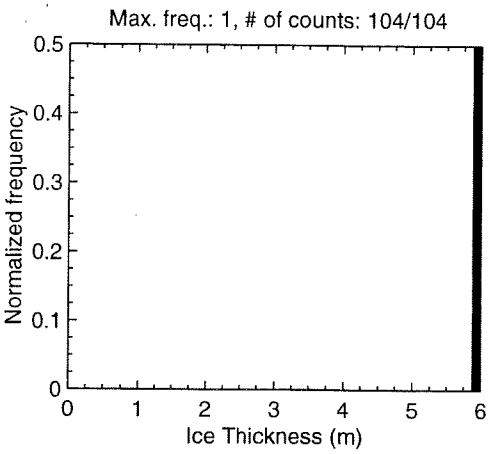

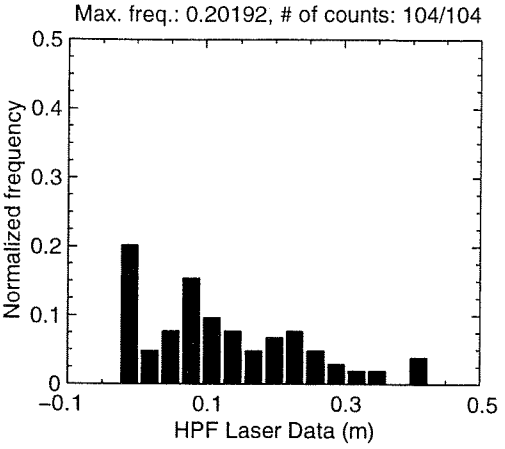

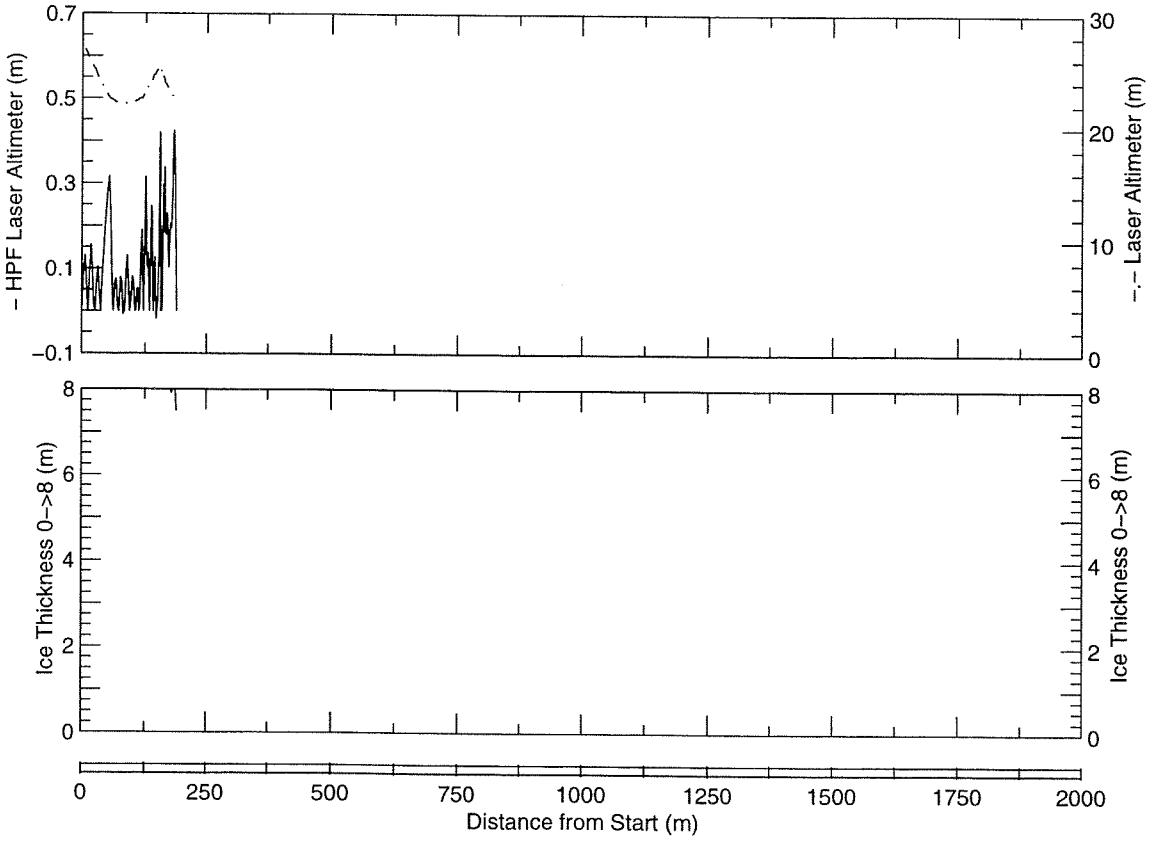

MAY 01 Flight #09 Line #10092 part 1 of 2

Line Starting Coordinates (74.5467,–96.9633) ending at (74.5643,–96.9532)

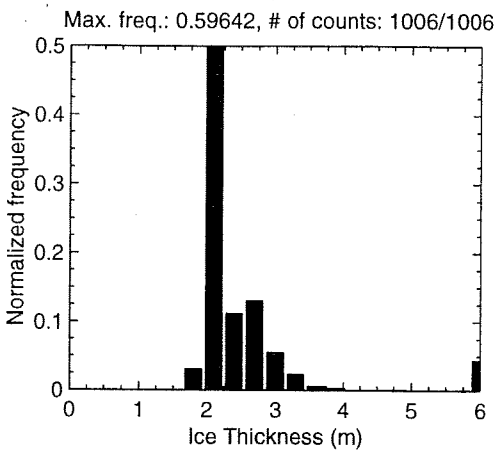

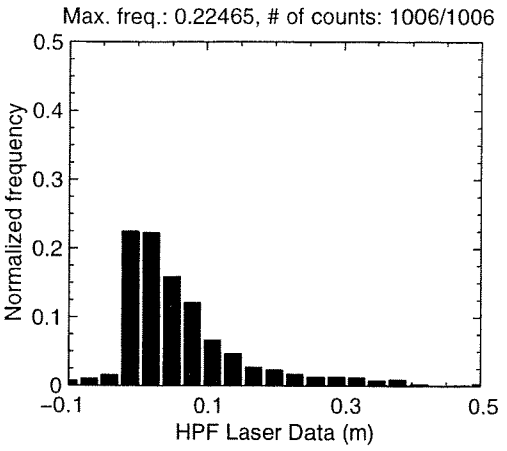

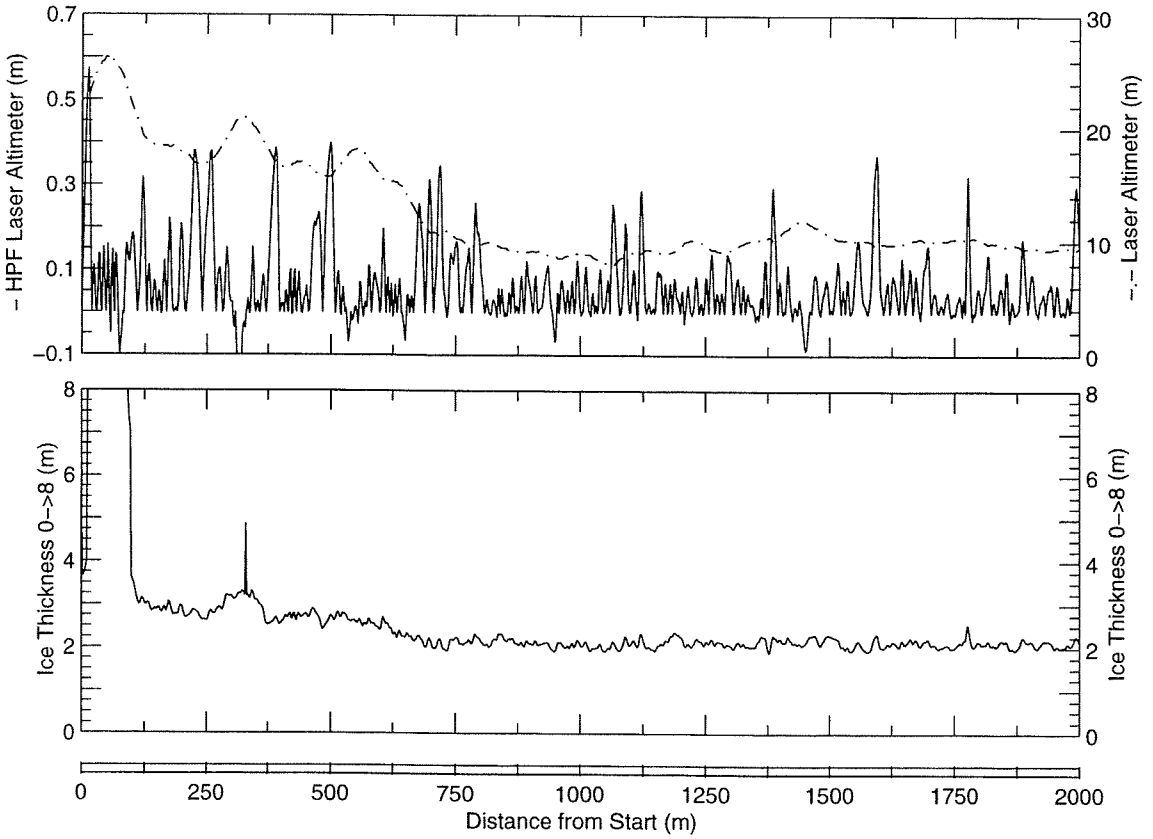

MAY 01 Flight #09 Line #10092 part 2 of 2

Line Starting Coordinates (74.5643,–96.9532) ending at (74.5678,–96.9500)

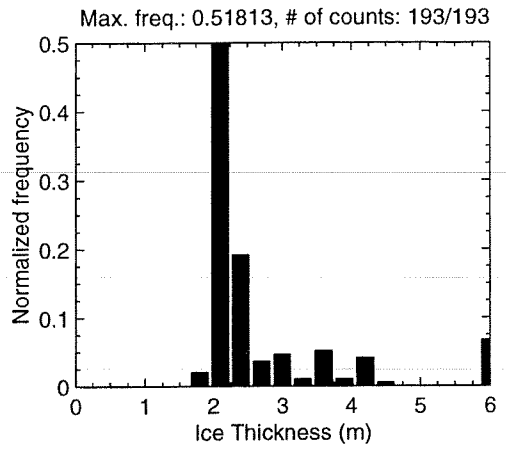

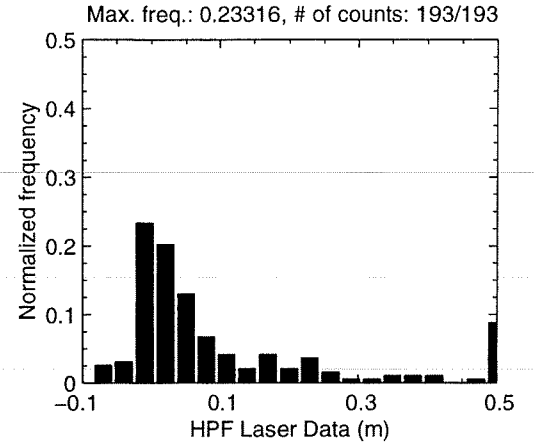

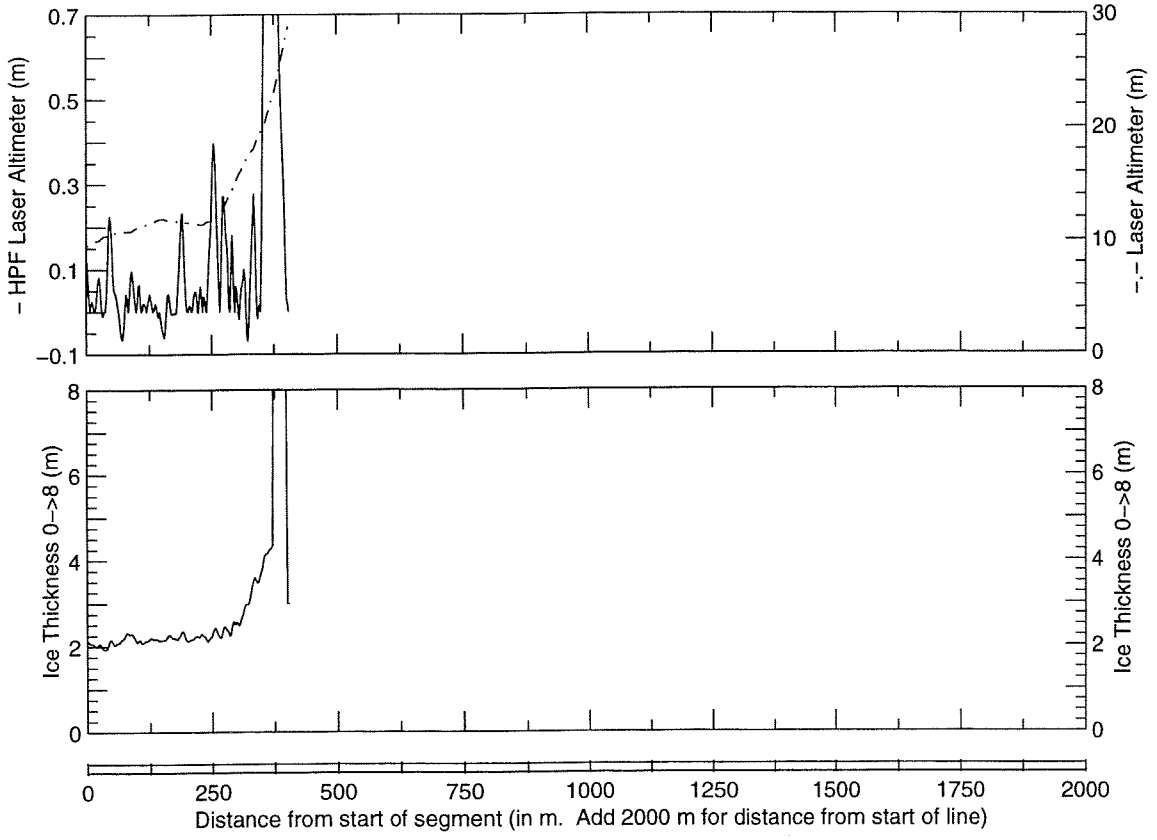

MAY 01 Flight #09 Line #10100 part 1 of 2

Line Starting Coordinates (74.5468,–96.9583) ending at (74.5646,–96.9551)

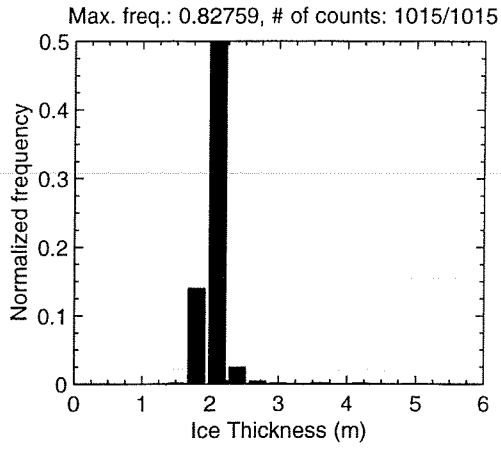

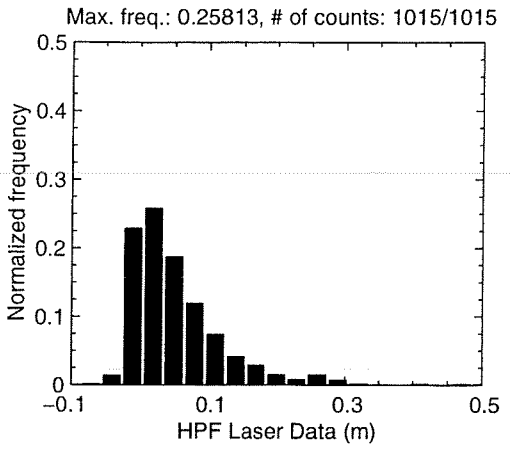

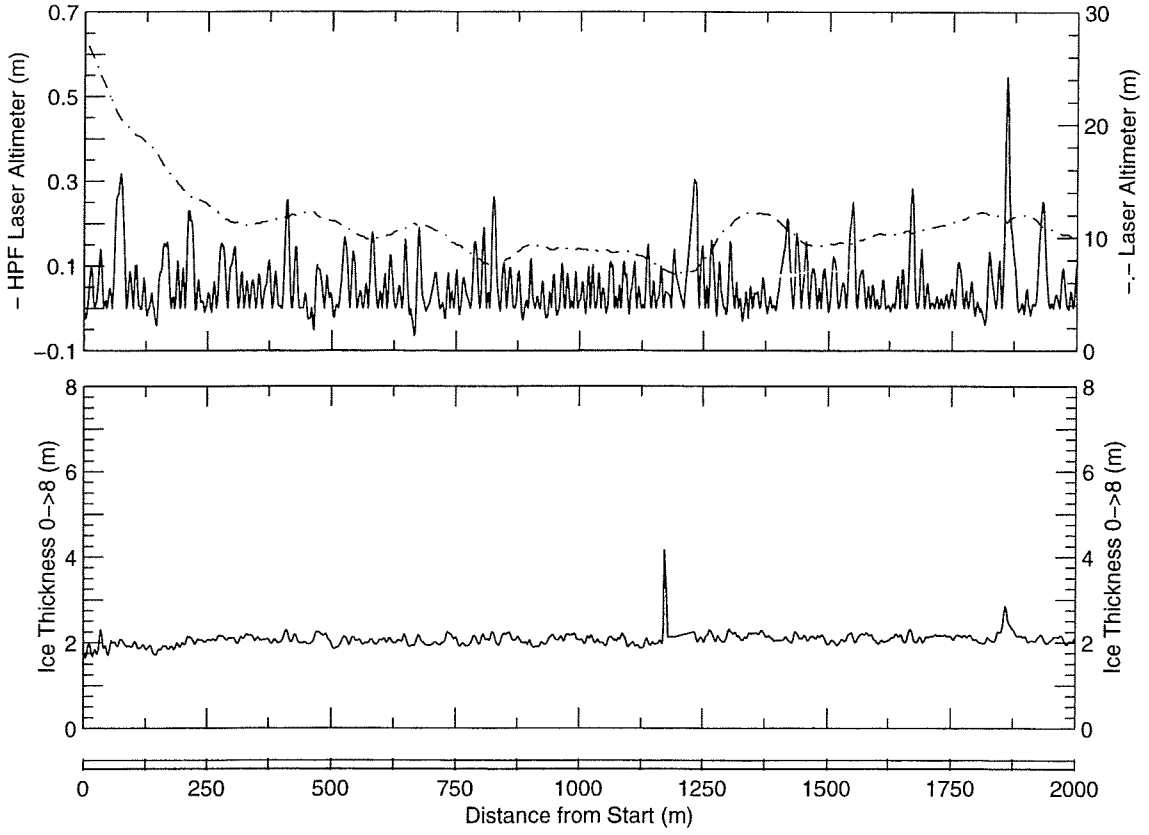

MAY 01 Flight #09 Line #10100 part 2 of 2

Line Starting Coordinates (74.5646,–96.9551) ending at (74.5711,–96.9453)

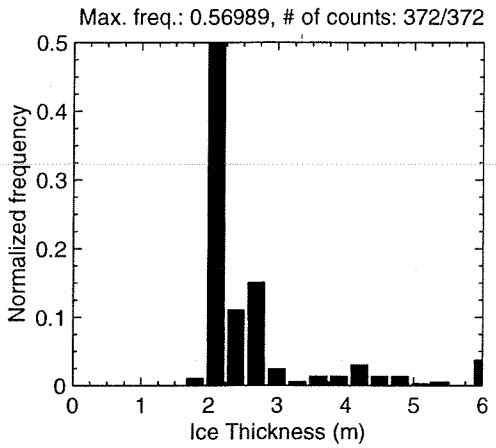

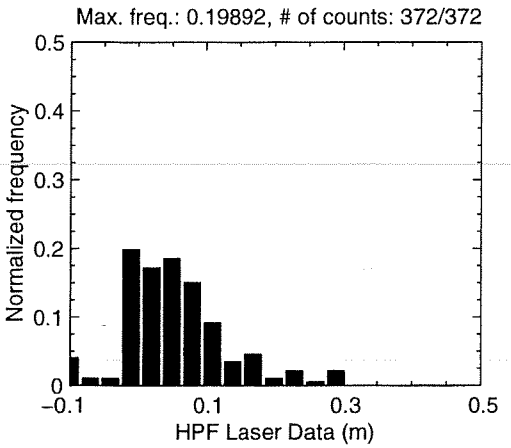

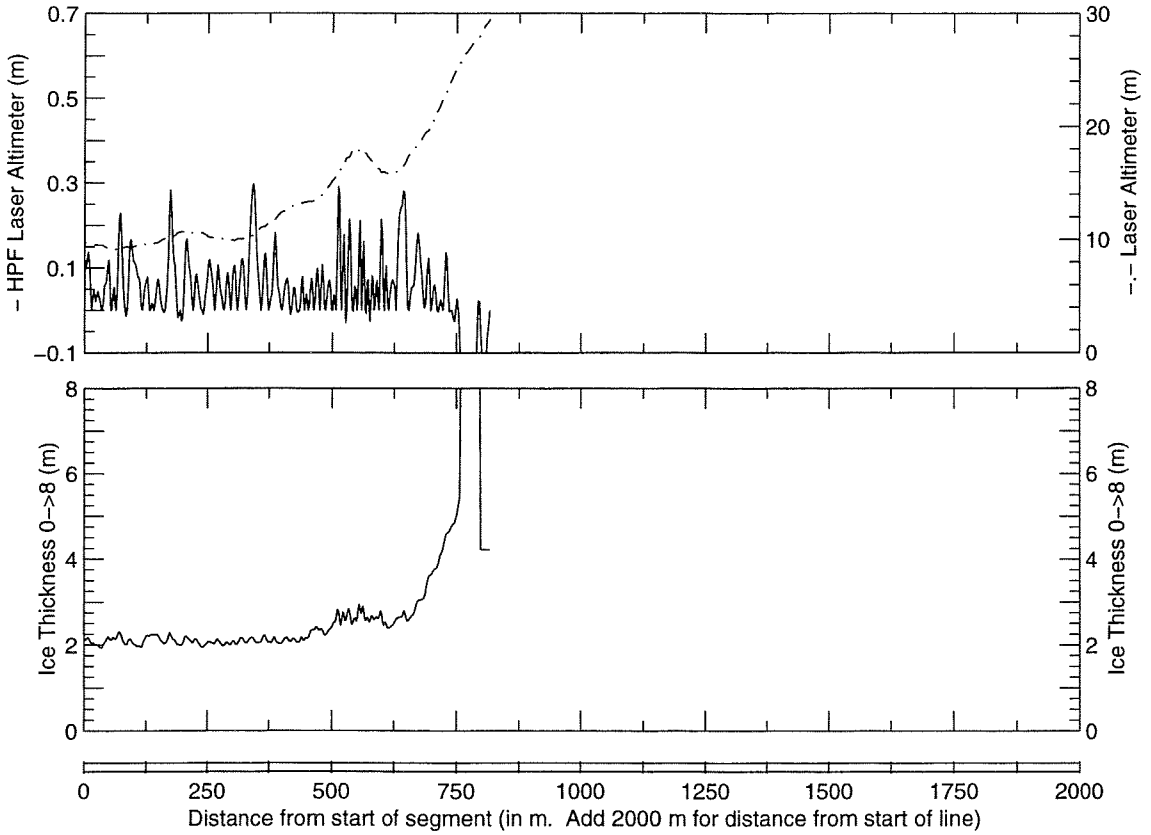

MAY 01 Flight #09 Line #10121 part 1 of 1

Line Starting Coordinates (74.5514,–96.9504) ending at (74.5509,–96.9626)

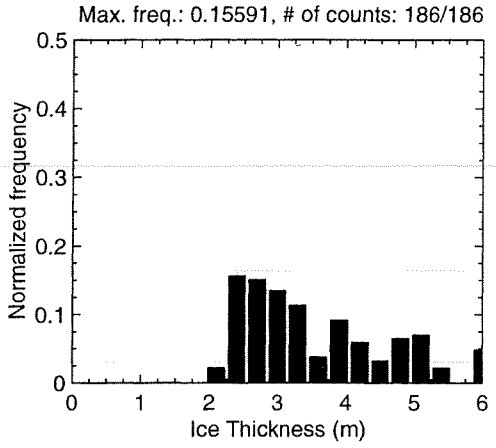

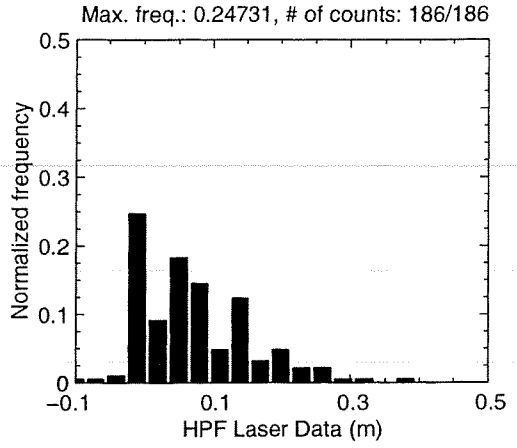

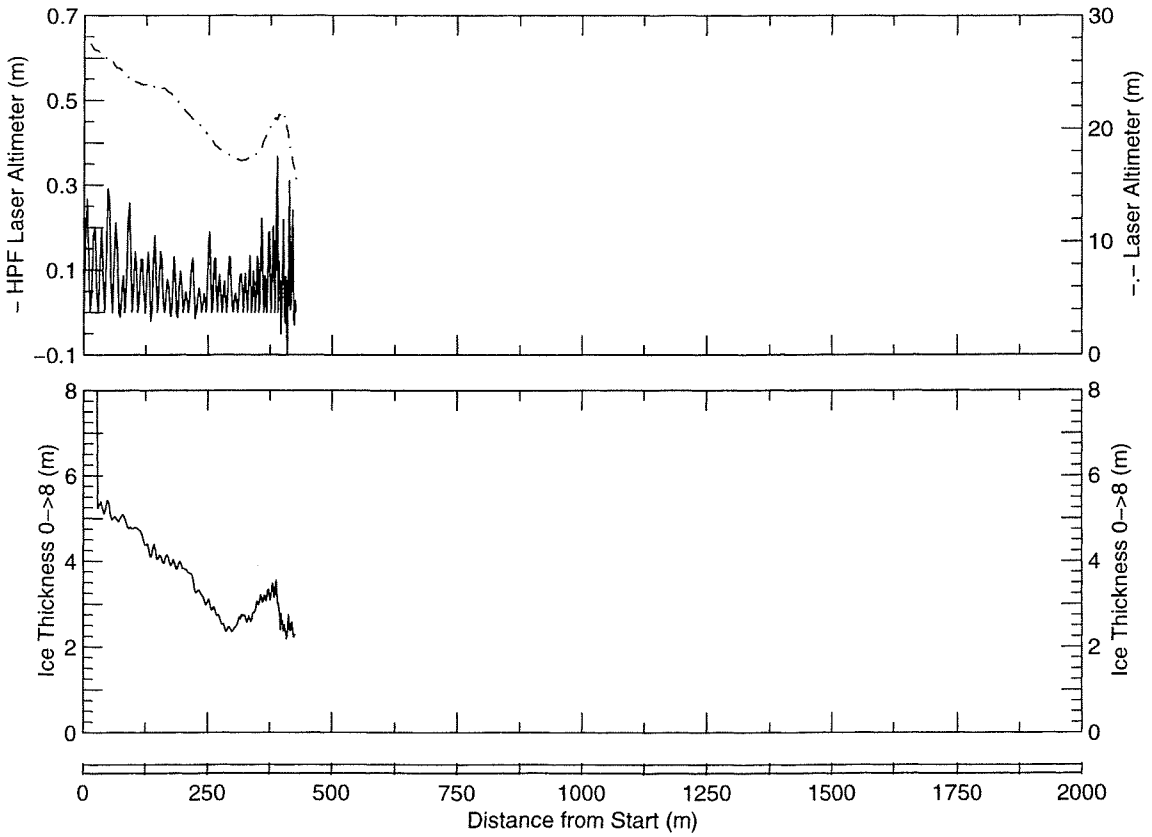

MAY 01 Flight #09 Line #10122 part 1 of 1

Line Starting Coordinates (74.5509,–96.9626) ending at (74.5674,–96.9551)

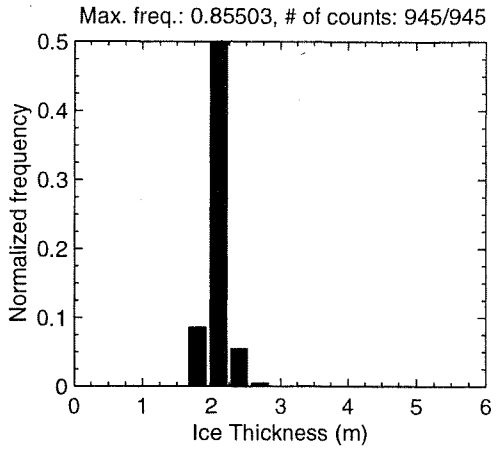

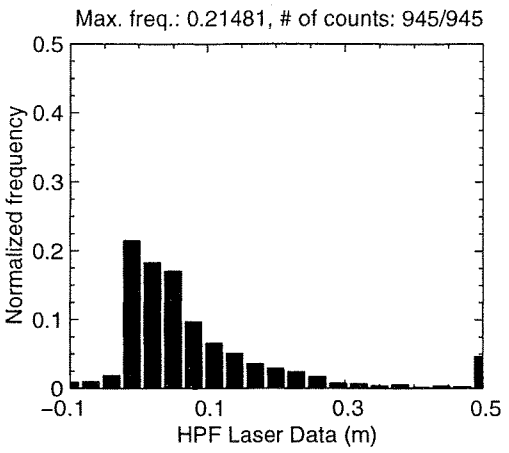

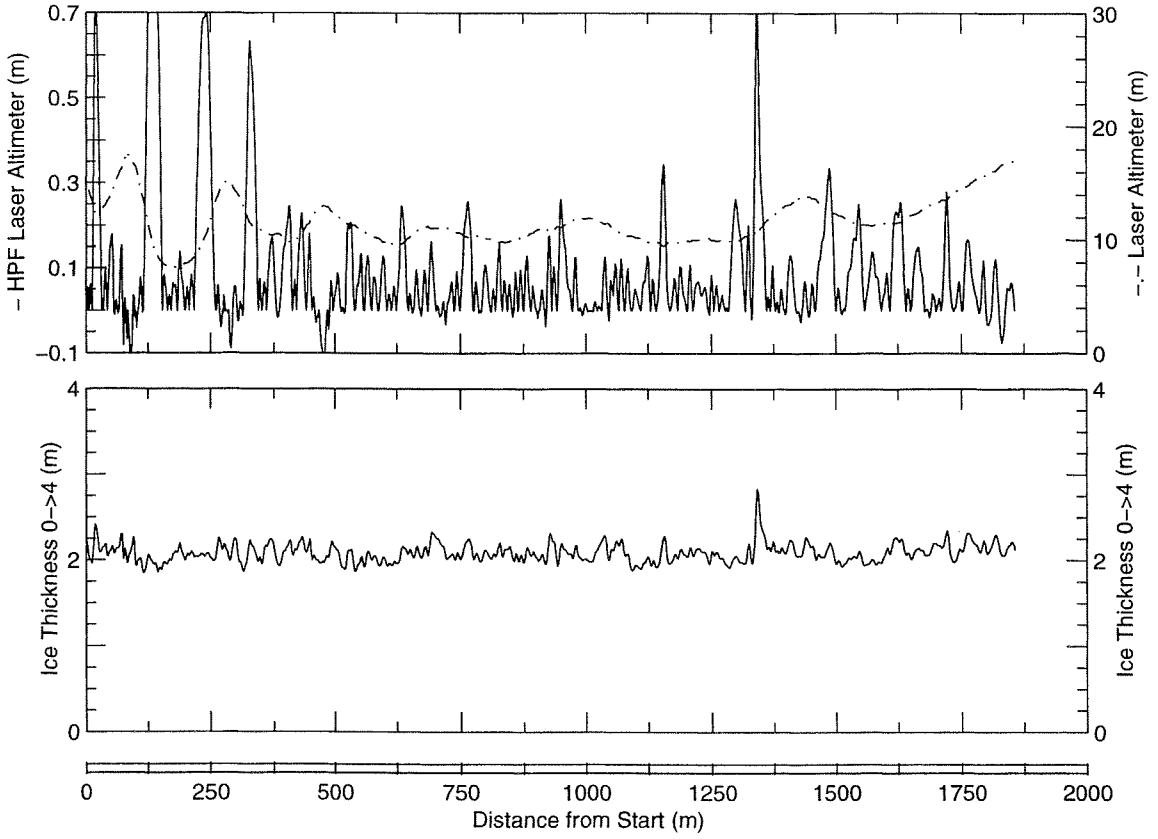

MAY 01 Flight #09 Line #10123 part 1 of 1

Line Starting Coordinates (74.5674,–96.9551) ending at (74.5769,–96.9732)

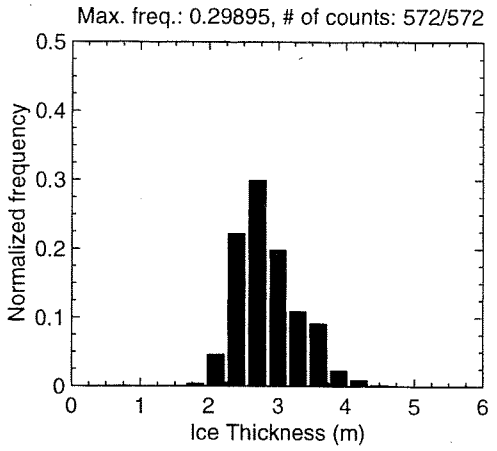

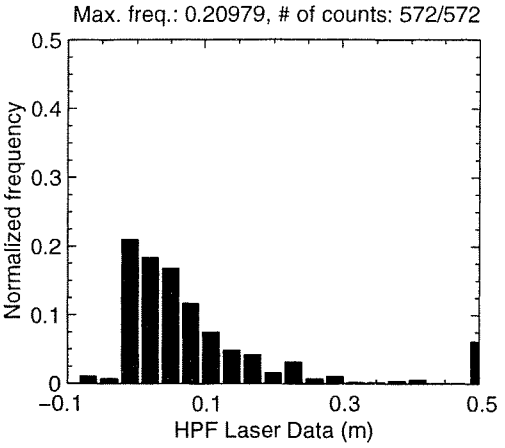

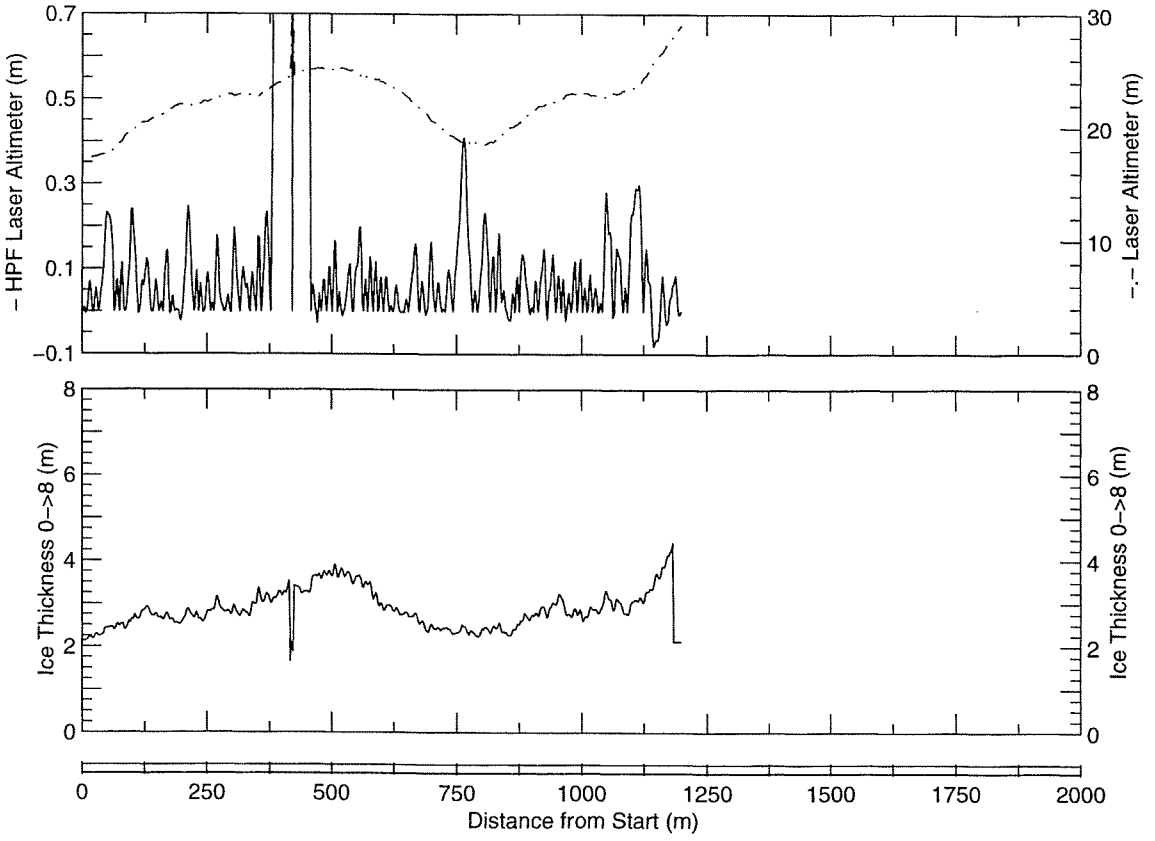

MAY 01 Flight #09 Line #10131 part 1 of 1

Line Starting Coordinates (74.5785,–96.9753) ending at (74.5805,–96.9893)

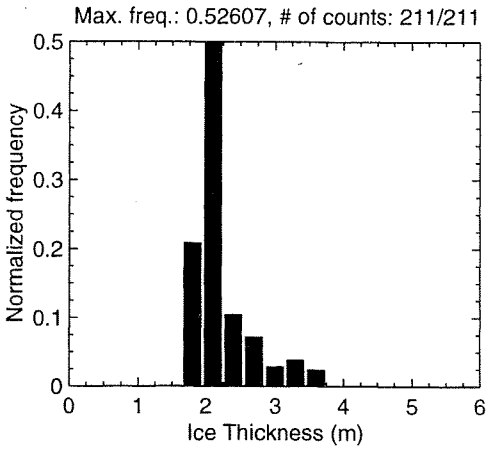

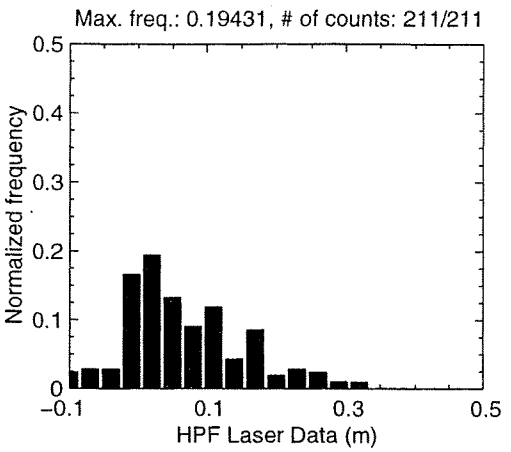

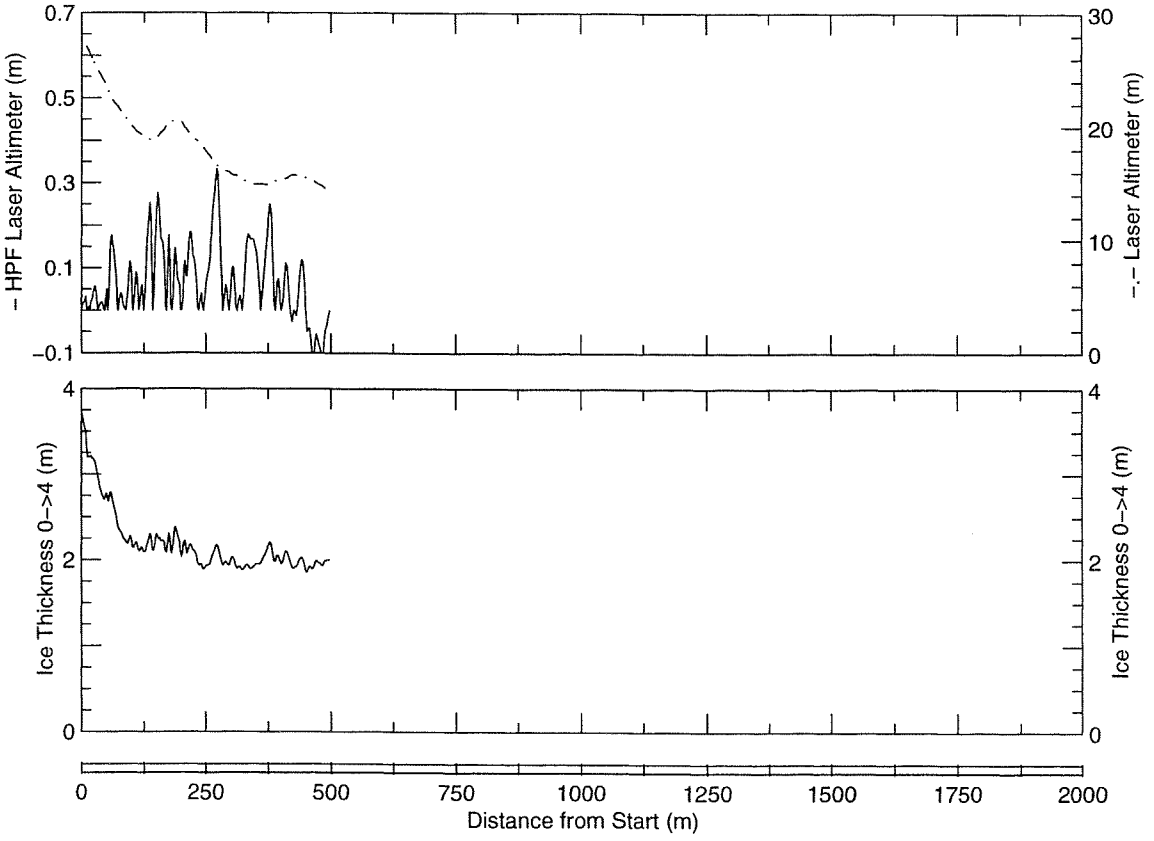

MAY 01 Flight #09 Line #10132 part 1 of 3

Line Starting Coordinates (74.5805,–96.9894) ending at (74.5799,–97.0569)

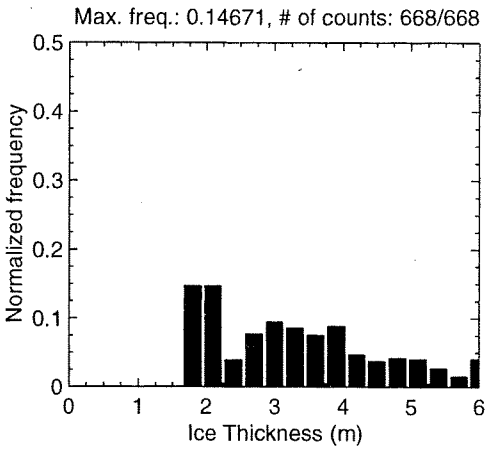

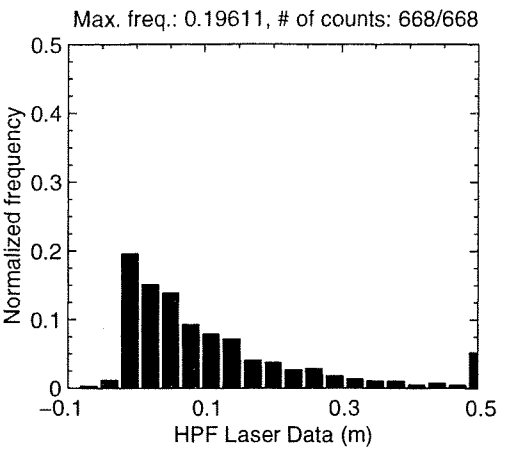

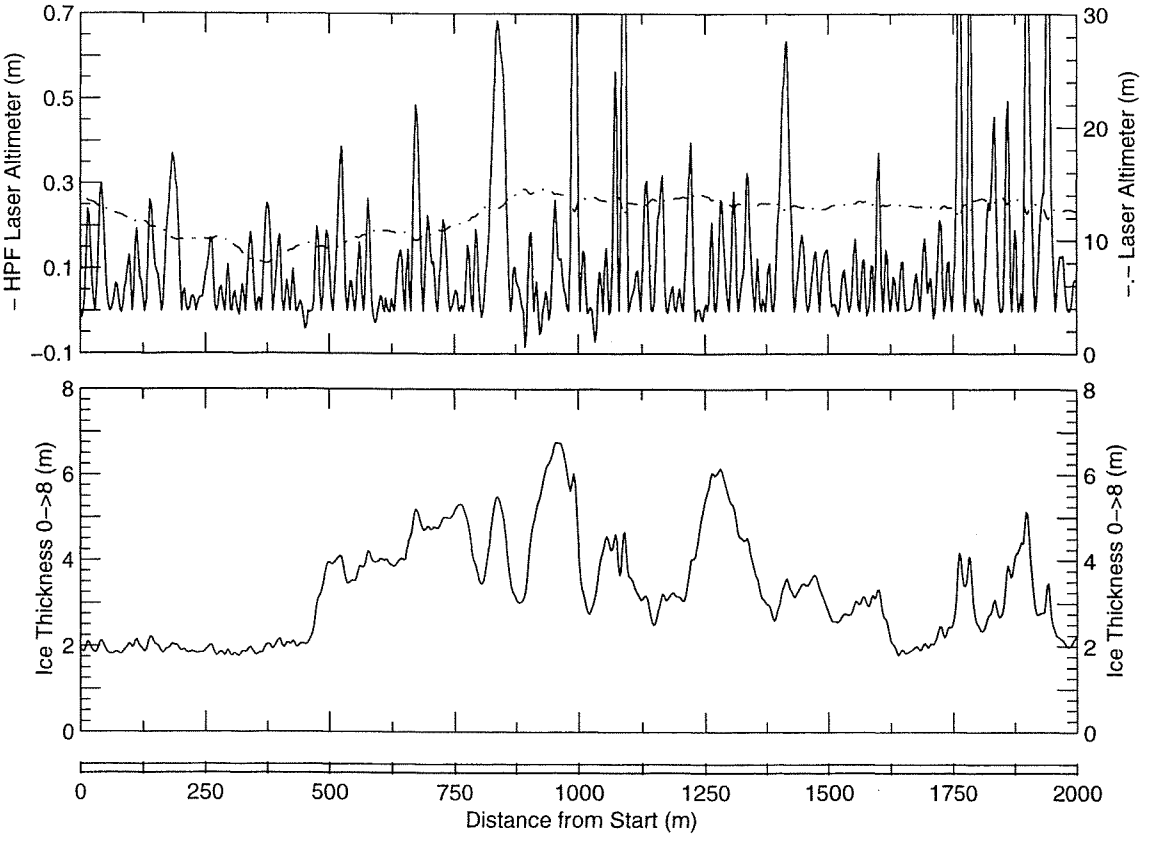

MAY 01 Flight #09 Line #10132 part 2 of 3

Line Starting Coordinates (74.5799,–97.0569) ending at (74.5779,–97.1240)

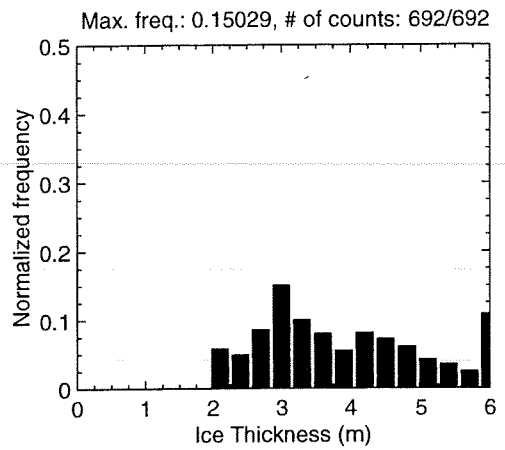

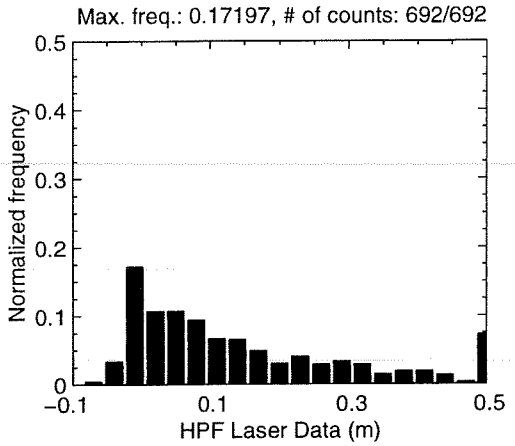

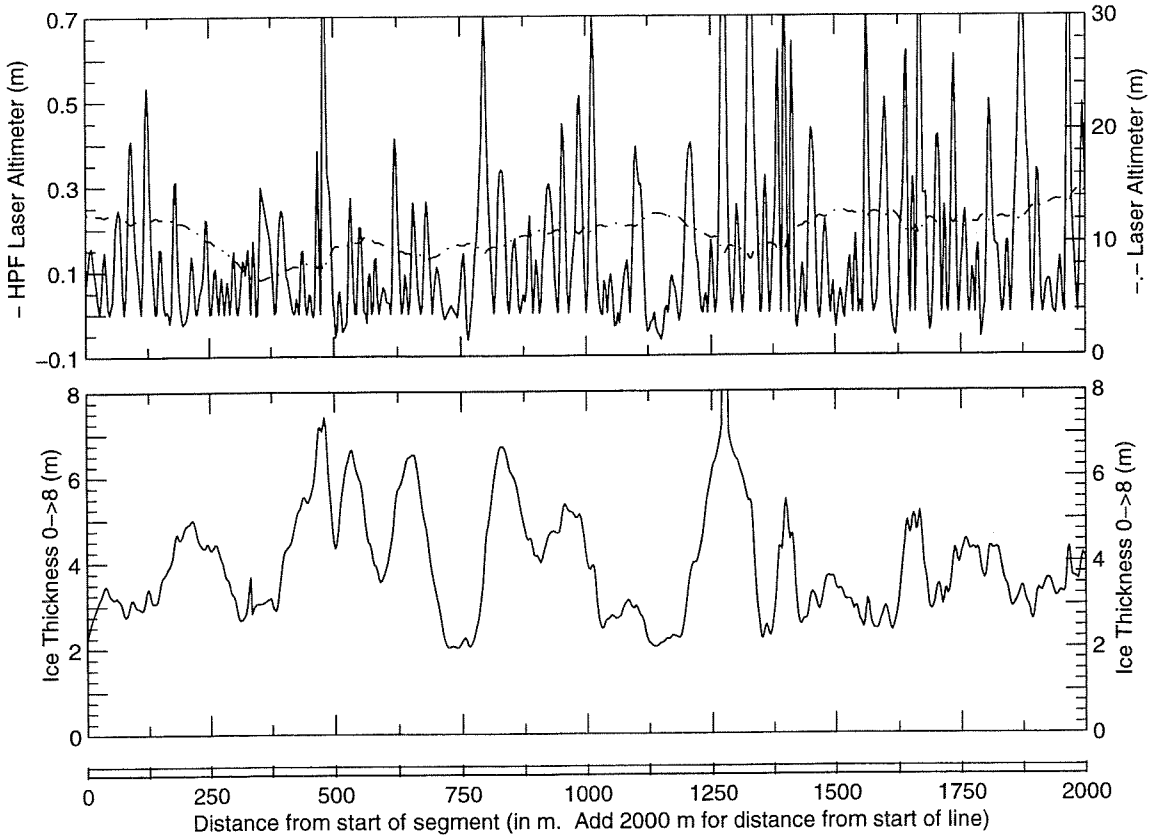

MAY 01 Flight #09 Line #10132 part 3 of 3

Line Starting Coordinates (74.5779,–97.1240) ending at (74.5777,–97.1761)

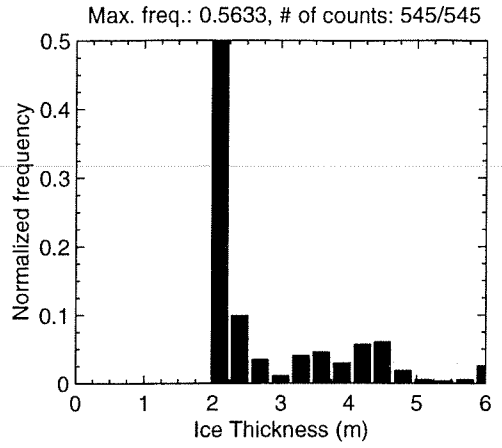

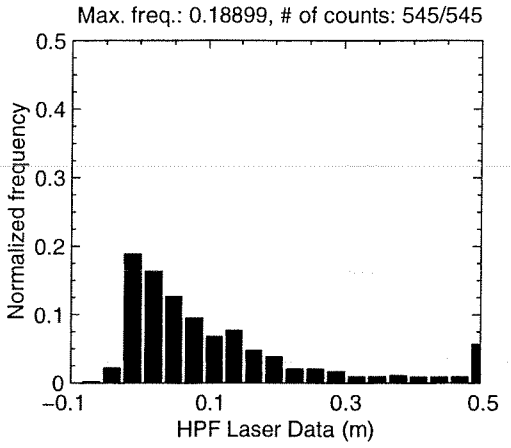

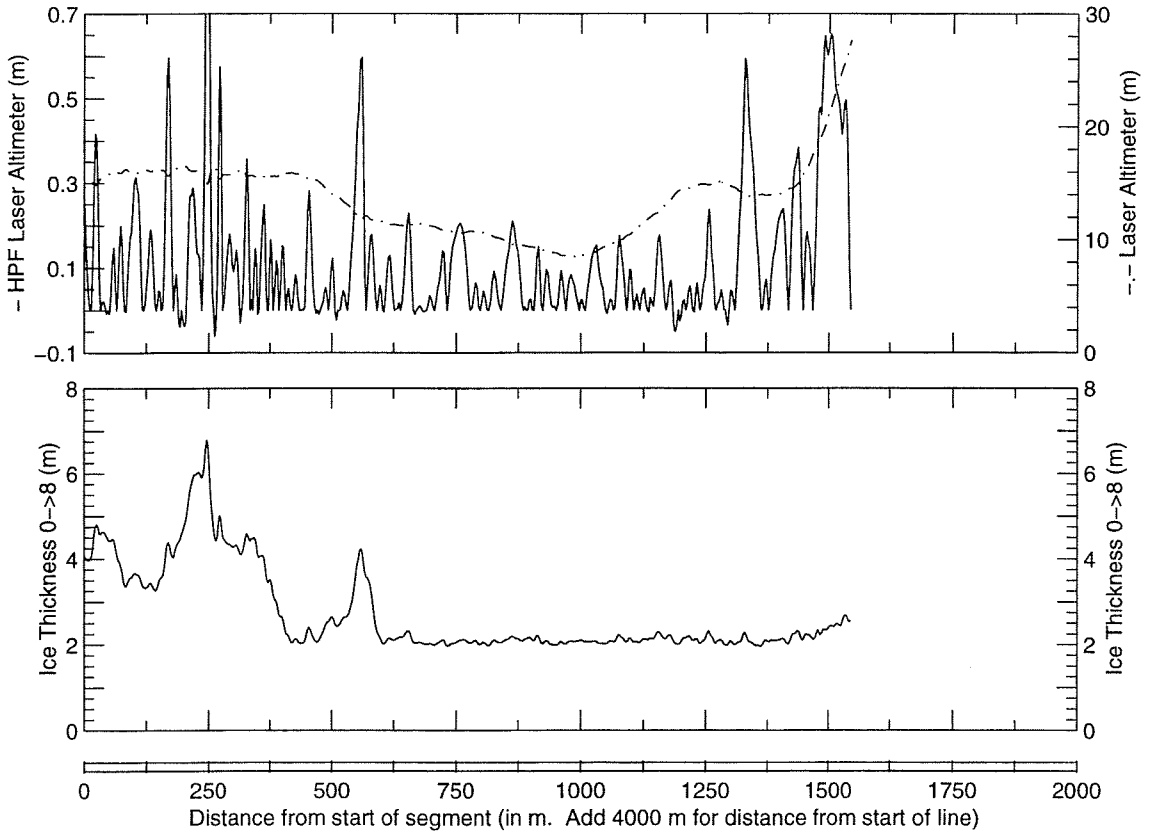

MAY 01 Flight #09 Line #10141 part 1 of 2

Line Starting Coordinates (74.5795,–97.1491) ending at (74.5669,–97.1911)

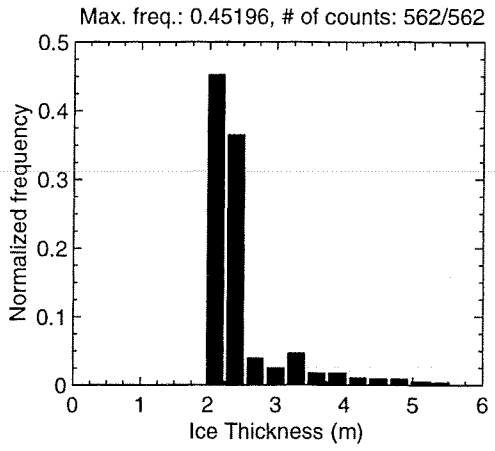

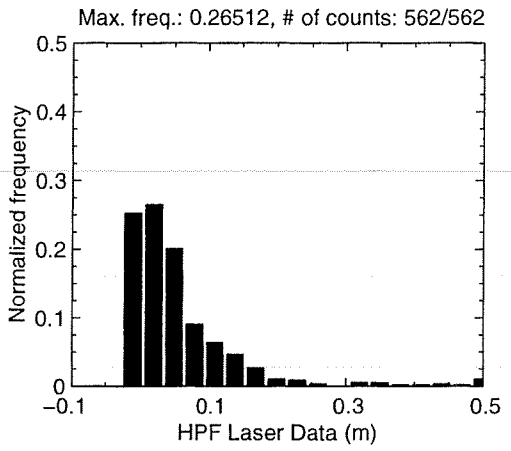

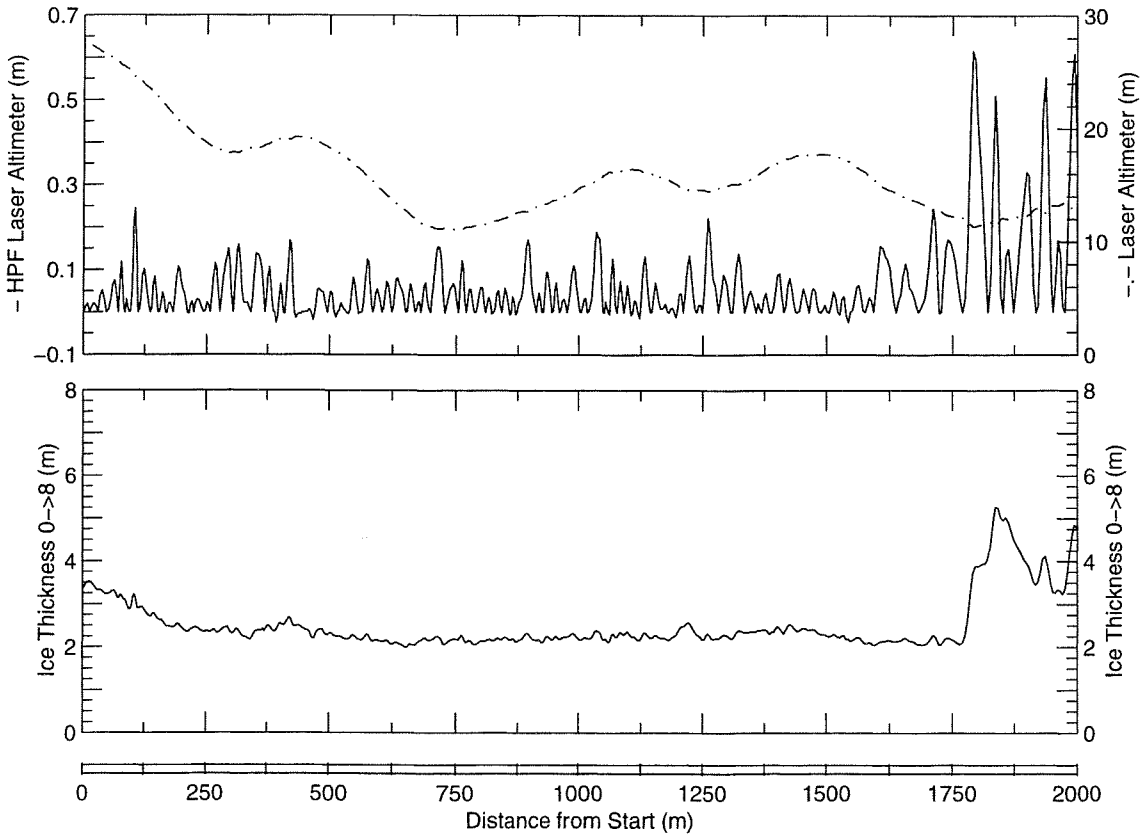

MAY 01 Flight #09 Line #10141 part 2 of 2

Line Starting Coordinates (74.5669,–97.1911) ending at (74.5649,–97.1913)

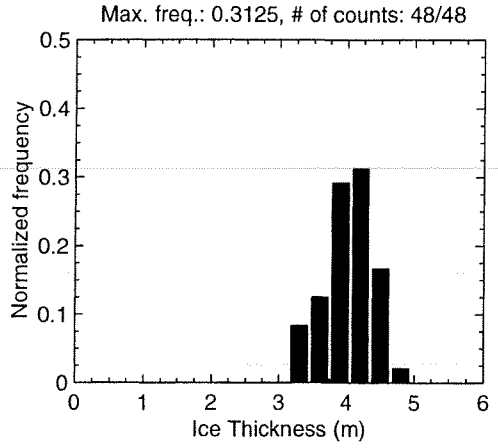

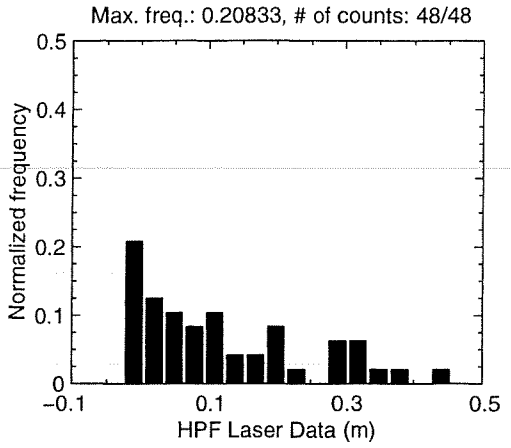

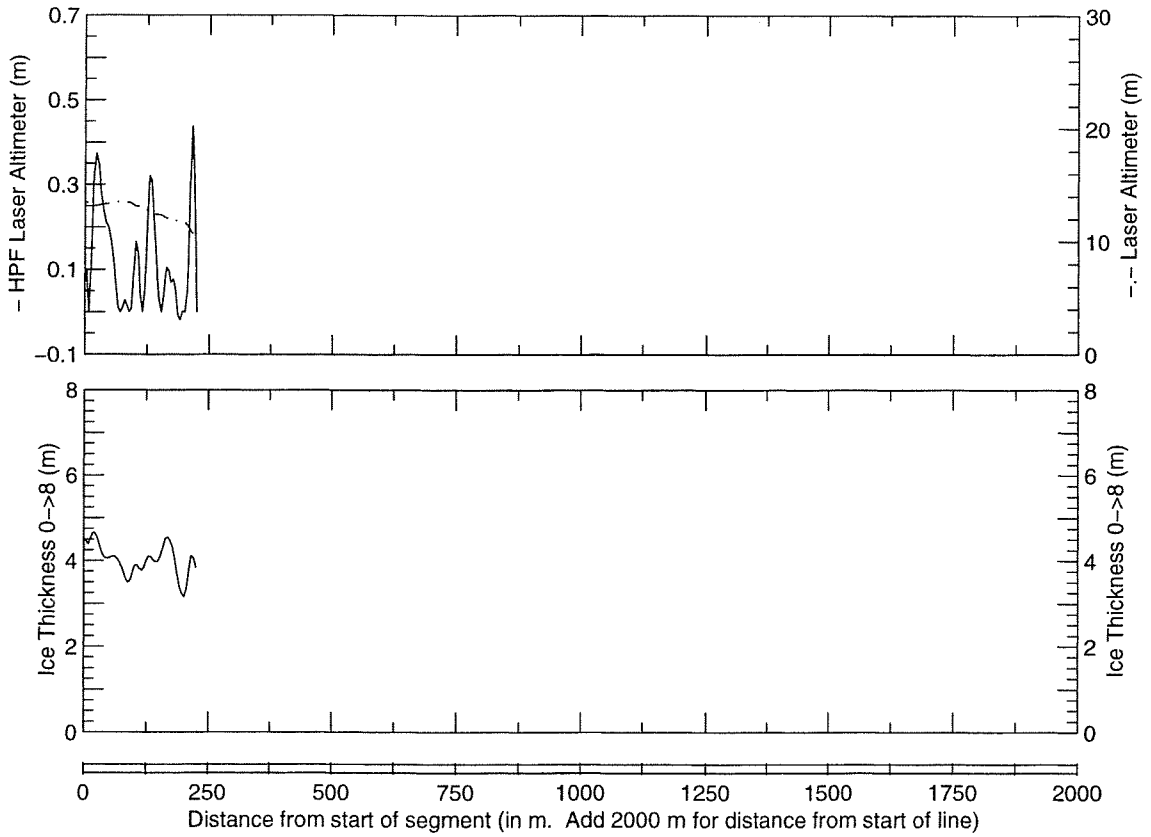

MAY 01 Flight #09 Line #10142 part 1 of 5

Line Starting Coordinates (74.5648,–97.1913) ending at (74.5473,–97.1767)

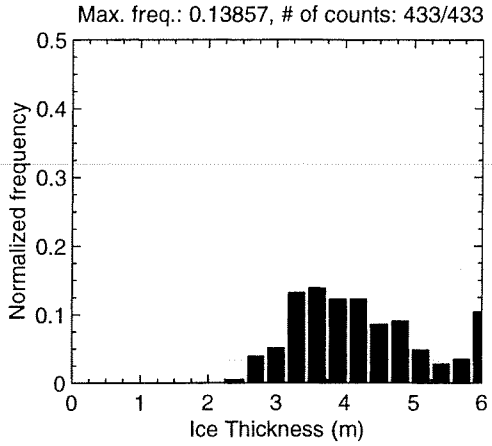

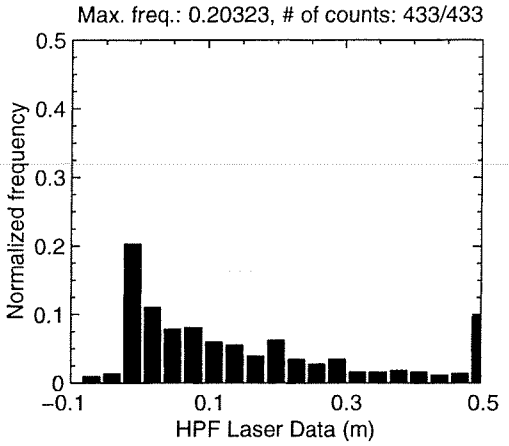

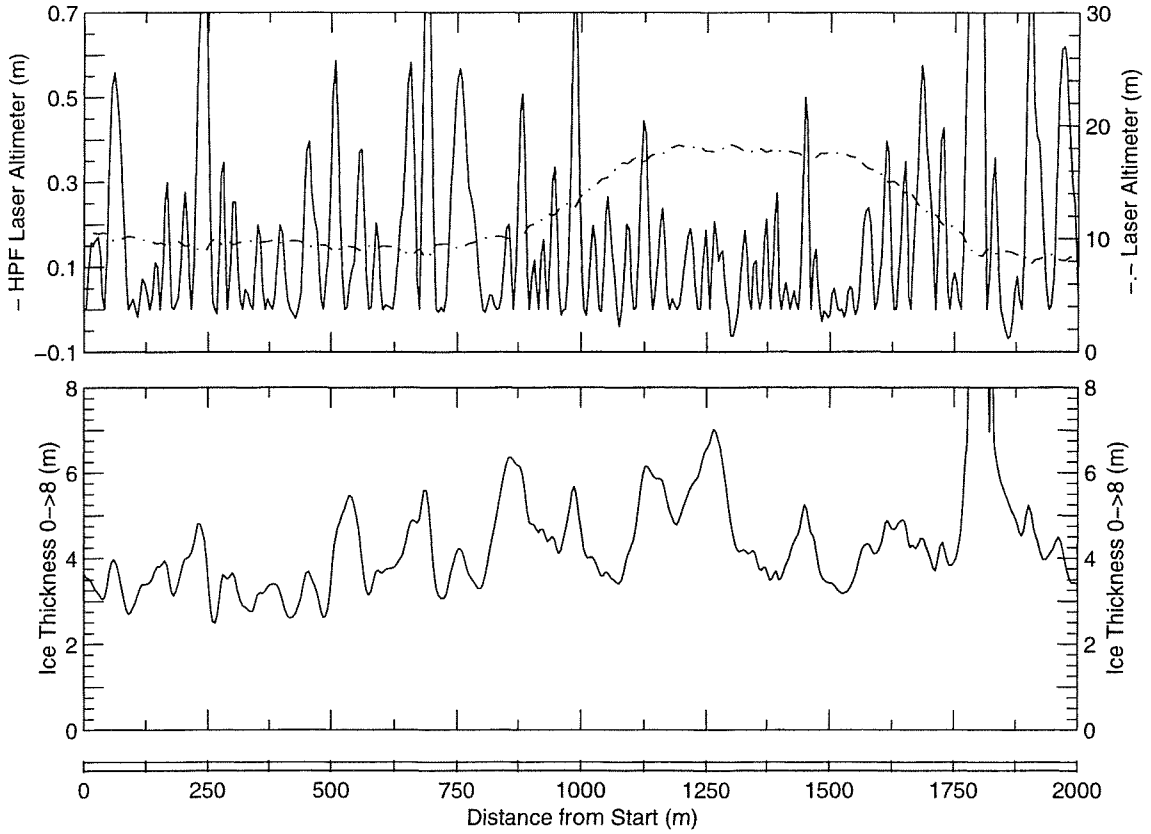

MAY 01 Flight #09 Line #10142 part 2 of 5

Line Starting Coordinates (74.5473,–97.1767) ending at (74.5303,–97.1554)

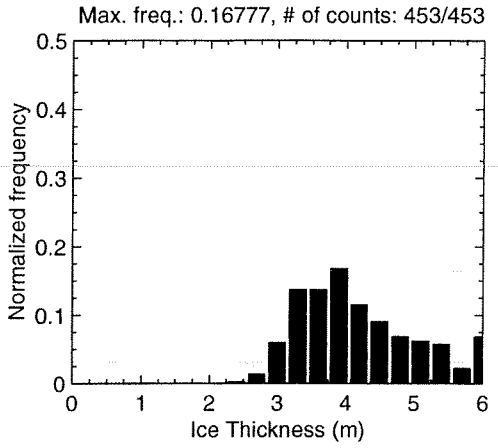

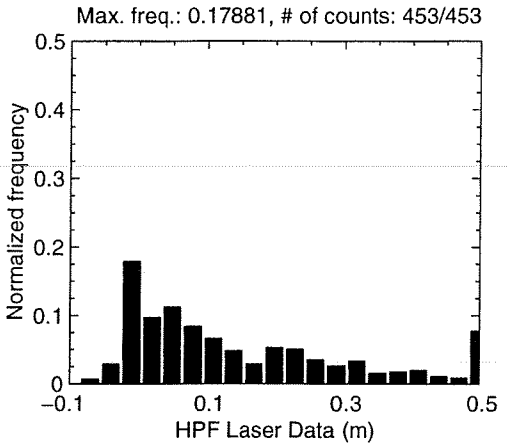

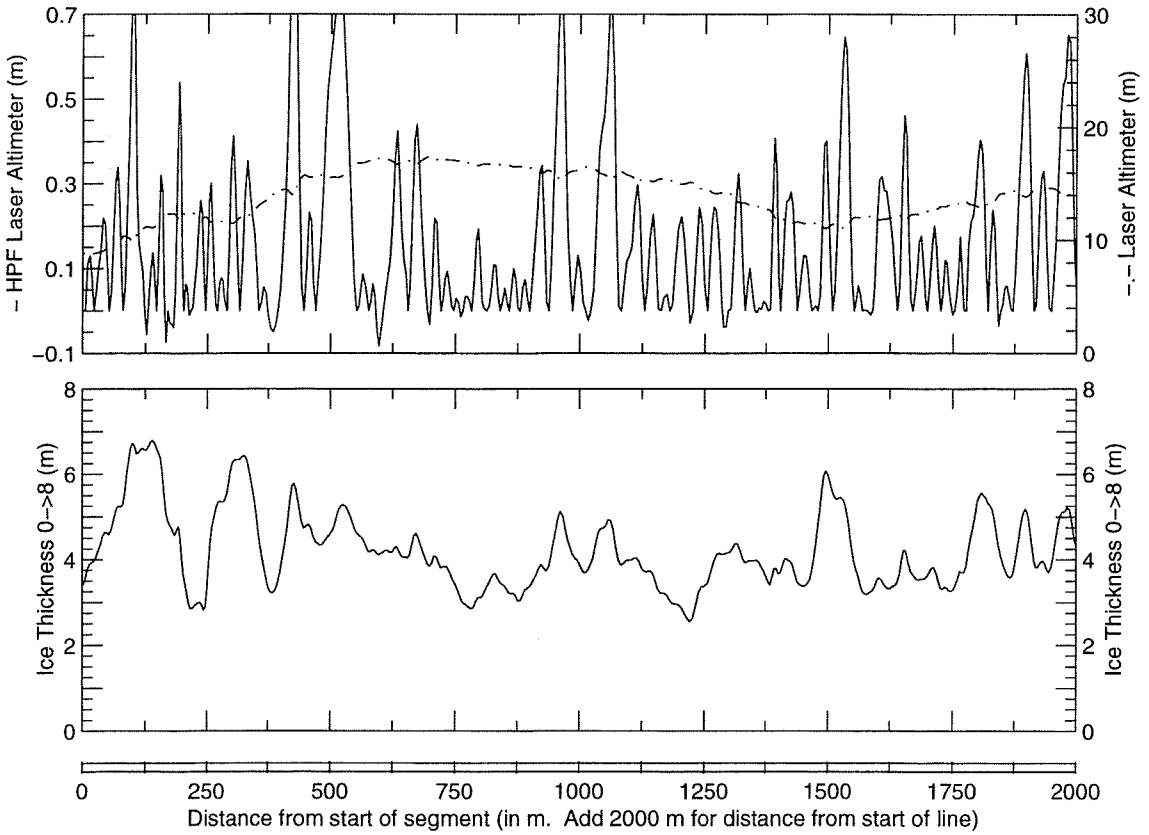

MAY 01 Flight #09 Line #10142 part 3 of 5

Line Starting Coordinates (74.5303,–97.1554) ending at (74.5133,–97.1333)

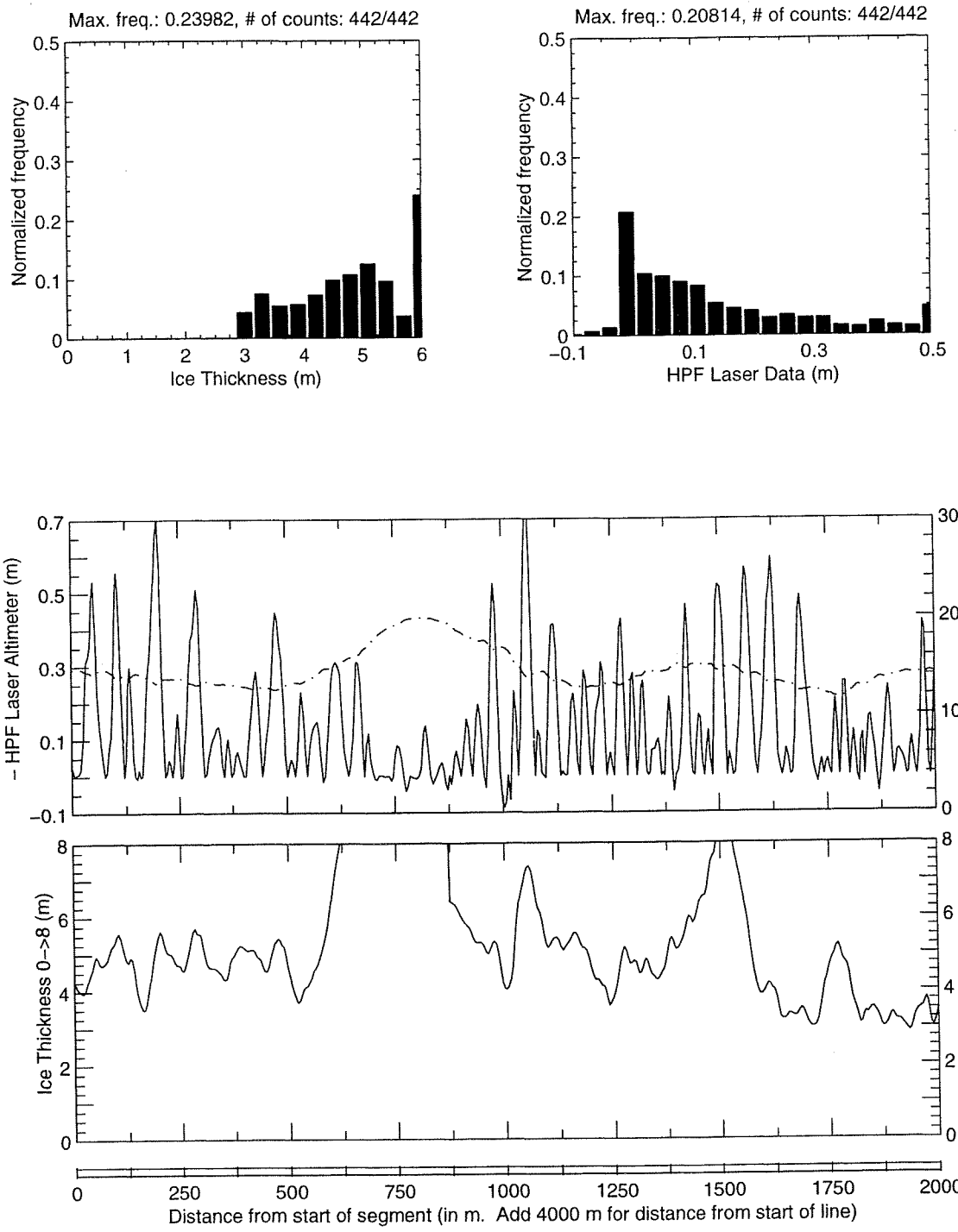

MAY 01 Flight #09 Line #10142 part 4 of 5

Line Starting Coordinates (74.5133,–97.1333) ending at (74.4963,–97.1114)

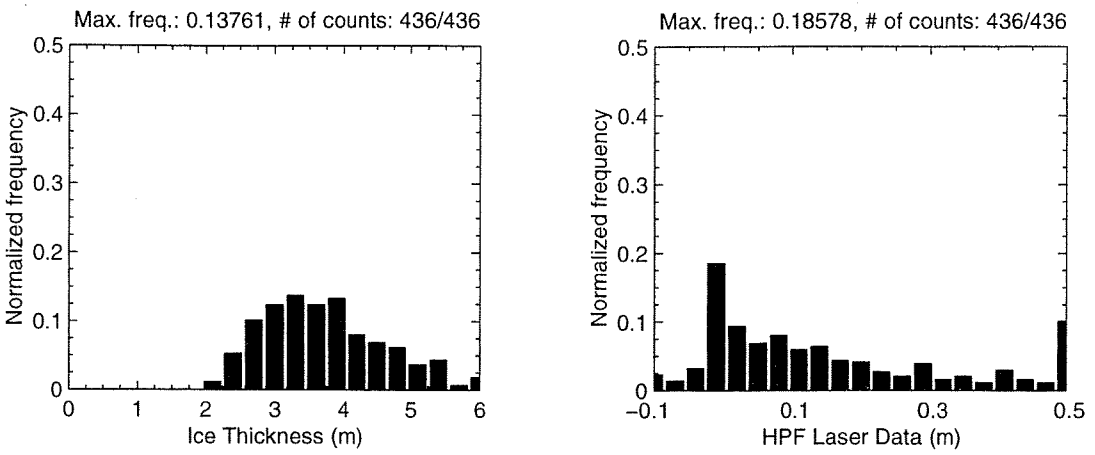

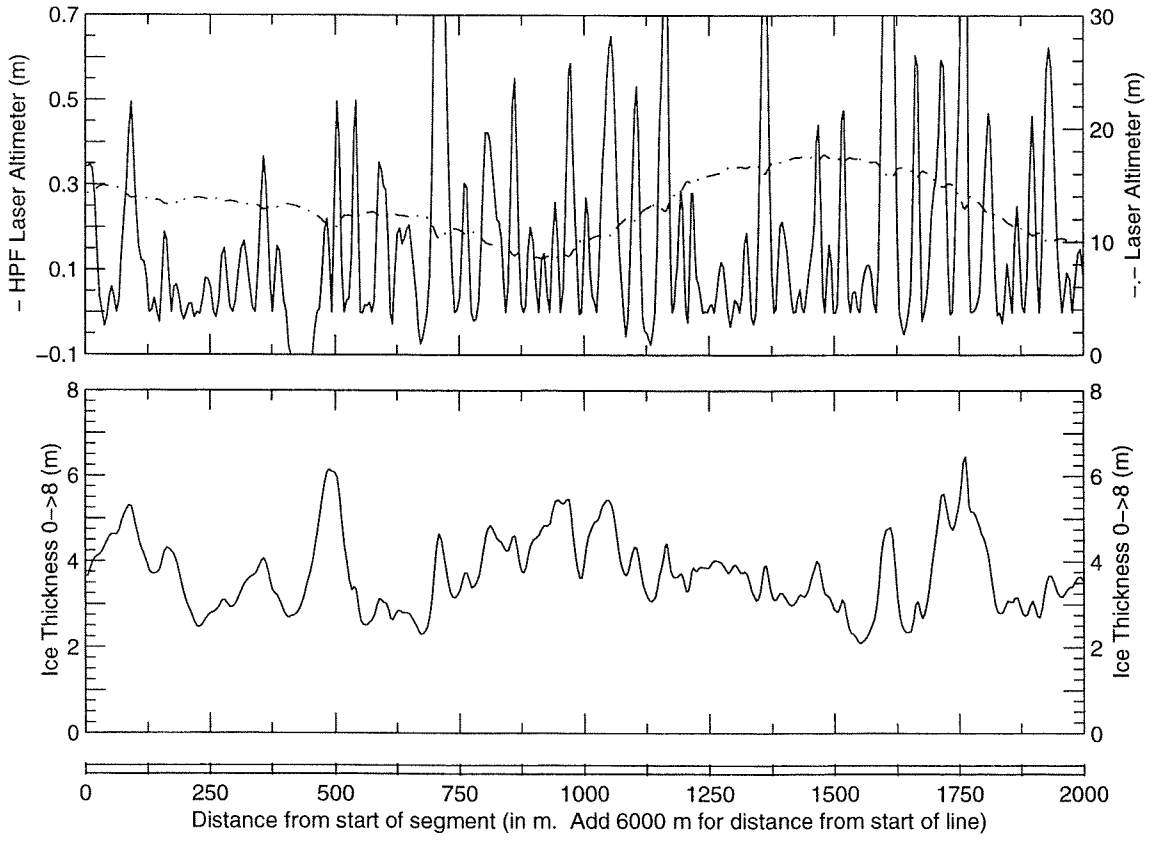

MAY 01 Flight #09 Line #10142 part 5 of 5

Line Starting Coordinates (74.4963,–97.1114) ending at (74.4858,–97.0936)

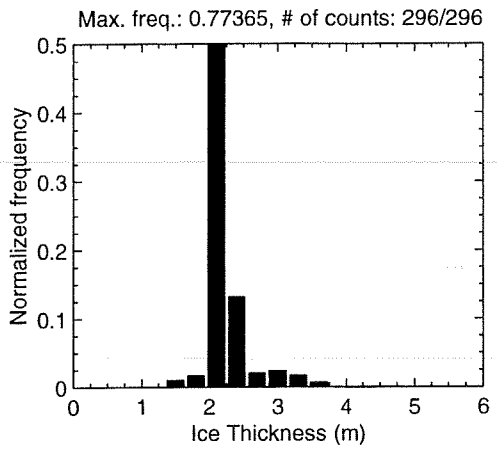

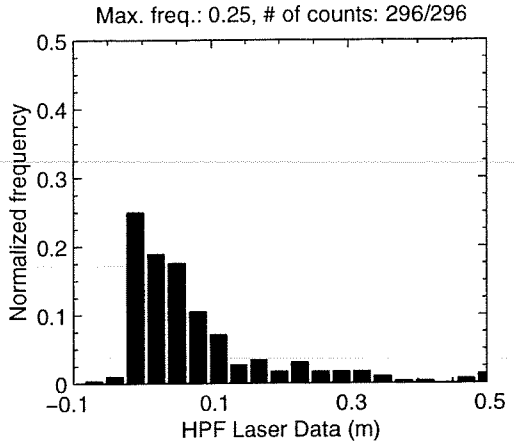

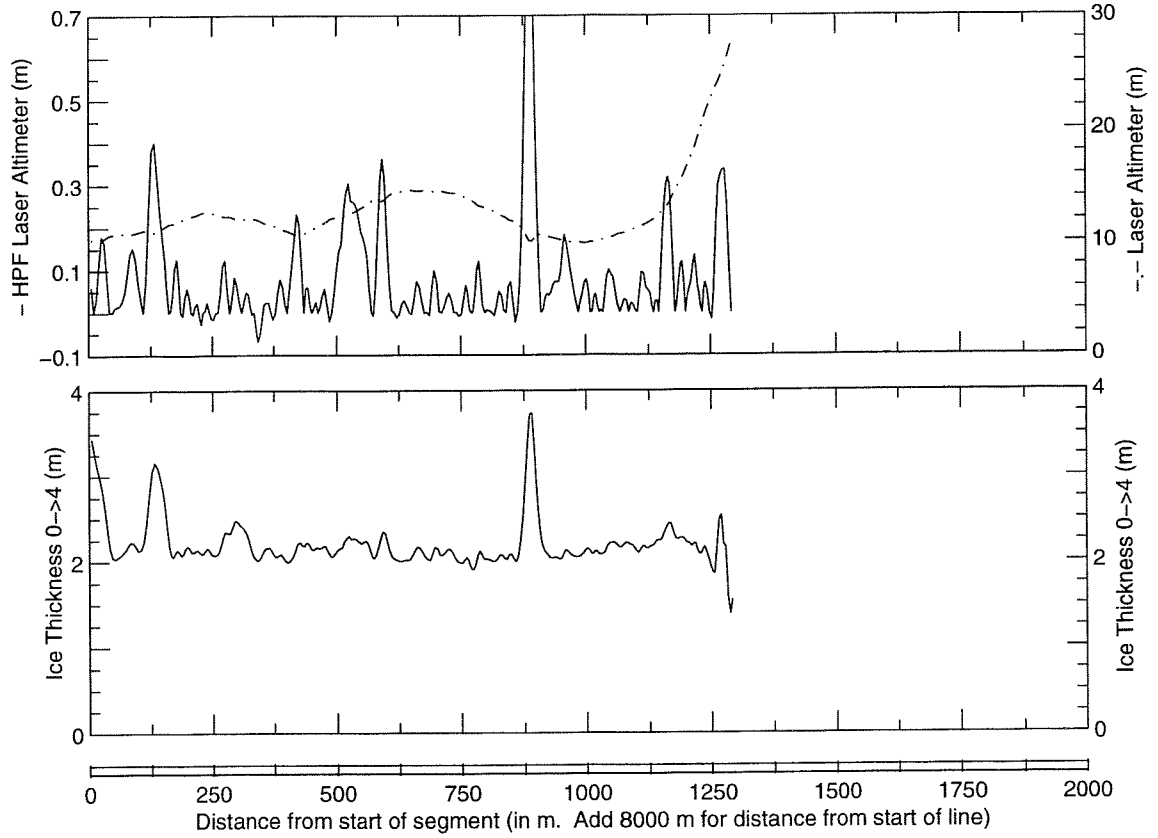

MAY 01 Flight #09 Line #10150 part 1 of 7

Line Starting Coordinates (74.4847,–97.0429) ending at (74.5006,–97.0747)

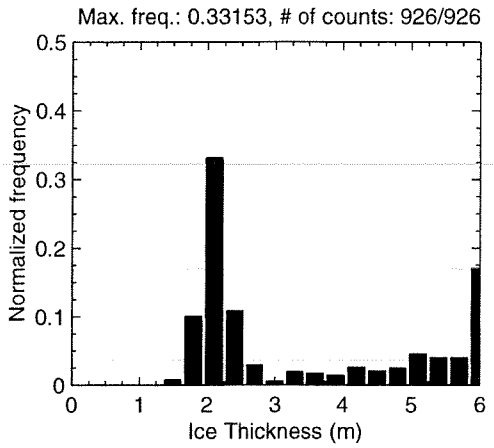

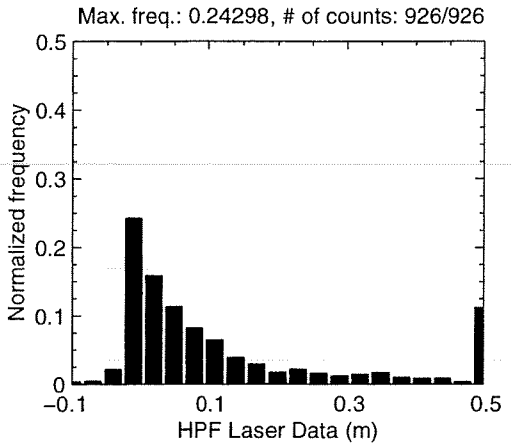

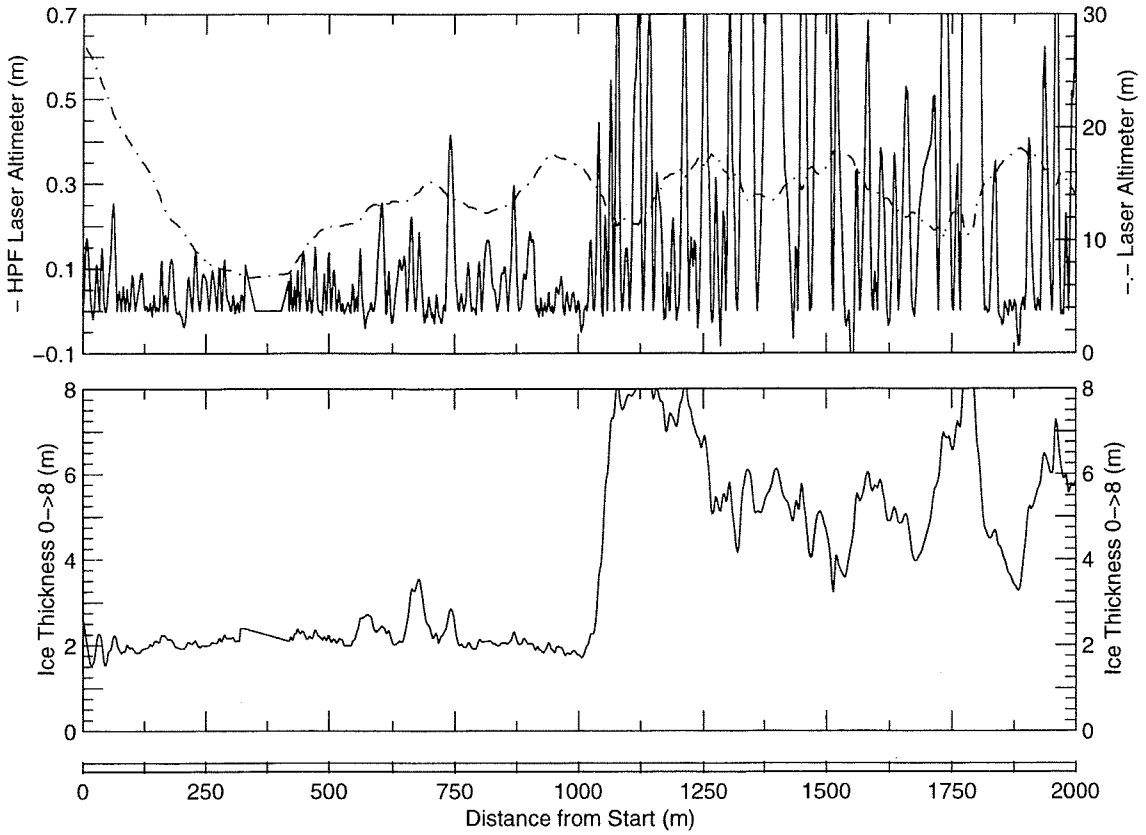

MAY 01 Flight #09 Line #10150 part 2 of 7

Line Starting Coordinates (74.5006,–97.0747) ending at (74.5178,–97.0919)

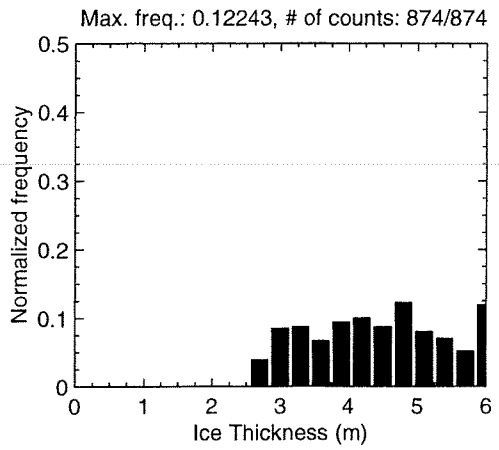

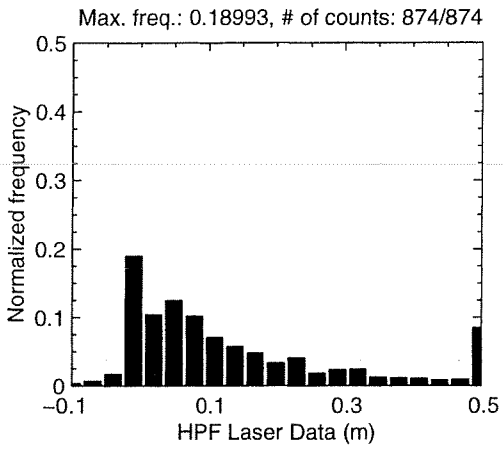

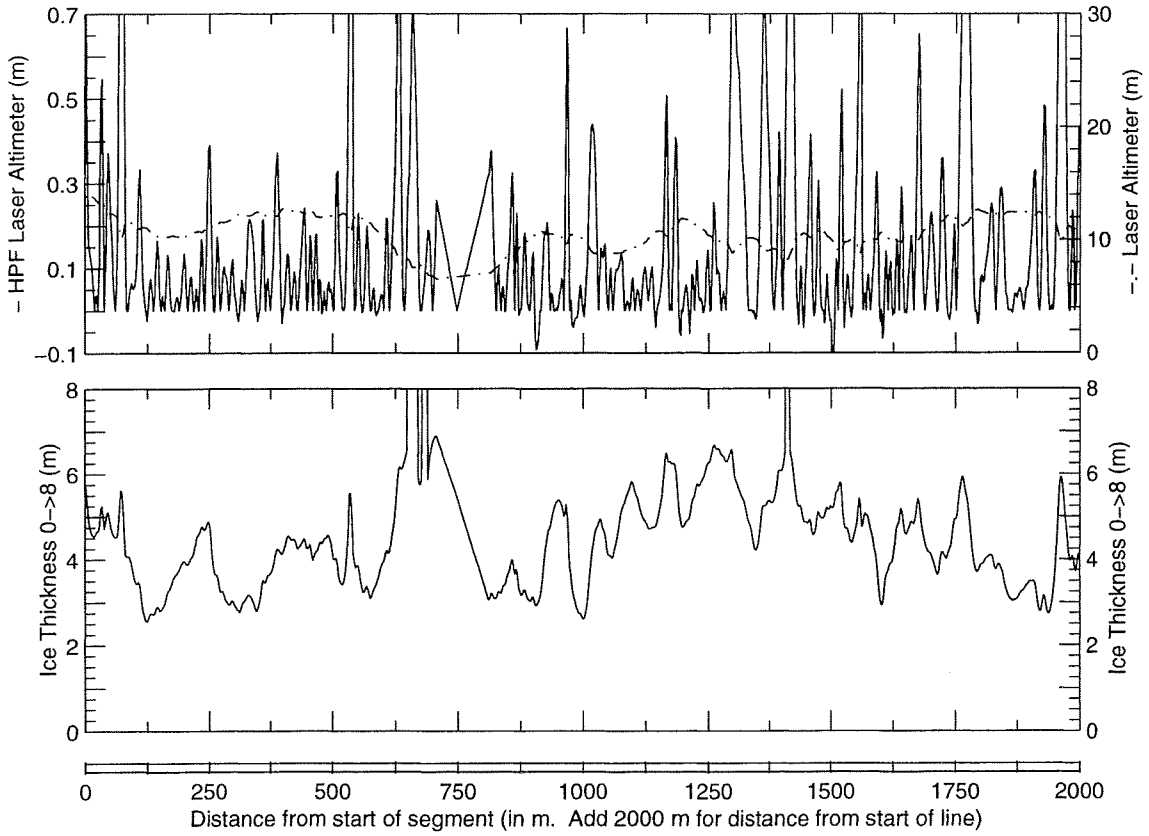

MAY 01 Flight #09 Line #10150 part 3 of 7

Line Starting Coordinates (74.5178,–97.0919) ending at (74.5354,–97.1052)

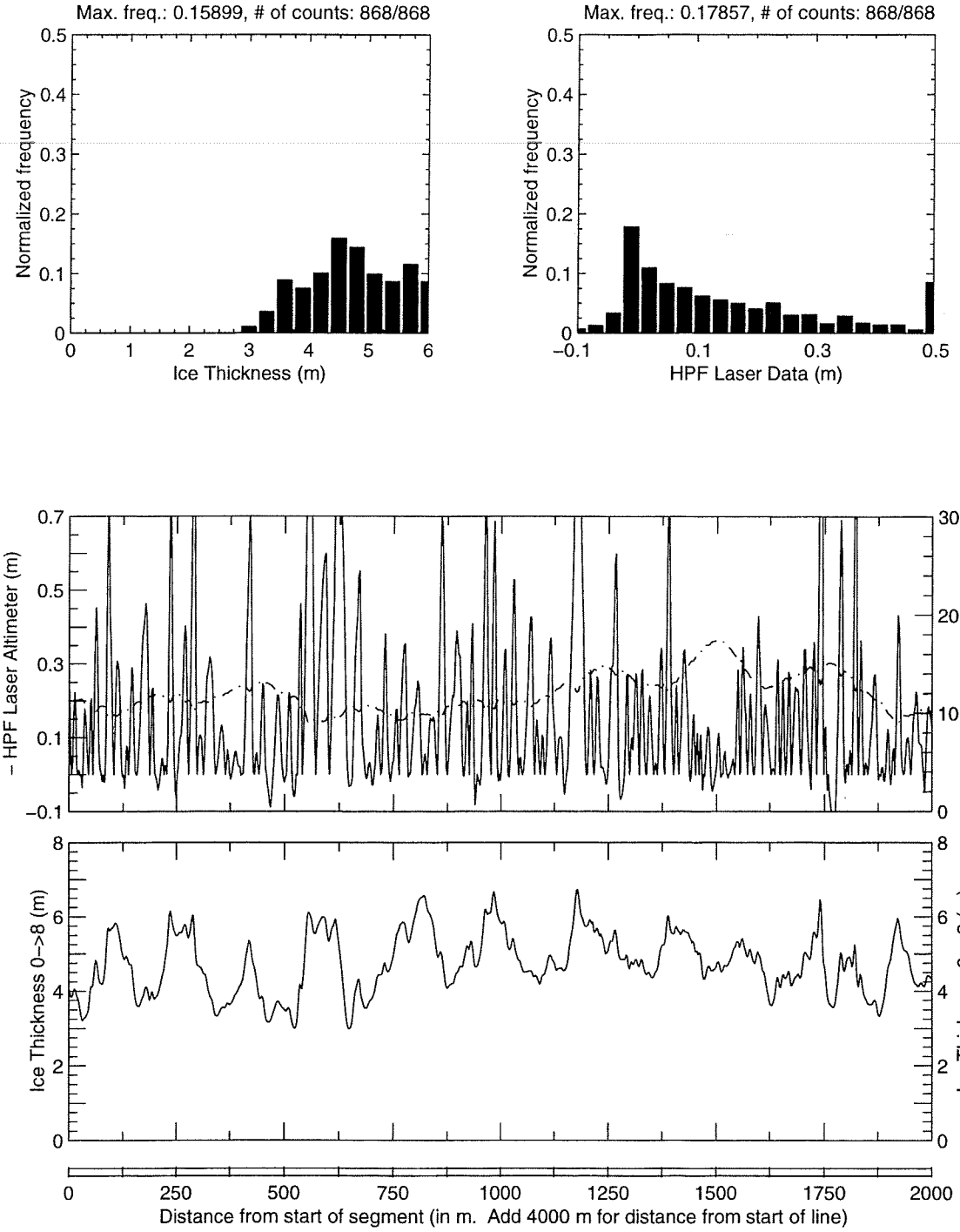

MAY 01 Flight #09 Line #10150 part 4 of 7

Line Starting Coordinates (74.5354,–97.1052) ending at (74.5531,–97.1154)

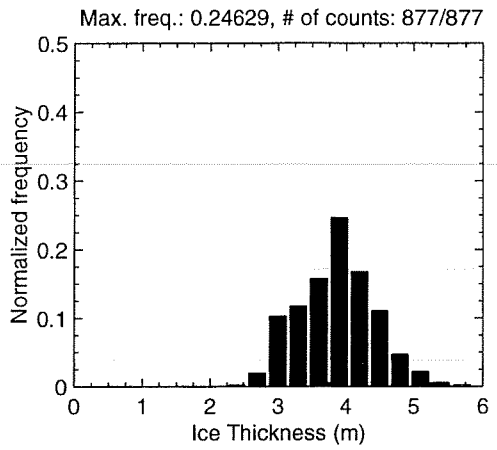

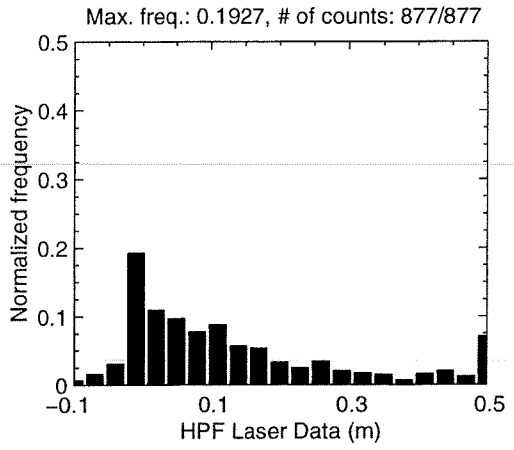

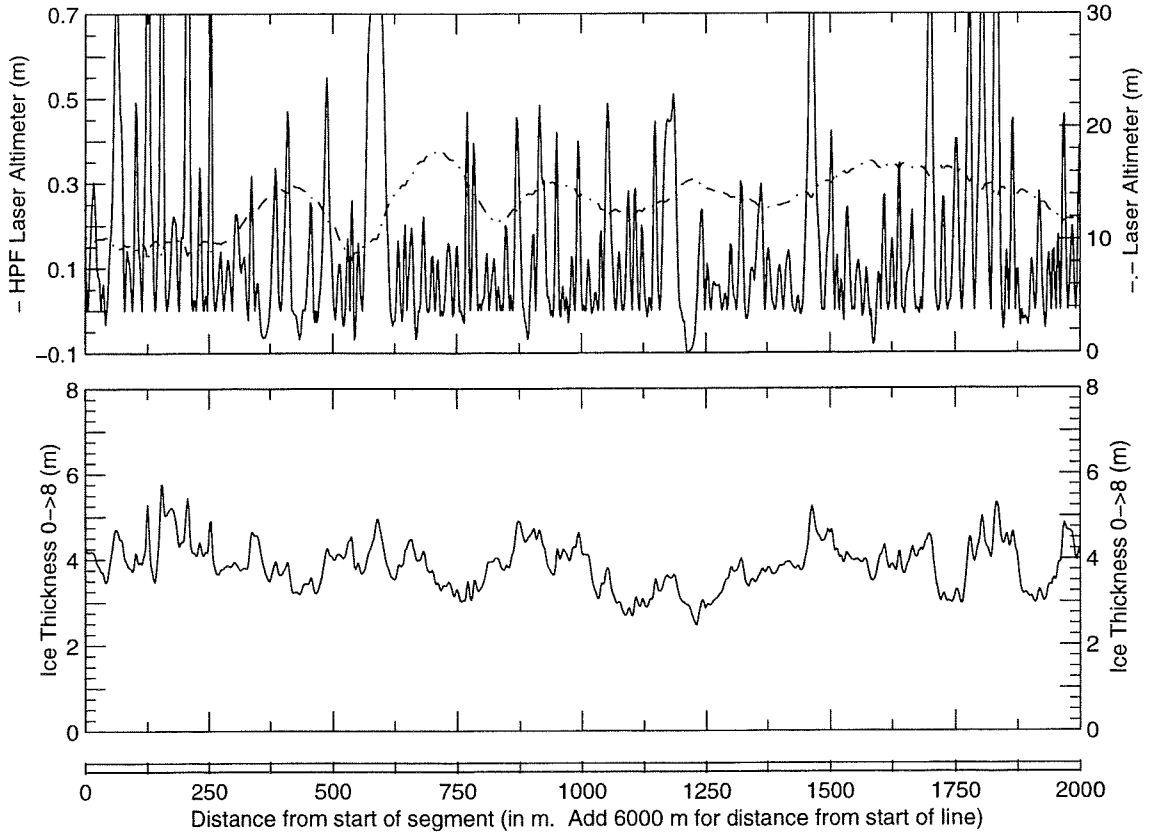

MAY 01 Flight #09 Line #10150 part 5 of 7

Line Starting Coordinates (74.5531,–97.1154) ending at (74.5705,–97.1322)

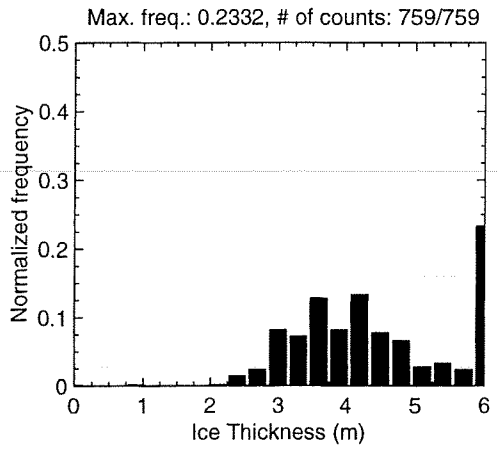

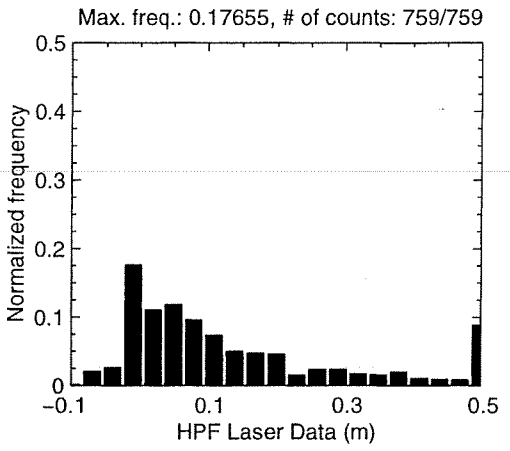

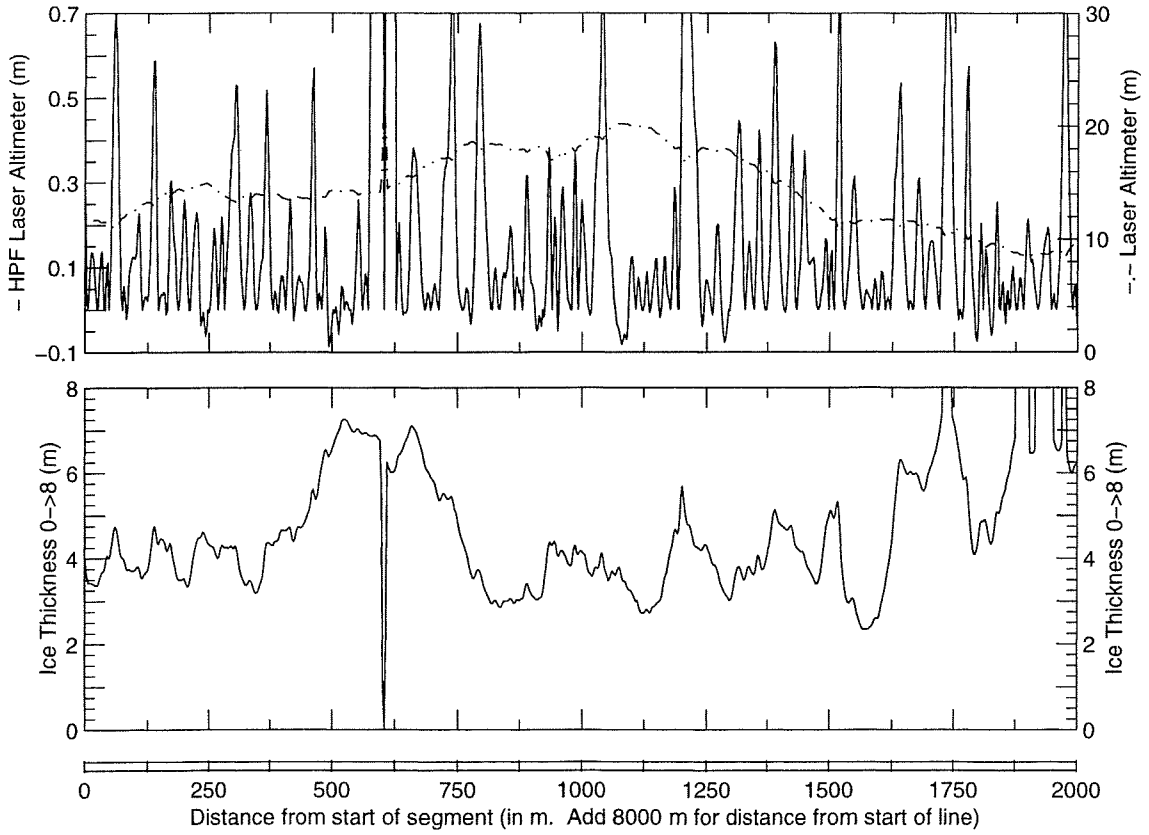

MAY 01 Flight #09 Line #10150 part 6 of 7

Line Starting Coordinates (74.5705,–97.1322) ending at (74.5877,–97.1526)

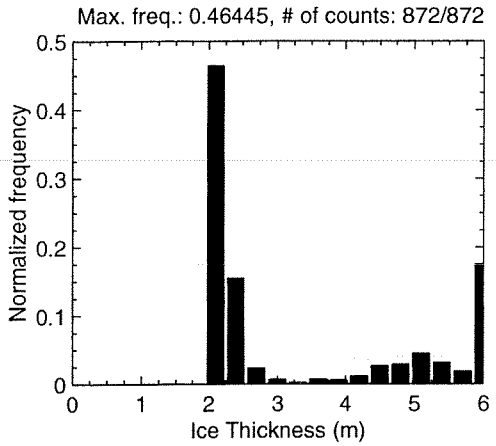

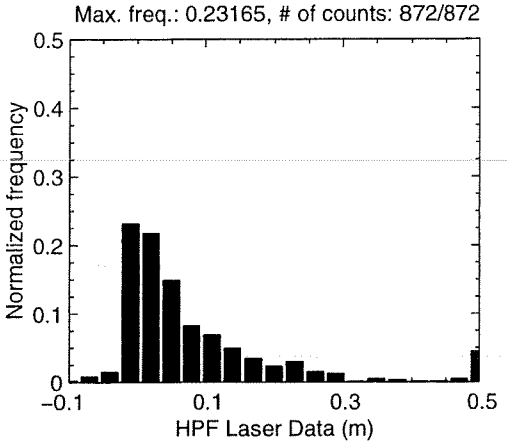

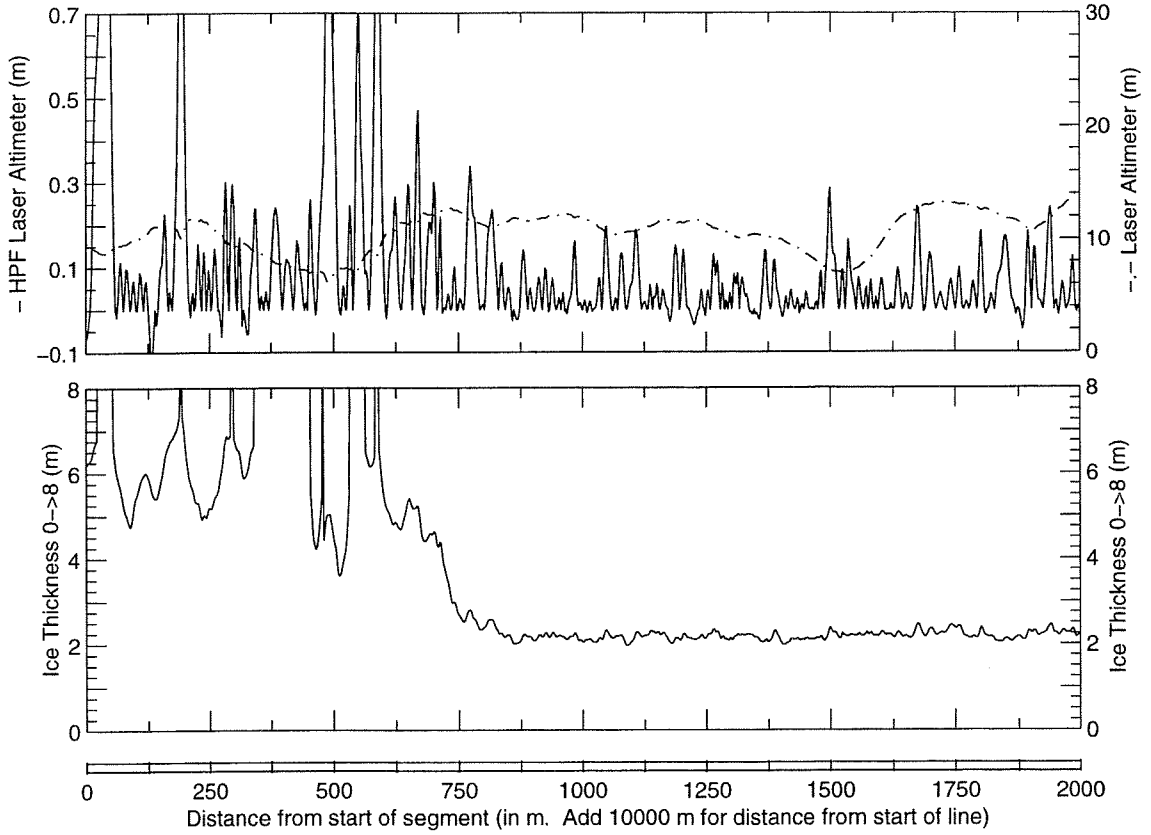

MAY 01 Flight #09 Line #10150 part 7 of 7

Line Starting Coordinates (74.5877,–97.1526) ending at (74.5937,–97.1610)

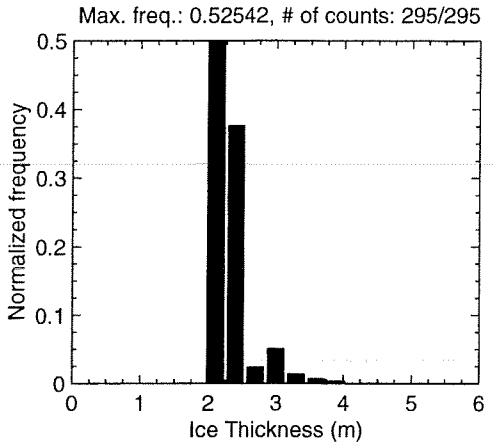

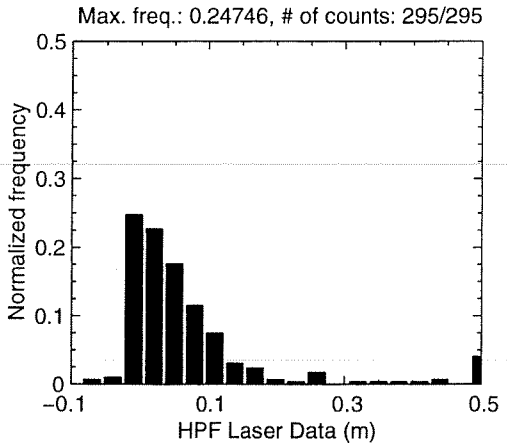

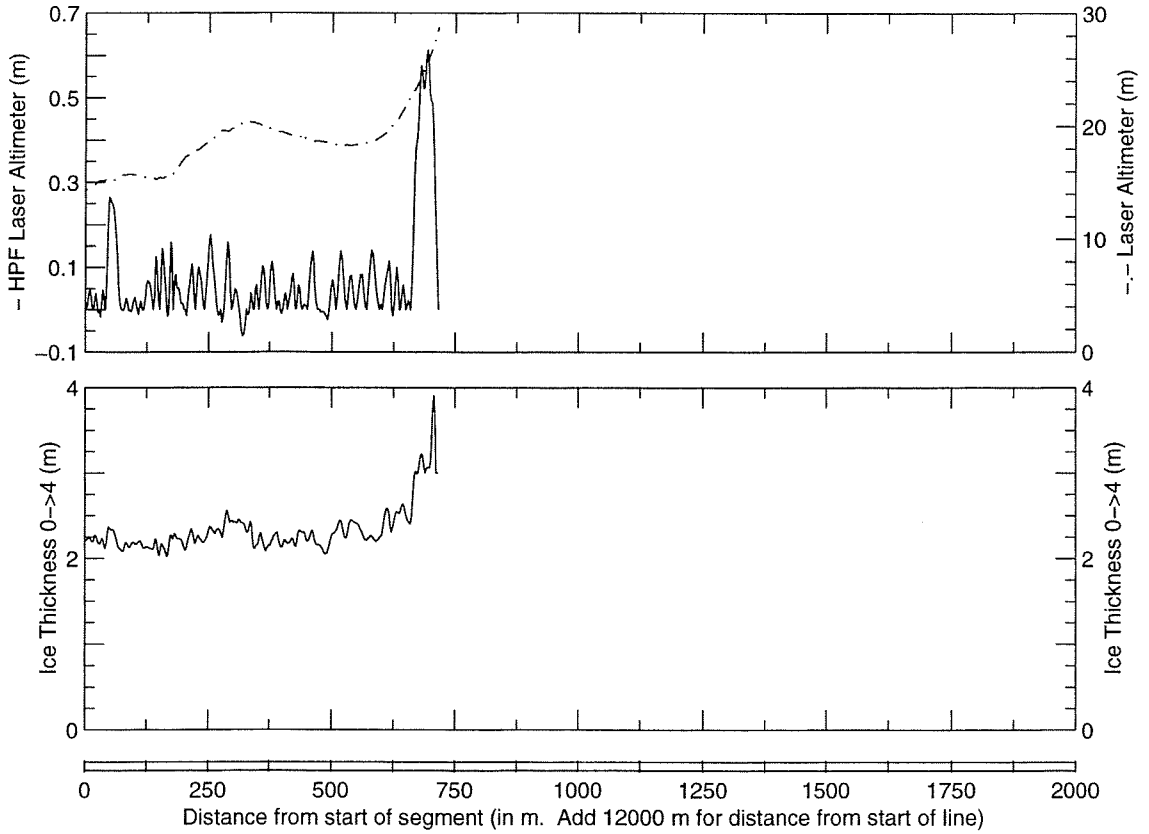

MAY 01 Flight #09 Line #10160 part 1 of 3

Line Starting Coordinates (74.6119,–97.0588) ending at (74.5961,–97.0265)

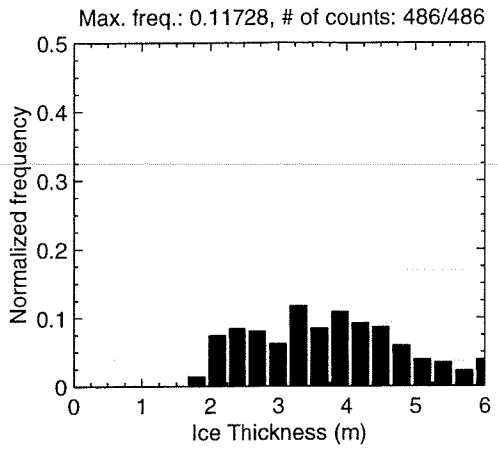

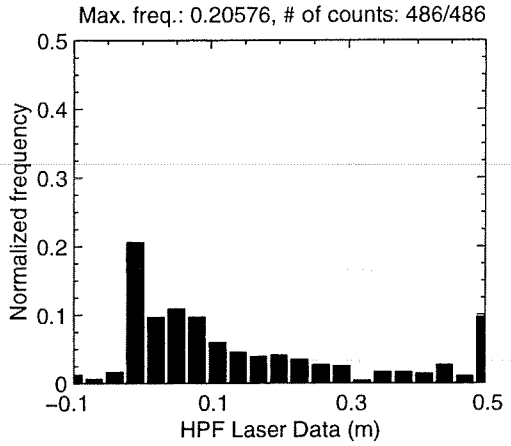

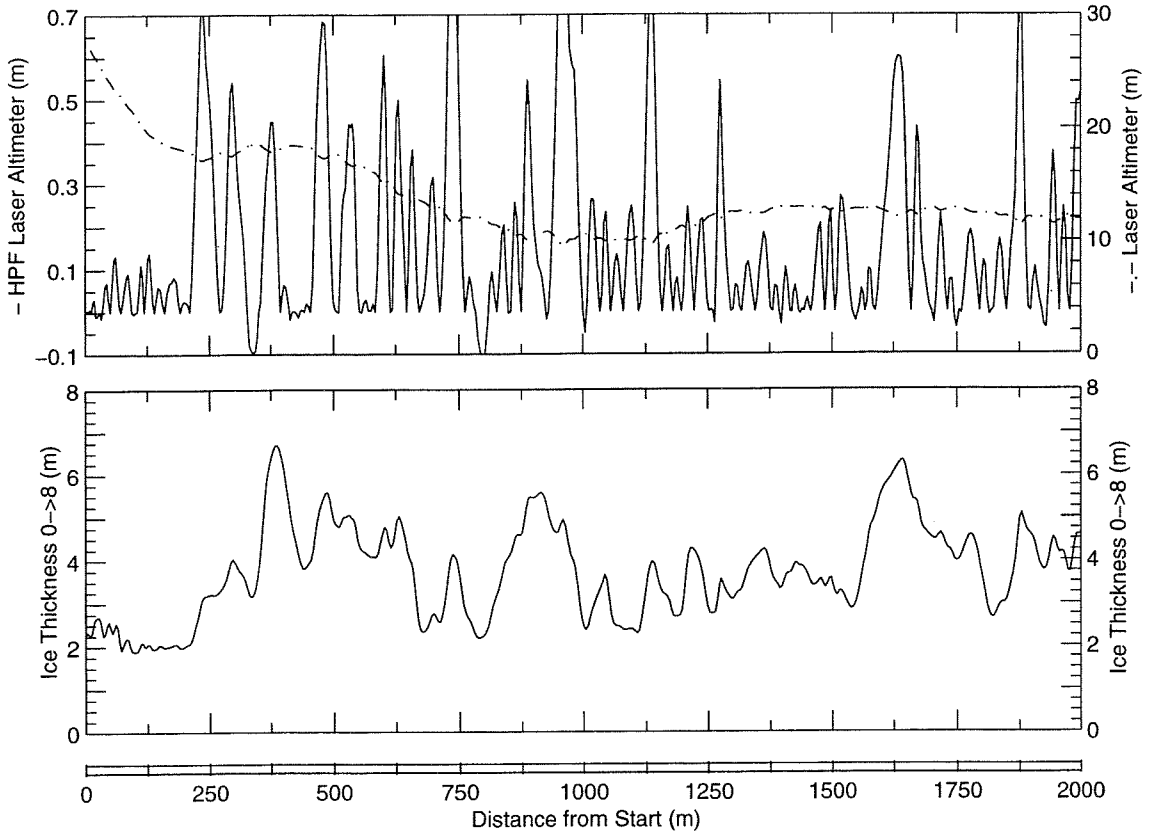

MAY 01 Flight #09 Line #10160 part 2 of 3

Line Starting Coordinates (74.5961,–97.0265) ending at (74.5812,–96.9891)

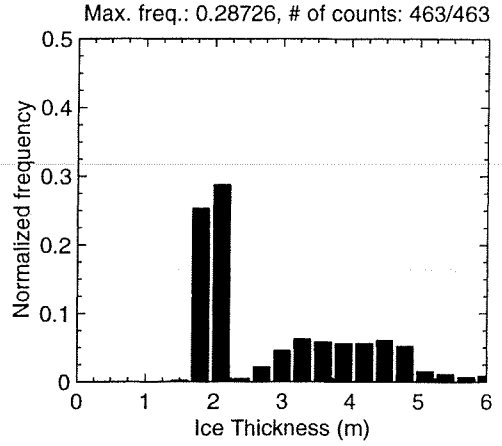

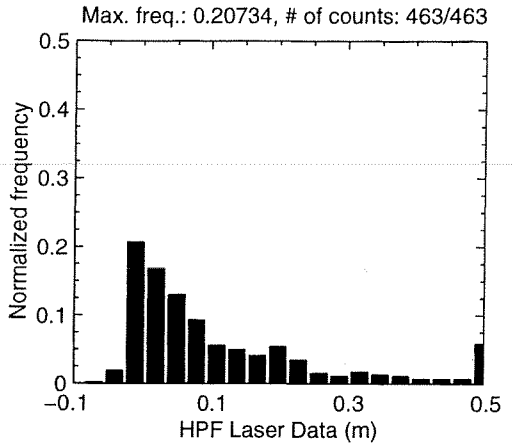

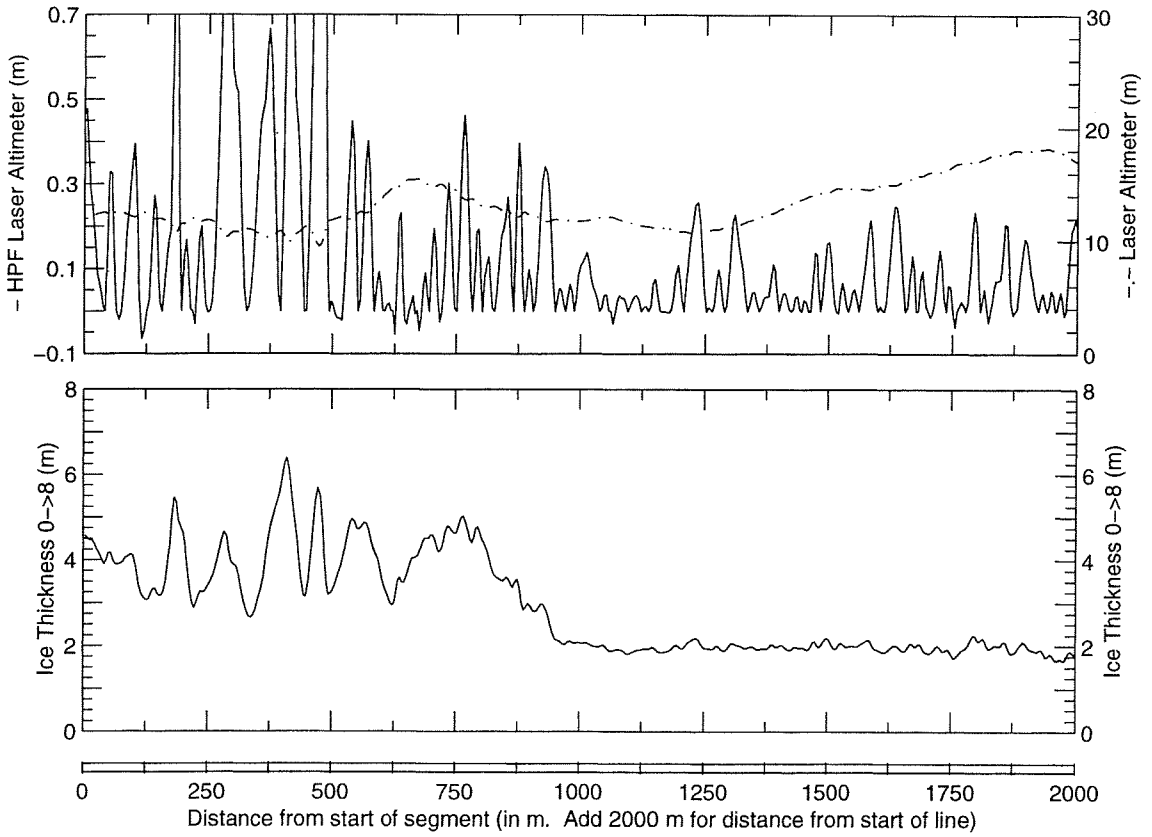

MAY 01 Flight #09 Line #10160 part 3 of 3

Line Starting Coordinates (74.5812,–96.9891) ending at (74.5798,–96.9673)

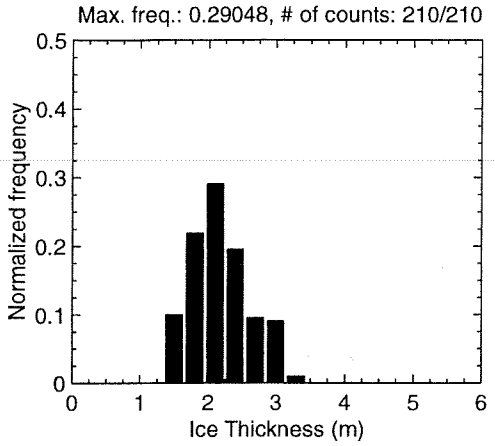

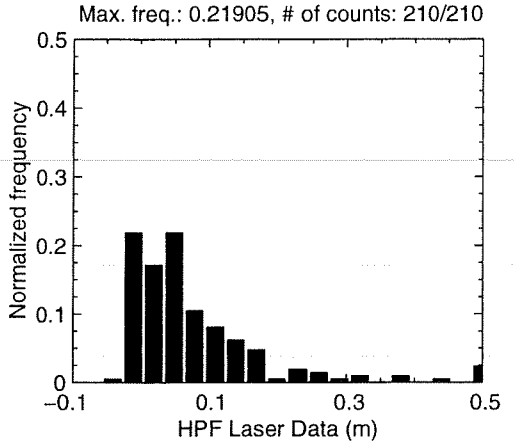

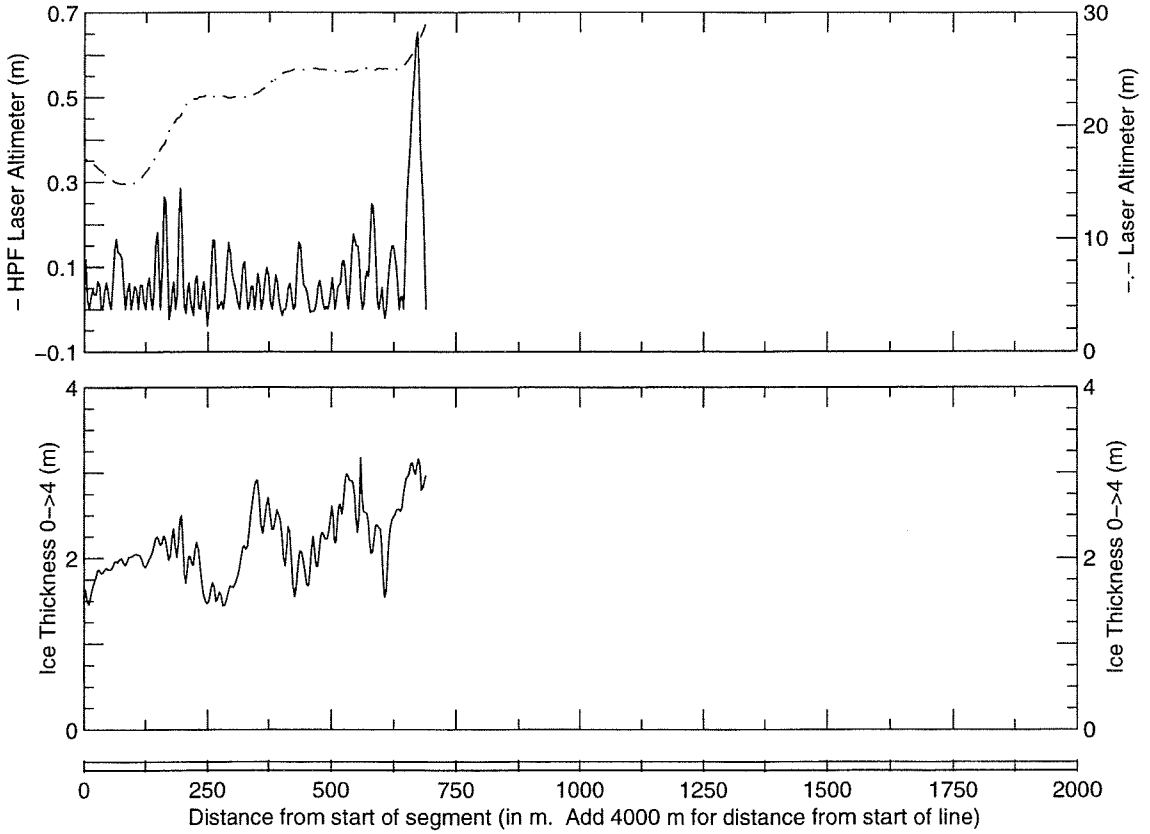

MAY 01 Flight #09 Line #10171 part 1 of 1

Line Starting Coordinates (74.5813,–96.9719) ending at (74.5813,–96.9765)

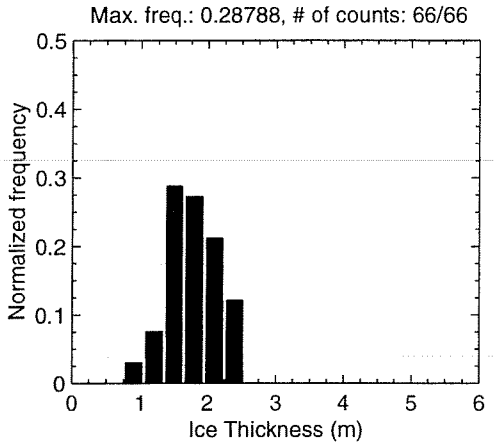

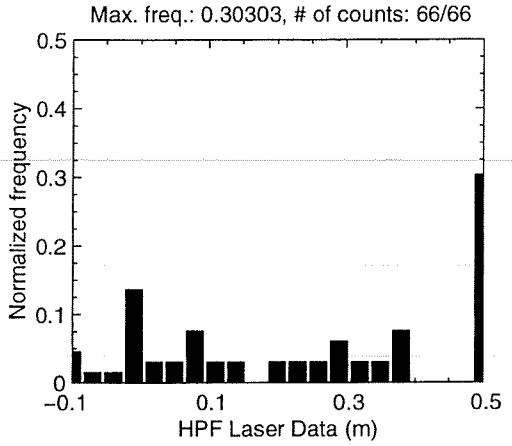

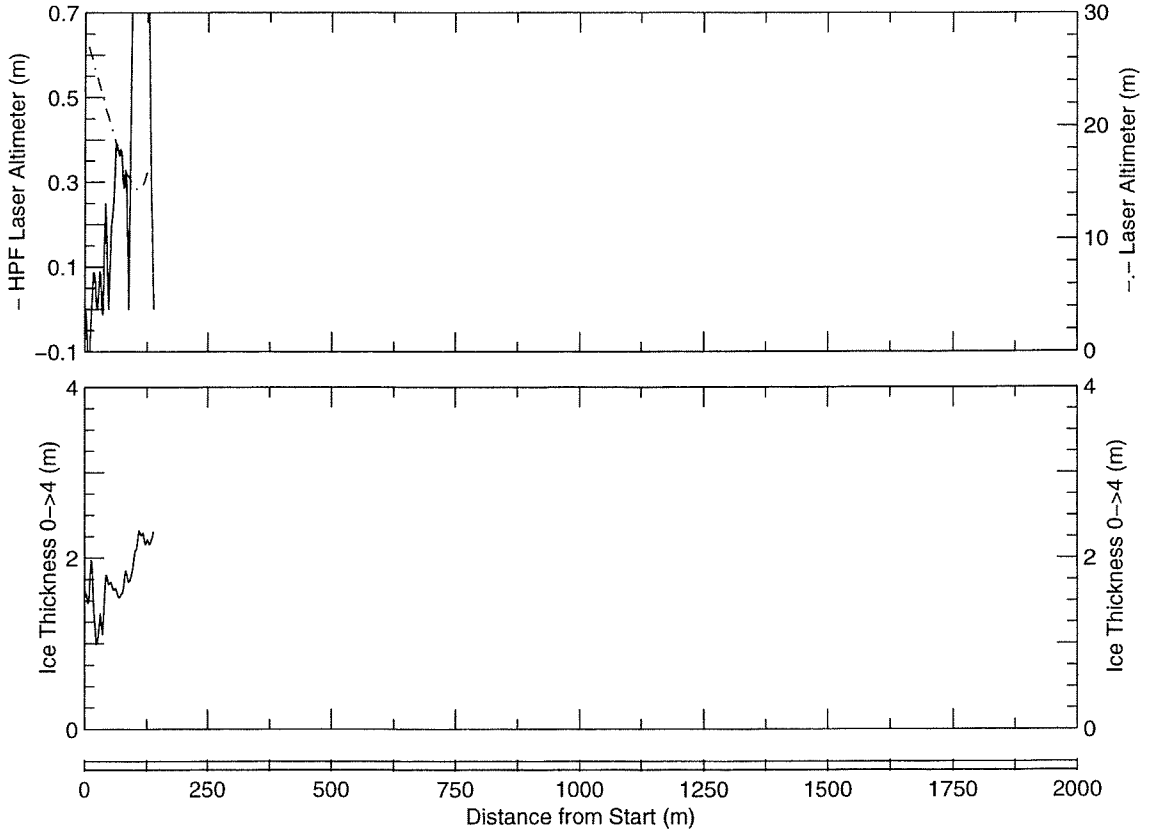

MAY 01 Flight #09 Line #10172 part 1 of 1

Line Starting Coordinates (74.5813,–96.9766) ending at (74.5811,–96.9823)

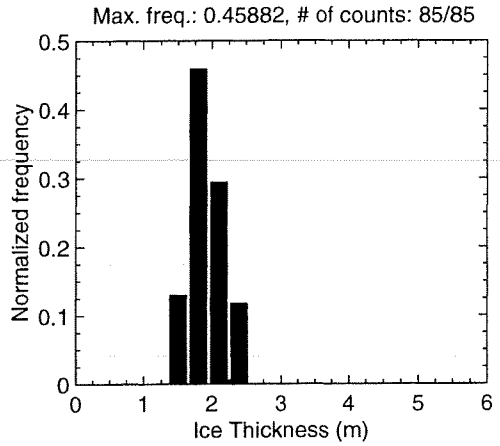

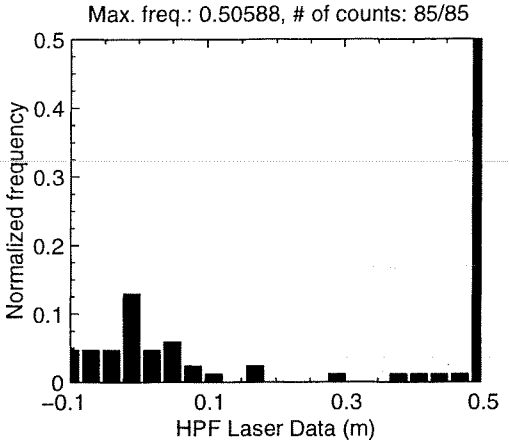

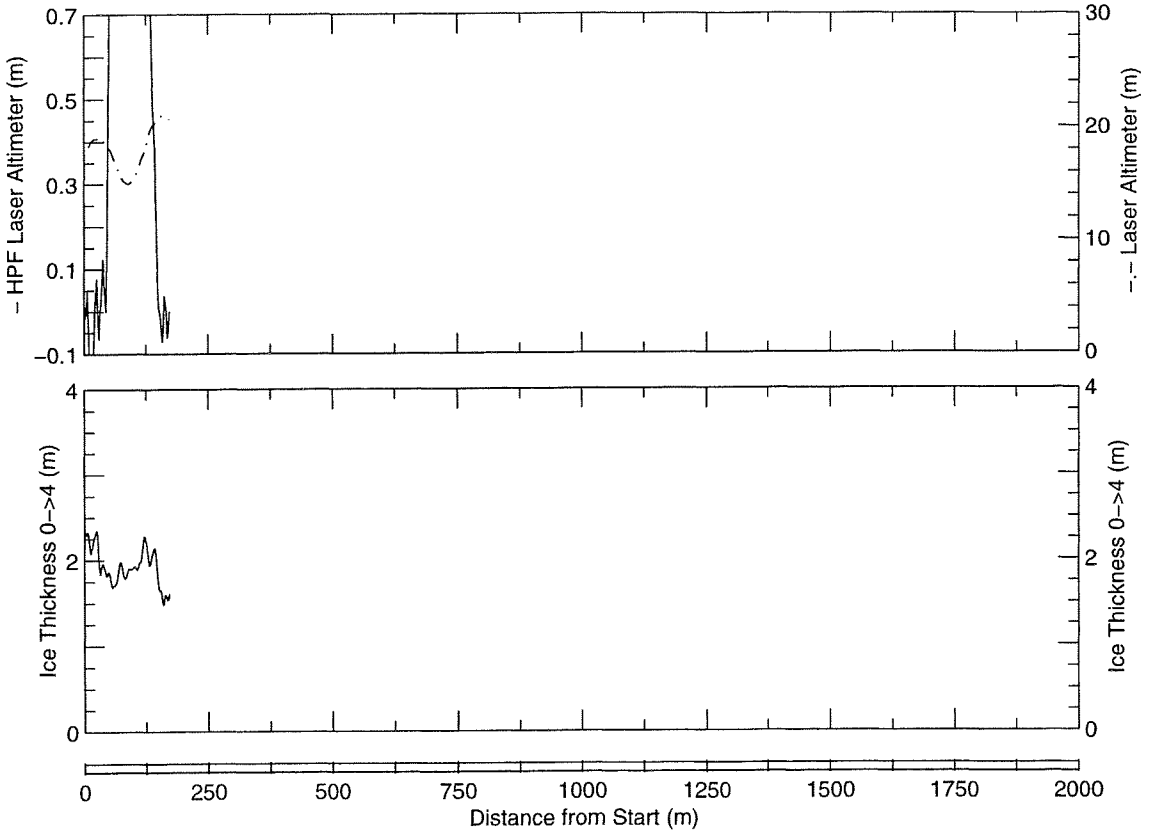

MAY 01 Flight #09 Line #10173 part 1 of 1

Line Starting Coordinates (74.5811,–96.9824) ending at (74.5805,–96.9980)

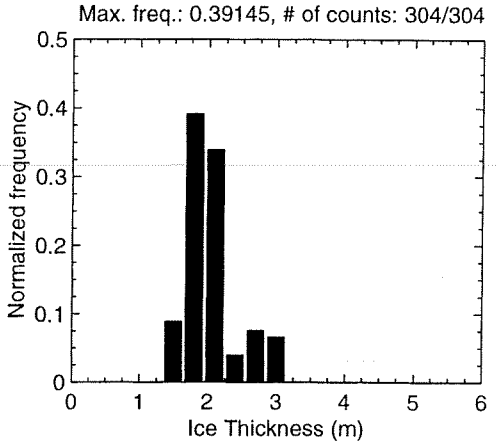

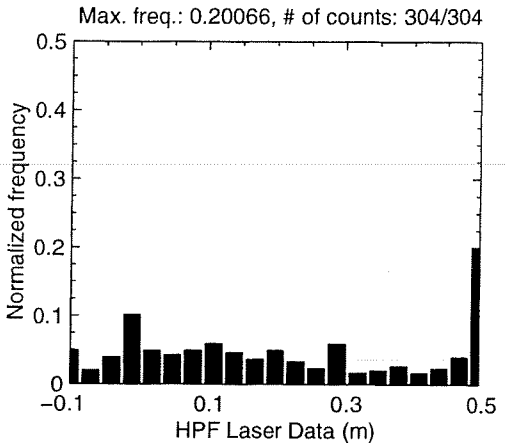

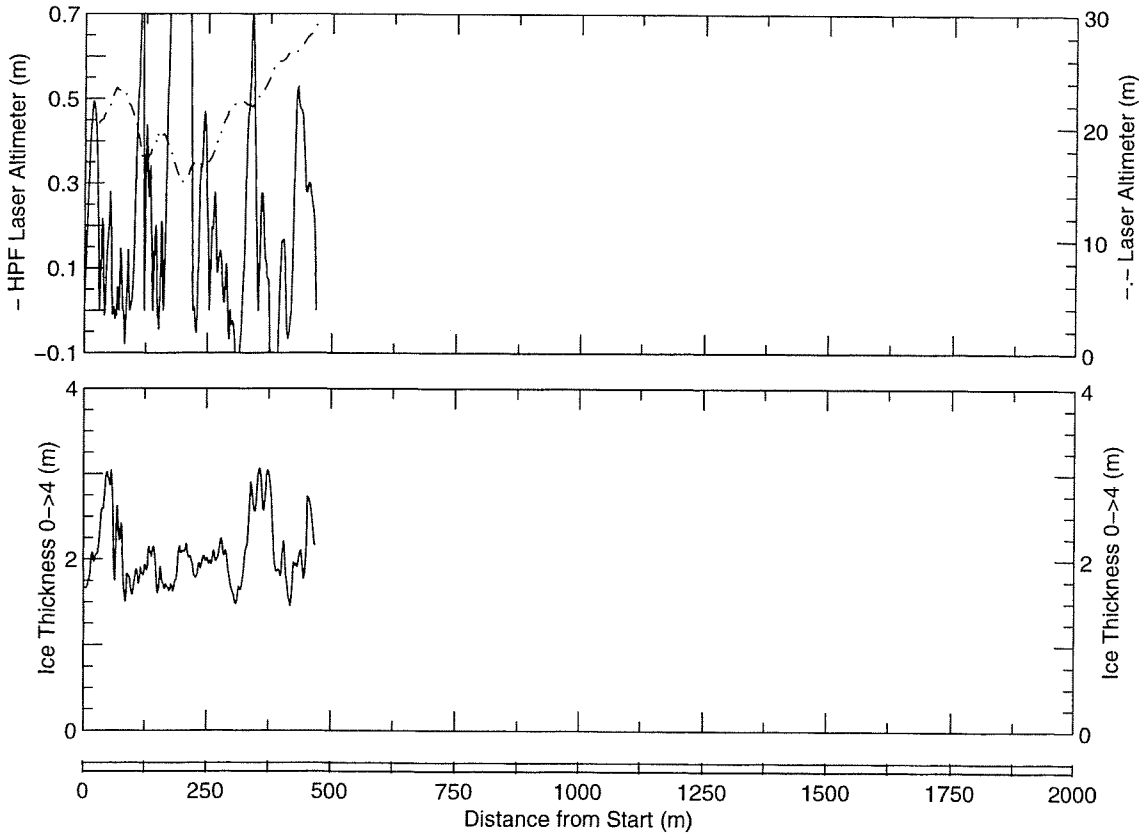

MAY 01 Flight #09 Line #10180 part 1 of 1

Line Starting Coordinates (74.5816,–96.9871) ending at (74.5810,–97.0284)

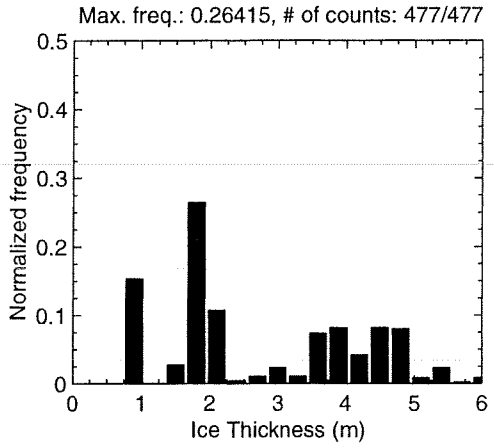

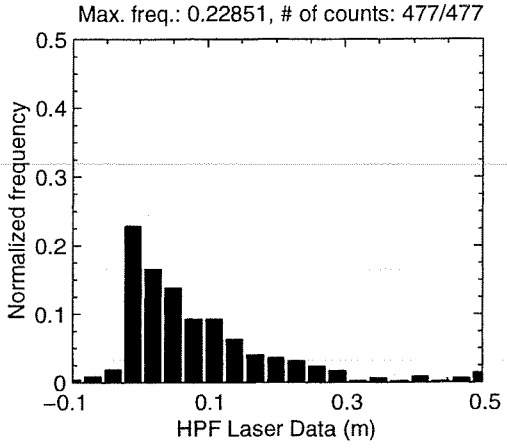

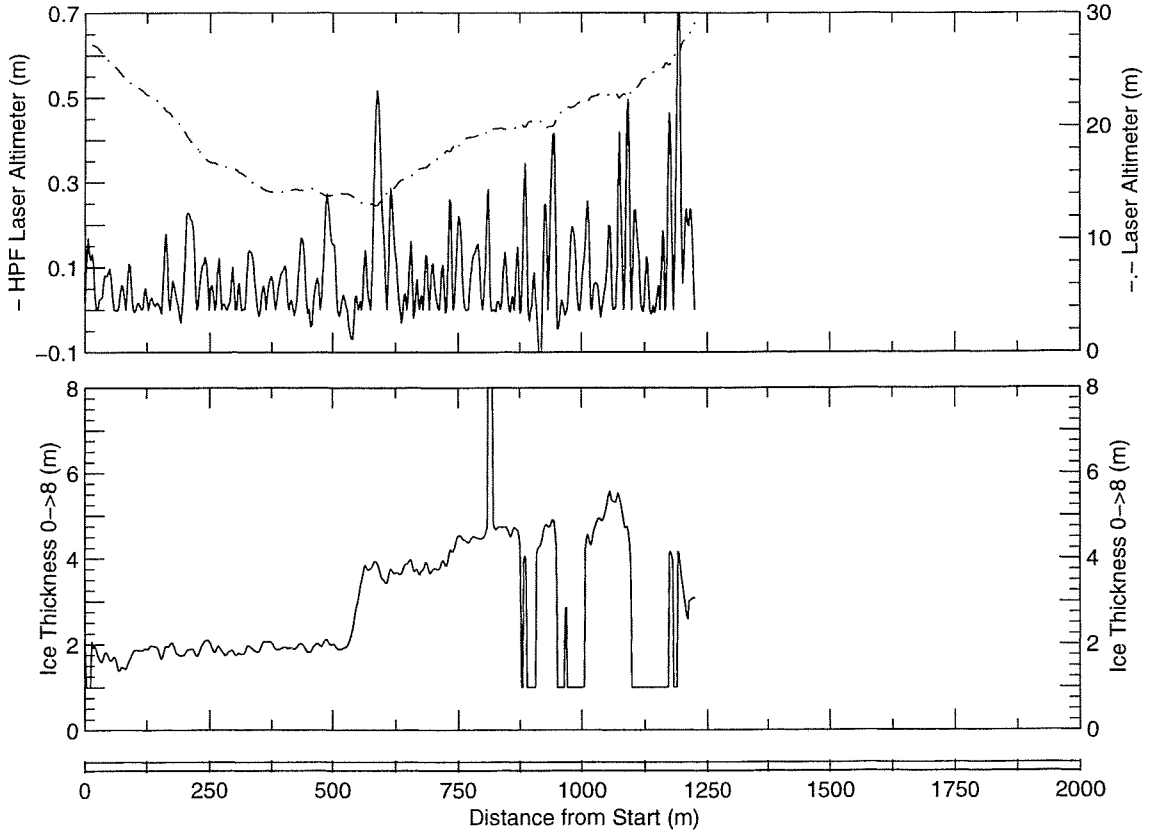

MAY 01 Flight #09 Line #10190 part 1 of 1

Line Starting Coordinates (74.5801,–97.0476) ending at (74.5807,–97.0295)

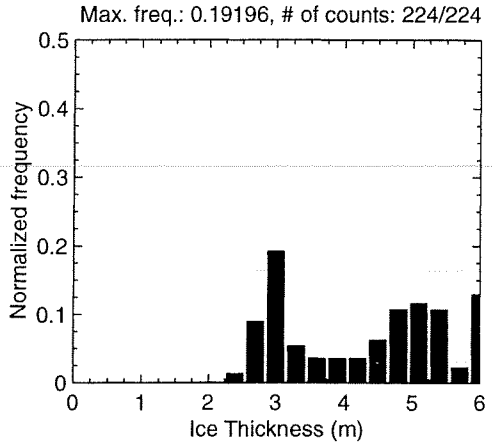

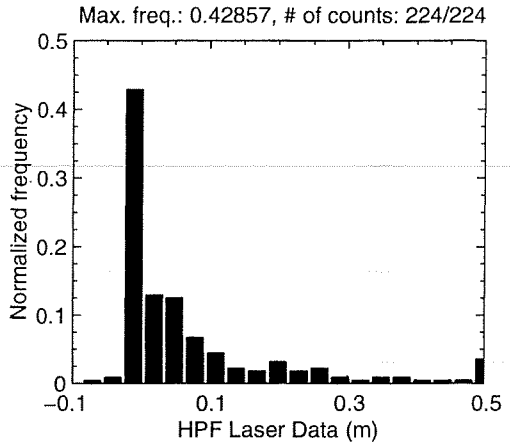

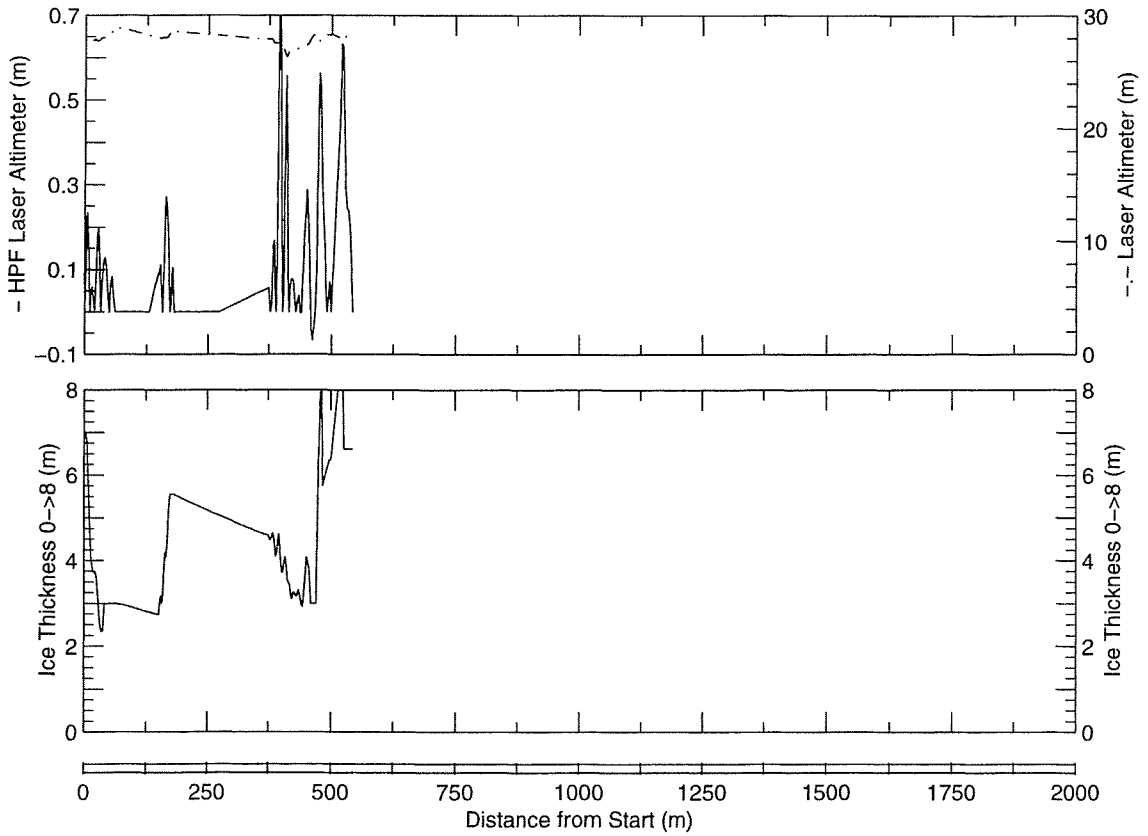

MAY 01 Flight #10 Line #10010 part 1 of 1

Line Starting Coordinates (74.5555,–96.9587) ending at (74.5683,–96.9529)

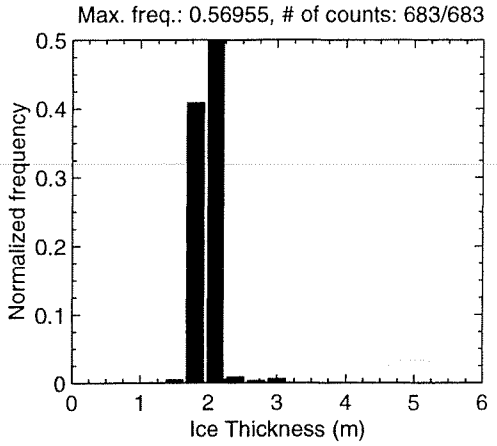

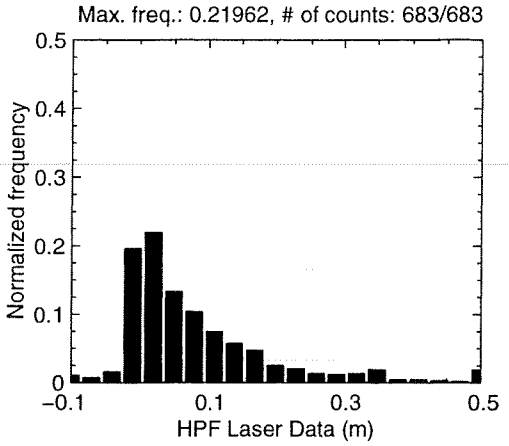

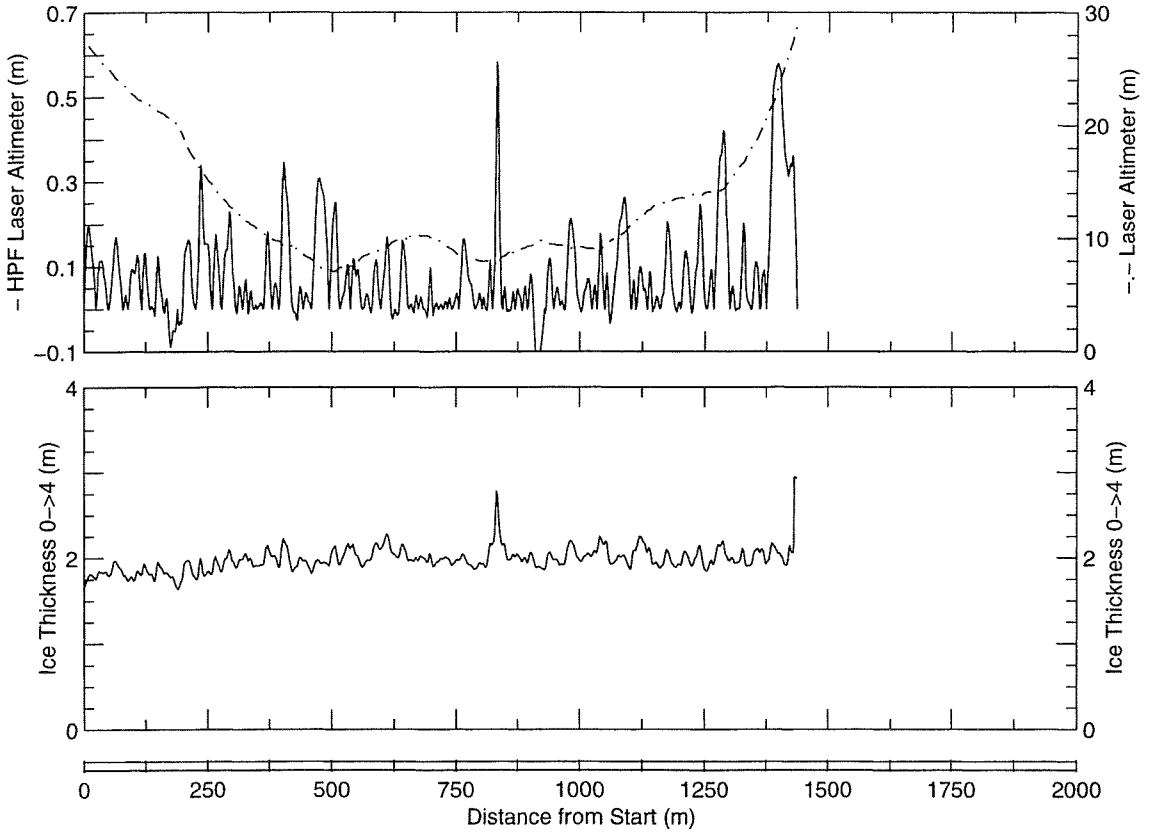

MAY 01 Flight #10 Line #10021 part 1 of 1

Line Starting Coordinates (74.5540,–96.9594) ending at (74.5686,–96.9536)

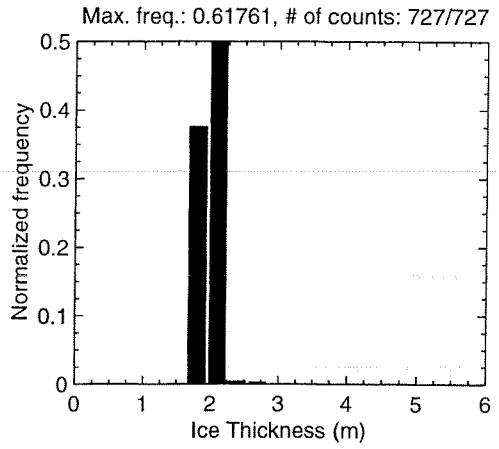

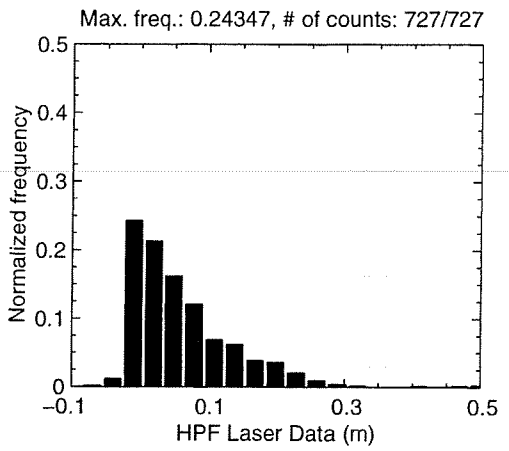

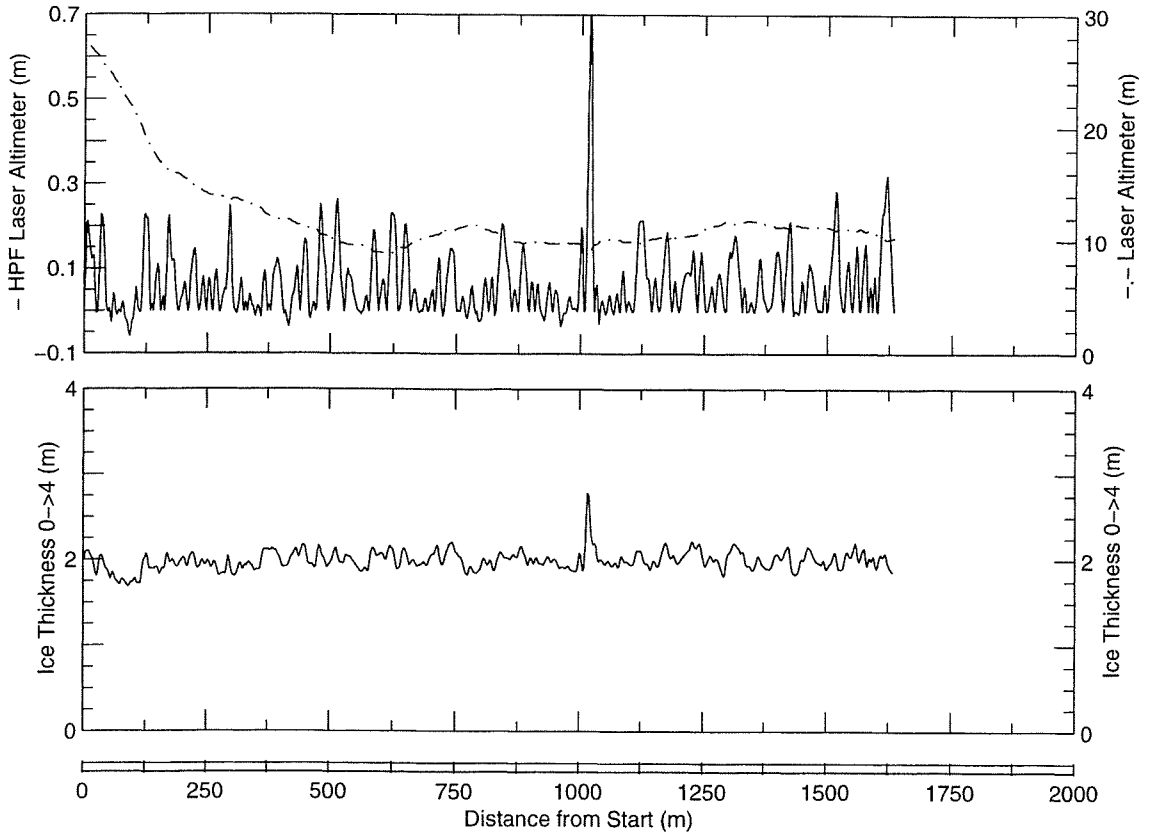

MAY 01 Flight #10 Line #10022 part 1 of 2

Line Starting Coordinates (74.5686,–96.9536) ending at (74.5864,–96.9629)

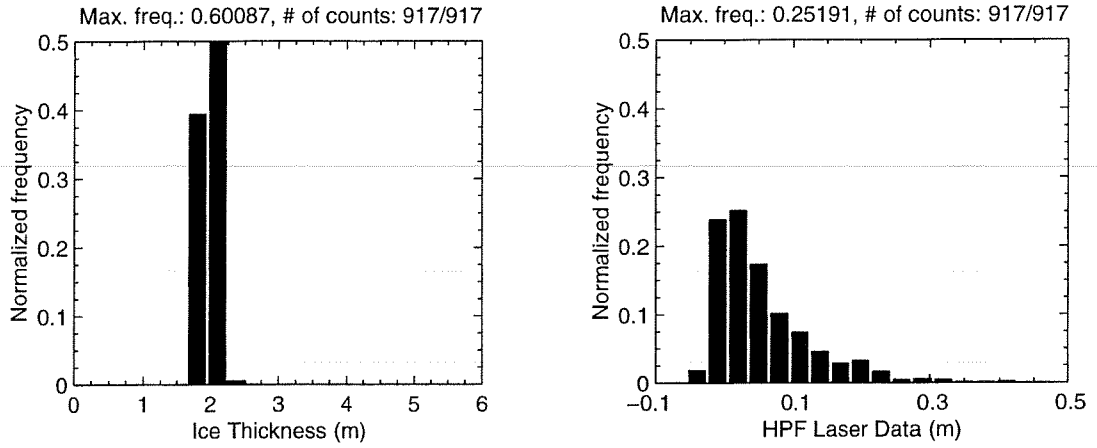

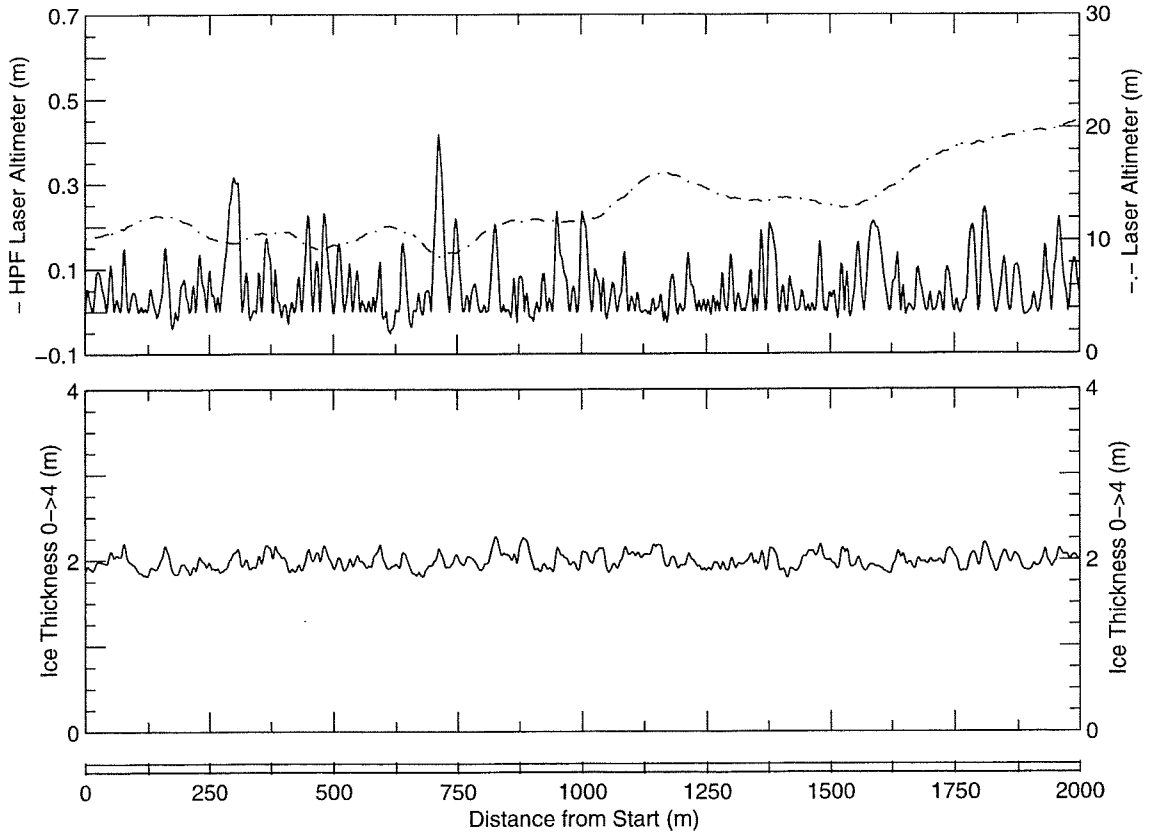

MAY 01 Flight #10 Line #10022 part 2 of 2

Line Starting Coordinates (74.5864,–96.9629) ending at (74.5963,–96.9661)

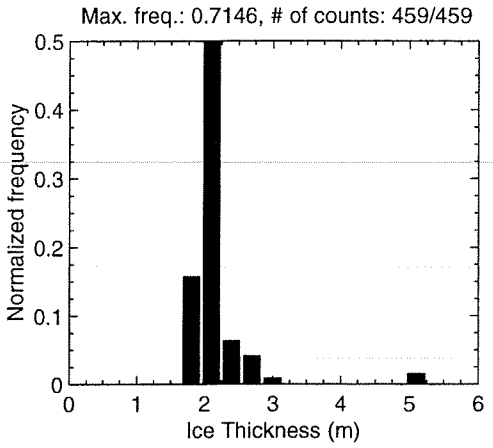

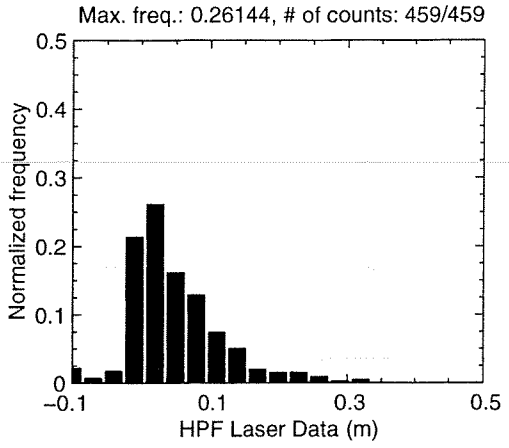

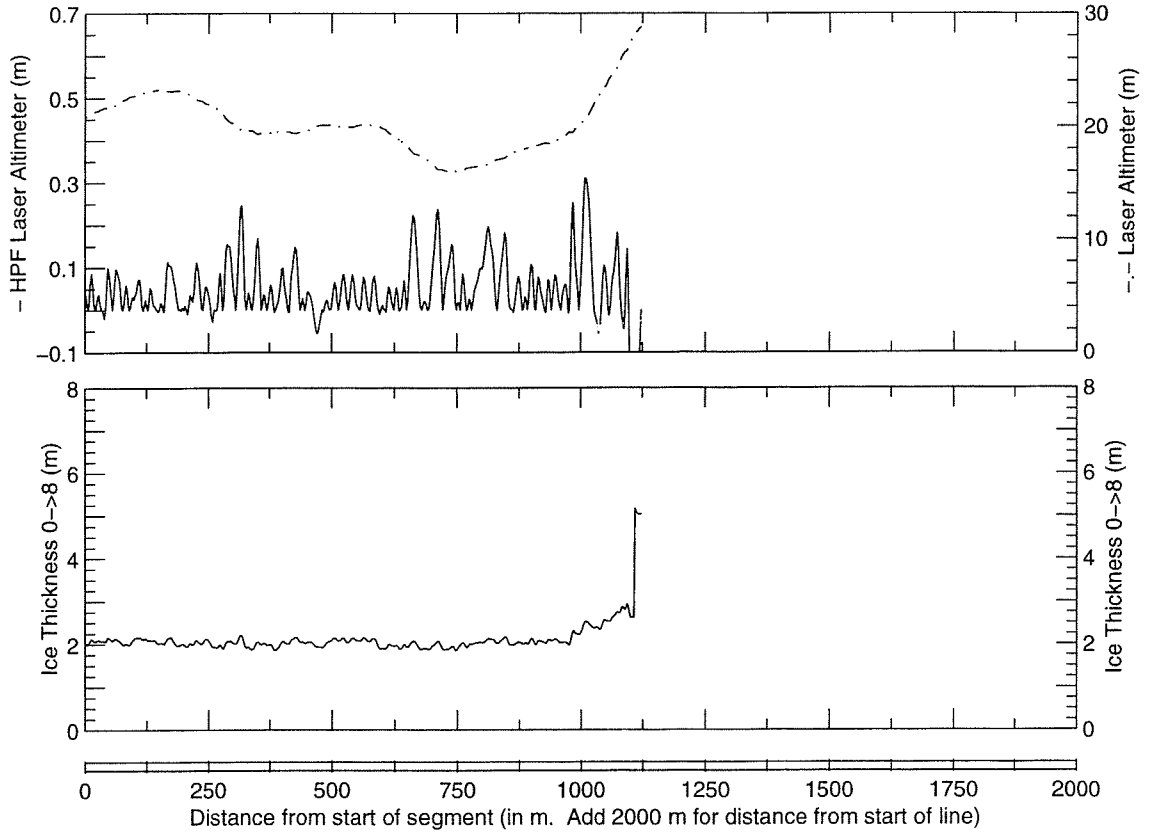

MAY 01 Flight #10 Line #10030 part 1 of 1

Line Starting Coordinates (74.5904,–96.9575) ending at (74.5858,–96.9799)

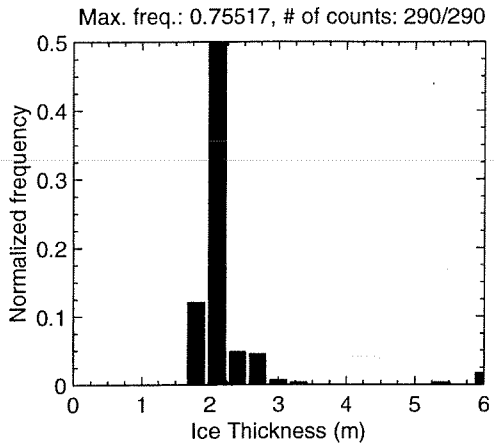

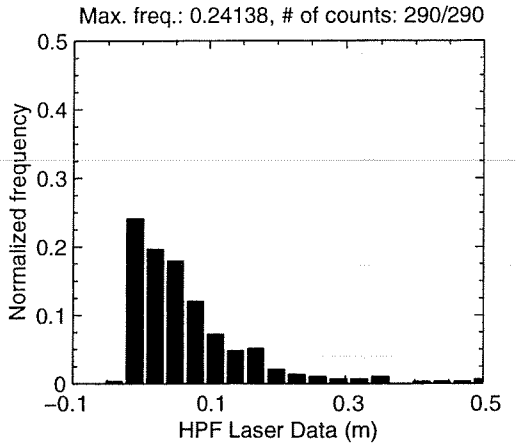

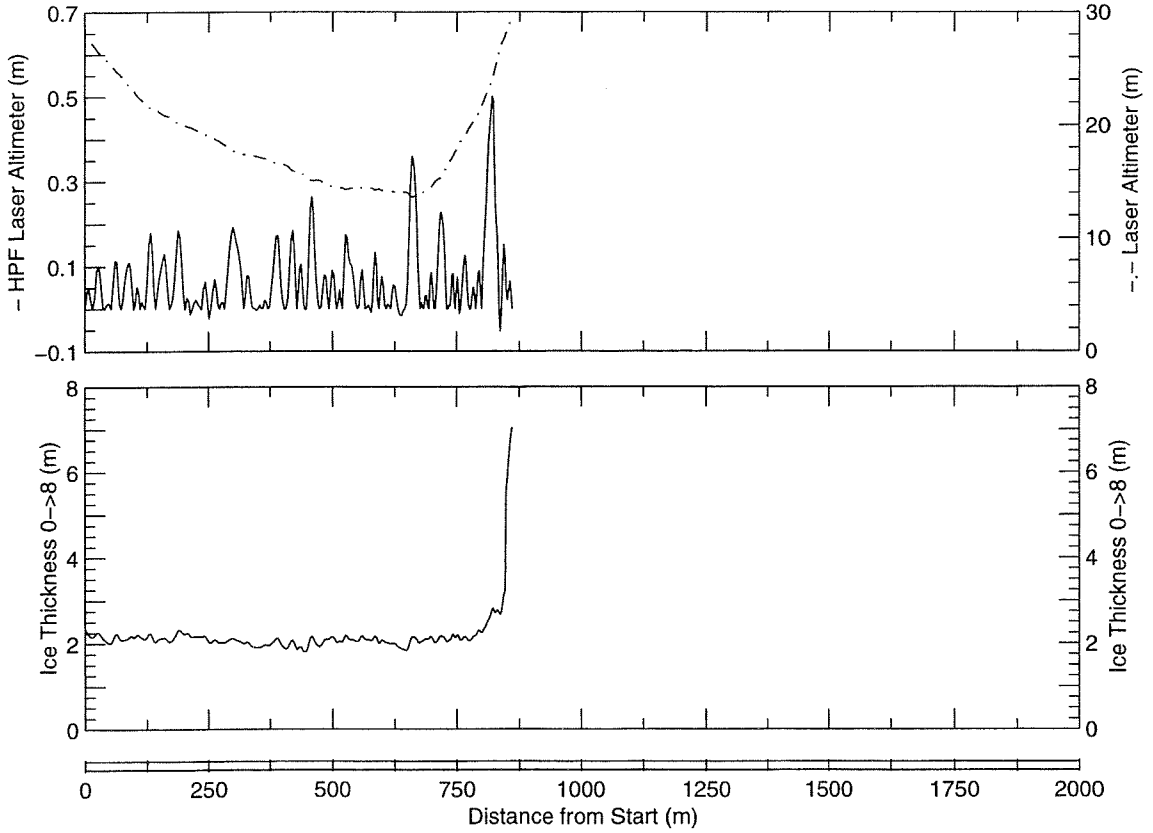

MAY 01 Flight #10 Line #10040 part 1 of 1

Line Starting Coordinates (74.5850,–96.9612) ending at (74.5802,–96.9618)

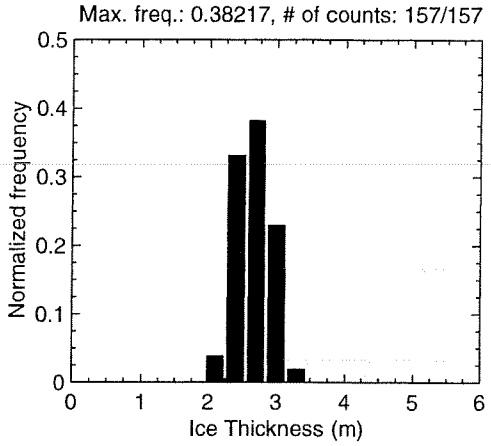

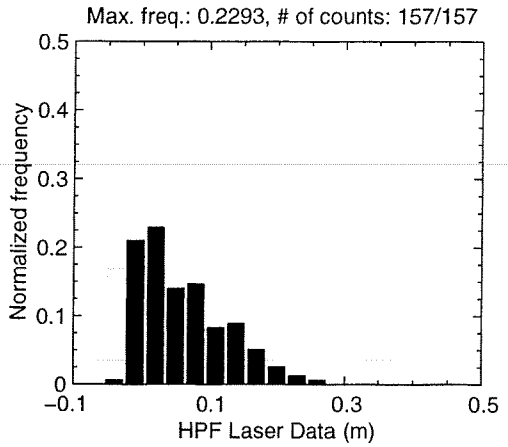

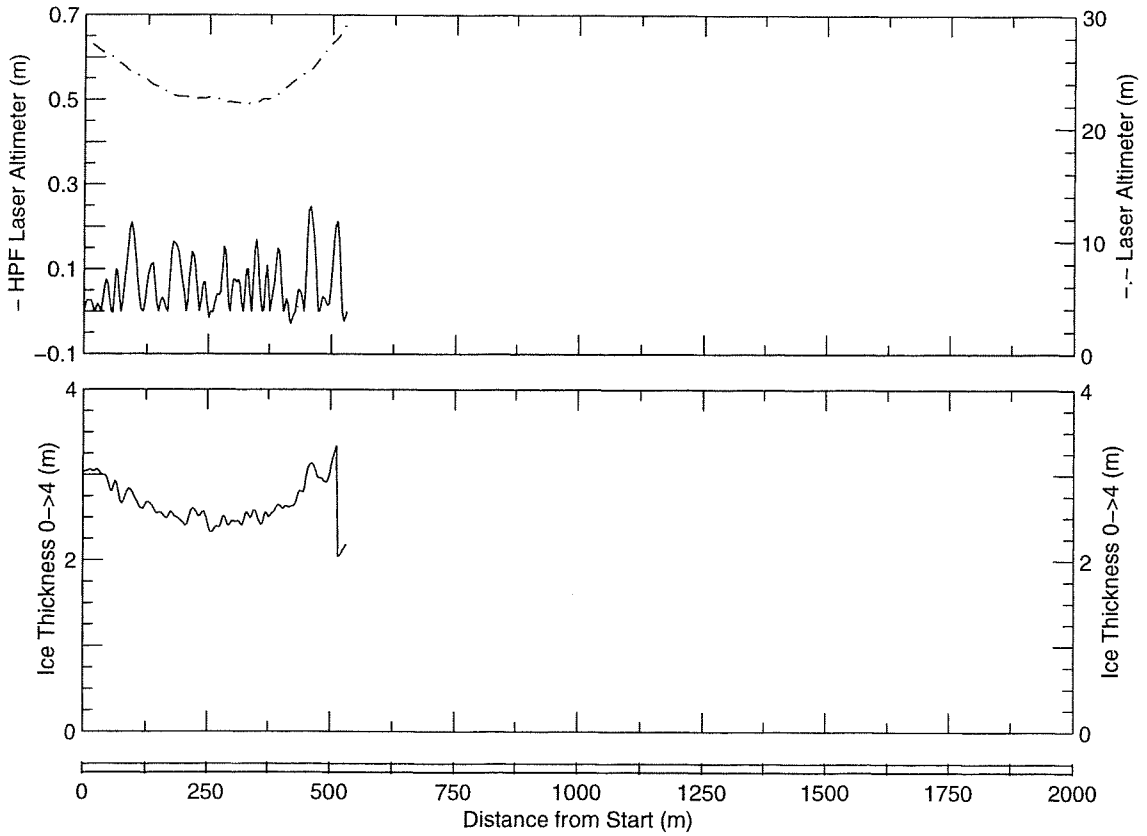

MAY 01 Flight #10 Line #10051 part 1 of 1

Line Starting Coordinates (74.5796,–96.9532) ending at (74.5860,–96.9598)

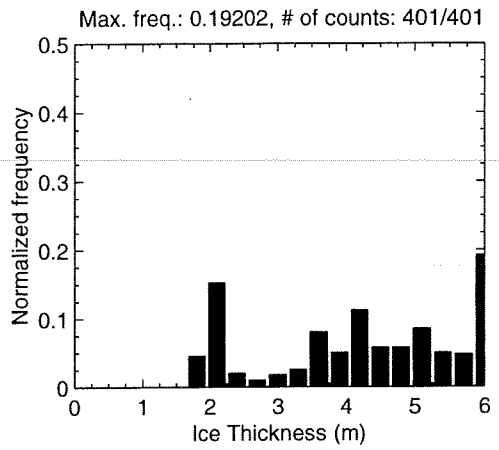

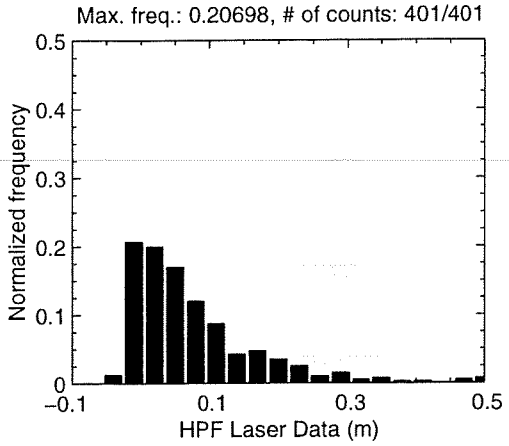

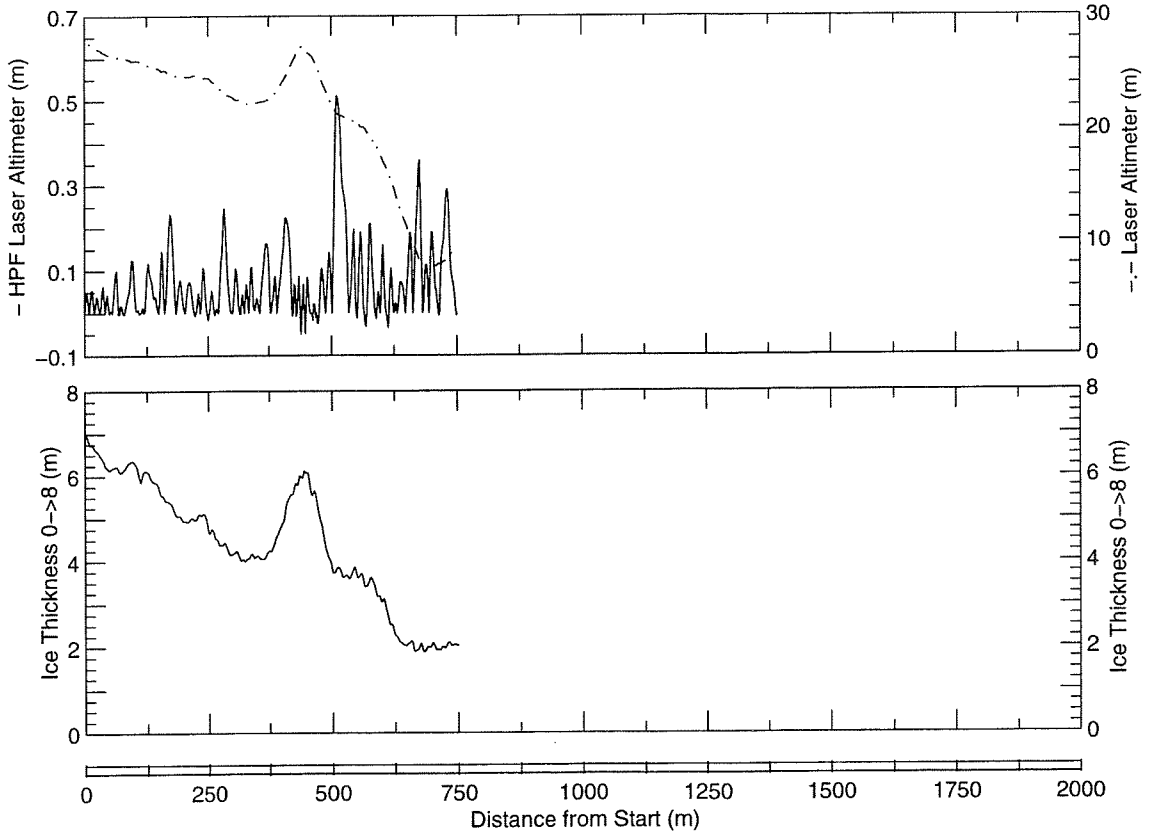

MAY 01 Flight #10 Line #10052 part 1 of 1

Line Starting Coordinates (74.5860,–96.9598) ending at (74.5924,–96.9555)

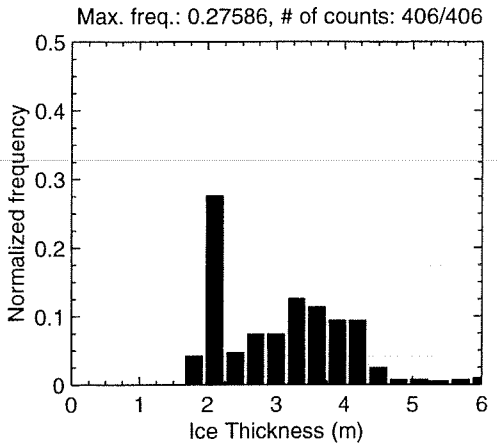

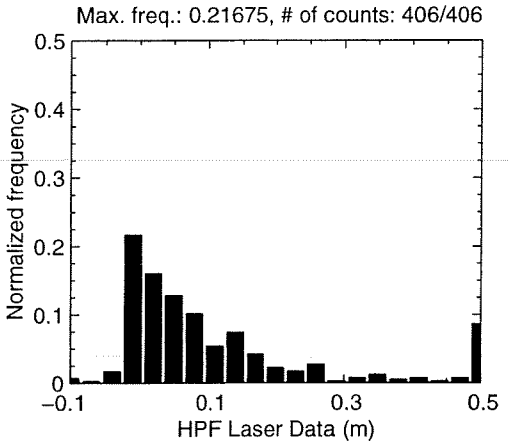

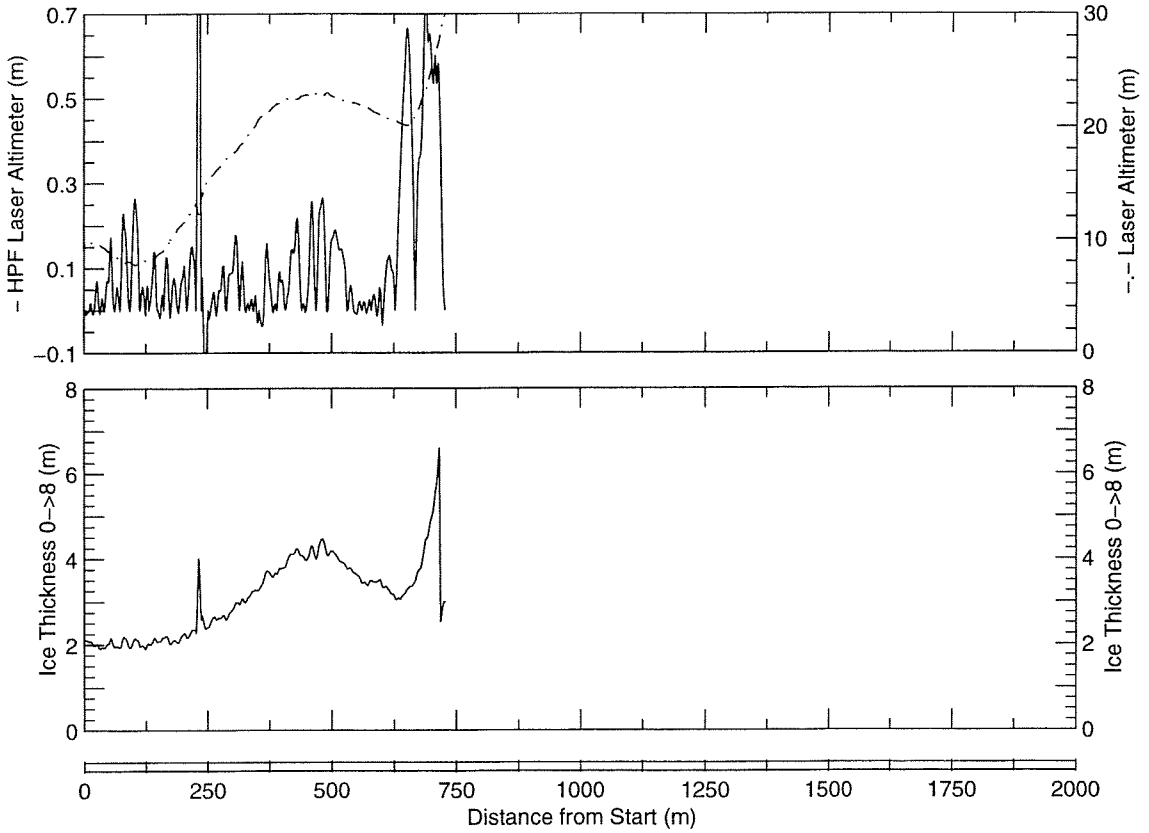

MAY 01 Flight #10 Line #10060 part 1 of 2

Line Starting Coordinates (74.5933,–96.9580) ending at (74.5975,–97.0236)

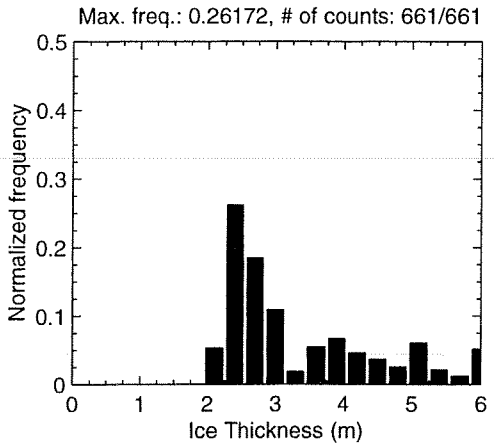

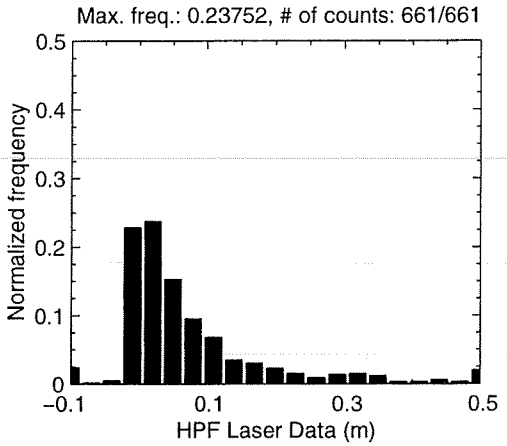

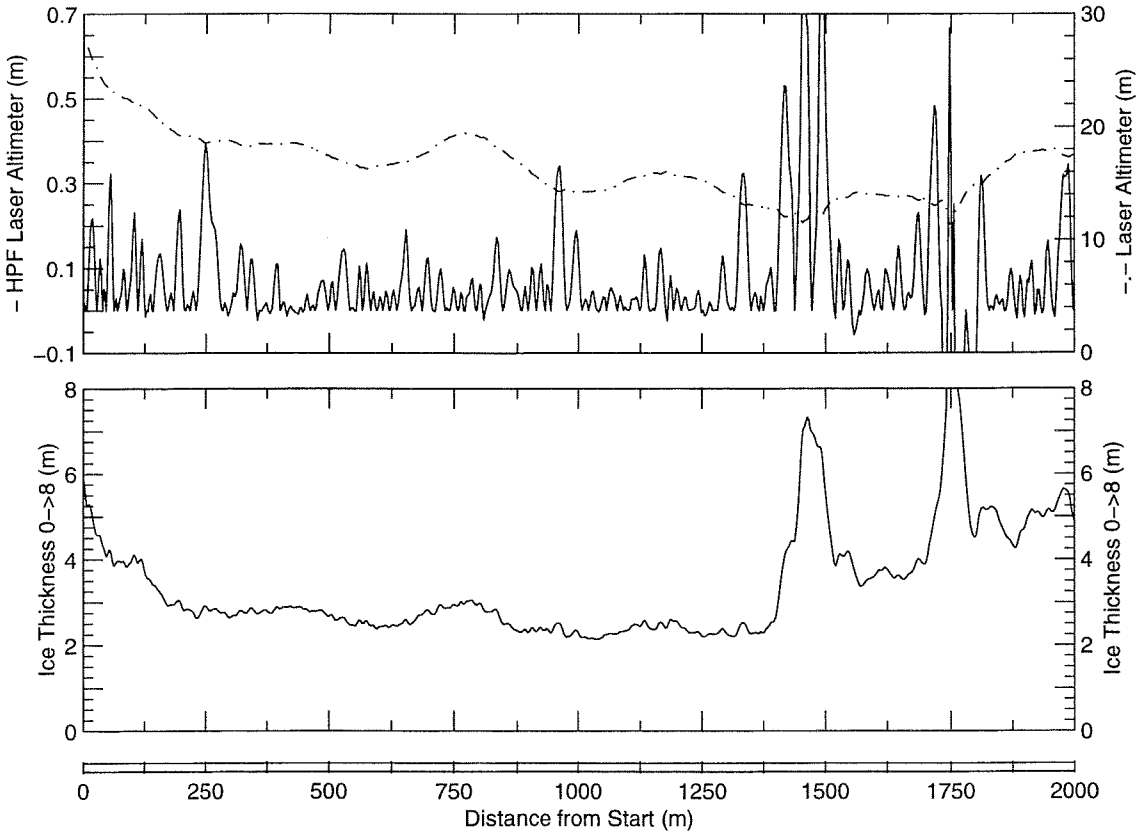

MAY 01 Flight #10 Line #10060 part 2 of 2

Line Starting Coordinates (74.5975,–97.0236) ending at (74.5978,–97.0392)

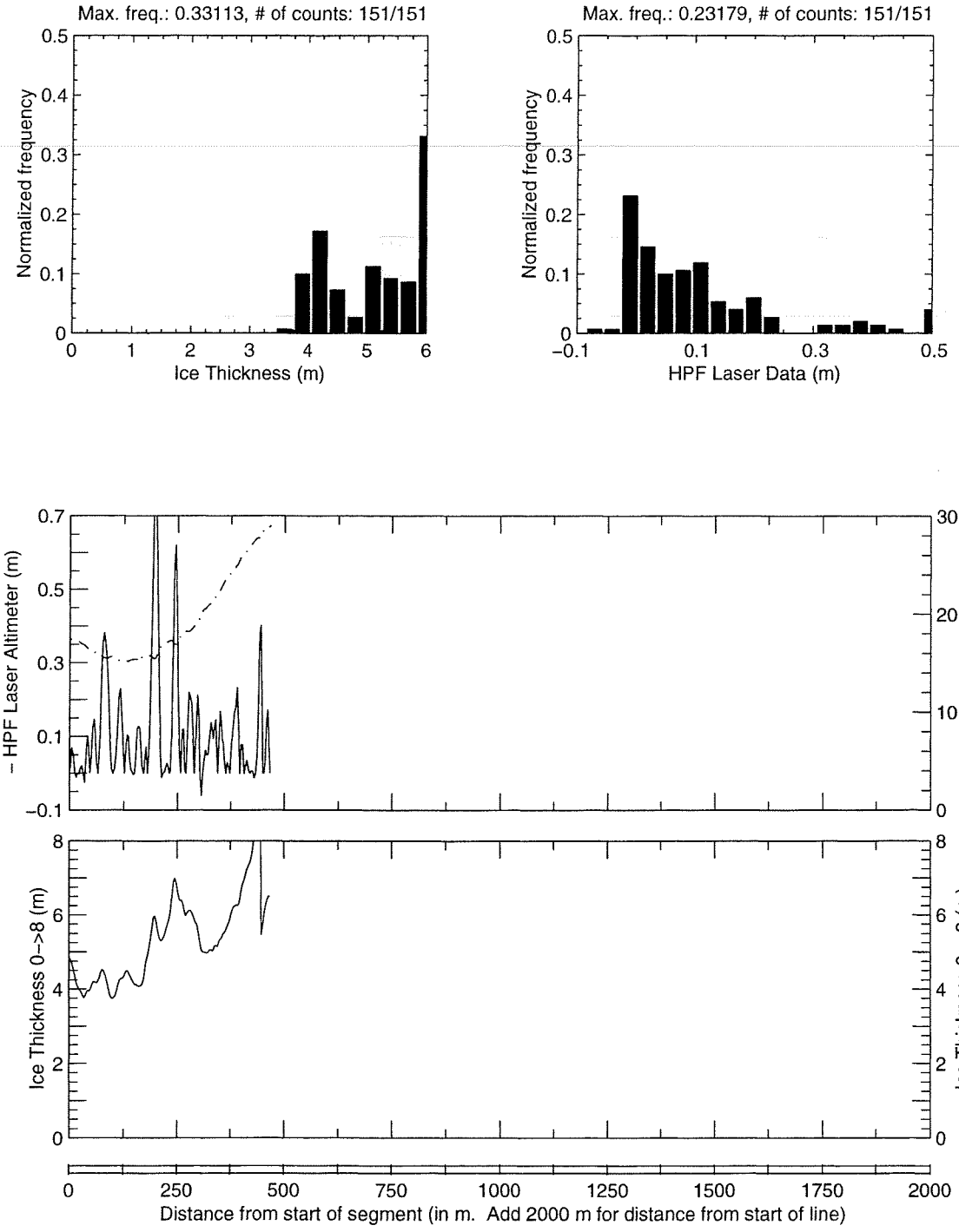

MAY 01 Flight #10 Line #10070 part 1 of 2

Line Starting Coordinates (74.5935,–97.0463) ending at (74.5895,–96.9832)

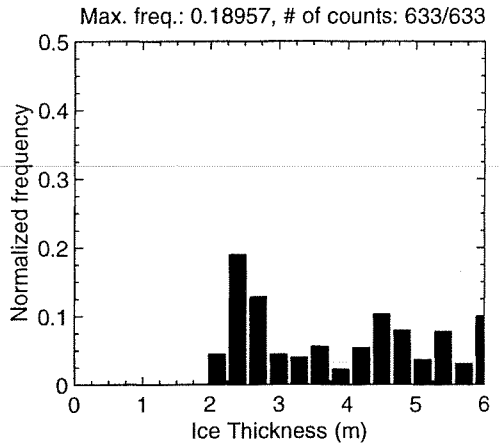

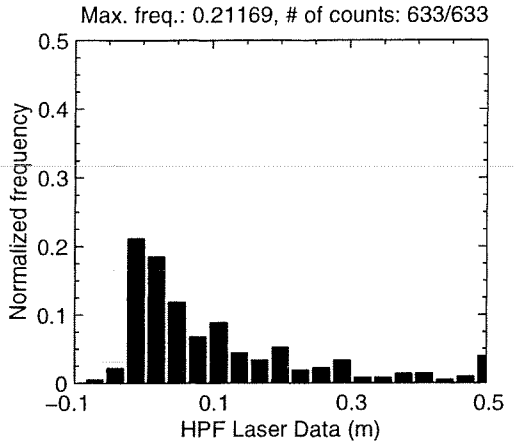

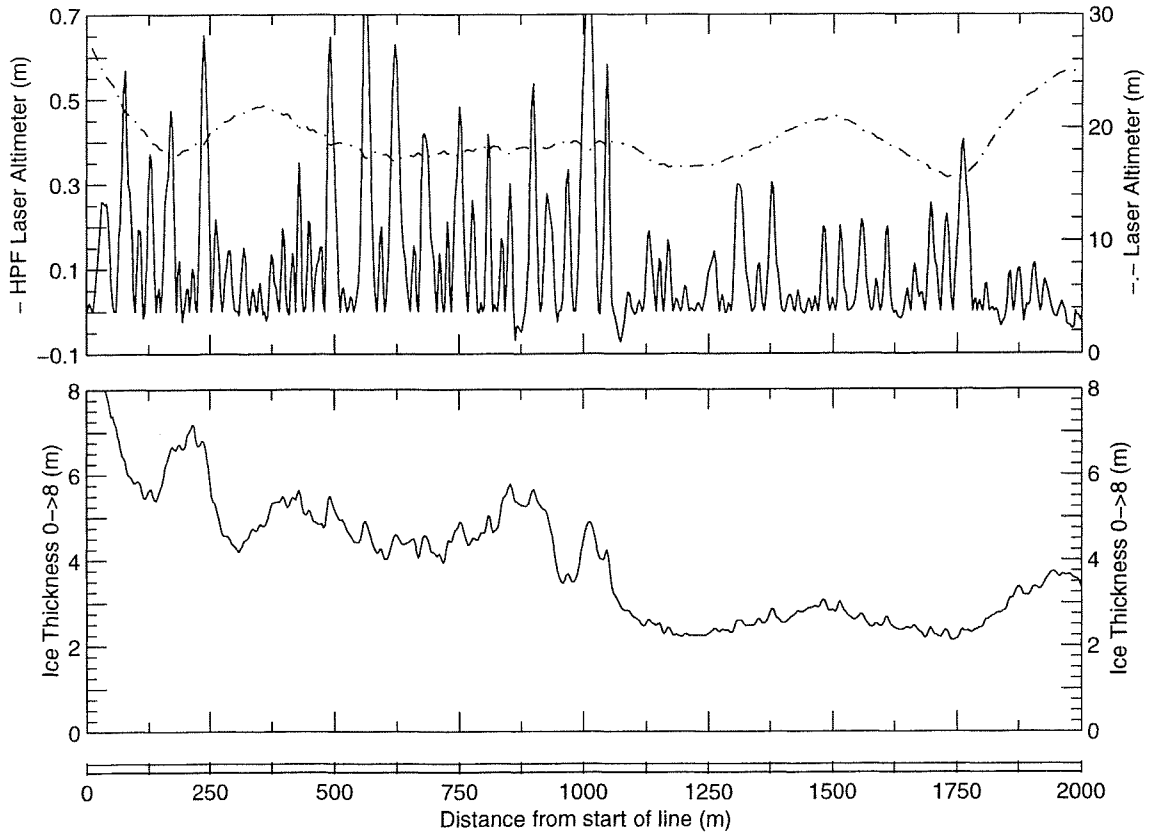

MAY 01 Flight #10 Line #10070 part 2 of 2

Line Starting Coordinates (74.5895,–96.9832) ending at (74.5865,–96.9464)

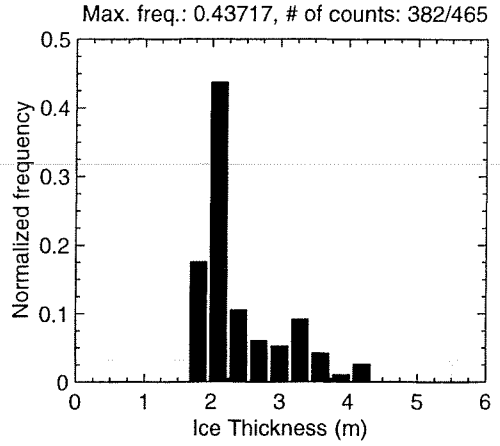

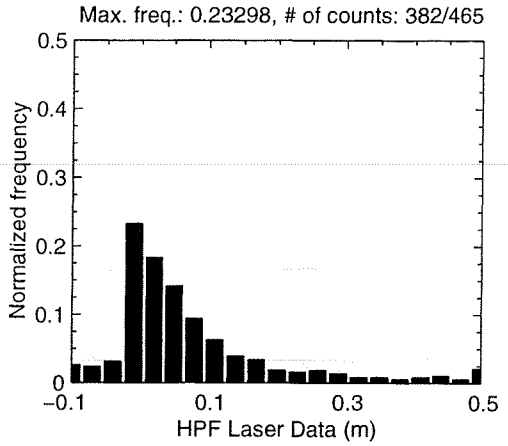

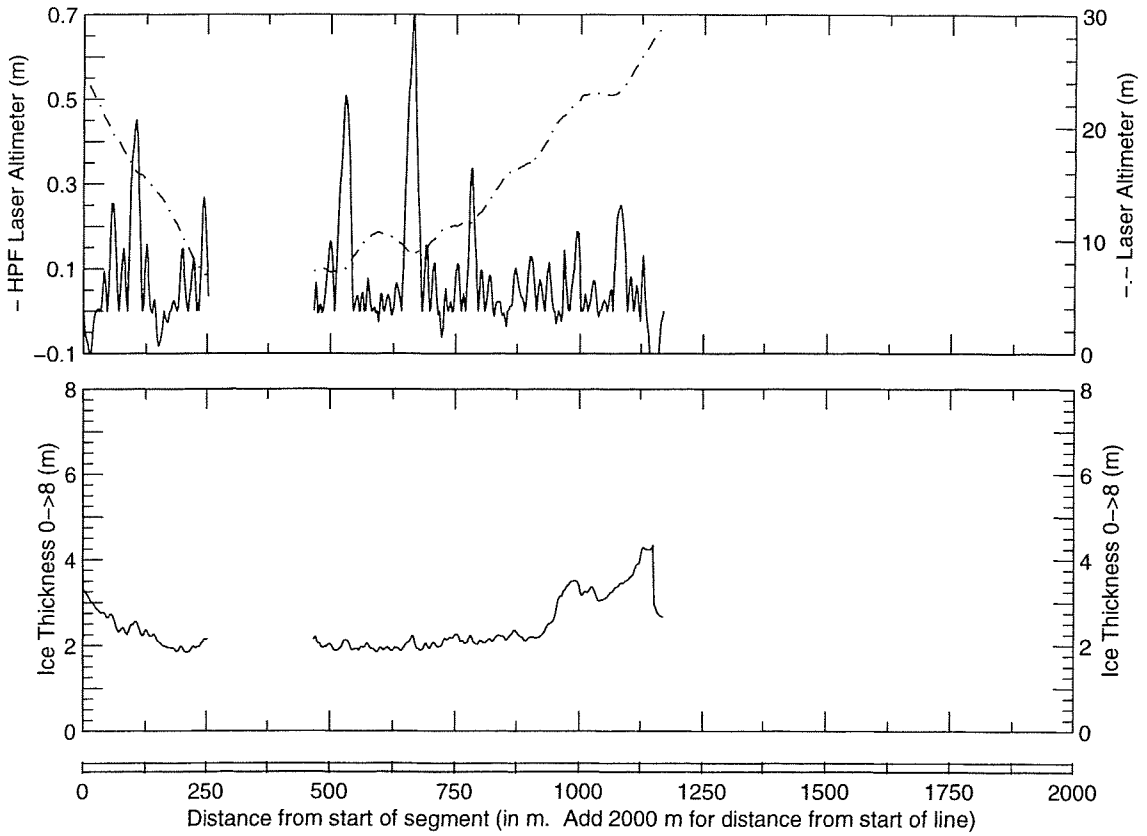

MAY 01 Flight #10 Line #10081 part 1 of 1

Line Starting Coordinates (74.5863,−96.9364) ending at (74.5870,−96.9432)

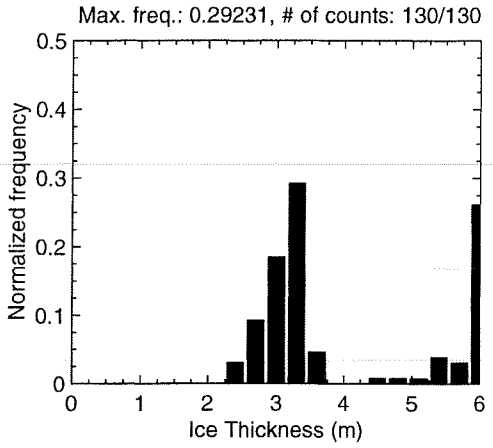

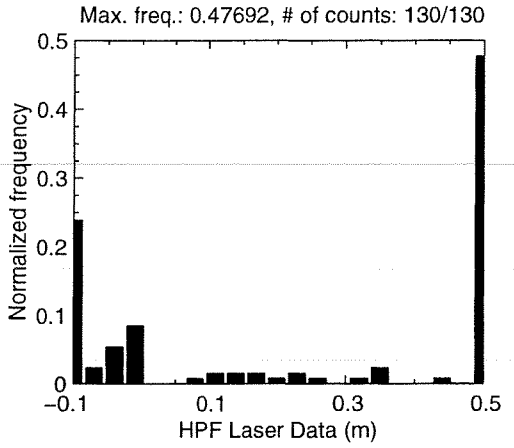

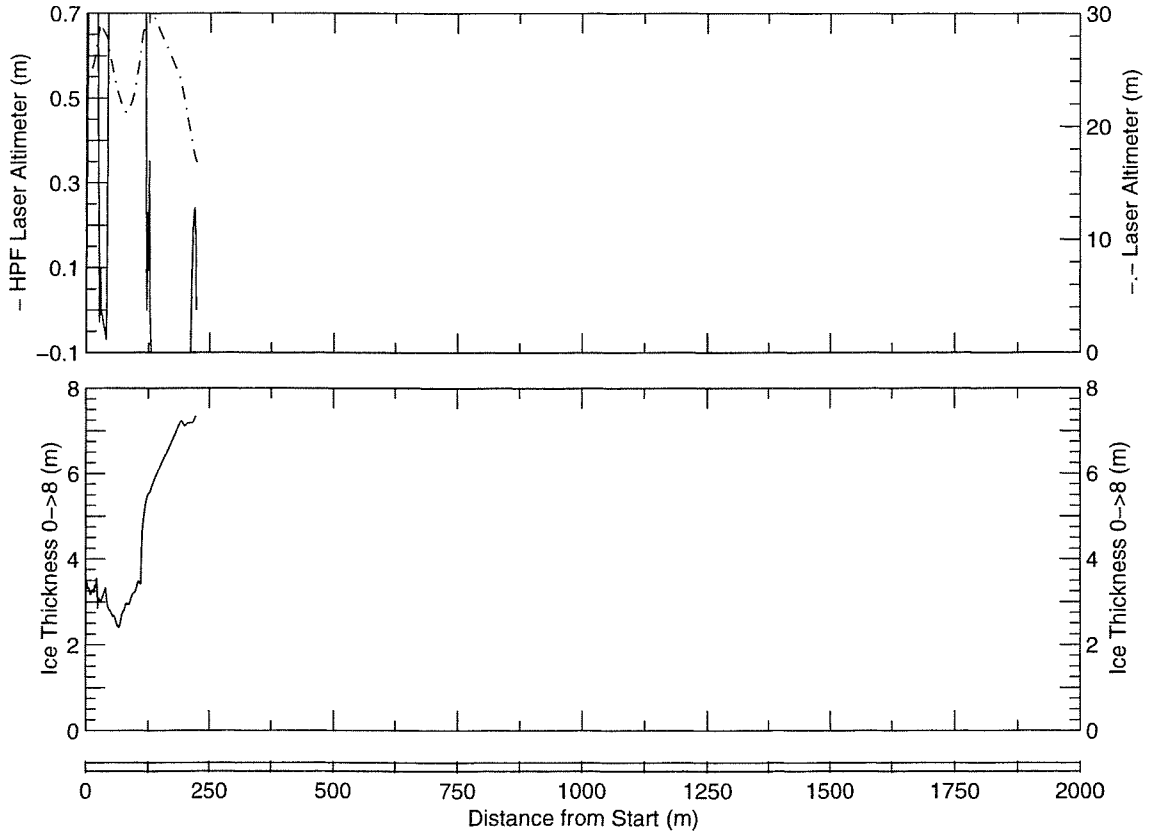

MAY 01 Flight #10 Line #10082 part 1 of 1

Line Starting Coordinates (74.5870,–96.9432) ending at (74.5868,–96.9519)

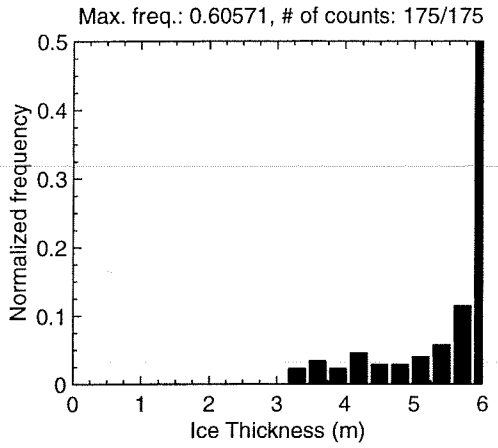

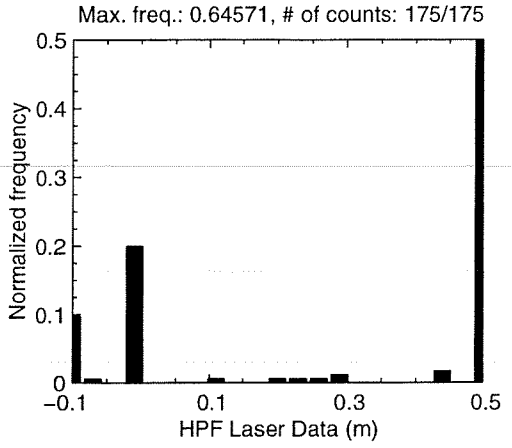

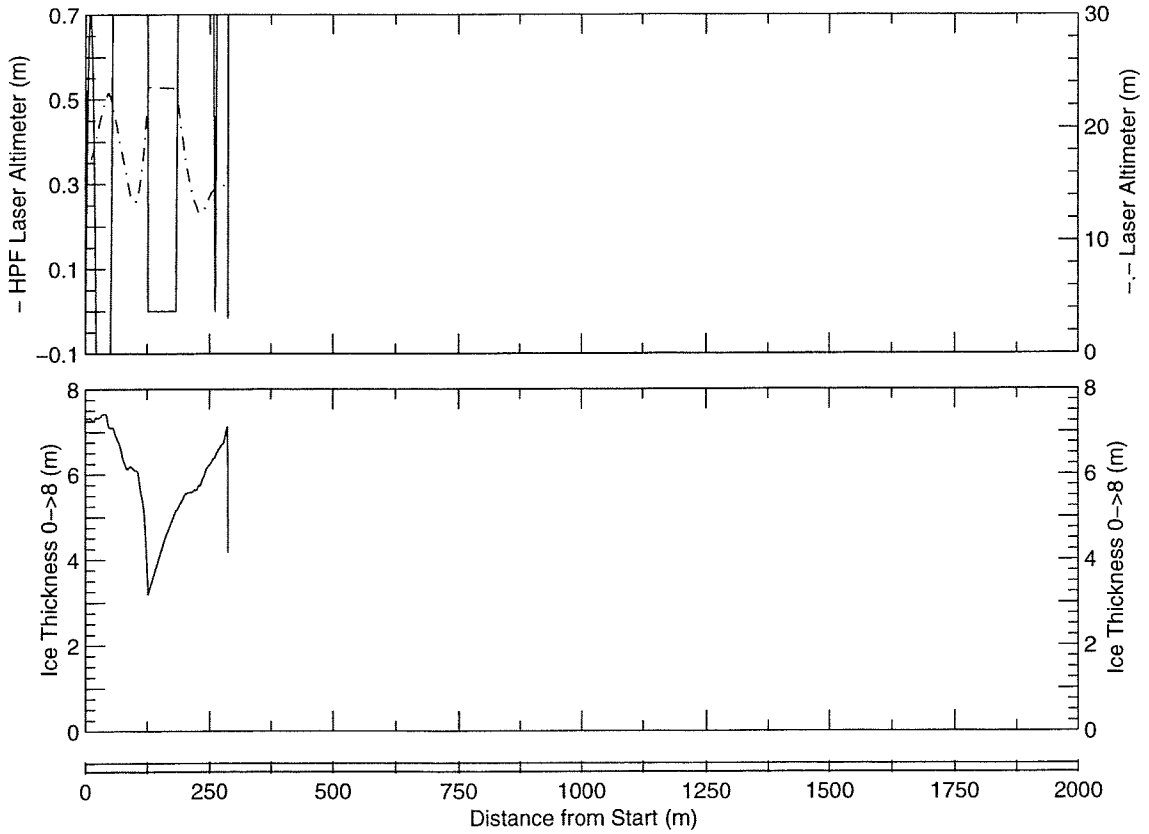

MAY 01 Flight #10 Line #10083 part 1 of 1

Line Starting Coordinates (74.5868,–96.9519) ending at (74.5880,–96.9526)

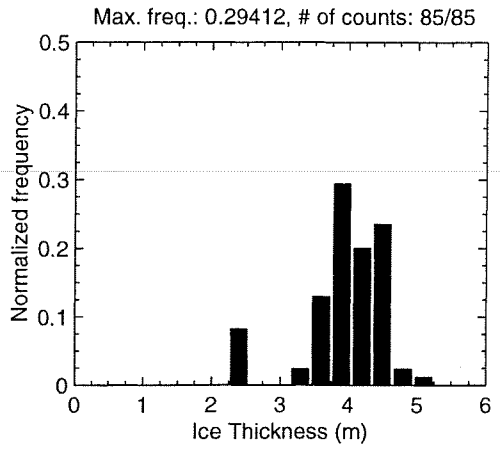

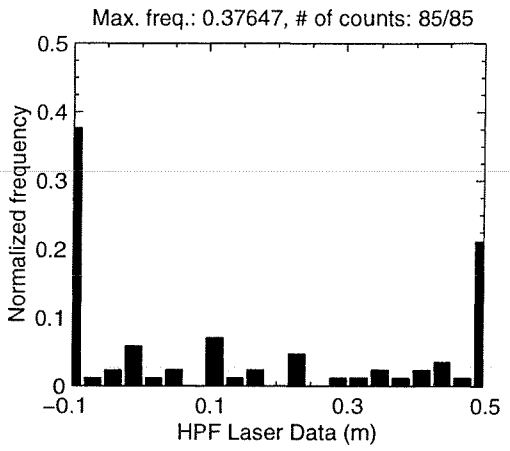

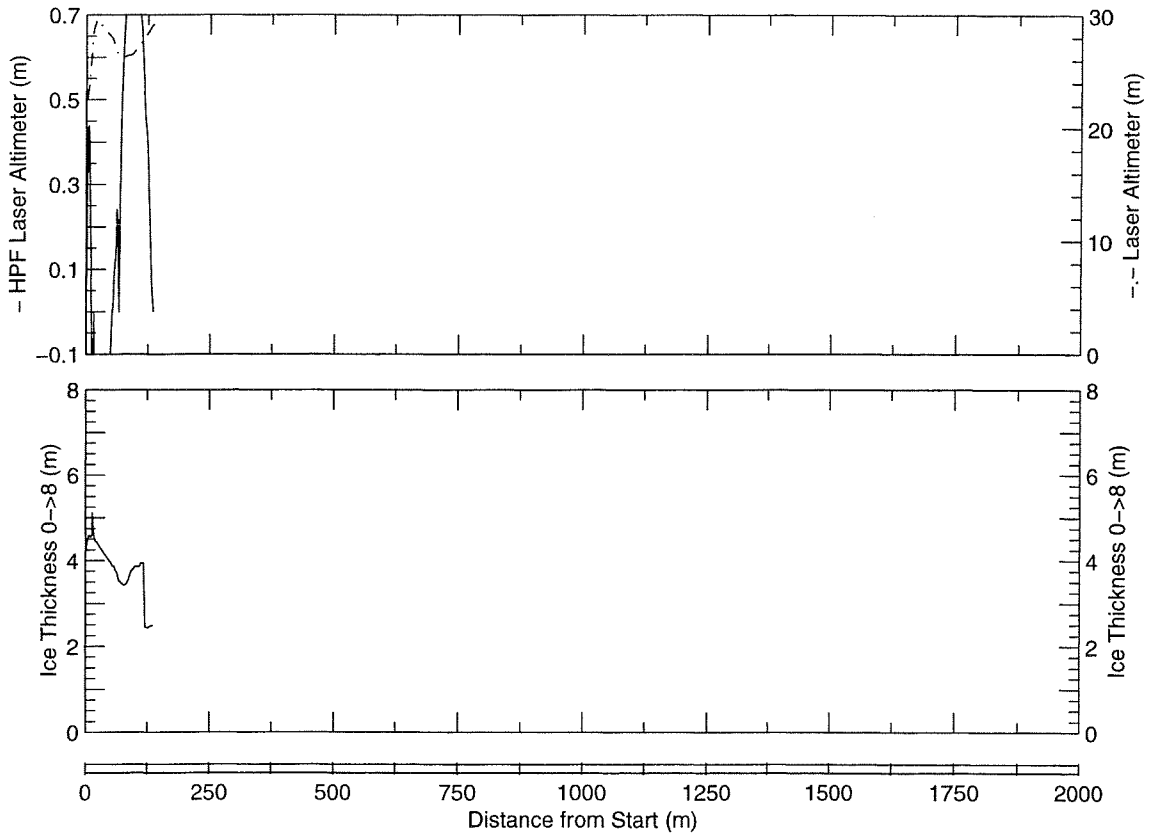

MAY 01 Flight #10 Line #10091 part 1 of 1

Line Starting Coordinates (74.5864,–96.9343) ending at (74.5866,–96.9407)

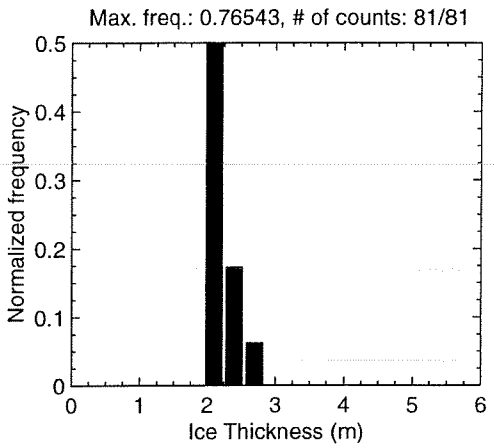

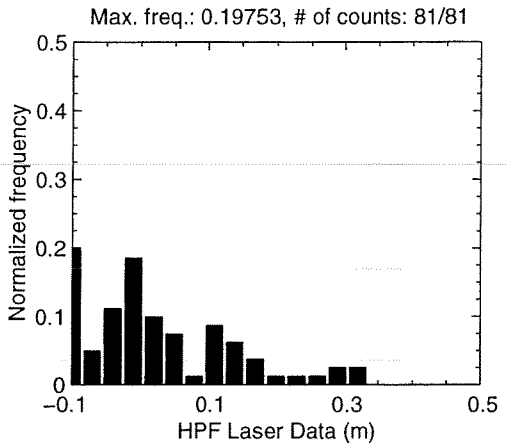

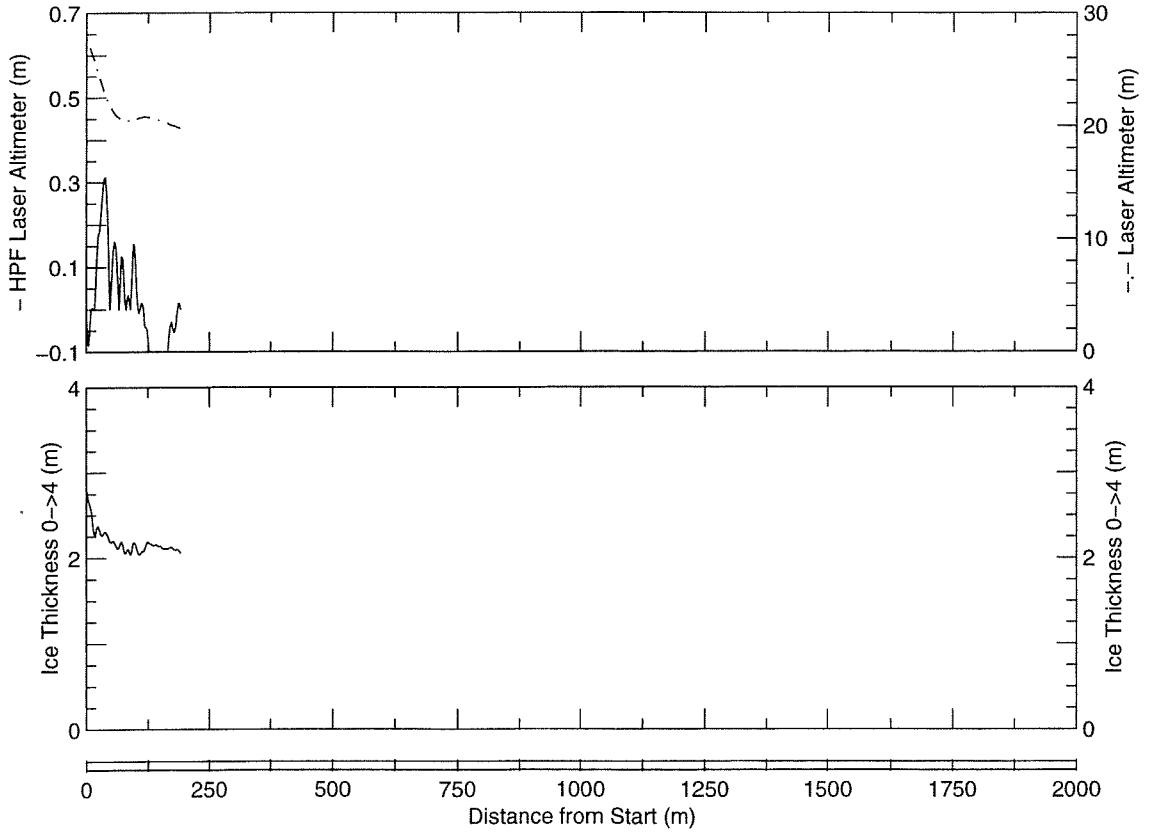

MAY 01 Flight #10 Line #10092 part 1 of 1

Line Starting Coordinates (74.5866,–96.9408) ending at (74.5901,–96.9769)

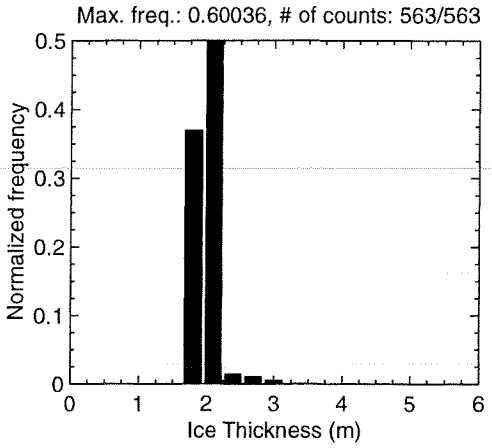

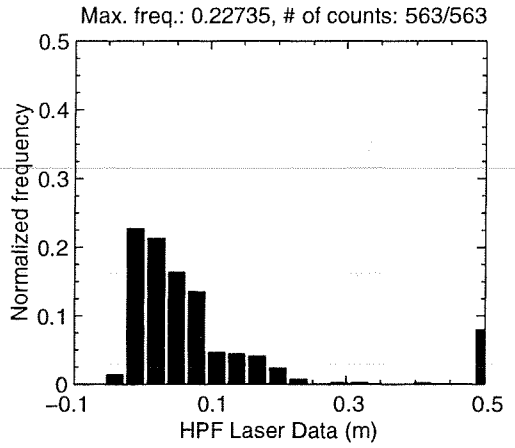

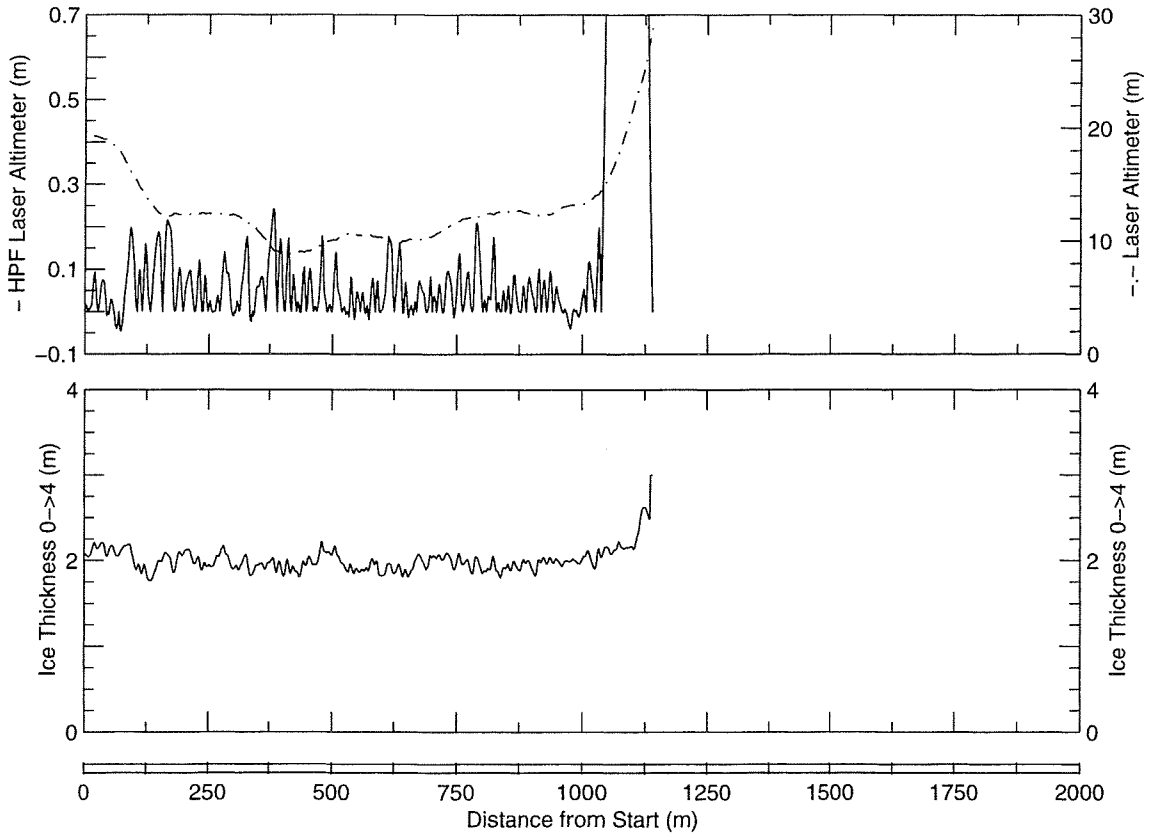

MAY 01 Flight #10 Line #10111 part 1 of 1

Line Starting Coordinates (74.5894,–96.9917) ending at (74.5865,–96.9484)

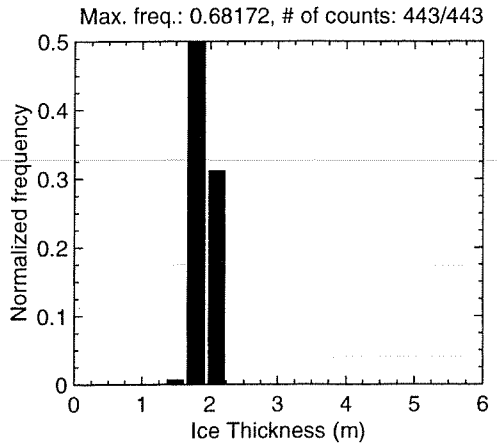

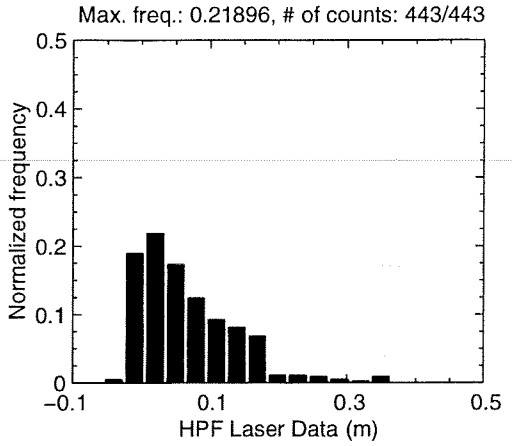

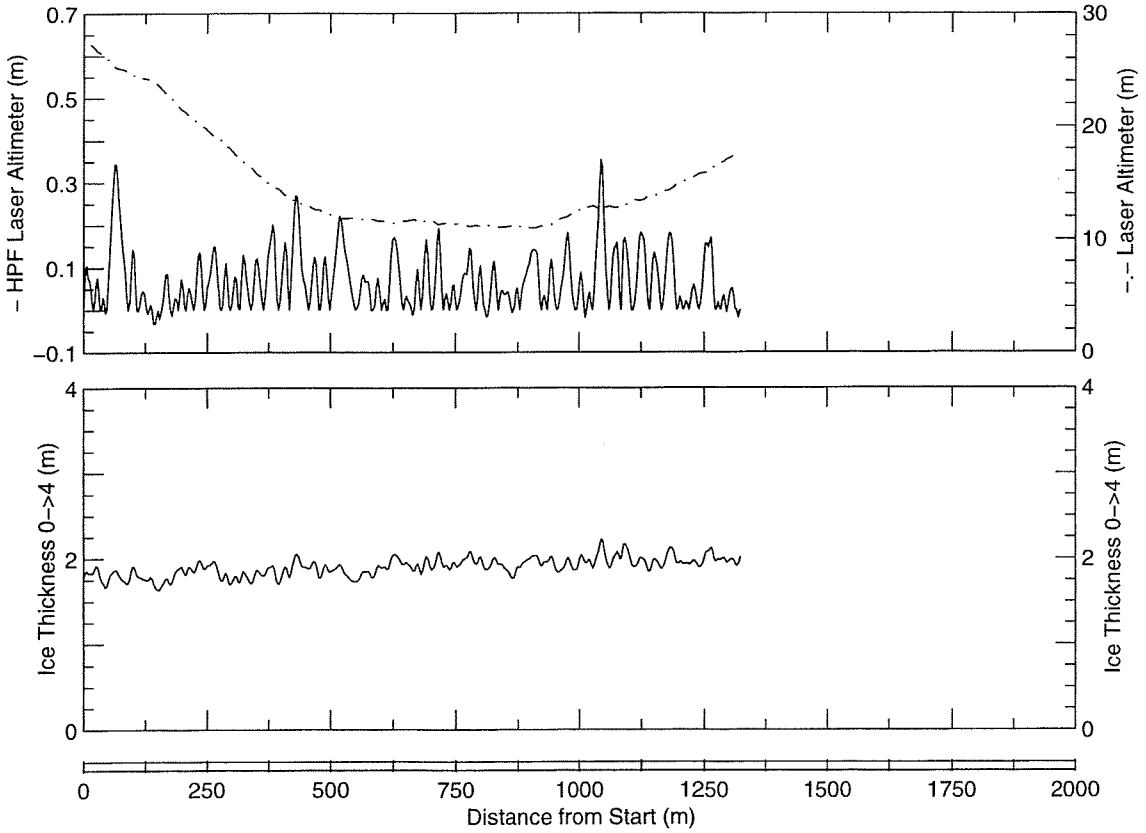

MAY 01 Flight #10 Line #10112 part 1 of 1

Line Starting Coordinates (74.5869,–96.9439) ending at (74.5881,–96.9782)

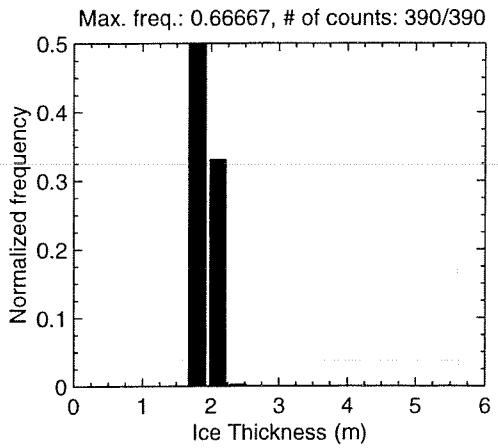

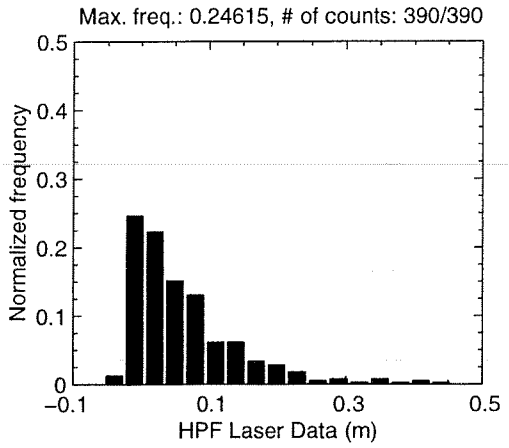

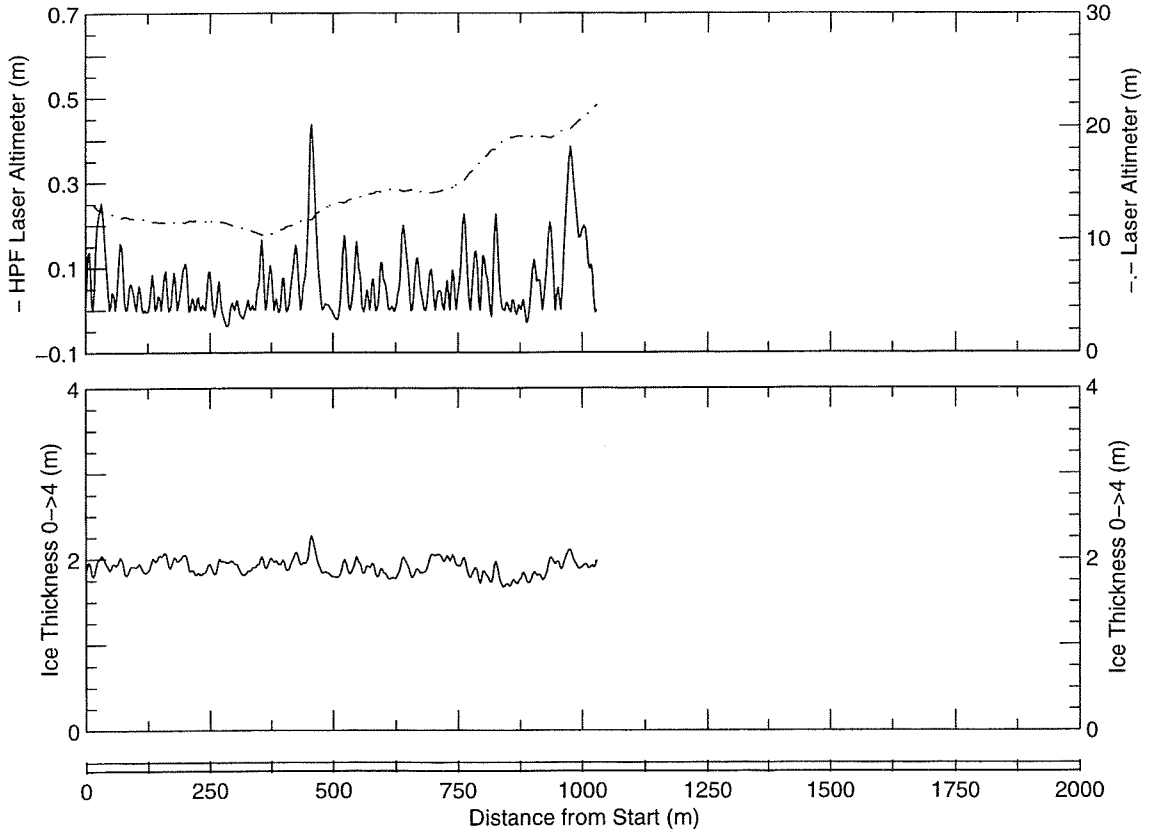

MAY 01 Flight #10 Line #10113 part 1 of 1

Line Starting Coordinates (74.5891,–96.9835) ending at (74.5863,–96.9440)

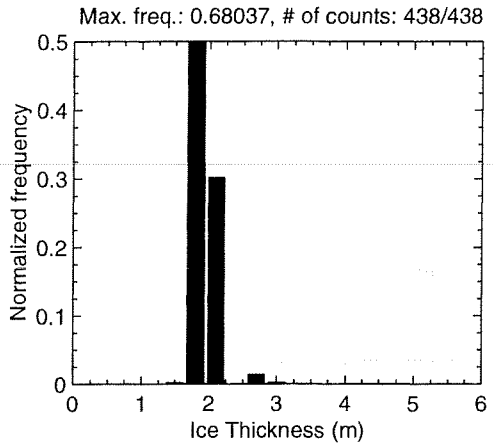

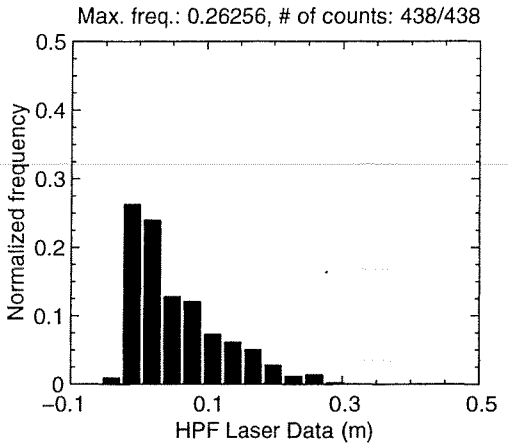

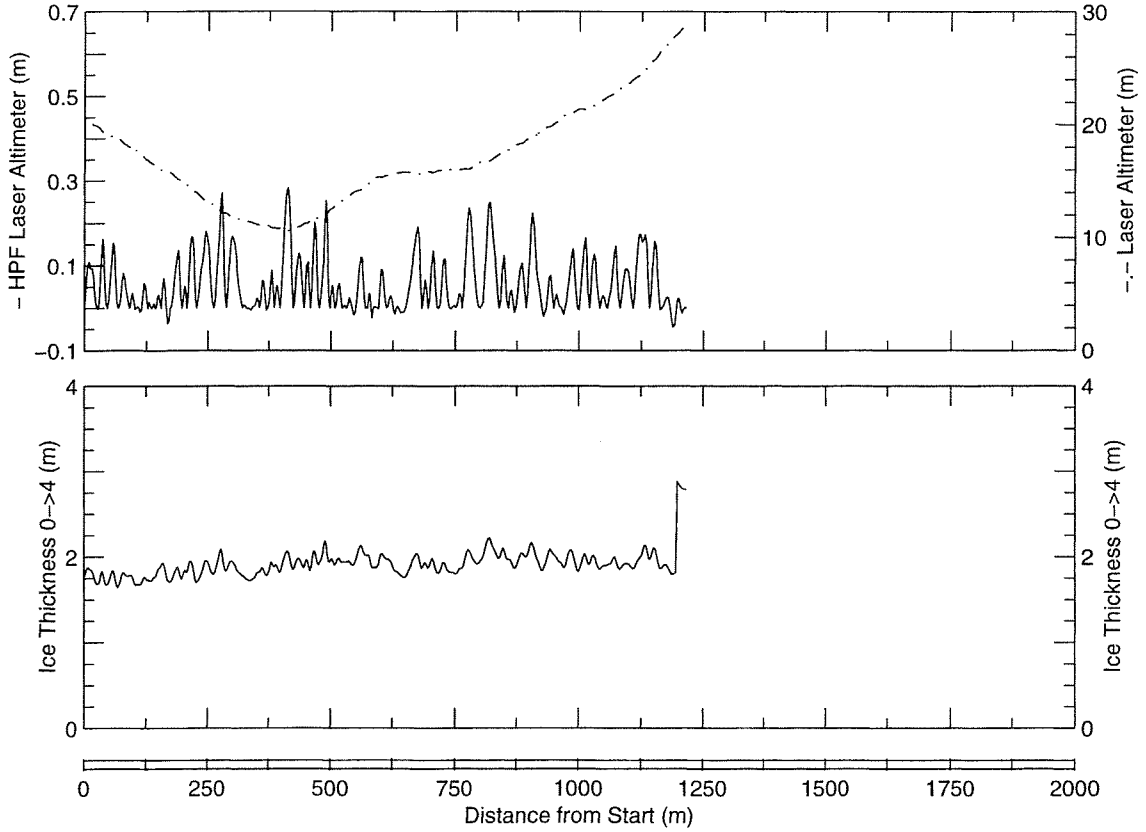

MAY 01 Flight #10 Line #10121 part 1 of 1

Line Starting Coordinates (74.5865,–96.9379) ending at (74.5892,–96.9696)